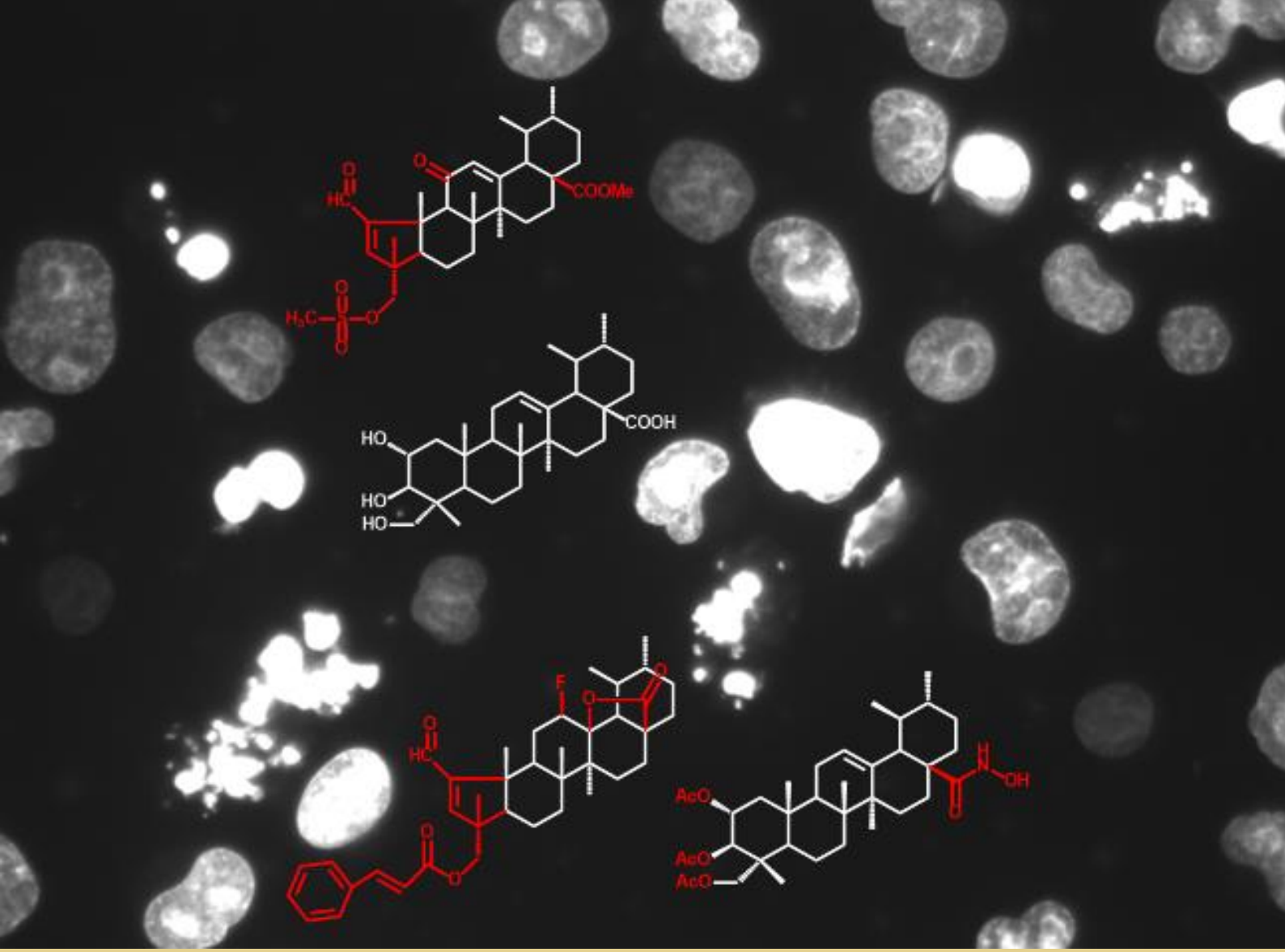

Bruno Miguel Ferreira Gonçalves

Preparation and Preclinical Evaluation of New Triterpenoid Compounds

Doctoral Thesis in Pharmaceutical Sciences with specialization in Pharmaceutical Chemistry, supervised by Professor Jorge António Ribeiro Salvador and presented to the Faculty of Pharmacy of the University of Coimbra

July 2016

· U C ·

UNIVERSIDADE DE COIMBRA

Preparation and Preclinical Evaluation of New Triterpenoid Compounds

Thesis submitted to the Faculty of Pharmacy of the University of Coimbra, to obtain the degree of Doctor of Philosophy in Pharmaceutical Sciences, in the specialty of Pharmaceutical Chemistry

Bruno Miguel Ferreira Gonçalves

July 2016

UNIVERSIDADE DE COIMBRA

Preparation and Preclinical Evaluation of New Triterpenoid Compounds

The research work presented in this thesis was developed under the scientific supervision of

Professor Jorge António Ribeiro Salvador, PhD

In Laboratory of Pharmaceutical Chemistry, Faculty of Pharmacy, University of Coimbra, and in Center for Neuroscience and Cell Biology of the University of Coimbra.

With the collaboration of:

Professor Marta Cascante Serratosa, PhD

Part of the work was developed in Department of Biochemistry and Molecular Biology, Faculty of Biology, University of Barcelona and in Institute of Biomedicine of University of Barcelona (IBUB), Unit Associated with CSIC.

Preparation and Preclinical Evaluation of New Triterpenoid Compounds

This work was supported by **Fundação Para a Ciência e Para a Tecnologia (FCT)** under the Programa Operacional Potencial Humano (POPH) of Quadro de Referência Estratégico Nacional (QREN) Portugal 2007-2013.

SFRH / BD / 69193 / 2010

UNIÃO EUROPEIA
Fundo Social Europeu

Front cover:

Picture: Microscope image of HeLa cells stained with Hoechst 33258 after treatment with a semisynthetic derivative of asiatic acid. The image was acquired using a fluorescence microscope (DMRB, Leica Microssystems, Wetzlar, Germany) and a DAPI filter.
Chemical structures: Representation of the chemical structures of asiatic acid and its semisynthetic derivatives with higher antiproliferative activity.

“Science is a way of life. Science is a perspective. Science is the process that takes us from confusion to understanding in a manner that's precise, predictive and reliable - a transformation, for those lucky enough to experience it, that is empowering and emotional.”

Brian Greene

Aos meus pais, aos meus irmãos

Aos meus familiares e amigos

Agradecimentos/Acknowledgments

Ao Professor Doutor Jorge Salvador pela confiança que sempre teve em mim e nas minhas capacidades, pelos vastos conhecimentos científicos, pelo entusiasmo, espírito inovador, pela disponibilidade constante e visão alargada que emprestou à realização deste trabalho. Agradeço ainda pela revisão científica da presente tese e por todas as sugestões feitas. Foi um enorme privilégio poder trabalhar e aprender com o professor ao longo destes anos.

To Professor Marta Cascante Serratosa, PhD for the opportunity to work in your laboratory and for providing all the conditions that I needed to perform the biological assays presented in this thesis. I am also grateful for your kindness and your concern about my work and my well-being. Finally, I thank you for the revision of my papers. It was an honor to work under your supervision.

To Sílvia Marin, PhD for welcoming me into the lab and for the teachings and support in the biological studies. I am also grateful that you shared your know-how with me and for your corrections of, and suggestions for my papers.

À Professora Doutora Maria Manuel por partilhar os vastos conhecimentos científicos que possui, pela simpatia com que sempre me tratou e pelo apoio prestado.

Ao Dr. Pedro Cruz e à Dra. Fátima Nunes, pelo auxílio prestado na discussão de alguns aspetos relacionados com a elucidação estrutural dos compostos.

À Graça Santiago e aos restantes funcionários do Laboratório de Química Farmacêutica da Faculdade de Farmácia da Universidade de Coimbra pela simpatia com que sempre me brindaram e por todo o apoio prestado.

A todos os colegas do Laboratório de Química Farmacêutica com quem trabalhei ao longo destes anos pelo companheirismo, amizade e agradáveis momentos que partilhamos. Ainda uma palavra de apreço por todos os debates de ideias e por todo o apoio que voluntariamente deram para que a realização da presente tese fosse possível.

To all the colleagues at Marta Cascante's lab for the friendship and for the assistance in some experiments. It was a pleasure to work with you.

Aos meus pais pelo apoio incondicional, pelo incentivo e por terem estado presentes em todos os momentos. Obrigado por me facilitarem a vida sempre que eu precisei de tempo para me dedicar a este trabalho. São sem dúvida as pessoas mais importantes para mim, agradeço-vos pela pessoa que sou hoje.

Aos meus irmãos por estarem sempre disponíveis para me apoiar e dar ânimo. São verdadeiros companheiros para a vida.

A todos os amigos que conheci em Barcelona (Pedro, Inês, Álvaro, Sandra, Nuno, Cláudia e Ariel) pela amizade e companheirismo e por tornarem a minha estadia na cidade muito mais agradável.

A todos os meus amigos por me trazerem equilíbrio à vida, o qual foi essencial para levar este trabalho até ao fim.

À Mariana pelo apoio que me deu e por ter alegrado os meus dias na parte final de escrita.

À minha restante família pelo interesse que sempre demonstraram no meu trabalho e pelas palavras de incentivo.

À Fundação para a Ciência e para a Tecnologia pelo apoio financeiro a este projeto, sem o qual a realização do mesmo não teria sido possível. SFRH / BD / 69193 / 2010.

Não querendo cometer nenhuma injustiça por omissão, deixo os meus profundos agradecimentos a todos os demais que contribuíram, de uma forma ou de outra, para a realização deste trabalho.

A todos,

MUITO OBRIGADO

Table of contents

Abbreviations

5-LOX	5-lipoxygenase
ABC	ATP-binding cassette
AIDS	acquired immune deficiency syndrome
AIF	apoptosis-inducing factor
Akt	protein kinase B
AMPK	AMP-activated protein kinase
Apaf-1	apoptotic protease-activating factor 1
ATP	adenosine triphosphate
BBB	blood-brain barrier
BCA	bicinchoninic acid
Bcl-2	B-cell lymphoma gene-2
BH	Bcl-2-homologous domain
br	broad signal
BSA	Bovine serum albumin
CARD	caspase activation and recruitment domain
CBMI	1,1′-carbonylbis(2′methlyimidazole)
CDI	1,1′-carbonyldiimidzole
CDKIs	cyclin-dependent kinase inhibitors
CDKs	cyclin-dependent kinases
CI	combination index
CML	chronic myeloid leukemia
Con A	concanavalin A
COX	cyclooxygenase
d	doublet
DAST	diethylaminosulfur trifluoride
DCM	dichloromethane
dd	doublet of doublets
DED	death-effector domain
DEPT	distortioneless enhancement by polarization transfer
D-GaIN	D-galactosamine
DIABLO	direct inhibitor of apoptosis-binding protein with low isoeletric point

DI-ESI-MS direct infusion electrospray ionization mass spectrometry
DISC death-inducing signaling complex
DMAP 4-dimethylaminopyridine
DMAPP dimethylallyl diphosphate
DMEM Dulbecco's modified eagle medium
DMSO dimethyl sulfoxide
DNA deoxyribonucleic acid
DPBS Dulbecco's phosphate buffered saline
dq doublet of quartets
dt doublet of triplets
E2F transcription factor activating adenovirus E2 gene
EDTA ethylenediamine tetra-acetic acid
EGTA glycol ether diamine tetra-acetic acid
EMA European Medicines Agency
eNOS endothelial nitric oxide synthase
ERK extracellular signal regulated kinase
ESI-HRMS electrospray ionization high resolution mass spectrometry
FACS fluorescence activated cell sorting
FADD Fas-associated death domain protein
FAK focal adhesion kinase
FasL ligand of Fas death receptor
FBS fetal bovine serum
FCC flash column chromatography´
FDA Food and Drug Administration
FLICE FADD-like interleukin-1β-converting enzyme inhibitory protein
FLIP FLICE-inhibitory protein
FPP pharnesyl diphosphate
FT-ICR Fourier transform ion cyclotron resonance
GP glycogen phosphorylase
HBMEC human brain microvascular endothelial cells
HDAC histone deacetylases
HPV Human papilloma virus
HRMS high resolution mass spectrometry

HTS	high-throughput screening
HUVEC	human umbilical vein endothelial cells
IAPs	inhibitor of apoptosis proteins
IC_{50}	concentration required to obtain 50% inhibition
IL	interleukin
iNOS	nitric oxide synthase
IPP	isopentenyl diphosphate
IR	infrared spectroscopy
J	coupling constant
L-NAME	Nω-nitro-L-arginine methyl ester hydrochloride
LPS	lipopolysaccharide
LTC_4S	leukotriene C_4 synthase
m	multiplet
m/z	ion mass/charge ratio
MAPK	mitogen-activated protein kinases
MEM	minimum essential medium
MEP	2-C-methyl-D-erythritol 4-phosphate
MIC	minimum inhibitory concentration
MMP	matrix metalloproteinases
MOMP	mitochondrial outer membrane permeabilization
Mp.	melting point
MPTP	1-methyl-4-phenyl-1,2,3,6-tetrahydropyridine
MS	mass spectrometry
mTOR	mammalian target of rapamycin
MTT	3-(4,5-dimethylthiazol-2-yl)-2,5-diphenyltetrazolium bromide
MVA	mevalonic acid
NF-κB	nuclear factor κB
NMR	nuclear magnetic resonance spectroscopy
NO	nitric oxide
NOx	nitric oxide metabolite
NSCLC	non-small cell lung cancer
PARP	poly-(ADP-ribose)-polymerase
PDC	pyridinium dichromate

PGE-2	prostaglandin E2
PI	propidium iodide
PI3K	phosphatidylinositol 3-kinase
PPARγ	peroxisome proliferator-activated receptor γ
PS	phosphatidylserine
PTs	pentacyclic triterpenoids
q	quartet
QIT-MS	Quadrupole/Ion Trap Mass Spectrometer
Rb	retinoblastoma protein
ROS	reactive oxygen species
RPMI	Roswell Park Memorial Institute medium
rt	room temperature
s	singlet
SAR	structure-activity relationship
SD	standard deviation
SDS	Sodium dodecyl sulfate
SLNs	solid lipid nanoparticles
Smac	second mitochondria-derived activator of caspase
STAT3	signal transducer and activator of transcription 3
STZ	streptozotocin
t	triplet
TBS	Tris-buffered saline
TGF	transforming growth factor
THF	tetrahydrofuran
TLC	thin layer chromatography
TNF	tumor necrosis factor
TOP1	topoisomerase I
TOP2	topoisomerase II
TPA	12- O-tetradecanoylphorbol-13-acetate
TRAIL	TNF-related apoptosis-inducing ligand
VDAC	voltage-dependent anion channel
VEGF-A	vascular endothelial grow factor-A
vs	versus

WHO	World Health Organization
XTT	2,3-bis-(2-methoxy-4-nitro-5-sulfophenyl)-2H-tetrazolium-5-carboxanilide
δ	chemical shift (NMR)
≈	approximately

Resumo

O cancro continua a ser uma das principais causas de morte a nível mundial. De acordo com os dados estatísticos, em 2012 morreram cerca de 8.2 milhões de pessoas devido a esta doença. Além disso, prevê-se que o número de novos casos diagnosticados de cancro aumente consideravelmente nas próximas décadas. Considerando que os fármacos antineoplásicos usados atualmente na clínica continuam a ter diversas limitações e efeitos secundários graves, é urgente desenvolver novos fármacos que tenham uma maior eficácia terapêutica no tratamento do cancro.

Os produtos naturais têm sido uma fonte importante de *leads* para a descoberta e desenvolvimento de novos fármacos, nomeadamente os anticancerígenos. Na verdade, alguns dos medicamentos anticancerígenos mais usados na prática clínica são derivados de produtos naturais. Os triterpenóides pentacíclicos representam uma vasta classe de produtos naturais que exibe diversas actividades biológicas, incluindo a atividade anticancerígena. Devido a essa atividade, ao seu perfil relativamente seguro e à sua elevada disponibilidade na natureza, os triterpenóides pentacílicos são compostos interessantes para desenhar novos *leads* visando o desenvolvimento de fármacos inovadores para a prevenção e tratamento do cancro. O ácido asiático é um triterpenóide pentacíclico da série ursano cujas propriedades anticancerígenas têm vindo a ser extensivamente estudadas ao longo dos últimos anos. Este composto demonstrou ter efeitos anticancerígenos promissores tanto em ensaios *in vitro* como em ensaios *in vivo*. Além disso, estudos prévios demonstraram também que a modificação estrutural do ácido asiático pode potenciar a sua atividade anticancerígena. Sendo assim, o presente trabalho teve como objetivo a preparação de novos derivados semissintéticos do ácido asiático, visando aumentar a sua actividade anticancerígena e obter compostos que possam vir a ser úteis para o desenvolvimento de novos tratamentos para o cancro.

No decorrer desde trabalho foram idealizados e preparados com sucesso três painéis de novos derivados semissintéticos do ácido asiático. Esses painéis incluem derivados fluorados (**3.1**–**3.26)**, A-nor (**4.2, 4.5, 4.8, 4.12–4.30)**, amidas e ácidos hidroxâmicos **(5.6–5.16)**. As estruturas químicas dos novos compostos foram elucidadas fazendo uso de várias técnicas analíticas incluindo ^{1}H e ^{13}C RMN, espectroscopia de infravermelho, espectrometria de massa e espectrometria de massa de alta resolução.

As atividades antiproliferativas dos novos derivados preparados foram avaliadas num painel de linhas celulares cancerígenas (HT-29, HeLa, MCF-7, Jurkat, PC-3, A-375, e MiaPaca-2), e determinaram-se os valores IC_{50}. A maioria dos novos compostos demonstrou maior atividade antiproliferativa que o ácido asiático. Alguns dos derivados exibiram valores de IC_{50} inferiores aos exibidos pela cisplatina nas células HeLa (2.28 μM), tendo apresentado, inclusive, valores de IC_{50} inferiores a 1 μM em várias linhas celulares. Foi estabelecida uma relação estrutura-actividade com base nos valores de IC_{50} determinados nas células HeLa. Os melhores compostos de cada painel foram posteriormente testados numa linha celular não tumoral (BJ) para avaliar a seletividade, tendo exibido menor toxicidade nas células não tumorais do que nas cancerígenas.

De seguida, efetuou-se um estudo preliminar do mecanismo de ação responsável pelo efeito anticancerígeno dos compostos mais ativos de cada painel, **3.14**, **4.29** e **5.6**. Estes compostos foram avaliados relativamente ao seu efeito no ciclo celular e à sua capacidade para induzir apoptose nas células HeLa. Os três compostos induziram a paragem do ciclo celular na fase G0/G1 e morte celular por apoptose. O composto **3.14** induziu apoptose com ativação das caspases 8 e 3, clivagem da PARP, aumento dos níveis de Bax e uma redução dos níveis de Bcl-2, sugerindo o envolvimento das vias intrínseca e extrínseca no processo apoptótico. O derivado **4.29** induziu a morte celular por apoptose nas células HeLa através da ativação das caspases 9, 8 e 3. Este composto conduziu ainda a uma redução dos níveis das proteínas Bcl-2 e Bid e a um aumento dos níveis da proteína Bax. O composto **5.6** induziu apoptose nas células HeLa através de um mecanismo relacionado com activação das caspases. Por fim, verificou-se a existência de sinergismo quando as células HeLa foram tratadas simultaneamente com o composto **5.6** e com a cisplatina.

Alguns dos novos derivados semissintéticos do ácido asiático preparados no decorrer deste trabalho, demonstraram efeitos anticancerígenos promissores em ensaios *in vitro* e justificam estudos pré-clínicos adicionais. Estes derivados podem vir a ser compostos úteis para o desenvolvimento de novos fármacos anticancerígenos.

Palavras-chave: Cancro, triterpenóides pentacíclicos, ácido asiático, atividade anticancerígena, derivados fluorados, derivados A-nor, derivados ácidos hidroxâmicos, paragem do ciclo celular, apoptose.

Summary

Cancer is a leading cause of death worldwide, with an estimated 8.2 million cancer-related deaths registered in 2012. Moreover, the number of new cancer cases diagnosed each year is expected to rise significantly over the next decades. Considering that antineoplastic agents available currently in the clinic have several limitations and some serious side effects, it's urgent the development of new chemotherapeutic agents with increased efficacy.

Natural products have been an important source of leads for the development of new drugs, including new anticancer drugs. In fact, some of the most important antineoplastic agents used in the clinic are derived from natural products. Pentacyclic triterpenoids represent a large and structurally diverse class of natural products that display diverse biological activities, including anticancer activity. Because of this activity, their relatively safe profile, and readily availability in nature, pentacyclic triterpenoids are interesting compounds for the design of new leads aimed at the development of new anticancer agents. Asiatic acid is an ursane-type pentacyclic triterpenoid whose anticancer properties have been extensively studied over the last few years. This compound exhibited promising anticancer effects in both *in vitro* and *in vivo* studies. Moreover, previous studies reported that structural modification of asiatic acid backbone may improve its anticancer activity. Therefore, the aim of this project was to synthesize new semisynthetic derivatives of asiatic acid in order to improve its anticancer activity and obtain compounds that may be valuable for the development of new anticancer treatments.

During this project, three panels of new semisynthetic derivatives of asiatic acid were designed and successfully synthesized. These panels include new fluorinated (**3.1**–**3.26)**, A-nor (**4.2**, **4.5**, **4.8**, **4.12–4.30),** amide and hydroxamic acid **(5.6–5.16)** derivatives of asiatic acid. The chemical structures of the new compounds were elucidated using techniques such as ^{1}H and ^{13}C NMR, IR, MS and HRMS.

The antiproliferative activities of the new derivatives were evaluated against several tumor cell lines (HT-29, HeLa, MCF-7, Jurkat, PC-3, A-375, and MiaPaca-2), and the IC_{50} values were determined. The great majority of the new compounds showed improved growth-inhibitory activity compared with asiatic acid. Some of the new derivatives exhibited a lower IC_{50} value than that of the reference drug cisplatin (2.28 μM) in the HeLa cell line, and even

showed IC_{50} values that were lower than 1 μM in several cancer cell lines. A structure–activity relationship was established based on the IC_{50} values determined in the HeLa cell line. The best compounds of each panel were further tested against a nontumor cell line (BJ), to assess selectivity, and exhibited lower toxicity toward nontumor cells than they did toward tumor cells.

A preliminary study of the mechanism underlying the anticancer effect of the most active compounds of each panel, **3.14**, **4.29** and **5.6,** was performed. These compounds were evaluated regarding their effects on the cell cycle and their ability to induce apoptosis in HeLa cells. All three compounds arrested the cell cycle at the G0/G1 phase and induced apoptotic cell death. Compound **3.14**-induced apoptosis was driven by caspases, with activation of caspases 8 and 3, cleavage of PARP, upregulation of Bax, and downregulation of Bcl-2, suggesting the involvement of intrinsic and extrinsic pathways in the apoptotic process. The derivative **4.29** induced apoptotic HeLa cell death via the activation of caspases 9, 8, and 3. This compound also induced the downregulation of the Bcl-2 and Bid proteins and the upregulation of the Bax protein. The compound **5.6** induced apoptosis through activation of caspases. Finally, a synergistic effect was observed after simultaneous treatment of HeLa cells with compound **5.6** and cisplatin.

Some of the newly synthesized derivatives of asiatic acid showed promising *in vitro* anticancer effects and clearly warrant further preclinical evaluation. These derivatives may be useful molecules for the development of new anticancer drugs.

Keywords: Cancer, pentacyclic triterpenoids, asiatic acid, anticancer activity, fluorinated derivatives, A-nor derivatives, hydroxamic acid derivatives, cell-cycle arrest, apoptosis.

List of figures

List of tables

List of schemes

Thesis organization

The current thesis is divided into 7 chapters. The first chapter consists in a general introduction in which a general overview of cancer, including some statistics and details of the biology of the disease, is given. This chapter also focuses on the importance of natural products for the treatment of cancer and on the therapeutic potential of pentacyclic triterpenoids, with special emphasis on the anticancer properties of asiatic acid. The final part of the chapter is dedicated to the description of selected asiatic acid derivatives that have been synthesized and investigated for their anticancer activities.

Chapter 2 explains the objectives underlying the work described in this thesis.

Chapters 3, 4, and 5 are dedicated to the description of the synthesis and anticancer evaluation of the new semisynthetic derivatives of asiatic acid and are organized in a similar way: each chapter starts with a short introduction, followed by the description of the synthetic strategies used for the preparation of a panel of new derivatives. Selected aspects of the structural elucidation of the new derivatives based on techniques such as IR, ^{1}H NMR, ^{13}C NMR and MS are provided. In each chapter are also presented the results and the discussion of the biological studies performed with the synthesized compounds, including their effects on cell viability with establishment of the SAR, and a preliminary study on their mechanism of action. Each chapter finishes with the conclusions and the description of the experimental procedures. In more detail: Chapter 3 is dedicated to the synthesis and anticancer evaluation of fluorinated asiatic acid derivatives, Chapter 4 is dedicated to the synthesis and anticancer evaluation of A-nor asiatic acid derivatives and finally, Chapter 5 is dedicated to the synthesis and anticancer evaluation of amide and hydroxamic acid derivatives of asiatic acid.

Chapter 6 outlines the concluding remarks of this work. Chapter 7 is dedicated to the bibliographic references used in this thesis.

For a better understanding of the structural elucidation of the new compounds discussed in chapters 3, 4, and 5, please consider the following representation of the chemical structure of asiatic acid, with the carbons numbered.

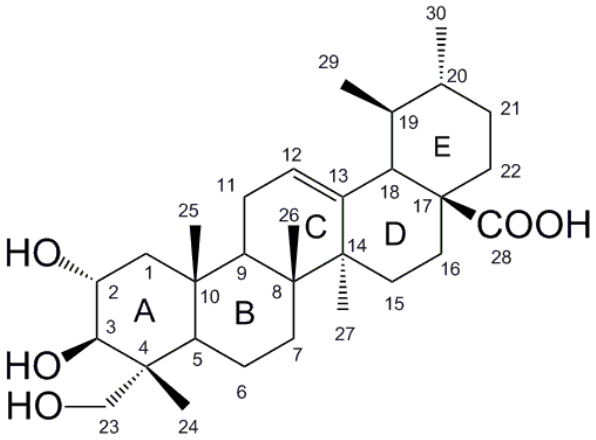

The attribution of nomenclature to the organic compounds presented in this thesis followed the recommendations of the IUPAC commission on nomenclature of organic chemistry, described by P. M. Giles Jr. in *Revised section F: natural products and related compounds*, Pure Appl. Chem., Vol. 71, Nº 4, pp. 587–643, 1999 and reviewed by H. A. Fabre et al. in *Errata Revised section F: natural products and related compounds*, Pure Appl. Chem., Vol. 76, Nº 6, pp. 1283–1292, 2004. However, some compounds are designated within this thesis by their trivial name. The compounds are also numbered according to the chapter in which they are mentioned and according to their order of appearance in the text. Asiatic acid is an exception, as it keeps the same number (**1.27**) throughout the entire thesis.

The main databases used for the bibliographic research were the ISI Web of Knowledge (Thompson Reuters) and PubMed.

Chapter 1

Introduction

Ursane-type pentacyclic triterpenoids as useful platforms to discover anticancer drugs

Jorge A. R. Salvador, Vânia M. Moreira, Bruno M. F. Gonçalves, Ana S. Leal and Youngkui Jing

Natural Products Reports, 2012, 29, 1463–1479.

Highlights of pentacyclic triterpenoids in the cancer settings

Jorge A. R. Salvador, Ana S. Leal, Daniela P. S. Alho, Bruno M. F. Gonçalves, Ana S. Valdeira, Vanessa I. S. Mendes and Youngkui Jing

Studies in Natural Products Chemistry, Atta-ur-Rahman Editors, Elsevier, Volume 41, 2014, 33–73.

1.1 Cancer

1.1.1 Cancer as a public health problem: some numbers

Cancer is one of the most devastating diseases of our era. It is a leading cause of death worldwide, thus representing a major public health problem.[1,2] About 8.2 million people were expected to die from cancer in 2012 worldwide, of which 1.75 million deaths were expected to occur in Europe. In the same year, an estimated 14.1 million new cancer cases were diagnosed worldwide, of which 3.45 million were diagnosed in Europe.[1,3,4]

Lung cancer, with an estimated 1.8 million new cases diagnosed (13% of all cancers diagnosed) in 2012, was the most common cancer worldwide in both sexes. In Europe, the most frequent cancers were breast cancer, with an estimated 464000 new cases diagnosed in 2012, followed by colorectal cancer, with an estimated 474000 new cases diagnosed in 2012 (Fig. 1.1).[1,3]

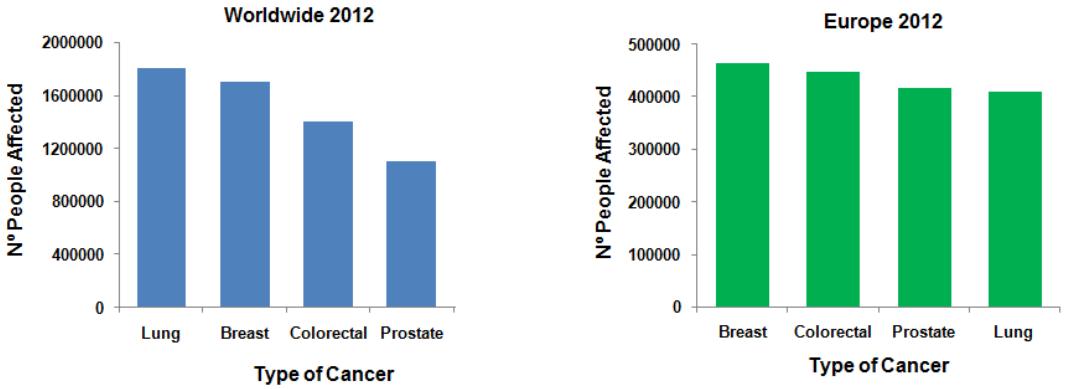

Figure 1.1 Leading cancer types for estimated new cancer cases worldwide and in Europe in 2012 for both sexes.

Lung cancer was the leading cause of cancer-related death in both sexes in 2012, with an estimated 1.6 million deaths (19% of all cancer deaths) worldwide, of which 353000 occurred in Europe (Fig. 1.2).[1,3]

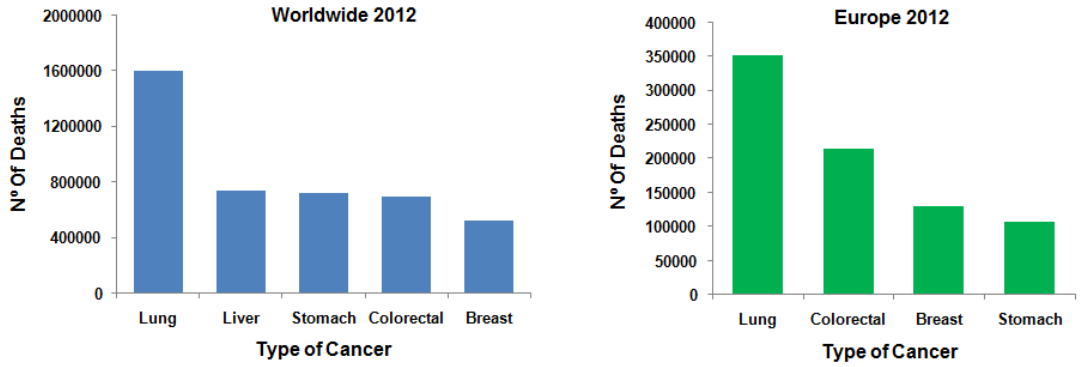

Figure 1.2 Leading cancer types for estimated death worldwide and in Europe in 2012 for both sexes.

The incidence and mortality of different cancer types vary with sex. Breast cancer was the most frequent cancer among women, with an estimated 463800 new cases diagnosed in Europe, in 2012 (29% of all cancers diagnosed in Europe). This cancer is also the leading cause of cancer-related death among women, with an estimated 131200 deaths in 2012 (17% of all cancer deaths in women). Colorectal and lung cancers are other cancers with a high incidence and mortality among women (Fig. 1.3).[3]

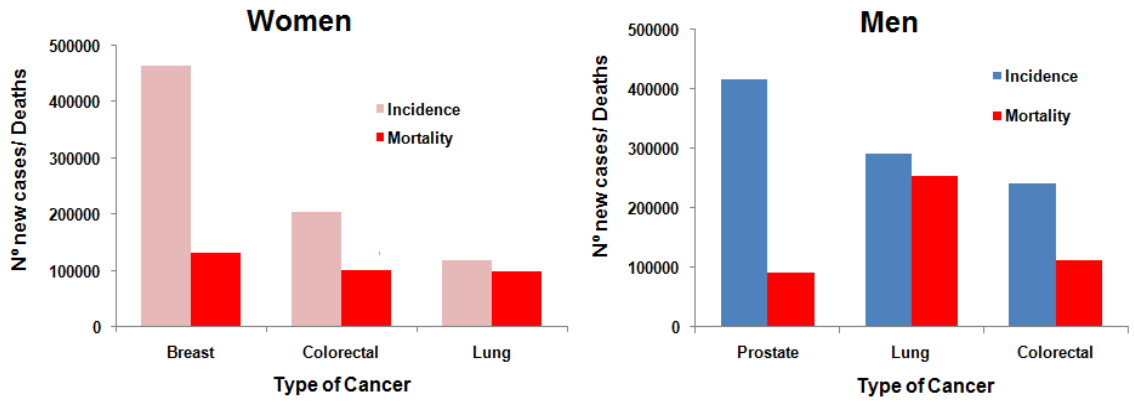

Figure 1.3 Leading cancer types for estimated new cancer cases and deaths in Europe for women and men in 2012.

Among men, lung, prostate, and colorectal cancers were the types of cancer with higher incidence and mortality in 2012 in Europe (Fig. 1.3). Prostate cancer is the most frequent cancer among men, with an estimated 416700 new cases diagnosed and lung cancer is the first-leading cause of cancer-related death among men in Europe, with an estimated 254400 deaths (26.1% of all cancer-related deaths in men) occurring in 2012.[3]

In Portugal, prostate cancer is the most frequent cancer among men, with an expected 6620 new cases diagnosed in 2012, while breast cancer is the most frequent cancer among women, with an estimated 6090 new cases diagnosed (Fig. 1.4).[3] Colorectal and lung cancers are the leading and second-leading causes of cancer-related death among both sexes. Lung cancer is the leading cause of cancer-related death among men, whereas breast cancer is the leading cause of cancer death among women.[3,5] In 2012, it was estimated that colorectal cancer was responsible for 3800 deaths (2240 men, 1560 women), lung cancer was responsible for 3440 deaths (2640 men, 800 women), female breast cancer was responsible for 1570 deaths, and prostate cancer was responsible for 1580 deaths.[5]

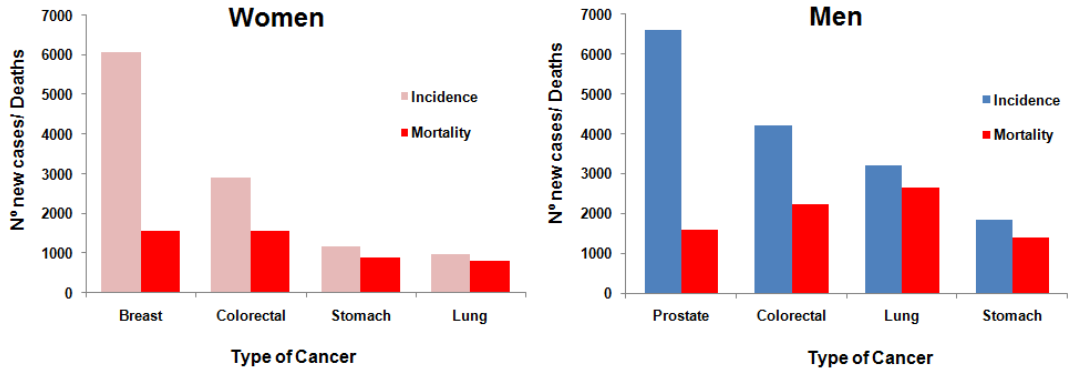

Figure 1.4 Leading cancer types for estimated new cancer cases and deaths in Portugal for women and men in 2012.

Environmental and lifestyle factors, such as smoking, poor nutrition, heavy alcohol use, obesity, exposure to pollutants, food additives, and pesticides, are at the origin of one third of cancer-related deaths. Because of the increasing prevalence of these risk factors and the growth and aging of populations in developing countries, the burden of cancer is expected to rise worldwide.[4]

According to World Health Organization (WHO) the annual number of new cancer cases is expected to rise from the 14 million recorded in 2012 to 22 million within the next two decades.[6] To reduce the global burden of cancer on society, it is urgent to change some behaviors and lifestyles and adopt several evidence-based measures, including the control of tobacco and alcohol abuse, vaccination against the human papilloma virus (HPV), promotion of physical activity and healthy diet, among others.[1,4,7] The use of tests that allow the early detection of cancers is also essential to increase the effectiveness of cancer treatment.[1,4]

Furthermore, is crucial to develop more effective anticancer medicines for the treatment of cancer patients.

1.1.2 Understanding the disease

To develop new effective medicines for the treatment of cancer, it is essential understand the disease. Cancer is a term used to define a group of diseases that are characterized by abnormal cells that grow in an uncontrolled manner and have the ability to invade adjacent tissues. These cells may also spread to other organs in a process called metastasis. Usually, in the body, cells divide, proliferate, and die in a controlled and regulated manner, which allows the maintenance of tissue homeostasis. Cancer can begin in any place of the body when a normal cell suffers several mutations in its DNA and evolves into a cancer cell, which starts to grow and divide without control. The transformation of normal cells into malignant cancers occurs through a multistep process across time, known as carcinogenesis. During this process normal cells progressively become cancerous and then malignant via the accumulation of successive genetic mutations.[8–10] These genetic mutations can occur spontaneously, because of personal genetic factors, or can be induced by exogenous carcinogens (ultraviolet and ionizing radiation, components of tobacco smoke, HPV virus, etc.).[11]

The most common genetic mutations implicated in carcinogenesis affect two groups of genes, the proto-oncogenes and the tumor suppressor genes. Proto-oncogenes regulate cell growth and proliferation, and tumor suppressor genes inhibit progression through the cell cycle. Mutations in these genes disrupt homeostasis and the regulation of cell grow, thus contributing to the development of tumors.[12,13] The proto-oncogenes are usually activated into oncogenes via gain-of-function mutations. Conversely, loss-of-function mutations lead to the inactivation of tumor suppressor genes.[14–16]

Carcinogenesis is a slow process, because normal cells require several genetic changes to evolve to cancer cells.[9] During this multistep process, cells acquire the so-called hallmarks of cancer, which are alterations in cell physiology that enable the development and metastatic dissemination of tumors. These hallmarks, proposed and described by Hanahan and Weinberg in 2000 and revised in 2011, are:[10,17]

- **Sustaining proliferative signaling:** One of the most important capabilities acquired by cancer cells is the ability to control their own proliferation by providing their own

growth signals or by increasing the level of cell surface receptors that transmit progrowth signals. Thus, cancer cells can proliferate indefinitely and independently from growth signals.[10,17]

- **Evading growth suppression:** Cancer cells also acquire the ability to ignore the antigrowth signals, which is often related with the inactivation of tumor suppressor genes.[10,17]
- **Resisting cell death:** Apoptosis is a mechanism of controlled cell death that is activated to eliminate old and damaged cells, therefore avoiding the accumulation of cells with DNA damage. Thus, apoptosis is a protection against the development of cancer. Cancer cells are not only able to sustain continuous cell growth, but they also acquire the capability to avoid or limit apoptosis. These cells can also avoid autophagy, which is another mechanism of regulated cell death. This acquired ability is determinant for the development of malignant tumors.[10,17,18]
- **Enabling replicative immortality:** The multiplication of normal cells is limited by telomeres, which are regions of replicative DNA that protect the end of chromosomes from degradation. The DNA replication machinery is unable to finish the duplication of telomeric DNA; thus, small amounts of telomeric DNA are lost in each replicative cycle. After a certain number of grow-and-division cycles, telomeres reach a critical length and normal cells undergo senescence or crisis, stop dividing, and die. It was found that 90% of immortalized cells, including cancer cells, exhibit high levels of telomerase, which is an enzyme that adds telomeric DNA to the end of chromosomes. In this way, cancer cells are able to maintain their telomeres, which allows their replication for an unlimited number of times.[10,17,19]
- **Inducing angiogenesis:** Cancer cells have the ability to stimulate the activation of angiogenesis, which is the process of formation of new vessels, via the upregulation of angiogenic activators, such as the vascular endothelial grow factor-A (VEGF-A), and the downregulation of inhibitors of angiogenesis. By activating angiogenesis, tumors create their own blood supply and, consequently, ensure the supply of the oxygen and nutrients that they need to expand.[10,17,20]
- **Activating invasion and metastasis:** In the last stages of tumor development, cancer cells acquire the ability to invade neighboring tissues and spread to other places in the body, in a process called metastasis. Metastasis occurs through a multistep process

that is usually initiated by cancer cells that enter the blood and lymphatic vessels, which transport them to a secondary anatomical site.[10,17,21]

- **Reprogramming energy metabolism:** In contrast with normal cells, which use glucose to produce energy via mitochondrial oxidative phosphorylation, cancer cells produce energy preferentially through glycolysis (oxygen-free glucose metabolism). This metabolic switch allows cancer cells to proliferate even in conditions with lower levels of oxygen.[17]
- **Avoiding immune destruction:** In normal conditions, the immune system can detect and eliminate abnormal cells, thus avoiding tumor formation and progression. In one way or another, cancer cells can avoid detection by the immune system and consequently evade destruction by immune cells.[17]

The acquisition of these distinctive capabilities is only possible because of the genetic instability associated with the accumulation of several changes in the DNA of cancer cells. Inflammation also contributes to the promotion of tumor proliferation and can potentiate the mutations in the DNA of cancer cells by generating reactive oxygen species (ROS).[17]

Tumors are no longer considered as a simple mass of proliferating malignant cells; rather, they comprise different types of cells and develop a specific tumor environment, which is extremely important to consider in the development of new anticancer therapies. For the effective treatment of tumors, more than eliminating cancer cells by inducing their death, it is necessary target the tumor environment to inhibit angiogenesis and prevent tumor promotion and progression.[10,17,22] The discovery of the hallmarks of cancer has contributed tremendously to a better understanding of the complex biology of tumors. This knowledge is essential to the discovery of new drug molecular targets and to the development of new targeted anticancer therapeutic strategies.

1.1.3 Targeted therapies for the treatment of cancer

1.1.3.1 Targeting the cell cycle

The cell cycle is a series of coordinated events that ensure proper cell division and proliferation. In Eukaryotes, the cell cycle is divided in two broad stages: interphase and mitosis (M phase). Mitosis is the process in which the nucleus of the cell divides into two identical nuclei. The interphase stage is the period of metabolic growth between cell division phases and is divided in three phases, G1 (gap 1), S (DNA synthesis), and G2 (gap 2). During the G1 phase, the cell grows, matures, and prepares for DNA replication, which occurs during the S Phase. The S phase is followed by a gap phase called G2, in which the cell prepares to enter mitosis. During the G1 phase, cells can pause and reversibly enter a quiescent phase called G0 (Fig. 1.5).[23,24]

Progression through the cell cycle is tightly regulated by the interactions between cyclins, cyclin-dependent kinases (CDKs), and cyclin-dependent kinase inhibitors (CDKIs). CDKs are a family of serine/threonine protein kinases that are expressed as inactive catalytic subunits. Their activation is dependent on the binding to regulatory subunit cyclins, giving origin to activated cyclin–CDK complexes. Cyclin–CDK complexes phosphorylate several protein substrates that are involved in cell-cycle progression. The expression of CDKs is constant along the cell cycle, in contrast to cyclins, which are expressed in an oscillatory way along the cell cycle. Thus, cyclins control the kinase activity of CDKs in a timely manner.[23,25–27]

Each phase of the cell cycle is regulated by specific cyclin–CDK complexes. The cyclin D–CDK4/6 and cyclin E–CDK2 complexes drive G1 progression and the transition through the restriction point (G1 checkpoint), after which cells are committed to entering the S phase. The passage through the restriction point is dependent on the phosphorylation of the Rb protein. This protein binds to and inactivates the E2F family of transcription factors, thus repressing the downstream transcription of genes that are involved in DNA synthesis and replication.[28,29] In the early G1 phase, cyclin D–CDK4/6 complexes partially phosphorylate the nuclear Rb protein, which results in partial activation of E2F and allows the E2F-mediated transcription of cyclin E. These events facilitate the activation of cyclin E–CDK2 complexes, which complete Rb phosphorylation, leading to its inactivation. The inactivated Rb protein releases the transcriptional factor E2F, which, once activated, initiates the transcription of the

genes that are required to enter the S phase (Fig. 1.5). After the G1/S transition, the cyclin E–CDK2 complexes are inactivated by the degradation of cyclin E. Concomitantly, cyclin A binds to CDK2, resulting in the formation of cyclin A–CDK2 complexes, which induce DNA synthesis and drive the progression of the cell cycle through the S phase and the transition to the G2 phase. At the end of the S phase, cyclin A interacts with CDK1 to give cyclin A–CDK1 complexes, which are inactivated during the G2 phase by the degradation of cyclin A. Meanwhile, cyclin B interacts with CDK1 at the end of the G2 phase, to form activated cyclin B–CDK1 complexes, which are responsible for the transition from the G2 to the M phase and for driving the cell cycle through mitosis (Fig. 1.5).[25,30]

The cell-cycle progression is negatively regulated by CDKIs, which bind to, and inactivate the kinase activity of cyclin–CDK complexes. There are two major classes of CDKIs: the Ink4 family ($p15^{Ink4b}$, $p16^{Ink4a}$, $p18^{Ink4c}$, and $p19^{Ink4d}$), which selectively inhibit the cyclin D–CDK4 and cyclin D–CDK6 complexes, and the CIP/KIP family ($p21^{cip1/waf1}$, $p27^{Kip1}$, and $p57^{kip2}$), which inhibit the activity of cyclins D–, E–, A–, and B–CDK complexes.[25,26]

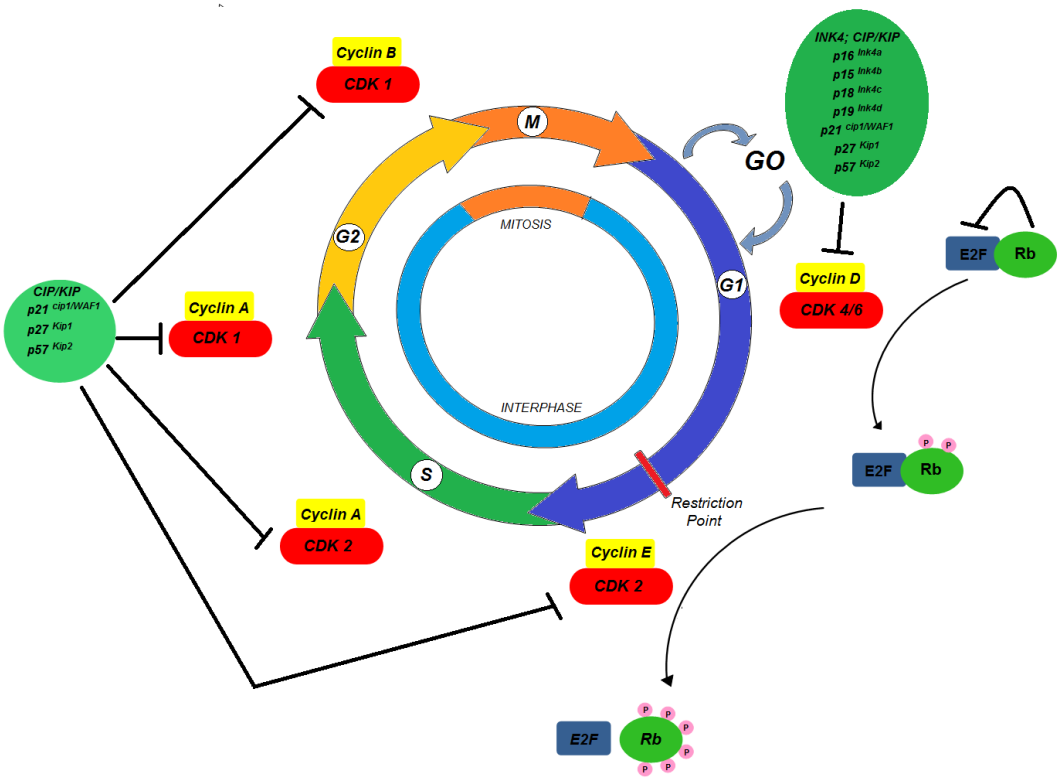

Figure 1.5 Schematic representation of cell cycle regulation.

The progression through the cell cycle is monitored at different regulatory points, known as checkpoints, which ensure an ordered sequence of events. These cell-cycle checkpoints sense possible defects in critical events, such as DNA synthesis and chromosome segregation. If any defect is detected, for example DNA damage, cell-cycle checkpoints induce the arrest of the cell cycle until the correction of the defects, thus preventing the division of compromised cells. If correction is not possible, a process of cell death is activated. In this way, it is possible to detect and correct genetic damage and ensure the faithful transmission of genetic information.[24–26]

Cancer is considered by many authors as a disease of the cell cycle.[25,31,32] The cell cycle controls cell proliferation, and cancer cells often present cell-cycle dysregulation (one of the main hallmarks of the cancer), which results in the genetic instability and aberrant cell proliferation that are characteristic of cancer.[33] This dysregulation of the cell cycle in tumors is related with mutations in several proteins of the cell regulatory machinery.[23,25] As CDK–cyclin complexes are the key regulators of the cell cycle, the defects in cell cycle of tumor cells are often related with alterations in CDK-dependent pathways. Therefore, the development of strategies that target the cell-cycle regulatory machinery and, in particular, that inhibit CDK–cyclin complexes represent valuable approaches for the discovery of new anticancer agents.[23,25,30]

1.1.3.2 Targeting apoptosis

Programmed cell death is essential to ensure physiological cell growth and survival in multicellular organisms.[34] Apoptosis is the most common mode of programmed cell death and regulates the homeostasis of tissues. This process of programmed cell death is activated during development, in the definition of the final shape of organs, to eliminate with high efficiency and precision cells that are no longer necessary or to remove cells that are in the wrong place.[34–36] Apoptotic cell death is also activated in response to irreparable damages in DNA and several other cellular stresses.[35,37,38]

Apoptosis is characterized by specific morphological changes, including cell retraction and rounding, dynamic membrane blebbing, compaction and condensation of chromatin, and nuclear fragmentation into smaller pieces, all of which are related with the proteolytic activity of caspases.[34,35,39–42] Caspases are a family of cysteine proteases that play a central role in the execution of apoptosis.[35,42] These cysteine proteases are synthesized as inactive precursor

enzymes (pro-caspases), which become active after proteolytic cleavage. Pro-caspases contain a C-terminal catalytic domain and an N-terminal prodomain. Caspases can be classified according to their function as proinflammatory caspases (caspases 1, 4, 5, 11, and 12) and as proapoptotic caspases (caspases 2, 3, 6, 7, 8, 9, and 10). The proapoptotic caspases, which mediate apoptotic cell death, can also be classified according to their position in the apoptotic signaling cascade as initiator caspases (caspases 2, 8, 9, and 10) and effector caspases (caspases 3, 6, and 7).[43–46] Initiator caspases have long prodomains containing caspase-recruitment domain (CARD) or death-effector domain (DED) motifs. These CARD and DED motifs regulate the activation of initiator caspases by mediating their dimerization and recruitment into caspase-activation complexes. The effector caspases have short prodomains and are activated through proteolytic cleavage by upstream initiator caspases.[45,46]

Two major pathways are involved in the initiation and execution of apoptosis: the extrinsic or death receptor pathway and the intrinsic of mitochondrial pathway. Both pathways converge in the activation of executioner caspases, caspases 3 and 7, which trigger events that result in apoptotic cell death (Fig. 1.6).[35,40]

The extrinsic pathway is initiated via the stimulation of death receptors that belong to the tumor necrosis factor (TNF) receptor superfamily, such as the Fas (CD95/APO-1) receptor or the TNF-related apoptosis-inducing ligand (TRAIL) receptor, which are localized at cell membrane, by specific death ligands (such as FasL and TNF-α).[47] The activation of death receptors causes a conformational change that leads to the recruitment of the adaptor protein Fas-associated death domain (FADD) and pro-caspase 8, thus leading to the formation of the death-inducing signaling complex (DISC). Caspase 8 is activated at DISC via dimerization or self-cleavage. The activation of caspase 8 can be inhibited by the FADD-like IL-1β-converting enzyme (FLICE)-inhibitory protein (c-FLIP), which binds to FADD and/or caspase 8 in a ligand-dependent and -independent manner, thus inhibiting DISC formation and, consequently, the activation of the caspase cascade.[48,49] Active caspase 8 can trigger apoptosis in two distinct ways: in some cells, active caspase 8 can directly induce the activation of the downstream effector caspase 3. In other cell types, caspase 8 can trigger the intrinsic pathway, to amplify the apoptotic signal.[37,50]

The intrinsic pathway is initiated in mitochondria, where several cellular stresses induce mitochondrial outer membrane permeabilization (MOMP), which is the crucial event that leads to the activation of the caspase cascade and apoptosis. MOMP is regulated by the interaction between the members of B cell lymphoma 2 (Bcl-2) family proteins, which are dimers that are located in the outer mitochondrial membrane. Bcl-2 family proteins are

divided into three groups: proapoptotic proteins (e.g., Bax, Bak, and Bok/Mtd), antiapoptotic proteins (e.g., Bcl-2, Bcl-xL, Mcl-1, and Bcl-w), and proteins that contain only a single BH3 domain (e.g., Bid, Bim, Puma, Noxa, and Bad). The proteins that contain only a single BH3 domain are stimulated by several cytotoxic stresses (such as DNA damage, grow-factor deprivation, and endoplasmic reticulum stresses) and activate Bax and Bak. Once activated, Bax and Bak oligomerize to form pores in the mitochondrial outer membrane, which leads to the release of proapoptogenic factors, such as cytochrome *c*, the apoptosis-inducing factor (AIF) and Smac/DIABLO, into the cytoplasm.[40,51,52] After release into the cytoplasm, cytochrome *c* binds to the apoptotic protease-activating factor 1 (Apaf1) and ATP, to form an apoptosome complex, which recruits, dimerizes, and activates the initiator caspase 9. Once activated, caspase 9 triggers the downstream executioner caspase 3, leading to apoptotic cell death (Fig. 1.6).[40,47,53] Moreover, Smac/DIABLO induces caspase activation by inhibiting the action of inhibitor of apoptosis proteins (IAPs).[46,47]

As mentioned previously, cross-talk between the intrinsic and extrinsic pathways can occur via the action of active caspase 8, which cleaves the proapoptotic BH3-only protein Bid, yielding t-Bid (truncated Bid). t-Bid translocates to the mitochondrial surface and induces the activation of proapoptotic Bcl2 family proteins (Bax) and the inhibition of the antiapoptotic ones (Bcl-2), thus leading to the activation of the intrinsic apoptotic pathway (Fig. 1.6).[50,54]

Apoptosis can also proceed through caspase-independent pathways. For example, AIF triggers apoptosis by inducing chromatin condensation and DNA fragmentation.[55]

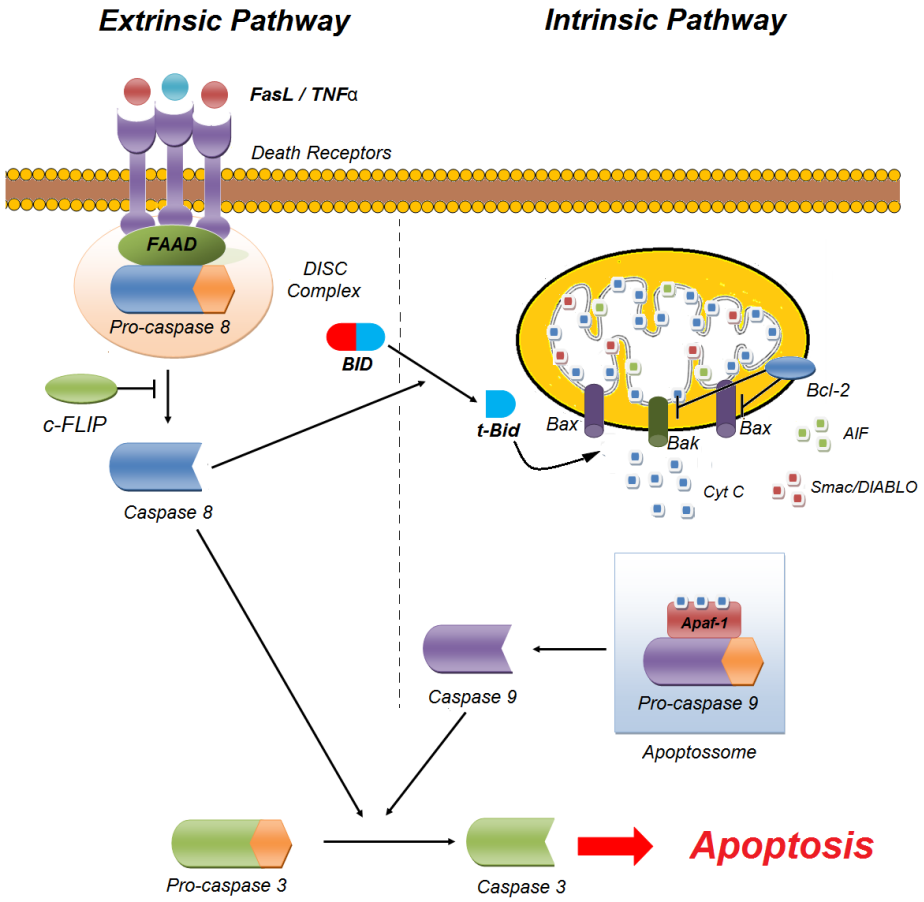

Figure 1.6 Simplified representation of the extrinsic and intrinsic apoptotic pathways

As outlined above, cancer is a disease that results from a succession of genetic mutations that drive the progressive transformation of normal cells into malignant ones. As apoptosis is triggered to discard cells with irreparably damaged DNA, it works as a natural protection against cancer.[53]

Defective or inefficient apoptotic processes have been found to play a vital role in the initiation and progression of cancer. In fact, the ability to avoid apoptotic cell death is an essential hallmark that is common to all tumors.[10,17,52,53,56] Cancer cells use several strategies to evade apoptosis, including the disruption of the balance between anti- and proapoptotic proteins via the overexpression of antiapoptotic proteins (such as Bcl-2) and the underexpression of proapoptotic proteins (such as Bid, Bax, and Bak).The downregulation of caspases and the upregulation of IAPs have also been related with development of

carcinogenesis and resistance to chemotherapy. Another mechanism of evasion from apoptosis is related with defects and mutations in the tumor suppressor gene p53. The downregulation of death receptors and the reduction of the levels of death signals can also lead to evasion from the extrinsic pathway of apoptosis.[18,52]

Most of the anticancer treatments that are available currently in clinical settings, such as chemotherapy, γ-radiation, suicide gene therapy, and immunotherapy, exert their anticancer effect via the induction of apoptosis.[47] Therefore, targeting apoptosis has been recognized as an effective strategy to fight cancer.[52,53] Based on these features, chemotherapeutic strategies that are designed to explore abnormalities in apoptotic signaling pathways aiming at the restoration of normality to induce the apoptosis of cancer cells selectively are an interesting approach to the treatment of cancer.[52,53]

1.2 Natural products

For many years, natural products have been one of the main sources of molecules for the development of new medicines. Many of the natural products that exhibit higher therapeutic potential are obtained essentially from readily accessible natural sources, such as plants, animals, microbes, and marine organisms. Plants in particular have been used since immemorial times for the relief of a wide spectrum of diseases and constitute the basis of many traditional medicine systems, such as the Egyptian, Chinese, or Indian systems. According to the WHO, it is estimated that approximately 65% of the worldwide population relies mainly on plant extracts for primary healthcare.[57,58] Since the discovery of penicillin in 1928, the microbial sources of natural products have been receiving a great deal of attention. The interest in marine natural products as a source of molecules for drug discovery only began in the 1970s, and the number of new marine natural products reported each year has been rising, from 332 in 1984 to 1378 in 2014. The marine environment is a rich source of new bioactive compounds, especially new anticancer agents; however, it is believed that "*the potential of the marine environment as a source of novel drugs remains virtually unexplored*".[58–60]

Despite the huge importance of natural products for drug discovery, a decline in the interest of the major pharmaceutical companies in the use of natural products in their drug discovery programs was observed in the last decades.[58,61–64] Pharmaceutical companies changed their focus from natural products to drug discovery approaches based on high-

throughput screening (HTS) directed at molecular targets and to combinational chemistry techniques. This decline of interest is justified in part by a higher regulation of the access to natural products; difficulties in obtaining appropriate amounts of natural products; an apparent incompatibility of natural products with HTS; difficulties related to the isolation, identification, or synthesis of natural products; and the expectation that combinational chemistry would provide large collections of new compounds.[62–65] Therefore, industries focused their efforts on the creation and use of synthetic chemical libraries.[63] However, these new approaches did not correspond to the initial expectations: combinational chemistry failed to increase the expected number of new leads, and the approval rates of new drugs declined (from 45 new drugs approved by the FDA in 1990 to 21 new drugs approved in 2010).[63,64] Moreover, natural products were also found to have a greater chemical diversity, degree of stereochemistry and steric complexity than compounds obtained from combinational chemistry and synthetic compounds. This diversity contributes to the biological utility of natural products, which translated into the higher hit rates obtained when using natural product collections.[62,63] In addition, recent technological advances have facilitated the screening of natural products in HTS assays.[62] Therefore, a renewed interest of major pharmaceutical companies in natural products has been observed.

Currently, natural products continue to play a crucial role in the field of drug discovery. It was found that 34% of all the new medicines that were approved between 1981 and 2010 were natural products or direct derivatives of natural products.[62,66]

1.2.1 Natural products as a source of anticancer drugs

Natural products have also played a crucial role in the discovery of new anticancer drugs. Among all the small molecules approved worldwide between 1981 and 2010 for cancer treatment, almost 70% were natural products or derived from natural products.[66]

Because the work presented in this thesis was developed using a plant-derived natural product, this section will focus on natural products obtained from plants. Plants have a long history of use in the treatment of cancer; more than 3000 plant species have been reported for their beneficial effects in the fight against cancer.[57,67–71] Additionally, some of the most important medicines available currently in the clinic for the treatment of cancer are derived from plant sources, including vinca alkaloids, taxanes, podophyllotoxins, and camptothecin.[68,69,72,73]

The first anticancer agents derived from plants that were approved for clinical use were the vinca alkaloids vinblastine **1.1** and vincristine **1.2**, which were originally isolated in the 1950s from the Madagascar periwinkle *Catarantus roseus.* Because of their potent cytotoxic activity, new semisynthetic analogs of vinca alkaloids were prepared and currently, four major vinca alkaloids are used in clinical settings: vinblastine **1.1**, vincristine **1.2**, vinorelbine **1.3**, and vindesine **1.4** (Fig. 1.7).[65,74–76] These compounds have been used mainly in combination therapies for the treatment of several types of cancer, including leukemias, non-small cell lung cancer, testicular and breast cancer, head and neck cancers, Kaposi sarcoma, and Hodgkin's and non-Hodgkin's lymphomas.[67,77] In 2009, a new synthetic vinca alkaloid, vinflunine, was approved by the European Medicines Agency (EMA) for clinical use in Europe.[73,74]

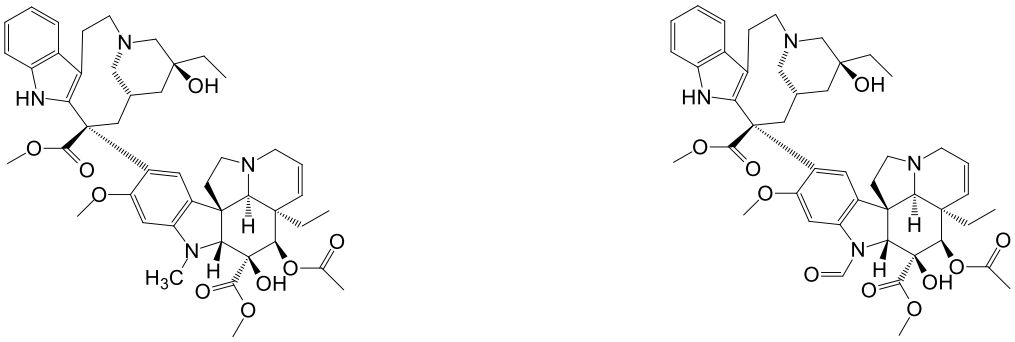

1.1 **1.2**

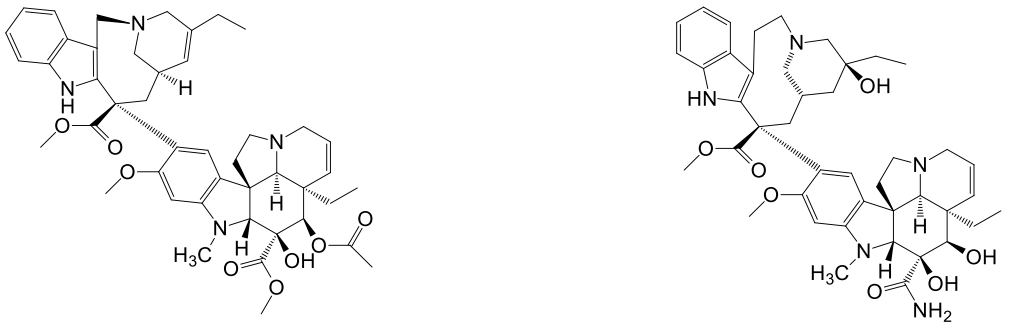

1.3 **1.4**

Figure 1.7 Chemical structures of vinca alkaloids: vinblastine **1.1**, vincristine **1.2**, vinorelbine **1.3**, and vindesine **1.4**.

The cytotoxic effect of vinca alkaloids is mediated mainly by perturbations in microtubule dynamics. These compounds interact with tubulin and block its polymerization

into microtubules, which results in the inhibition of mitotic split. Thus, the cell cycle is arrested at the mitotic phase and the division of cancer cells is prevented.[73,75,76,78]

The taxanes paclitaxel **1.5** (Taxol®) and docetaxel **1.6** (Taxotere®) (Fig. **1.8**) are among the most important drugs used in the treatment of cancer, thus enforcing the relevance of natural products in the development of effective anticancer agents. Paclitaxel **1.5** was discovered in 1962 as part of a National Cancer Institute Program. It was first isolated from the bark of the Pacific yew tree *Taxus brevifolia*, which was considered a finite source of the compound. Therefore, alternative sources were developed, and paclitaxel **1.5** was obtained through a semisynthetic process from the precursor 10-deacetylbaccatin, which was extracted from the needles of more abundant *Taxus* species, such as European yew *Taxus baccata.* [64,65,67,79,80]

Paclitaxel **1.5** was approved by the FDA in 1992 for the treatment of breast and ovary cancers and the AIDS-related Kaposi sarcoma. This compound has also been used in the treatment of non-small cell lung cancer (NSCLC). The huge success of paclitaxel **1.5** in cancer treatment led to the development of its semisynthetic analog docetaxel **1.6** (Fig. 1.8).[58] Docetaxel **1.6** was approved by the FDA for the treatment of breast, head, neck, prostate, and gastric carcinomas.[79] This compound has also been used in the treatment of NSCLC.[67] An albumin-bound formulation of paclitaxel **1.5** (nab-paclitaxel, Abraxane®) was approved by the FDA in 2005 for the treatment of breast metastasis, in 2012 for the treatment of NSCLC, and in 2013 for the treatment of late-stage pancreatic cancer.[58,79,81] In 2010, a novel taxane, cabazitaxel **1.7** (Jevtana®) (Fig. 1.8), was approved by the FDA for the treatment of metastatic hormone-refractory prostate cancer, in combination with prednisone.[58,73,82] Novel taxane derivatives are currently in clinical trials, including paclitaxel poliglumex (CT-2103; Xyotax), which is in a Phase III clinical trial for the treatment of NSCLC, and ortataxel (BAY-59-862), which showed promising activity in a phase II clinical trial of breast cancer patients who are resistant to paclitaxel or docetaxel combinations.[73]

Paclitaxel **1.5** and docetaxel **1.6** are microtubule inhibitors that are also known as mitotic poisons. Unlike the vinca alkaloids, which inhibit tubulin polymerization and prevent microtubule assembly, these taxanes bind to and stabilize tubulin, thus blocking microtubule depolymerization and cell division.The mechanisms via which cell death occurs after the stabilization of microtubules by taxanes are not fully understood.[73,80,83]

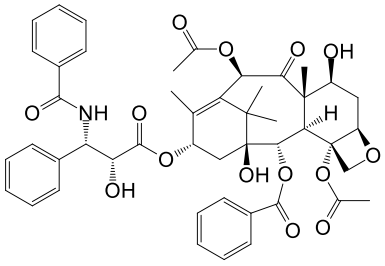

1.5

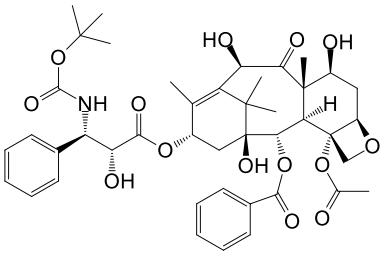

1.6

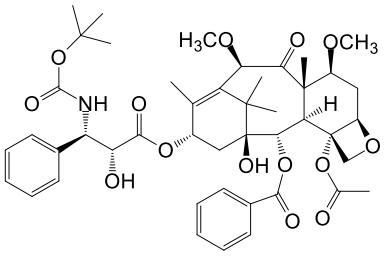

1.7

Figure 1.8 Chemical structures of the taxanes paclitaxel **1.5**, docetaxel **1.6**, and cabazitaxel **1.7**.

Other important clinically used anticancer agents derived from plants are the podophyllotoxin **1.8** derivatives etoposide **1.9** and teniposide **1.10** (Fig. 1.9). Podophyllotoxin **1.8** is a natural product that is extracted from *Podophyllum peltatum* and *Podophylum emodii* and exhibits anticancer activity. However, the severe side effects of this compound have limited its clinical use.[67,84,85] Posterior research led to the development of the semisynthetic derivatives etoposide **1.9** and teniposide **1.10**. These compounds have been used in the clinic for the treatment of several types of cancer, such as lymphomas, testicular and bronchial cancers, lung cancer, germ-cell malignancies, non-Hodgkin's lymphoma, Kaposi sarcoma, soft tissue sarcomas, and neuroblastoma.[67,86]

The anticancer effects of etoposide **1.9** and teniposide **1.10** are related with the inhibition of topoisomerase II (TOP2). These compounds induce the stabilization of TOP2–DNA complexes, thus resulting in DNA strand breaks and cell death by apoptosis.[84,86,87]

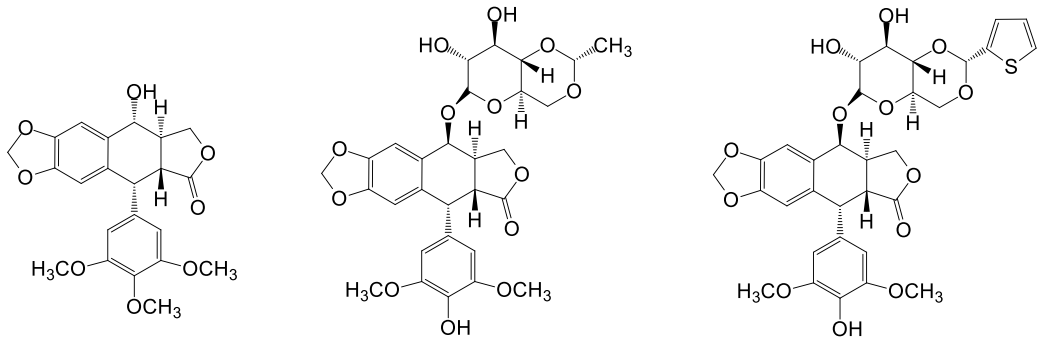

Figure 1.9 Chemical structures of podophyllotoxin **1.8**, etoposide **1.9**, and teniposide **1.10**.

Camptothecin **1.11** was isolated for the first time in 1966 from the bark of *Camptotheca acuminata* and its clinical use was tested in the 1970s; however, it exhibited low water solubility, low stability, and severe side effects. Further studies led to the development of water-soluble, safer, and more effective camptothecin derivatives: topotecan **1.12** and irinotecan **1.13** (Fig. 1.10).[67,88,89] Other derivatives of camptothecin **1.11**, such as diflomotecan, gimatecan, lurtotecan, and exatecan, are presently being tested in clinical trials.[90,91]

Topotecan **1.12** was approved by the FDA in 1996 for the treatment of ovary cancer and in 2007 for the treatment of NSCLC. In 2006, the FDA approved topotecan **1.12** in combination with cisplatin for the treatment of cervical cancer. Irinotecan **1.13** was approved by the FDA in 1994 for the treatment of colorectal cancers. In 2015, FDA approved the use of irinotecan **1.13** in combination with fluorouracil and leucovorin for the treatment of patients with advanced pancreatic cancer (whose were treated previously with gemcitabine-based chemotherapy).[67,91–93]

The potent anticancer effects of topotecan **1.12** and irinotecan **1.13** are attributed to their interaction with topoisomerase I (TOP1). These compounds specifically bind to and stabilize the covalent TOP1–DNA complexes, which blocks DNA religation, resulting in DNA impairment. It is expected that the replication fork will collide with stabilized TOP1–DNA complexes during the replication process, thus giving origin to double-strand breaks and, consequently, cell death by apoptosis.[88, 90,91,94]

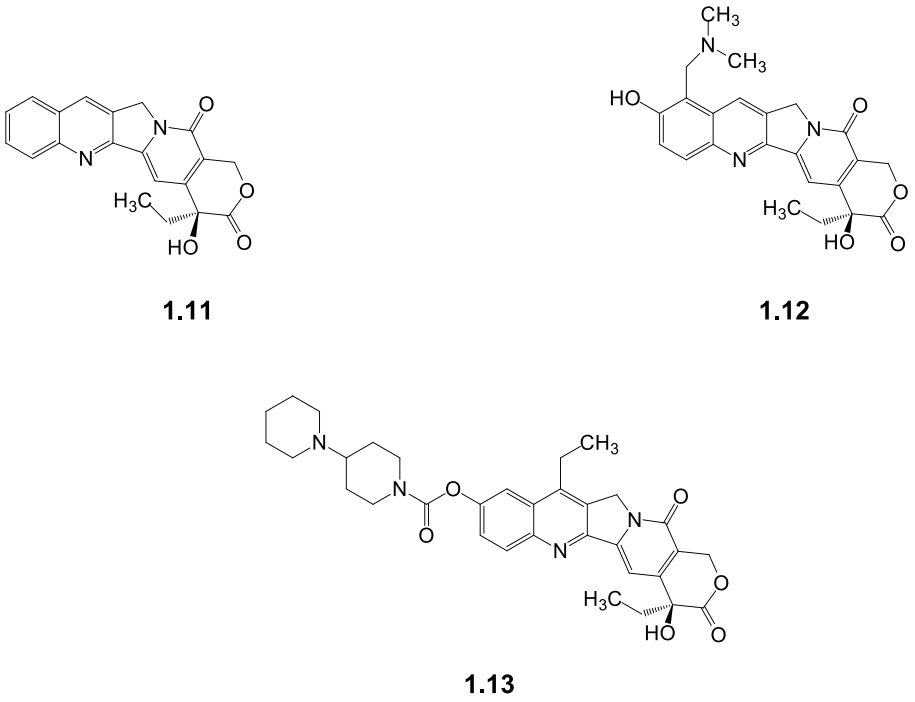

Figure 1.10 Chemical structures of camptothecin **1.11**, topotecan **1.12**, and irinotecan **1.13**.

Omacetaxine mepesuccinate **1.14** (Synribo®) (Fig. 1.11) is another plant-derived anticancer agent that was approved by the FDA in 2012 for the treatment of adult patients with chronic- or accelerated-phase chronic myeloid leukemia (CML) with resistance and/or intolerance to two or more tyrosine kinase inhibitors (TKIs).[73]

Several other chemotherapeutic agents derived from plants are currently in clinical trials, including the combretastatin A4 phosphate **1.15** (Fig. 1.11**)**, which is a tubulin-binding agent that targets and disrupts the existing tumor blood vessels. This compound is currently undergoing phase I and phase II clinical trials in combination with other chemotherapeutic agents against non-small-cell lung cancer (NSCLC), ovarian cancer, and anaplastic thyroid cancer. Combretastatin A4 phosphate appears to be safe and well tolerated in combination with other anticancer agents.[73,76,95–97] Another example is the flavopiridol **1.16** (Fig. 1.11), a synthetic flavone, which structure is based on the plant alkaloid rohitukine. This potent CDK inhibitor is currently being tested in several phase I and phase II clinical trials, either alone or in combinational therapies against different types of tumors, including leukemias, lymphomas, and solid tumors.[65,67,73]

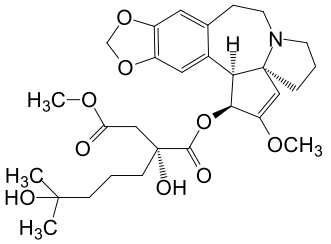

1.14

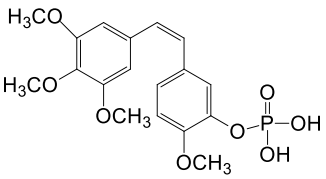

1.15

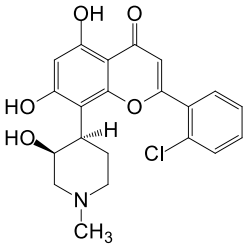

1.16

Figure 1.11 Chemical structures of omacetaxine mepesuccinate **1.14**, combrestatin A4 phosphate **1.15**, and flavopiridol **1.16**.

As described in this section, plants have been a rich source of anticancer agents and have made a huge contribution to the armamentarium against cancer. Currently, plants still play a significant role in the drug discovery of new anticancer agents. They can provide new leads that can be useful for the development of more effective anticancer drugs.

1.3 Terpenes

Terpenes are a group of secondary metabolites that are synthesized mainly by plants and represent the largest and most diverse class of natural products, with over 40 000 known compounds.[98] These compounds are widely distributed in the plant kingdom and take part in the human diet. All terpenes are built up from isoprene units, which is known as the "isoprene rule" described by Rutzica and Wallach. Based on the number of isoprene units, terpenes can be classified as hemiterpenes (C5), monoterpenes (C10), sesquiterpenes (C15), diterpenes (C20), triterpenes (C30), and tetraterpenes (C40).[99,100]

The chemical modification of terpenes by the addition of oxygen atoms or via the rearrangement of the carbon skeleton gives origin to compounds called terpenoids.[101] All terpenoids are synthesized through condensation of the universal five-carbon building blocks

isopentenyl diphosphate (IPP) (**1.17**) and its allylic isomer dimethylallyl diphosphate (DMAPP) (**1.18**) (Fig. 1.12).[98] IPP **1.17** and DMAPP **1.18** are synthesized in plants through two main pathways: the cytosolic mevalonic acid (MVA) pathway, which gives origin to IPP **1.17** from acetyl-CoA, and the plastidial 2-C-methylerythritol 4-phosphate (MEP) pathway, which produces IPP **1.17** and DMAPP **1.18** from pyruvate and glyceraldehyde-3-phosphate. The IPP **1.17** derived from the MVA pathway is converted to DMAPP **1.18** via the activity of an isopentenyl diphosphate isomerase (IPP isomerase). After their synthesis, the precursors IPP **1.17** and DMAPP **1.18** are condensed by the action of prenyltransferases into prenyl diphosphate intermediates, which are further converted into all terpenoids via the action of several terpene synthases/cyclases.[102]

1.3.1 Pentacyclic triterpenoids

The triterpenoids are a large group of structurally diverse natural products that consist of six isoprene units, with over 20 000 known members.[103–106] As shown in Figure 1.12, the starting molecule of the biosynthesis of triterpenes is DMAPP **1.18**, which is condensed with two IPP **1.17** units, to give pharnesyl diphosphate (FPP) **1.20**.[102] Subsequently, the enzyme squalene synthase catalyzes the condensation of two molecules of FPP **1.20**, to produce squalene **1.22**, which is oxidized into 2,3-oxidosqualene **1.23** via the action of squalene epoxidase. Triterpenoids are then synthesized through cyclization of 2,3-oxidosqualene **1.23**, by the action of enzymes known as oxidosqualene cyclases.[104,105] More than 100 types of triterpene scaffolds are known in nature. This remarkable structural diversity is related with the existence of several oxidosqualene cyclases and with the fact that each cyclase can produce different products.[101,104,105,107]

Triterpenoids can be classified according to the number of rings in their structure into acyclic (linear), monocyclic (one ring), bicyclic (two rings), tricyclic (three rings), tetracyclic (four rings), and pentacyclic (five rings). The two most-studied groups of triterpenoids are the tetracyclic triterpenoids and the pentacyclic triterpenoids (PTs). PTs can be classified according to their structural skeleton into three main types: oleanane, ursane, and lupane.[100,103]

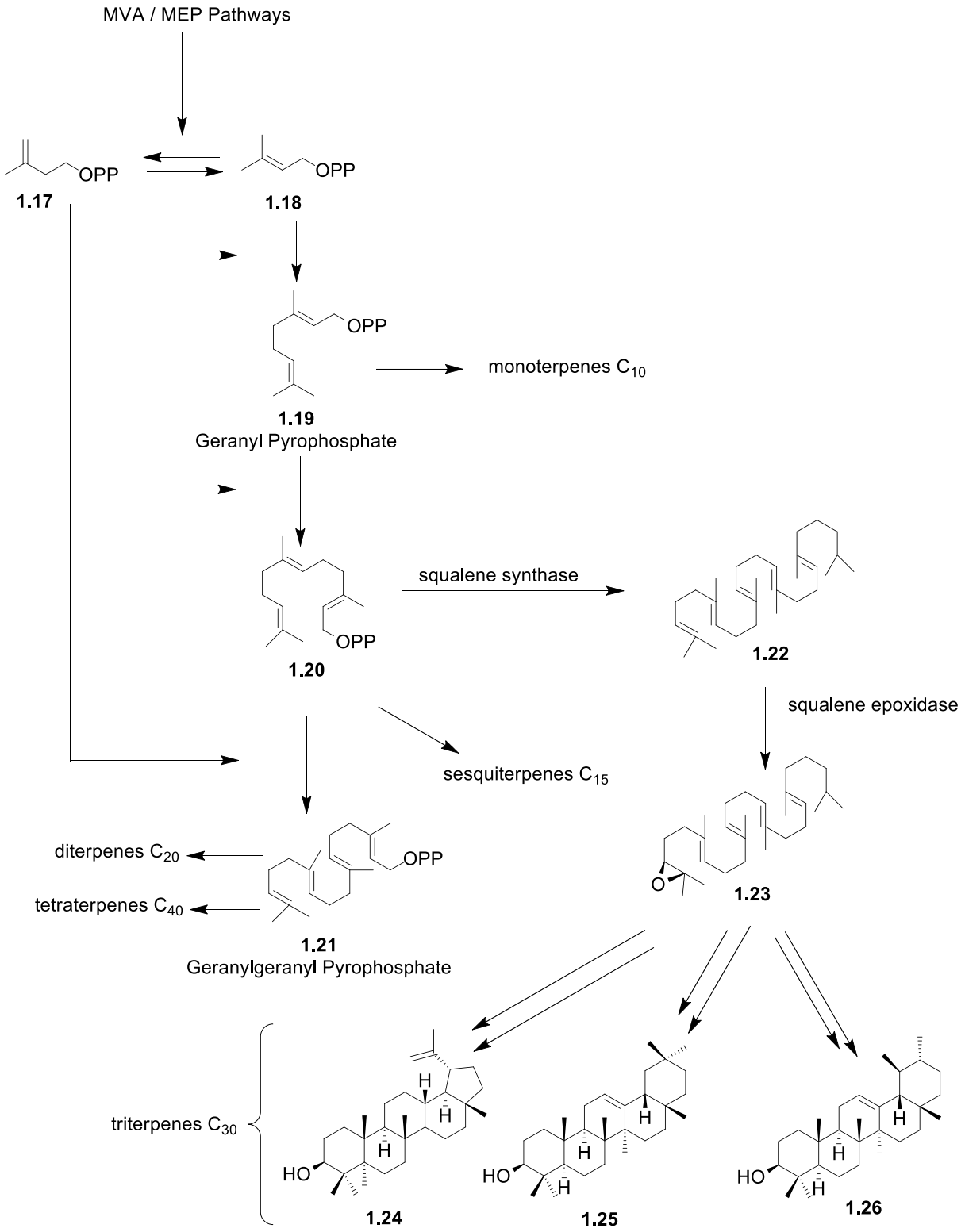

Figure 1.12 Schematic representation of the biosynthetic pathways of terpenoids.

Lupeol **1.24**, α-amyrin **1.25**, and β-amyrin **1.26** (the basic structures of lupane-, ursane-, and oleanane-type triterpenes, respectively) are obtained via the cyclization of 2,3-oxidosquelene **1.23** by the action of lupeol synthase, α-amyrin synthase, and β-amyrin synthase (oxidosqualene cyclases). Further modifications are then performed in these basic structures by tailoring enzymes, to obtain more functionalized PT scaffolds, such as betulinic acid (lupane type), oleanolic acid and glycyrrhetinic acid (oleanane type), and ursolic acid and asiatic acid (ursane type).[105,108,109]

PTs are widely distributed in nature, are an integral part of the human diet, and are present in several medicinal plants, especially in fruit peels, leaves, and stem backs. These compounds have attracted a great deal of attention because of their wide range of unique pharmacological activities such as antidiabetic, anti-inflammatory, antibacterial, antiviral, and anti-HIV, antihyperlipidemic, hepatoprotective, and cardioprotective functions, among others.[100,101,109] PTs have also been extensively studied regarding their promising anticancer activity.[22,101,103,110]

1.3.1.1 Pentacyclic triterpenoids as promising candidates for the development of new anticancer agents

Among all the biological activities of PTs, their anti-inflammatory and anticancer activities are the most studied.[111,112] Over the last two decades, the number of publications reporting the anticancer effects of PTs has risen exponentially, which reflects the potential interest of PTs for the development of new antineoplastic drugs.[112]

The most investigated PTs regarding their anticancer properties are lupane, oleanane, and ursane types and include, for example, ursolic acid, oleanolic acid, and betulinic acid. The extensive literature that exists in this field of research shows that the anticancer effects of PTs are mediated by several mechanisms, as they modulate a multiplicity of molecular targets and signaling pathways.[22,101,109,111–114] As PTs affect several molecular mechanisms, they exhibit various pharmacological effects that contribute to their anticancer potential (Fig. 1.13). For example, PTs exhibited the ability to suppress the proliferation of tumor cells and induce cell death by apoptosis in a large panel of cancer cell lines.[115,116] It is also important to note that some of these compounds present selectivity for cancer cells, none or reduced toxicity toward nontumor cells, and good safety profiles.[116,117] In addition, PTs and their semisynthetic derivatives possess organ-protective effects; they protect organs from chemotherapy-induced

toxicities by acting on several molecular targets.[113] PTs also revert the resistance of cancer cells to several anticancer agents by inhibiting the ATP-binding cassette (ABC) transporters[118] and sensitize cancer cells to the cytotoxic effect of anticancer drugs. Therefore, PTs and their semisynthetic derivatives could be used as multifunctional adjuvants in cancer chemotherapy.[113,118]

Several PTs, including betulinic, oleanolic, and ursolic acids, possess remarkable anti-inflammatory activities.[112,119,120] The association of prolonged inflammation with the development and progression of cancers has been reported for a long time. In the early stages of neoplastic progression, inflammatory cells work as tumor promoters by releasing growth and survival factors, promoting angiogenesis, contributing to the creation of tumor microenvironment, and stimulating DNA damage.[121,122] The mechanisms underlying the anti-inflammatory activity of PTs include, among others, the modulation of the expression of transcription factors, such as NF-κB and STAT3, the modulation of inflammatory enzymes, such as COX-2, 5-LOX, and MMP, and the downregulation of proinflammatory cytokines, such as TNF-α, IL-1β, and IL-6.[112,119] Therefore, because of their potent anti-inflammatory properties, PTs have the potential to prevent and treat cancer.

Pentacyclic triterpenoids and their semisynthetic derivatives also show antiangiogenic effects, both in *in vitro* and *in vivo* assays.[22,123,124] Based on the crucial importance of angiogenesis in tumor growth and dissemination, PTs can be useful agents in the prevention of tumor growth, invasion, and metastasis. Other biological effects of PTs that contribute to their promising anticancer potential include antioxidant effects, the promotion of the redifferentiation of tumor cells, and *in vivo* chemopreventive effects.[22,125]

Finally, it is also important to consider that the potential of PTs to design new drugs has been demonstrated by the clinical utility of compounds such as olenolic acid, glycyrrhetinic acid and asiaticoside. Additionally, some of the semisynthetic derivatives of PTs, including bevirimat, CDDO, CDDO-Me (CDDO methyl ester, bardoloxone methyl), and CDDO-Im (CDDO-imidazolide), have entered in clinical trials. The derivative bardoloxone methyl exhibited low toxicity and was well tolerated by the great majority of the patients in a phase III clinical trial, thus presenting a good safety profile.[103,111,126]

As described previously, cancer is a multifactorial disease that is characterized by a high level of complexity and involves multiple genes. The traditional treatments for cancer are based in surgery, chemotherapy, and radiotherapy, which exhibit a lack of effectiveness in the treatment of such a complex disease. Considering the complexity of cancer, modern therapeutic strategies focused on the development of new multifunctional drugs, rather than

monofunctional ones, represent a more rational approach for the prevention and treatment of the disease.[22,120] Therefore, PTs as multifunctional compounds that simultaneously inhibit various critical events in the initiation, promotion, progression, and dissemination of tumors (Fig. 1.13), are ideal candidates for the design of lead compounds aimin the development of new anticancer agents.[22,112,116,120] The fact that PTs are relatively safe, economic, and readily available in nature, strongly support this idea.

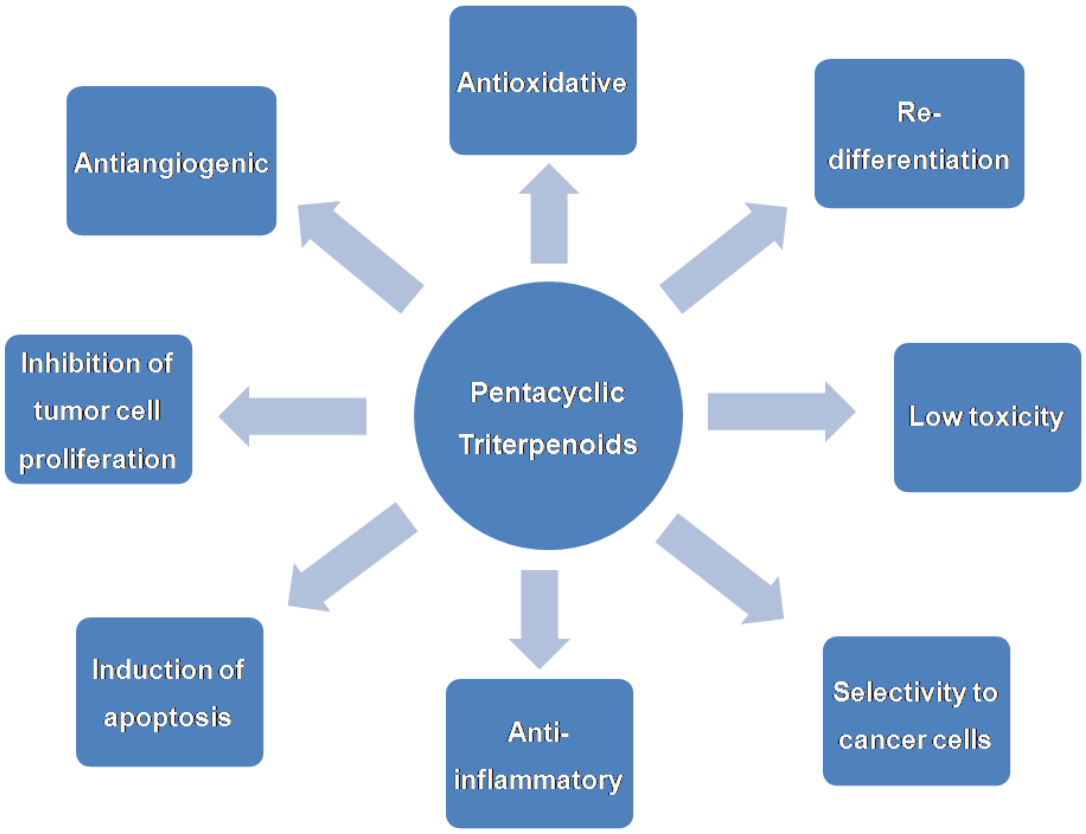

Figure 1.13 Pentacyclic triterpenoids exhibit multiple pharmacological effects that could be useful for the prevention and treatment of cancer.

1.4 Asiatic acid

Asiatic acid (2α,3β,23-trihydroxyurs-12-en-28-oic acid, **1.27**, Fig. 1.14) is a pentacyclic triterpenoid that is mainly extracted from the tropical medicinal plant *Centella asiatica* (L.) Urb. (family, Apiaceae Lindl.), also known as "Gotu Kola". The extracts of *Centella asiatica* have been widely used in traditional medicine as wound-healing, brain-tonic, memory-enhancing, antihypertensive, anti-inflammatory, antimicrobial, antiviral, and antifungal agents.[127–130] These extracts have also been used in the treatment of venous

diseases, chronic venous insufficiency, gastric ulcers, inflammatory diseases of the liver, and leprous lesions, among others.[128] The main constituents of the extracts of *C. asiatica* are four ursane-type pentacyclic triterpenoids: asiatic acid **1.27**, its analogue madecassic acid **1.28**, and the saponins asiaticoside **1.29** and madecassicoside **1.30** (Fig. 1.14).[127,131] These triterpenoids are believed to be responsible for the biological activities displayed by the *Centella asiatica* extracts.[130,131] According to the literature, asiatic acid **1.27** appears to be one of the most active constituents of these extracts.[132,133] Moreover, asiaticoside **1.29**, is presumably converted *in vivo* into its aglycone form asiatic acid **1.27**, which is responsible for the therapeutic effects. [132,134–137]

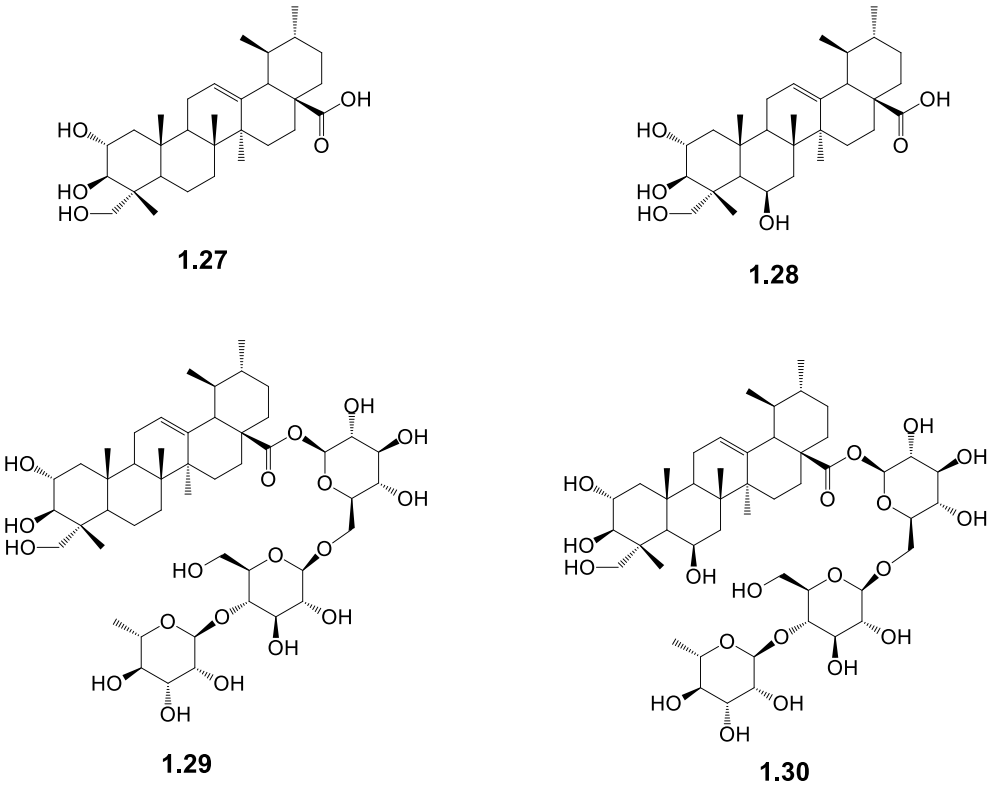

Figure 1.14 Chemical structures of asiatic acid **1.27**, madecassic acid **1.28**, asiaticoside **1.29**, and madecassoside **1.30**.

Asiatic acid **1.27** was isolated for the first time in 1941 by Bontems[138,139] and its chemical structure was elucidated by Polonsky and colleagues in the 1950s.[139–141] This triterpene has five functional groups: three hydroxyl groups at C2, C3, and C23, an olefin group at C12, and a carboxylic acid group at C28.

1.4.1 Pharmacological activities of asiatic acid

Asiatic acid **1.27** displays a wide range of pharmacological effects, including wound-healing, hepatoprotective, neuroprotective, antidiabetic, anti-inflammatory, and anticancer activities, among others.

1.4.1.1 Wound-healing activity

Wound healing is a dynamic process that is triggered by the body to repair a damaged tissue after injury. Asiatic acid **1.27** has long been used in the field of dermatology because of its wound-healing properties.[134] The extract of *Centella asiatica* is commercialized under the trade name Madecassol®, which has been successfully employed as a wound-healing product and for the prevention of scarring.[142] Asiatic acid **1.27** is considered the most therapeutically active ingredient of Madecassol® [132,134,143], which also contains madecassic acid **1.28** and asiaticoside **1.29**.[142] *In vitro* studies carried out with human foreskin fibroblast cultures revealed that the mechanism of action of the wound-healing process induced by asiatic acid **1.27** is related with the stimulation of collagen synthesis.[144,135] Moreover, some studies suggest that the sugar moiety in asiaticoside **1.29** is not required for the stimulation of the synthesis of collagen[135], and that its therapeutic activity is associated with its *in vivo* conversion to asiatic acid **1.27**.[134]

1.4.1.2 Hepatoprotective activity

Liver diseases are a significant health problem, with a high impact on the global burden of illness and mortality.[145] Asiatic acid **1.27** has been reported to have potent hepatoprotective effects against D-galactosamine (D-GaIN)[146,147], etanol[148], or high-fat diet-induced hepatotoxicity.[149] These results reveal the existence of different mechanisms for the hepatoprotection provided by asiatic acid **1.27**. This compound showed hepatoprotective effects against D-GaIN/lipopolysaccharide (LPS)-induced hepatotoxicity in mice via a mechanism that is apparently related with the upregulation of voltage-dependent anion channel (VDAC) levels and the inhibition of the process of mitochondrial permeability transition.[150] Using a co-culture system of D-GaIN/LPS-treated hepatocytes and kuppfer cells, Kufien Ma and coworkers showed that pretreatment with asiatic acid **1.27** protects against D-

GaIN/LPS-induced liver injury through the inhibition of redox-regulated leukotriene C_4 synthase (LTC_4S) expression.[151] Asiatic acid **1.27** inhibited CCl_4 and TGF-beta1-induced hepatic stellate cells (HSCs) activation and liver fibrosis *in vitro* and *in vivo* via the upregulation of hepatic Smad7.[152] Recently, Wenjie Guo et al. found that asiatic acid **1.27** alleviates Con A-induced T-cell-dependent liver injury in mice by triggering the apoptosis of activated T cells in a mitochondria-dependent manner.[153]

1.4.1.3 Neuroprotective activity

Historically, the extract of *Centella asiatica* has been used in Ayurvedic medicine as a brain tonic to stimulate learning and memory.[154] Several studies reported the neuroprotective and cognitive- and memory-enhancing effects of *Centella asiatica*. [155–157] Asiatic acid **1.27**, which is one of the main components of *Centella asiatica* extracts, has been reported to possess neuroprotective properties, both *in vivo* and *in vitro.* Furthermore, this compound was patented as a useful agent for the treatment of dementia and other cognitive disorders.[158,159]

In *in vitro* assays, asiatic acid **1.27** was found to protect B103 cells from Aβ-induced neurotoxicity.[160,161] This triterpenoid (at 0.01–100 nM) also protected SH-SY5Y neuronal cells against rotenone-, Oxygen peroxide (H_2O_2)-, or glutamate-induced cytotoxicity by decreasing voltage-dependent anion channel (VDAC) expression, reducing reactive oxidative stress, and preventing mitochondrial dysfunction.[162,163] Moreover, asiatic acid **1.27** (at 0.01–1.0 μM) exhibited neuroprotective effects against C2-ceramide-induced cell death in neuronal cells. This effect could be related with a decrease in oxidative stress and avoidance of mitochondrial dysfunction and may be regulated by the extracellular-signal-regulated kinase (ERK1/2) pathway.[164]

Regarding *in vivo* studies, Krishnamurthy et al. reported that asiatic acid **1.27** (at 75 mg/kg) significantly reduced infarct volume and improved neurological performances in a mouse model of permanent focal cerebral ischemia.[165] The mechanism underlying this effect could be related with the preservation of mitochondrial function and the inhibition of mitochondrial cytochrome *c* and AIF release from mitochondria.[165,166] The neuroprotective effect of asiatic acid **1.27** at 75 mg/kg was enhanced when combined with the tissue plasminogen activator (at 2.5 mg/kg) in a rat model of focal embolic stroke.[166] In other studies, asiatic acid **1.27** was found to attenuate cognitive deficits and to improve learning and memory in mice.[154,162,167,168] Asiatic acid **1.27** also exhibited neuroprotective effects against

Parkinson disease-like neurotoxicity in mice by attenuating 1-methyl-4-phenyl-1,2,3,6-tetrahydropyridine (MPTP)-induced apoptotic, oxidative, and inflammatory injury.[169]

Using a rat model of spinal cord injury, asiatic acid **1.27** was found to improve the recovery of neurological functions after spinal cord injury by suppressing inflammation and oxidative stress.[170]

1.4.1.4 Antidiabetic activity

Asiatic acid **1.27** has been reported to possess antidiabetic activities, which could be useful for the development of new treatments for both type 1 and 2 diabetes mellitus.[171,172] Diabetes mellitus type 2 is a disease that is characterized by high blood glucose levels as a result of defective insulin secretion and of insulin resistance. The main goal of the treatments for this disease is to maintain blood glucose homeostasis.[173] Glycogen phosphorylases (GPs) are enzymes that catalyze the release of glucose from its glycogen storage form (glycogenolysis), thus leading to an increase in the glucose levels in the blood.[174] Thus, the inhibition of GPs has been reported as a valuable therapeutic strategy for the treatment of type 2 diabetes.[175] Asiatic acid **1.27** has been reported to inhibit rabbit muscle GP with an IC_{50} value of 17 μM.[176,177] The analysis of the X-ray crystal structure of the GP–asiatic acid **1.27** complex showed that asiatic acid **1.27** binds to GP at the allosteric activator site, which leads to the stabilization of the inactive T-state quaternary conformation of the enzyme.[176]

In diabetes type 1, the high levels of glucose are related with insulin insufficiency caused by the loss or dysfunction of pancreatic beta cells. The administration of asiatic acid **1.27** to rats with streptozotocin (STZ)-induced diabetes was found to reduce the levels of plasma glucose and increase the levels of plasma insulin.[171,172,178,179] This glucose-lowering effect of asiatic acid **1.27** may be mediated by its ability to prevent the death and promote the proliferation of insulin-producing beta cells in islets, via a mechanism involving the activation of the pro-survival Akt kinase and the upregulation of Bcl-x_L.[171] The restoration of normal glucose levels by asiatic acid **1.27** could also be mediated by the stimulation of glucose uptake into skeletal muscle via the activation of the phosphatidylinositol 3-kinase (PI3K)-Akt signaling pathway.[179] Using the same *in vivo* model, asiatic acid **1.27** was found to modulate the key enzymes that are responsible for glucose metabolism, such as glucose-6-phosphatase, fructose-1,6-bis-phosphatase, glucose-6-phosphate dehydrogenase, pyruvate kinase, among others, thus restoring their normal activity and contributing to glucose homeostasis.[178] In

addition to its antidiabetic effects, asiatic acid **1.27** showed the ability to reduce hyperlipidemia (an associated complication in diabetes) in STZ-induced diabetic rats, thus preventing the development of vascular complications.[172]

1.4.1.5 Anti-inflammatory activity

The anti-inflammatory properties of asiatic acid **1.27**, both *in* vitro and *in vivo*, are well supported by a large number of studies. Fan et al. reported that TPA-induced ear edema was reduced by 54% after treatment with asiatic acid **1.27** at 0.3 mg/ear, a reduction that was similar to that obtained after treatment with the standard anti-inflammatory drug indomethacin (57%).[180] Asiatic acid **1.27** exhibited inhibitory activity against the production of pro-inflammatory molecules, such as NO and PEG-2, in LPS-stimulated RAW 264.7 macrophages.[181,182] Recently, Tsao and coworkers reported that 4 or 8 μM of asiatic acid **1.27** protected bronchial epithelial cells (16HBE and BEAS-2B cells) against hydrogen peroxide (H_2O_2)-induced apoptotic, oxidative, and inflammatory stress.[183] Moreover, asiatic acid **1.27** was found to reduce λ-carrageenan-induced paw edema in male ICR mice.[184]

The mechanisms underlying the anti-inflammatory effects of asiatic acid **1.27** have been studied and may involve the inhibition of inducible nitric oxide synthase (iNOS) and cyclooxigenase-2 (COX-2) expression levels, the downregulation of TNF-α, IL-1β, and IL-6, and IL-8 and nuclear factor κB (NF-κB) inactivation.[181,184,185]

1.4.1.6 Other activities

Asiatic acid **1.27** has been reported to have an antifibrotic effect in the kidneys of mice with unilateral ureteral obstruction. Mice that were treated orally with this compound showed a reduction in tubular injury, a decrease in the volume of extracellular matrix in the interstitium, and inhibition of myofibroblast activation and recruitment. The attenuation of tubule interstitial fibrosis by asiatic acid **1.27** was associated with the inhibition of the transforming growth factor (TGF)-β1/Smad signaling pathway, which plays central roles in the development of fibrotic diseases.[186,187,188] Asiatic acid **1.27** in combination with naringenin was found to produce an additive inhibitory effect on the TGF-β1/Smad pathway,

through the upregulation of the protective Smad 7 by asiatic acid **1.27** and the inhibition of the pathogenic Smad 3 by naringenin.[188]

The antibacterial activity of asiatic acid **1.27** has been reported against several bacteria. This triterpenoid had the ability to inhibit the growth of Gram-positive bacteria, such as *Streptococcus pneumoniae*, *Staphylococcus aureus* [minimum inhibitory concentration (MIC) = 28 μg/ml], *Listeria monocytogenes* (MIC = 36 μg/ml), *Enterococcus faecalis* (MIC = 20 μg/ml), and *Bacillus cereus* (MIC = 40 μg/ml); as well as of Gram-negative bacteria, such as *Helicobacter pylori*, *Escherichia coli* O157:H7 (MIC = 24 μg/ml), *Salmonella typhimurium* DT104 (MIC = 32 μg/ml), and *Pseudomonas aeruginosa* (MIC = 36 μg/ml).[189–191] The antibacterial effect of asiatic acid **1.27** may be mediated by the induction of damage in membrane integrity, changes in K^+ homeostasis, and promotion of nucleotide release.[189]

P. aeruginosa is a Gram-negative bacterium that is responsible for many hospital-related infections in immunodepressed patients.[192] In some cases, *P. aeruginosa* infections develop resistance to antibiotic therapy, at least in part because of the presence of a bacterial biofilm.[192,193] Asiatic acid **1.27** was found to increase the susceptibility of the *P. aeruginosa* biofilm to treatment with tobramycin.[193]

Asiatic acid **1.27** has been reported to attenuate the cardiac hypertrophy induced by TGF-β1, IL-1β, or angiotensin II *in vitro*, or that induced by pressure overload *in vivo*. The mechanisms underlying this effect are related with the downregulation of TGF-β1 and IL-1β, blockage of p38 and ERK1/2 phosphorylation, reduction of the NF-κB binding activity, and activation of the AMP-activated protein kinase α (AMPKα) signaling pathway.[194–196] The ability of asiatic acid **1.27** to inhibit the activation of the ERK1/2 and p38 MAPK pathways was found to be the mechanism underlying the inhibition of left ventricular remodeling and the increase of cardiac function in postinfarct rat hearts.[197] Asiatic acid **1.27** was also found to protect rat cardiomyoblast cells against high-glucose-induced oxidative, inflammatory, and apoptotic injury through a decrease in the production of inflammatory cytokines, inhibition of NF-*k*B and p38 MAPK activation, and downregulation of Bax and cleaved caspase-3.[198]

Asiatic acid **1.27** has also been reported to have antiosteoporotic effects. With age, the differentiation of bone marrow mesenchymal stromal cells (BMSCs) into osteoblasts decreases, while its differentiation into adipocytes increases, resulting in bone loss and the development of osteoporosis. The inhibition of the adipogenic differentiation of BMSCs by

suppressing the expression of the peroxisome proliferator-activated receptor γ (PPARγ) may be the mechanism underling this antiosteoporotic effect.[199]

The antihypertensive effects of asiatic acid **1.27** were evaluated in Nω-nitro-L-arginine methyl ester hydrochloride (L-NAME)-induced hypertensive rats. The blood pressure was reduced and vascular responses were restored after the administration of 10 or 20 mg/kg of asiatic acid **1.27**.[200,201] This antihypertensive effect was related with the decrease in the production of the superoxide anion ($O2^{-}$), the modulation of endothelial nitric oxide synthase (eNOS)/p^{47phox} expression, and consequent increase in NO metabolite (NOx) levels.[200] The ability of asiatic acid **1.27** to decrease hypertension and improve vascular function in an *in vivo* rat model of metabolic syndrome was associated with the decrease in the renin–angiotensin system and in sympathetic nerve activities and the restoration of eNOS protein expression.[202]

The microbicidal spermicide activity of asiatic acid **1.27** isolated from *Shorea robusta* resin was evaluated *in vivo*. Treatment of rat spermatozoa with asiatic acid **1.27** at 125 μg/mL resulted in 100% immobilization. The spermicidal activity of asiatic acid **1.27** was related with the loss of the integrity of the sperm membrane. This triterpene also showed microbicidal activity against bacteria (*Escherichia coli ATCC 25938* and Pseudomonas *aeruginosa* 71) and a fungus (*Candida tropicalis*), but did not affect the viability of the normal vaginal flora.[203]

Asiatic acid **1.27** showed useful effects in the prevention of malarial infection. This compound (at 10 mg/kg) suppressed the induction and progression of parasitemia when administered to Sprague–Dawley rats before they became infected with *Plasmodium berghe* and also inhibited the development of anemia associated with malaria. Moreover, animals that were pretreated with asiatic acid **1.27** exhibited an increase in food and water intake and in body weight compared with infected animals without pretreatment.[204]

Asiatic acid **1.27** was also reported to prevent UVA-induced photoaging. The mechanism underling this effect may be related with the ability of asiatic acid **1.27** to inhibit UVA-modulated signaling pathways. This compound decreased the expression of p53 and showed inhibitory effects on the activation and expression of metalloproteinase-2 (MMP-2), lipid peroxidation, and production of reactive oxygen species (ROS).[205]

1.4.1.7 Anticancer activity

The anticancer activity of asiatic acid **1.27** has been explored since the beginning of the current century[206] in both *in vitro* assays using cancer cell lines and *in vivo* assays using animal models. Asiatic acid **1.27** was found to suppress proliferation in several cancer cell lines, including liver, colon, breast, skin, prostate, lung, cervix, stomach, blood, brain, and ovary cell lines (Tables 1.1 and 1.2). The mechanisms underlying the anticancer effect of asiatic acid **1.27** have also been investigated in several studies, and various potential molecular targets have been identified (Table 1.3).

Asiatic acid **1.27** was found to inhibit the proliferation of human melanoma cells (SK-MEL-2) with an IC_{50} value of 40 μM (Table 1.1, entry 1).[207] Induction of apoptotic cell death was also observed after treatment of these cells with asiatic acid **1.27**. This effect was correlated with an increase in the reactive oxygen species, followed by upregulation of Bax and activation of caspase-3, and was p53 independent. Alterations in Ca^{2+} homeostasis apparently were not involved in the apoptosis mechanism.[207] The antitumor effect of asiatic acid **1.27** was also evaluated in an *in vivo* assay (mouse), in which topical application of compound (50 μM) inhibited TPA-induced skin tumor promotion by blocking the NO generation and decreasing the expression of iNOS and COX-2.[208]

The inhibitory effects of asiatic acid **1.27** on the proliferation of HepG2 human hepatoma cells have been reported.[206,209,210] Asiatic acid **1.27** induced apoptosis in HepG2 cells in a time- and concentration-dependent manner. This proapoptotic effect was mediated by an increase in the intracellular Ca^{2+} concentration, which led to the upregulation of p53 protein levels in the nucleus.[206] Additionally, Yapeng Lu and coworkers observed that asiatic acid **1.27** induced mitochondrial membrane potential dissipation, depletion of ATP levels, and release of cytochrome *c* from mitochondria to the cytosol. The induction of HepG2 cell death by asiatic acid **1.27** was found to be independent of caspases.[210]

NDR1/2 kinase is an enzyme that phosphorylates $p21^{cip1/\ waf1}$, thus promoting its degradation. Asiatic acid **1.27** at 10 μM was found to decrease NDR1/2 expression, leading to an increase in the levels of $p21^{cip1/\ waf1}$ and, consequently, to the inhibition of HepG2 cell proliferation.[209]

Table 1.1 Inhibitory effects of asiatic acid **1.27** on the proliferation of several human cancer cell lines.

Entry	Tumor type	Cell Line	IC_{50} [a] (μM)	Assay	Time (h)	Reference
1	**Skin**	SK-MEL-2	≈ 40	MTT	48	[207]
2	**Lung**	A549	18.8	CCK-8	72	[211]
3			> 100	CCK-8	48	[212]
4			> 60	CCK-8	48	[213]
5		NCI-H460	39.55	MTT	48	[214]
6	**Liver**	HepG2	4	CCK-8	72	[211]
7			>10	MTT	72	[215]
8			34.9	MTT	48	[214]
9			120	XTT	48	[216]
10			119.70	XTT	48	[217]
11		BEL-7404	40.78	MTT	48	[214]
12	**Stomach**	MGC-803	22.57	MTT	48	[214]
13		SGC-7901	36.8	CCK-8	72	[211,218]
14		BGC-823	>10	MTT	72	[215]
15		MK-1	40	MTT	-	[219]
16		HGC-27	61.23	CCK-8	72	[218]
17	**Colon**	HT-29	75.7	MTS	24	[220]
18		SW620	130	XTT	48	[216]

[a] IC_{50} is the concentration of compound that inhibits 50% of cell growth.

Asiatic acid **1.27** was also found to inhibit proliferation and to induce apoptosis in human colon cancer cells (HT-29 and SW480 cells, Table 1.1, entries 17 and 18).[220,221] In HT-29 cells, asiatic acid **1.27** induced apoptosis via the downregulation of the antiapoptotic Bcl-2 and Bcl-xL proteins and the activation of the effector caspase 3. Moreover, a synergistic effect between asiatic acid **1.27** and irinotecan hydrochloride was observed when HT-29 cells were treated with irinotecan hydrochloride prior to the treatment with asiatic acid **1.27**.[220] Asiatic acid **1.27** triggered the apoptosis of SW480 cells via the activation of the

mitochondrial pathway. Treatment with asiatic acid **1.27** induced mitochondrial membrane permeabilization and the release of cytochrome *c* into the cytosol. Once in the cytosol, cytochrome *c* induced the activation of caspase 9, which in turn led to the activation of caspase 3, resulting in the activation of PARP and apoptotic cell death.[221]

Table 1.2 Inhibitory effects of asiatic acid **1.27** on the proliferation of several human cancer cell lines.

Entry	Tumor type	Cell Line	IC_{50} [a] (μM)	Assay	Time (h)	Reference
1	**Breast**	MCF-7	32.8	CCK-8	72	[211]
2			5.95	XTT	48	[222]
3			67.58	CCK-8	48	[212]
4			57.9	MTT	-	[223]
5		MDA-MB-231	8.12	XTT	48	[222]
6	**Cervix**	HeLa	55.1	CCK-8	72	[211]
7			91.07	CCK-8	48	[212]
8			37.26	MTT	48	[214]
9			>10	MTT	72	[215]
10			38.9	MTT	-	[223]
11			34	MTT	-	[219]
12			80.4	MTS	72	[224]
13	**Ovary**	SKOV3	81.85	MTT	72	[225]
14		OVCAR3	81.85	MTT	72	[225]
15	**Prostate**	PCC-1	42	MTS	24	[226]
16		PC-3	53.6	CCK-8	72	[211]
17	**Blood**	RPMI 8226	24.88	MTT	48	[227]
18	**Brain**	U-87 MG	38.8-61.0	MTT	72	[228]

[a] IC_{50} is the concentration of compound that inhibits 50% of cell growth.

An antiproliferative effect of asiatic acid **1.27** has been observed toward the human breast cancer cells MCF-7 and MDA-MB-231 (Table 1.2, entries 1–6).[211,212,222,223] Asiatic

acid **1.27** (at 10 μM) was found to induce cell-cycle arrest at the S–G2/M phase and apoptosis in both cell lines. The cell-cycle arrest was mediated by a decrease in the expression of cell-cycle-related proteins cyclin B1, cyclin A, cdc2, and cdc25c and an increase in the expression of $p21^{cip1/waf1}$, independent of p53. Asiatic acid **1.27** induced apoptosis through the activation of the mitochondrial pathway, with upregulation of Bax and downregulation of Bcl-2 and Bcl-x_L, followed by the release of cytochrome *c* and the activation of caspase 9. The cell-cycle arrest and apoptotic cell death induced by asiatic acid **1.27** were apparently mediated by the activation of the ERK1/2 and p38 MAPK pathways.[222]

Asiatic acid **1.27** exhibited growth-suppressive effects against the SKOV3 and OVCAR3 ovary cancer cells (Table 1.2, entries 13 and 14).[225] This compound induced cell-cycle arrest at the G0/G1 phase by decreasing the expression of cyclin D1, cyclin E, CDK2, CDK4, and CDK6 and increasing the expression of $p21^{cip1/waf1}$ and $p27^{kip1}$. Moreover, SKOV3 and OVCAR3 cells treated with asiatic acid **1.27** underwent apoptosis via a mechanism involving the alteration of the Bax/Bcl-2 ratio, the activation of caspases 9 and 3 and the cleavage of PARP.[225] The anticancer effects of asiatic acid **1.27** on SKOV3 and OVCAR3 cells were related with the inactivation of the PI3K/Akt/mammalian target of rapamycin (mTOR) pathway[225], which is believed to be critical for the development of ovarian cancers.[229]

Antiproliferative and proapoptotic effects of asiatic acid **1.27** have been reported on human prostate cancer cells (PPC-1) (Table 1.2, entry 15).[226] Treatment of PPC-1 cells with asiatic acid **1.27** at 100 μM for 7.5 h led to the disruption of the endoplasmic reticulum, with subsequent release of Ca^{2+} into the cytoplasm. Once in the cytoplasm, Ca^{2+}induced the loss of mitochondrial potential and the activation of caspases 2, 3, and 8. These results revealed that asiatic acid **1.27** induced apoptosis via a caspase-dependent mechanism.[226] However, cell death through a caspase-independent mechanism was also observed when PPC-1 cells were treated with asiatic acid **1.27** for 24 h.[226]

The proliferation of multiple myeloma RPMI 8226 cells was inhibited by asiatic acid **1.27** in a time- and dose-dependent manner, with an IC_{50} value of 24.88 μM (Table 1.2, entry 17). Cell-cycle arrest at the G2/M phase and decreased expression levels of focal adhesion kinase (FAK) and p-FAK were observed after treatment of RPMI 8226 cells with asiatic acid **1.27**.[227] FAK is a tyrosine kinase that plays critical roles in angiogenesis and cancer

progression.[230] Thus, the antiproliferative effect of asiatic acid **1.27** against RPMI 8226 cells may be mediated by cell-cycle arrest at the G2/M phase and inhibition of the FAK signaling pathway.[227]

Malignant gliomas are one of the most deadliest types of cancers. This type of cancer has very poor prognosis, mainly because of sustained and excessive angiogenesis by glioma cells.[231] Asiatic acid **1.27** has been found to possess strong antiangiogenic effects, both *in vitro* and *in vivo*. This compound (at 20 μM) prevented the proliferation, invasion, and migration of human umbilical vein endothelial cells (HUVEC) and human brain microvascular endothelial cells (HBMEC). Moreover, asiatic acid **1.27** decreased the secretion of the vascular endothelial growth factor (VEGF) by glioblastoma cells (LN18 and U-18 MG), which resulted in the inhibition of the VEGF-induced tube formation and invasiveness of endothelial cells toward glioma cells.[231] Using the Matrigel plug assay, asiatic acid **1.27** was also shown to inhibit VEGF-stimulated angiogenesis *in vivo.*[231]

Asiatic acid **1.27** was found to induce the death of human glioblastoma cells (U-87 MG, LN-18, and U-118 MG cells)[232,233] with greater efficacy than did temozolomide, which is a drug that is used in the clinic for the treatment of glioblastoma.[233] Glioblastoma cells treated with asiatic acid **1.27** underwent apoptosis through a mechanism related with the induction of endoplasmic reticulum stress, increase of intracellular Ca^{2+} levels, decrease of mitochondrial membrane potential, activation of caspases 9, 8, and 3, downregulation of Bid and Bcl-2, and upregulation of Bad.[232,233] Asiatic acid **1.27** also decreased the expression of *survivin* in LN-18 and U-118 MG cells.[233] In U-87 MG cells, asiatic acid **1.27** not only induced apoptosis, but also necrosis, apparently with prevalence of the latter. The increase in the intracellular Ca^{2+} levels observed after treatment with asiatic acid **1.27** may be involved in the process of necrotic cell death.[232]

Asiatic acid **1.27**-loaded solid lipid nanoparticles (SLNs) were successfully prepared to deliver asiatic acid **1.27** with higher efficiency across the blood–brain barrier (BBB) to cancer tissues. It was found that U-87 MG cells preferentially internalized the asiatic acid **1.27**-loaded SLNs compared with SVG P12 human fetal glial nontumor cells, which was reflected in the higher toxicity of asiatic acid **1.27**-loaded SLNs towards cancer U-87 MG cells vs SVG P12 cells. Both apoptotic and necrotic types of cell death were induced by asiatic acid **1.27**-loaded SLNs in U-87 MG cells.[228]

The antiproliferative effects of asiatic acid **1.27** against glioblastoma were also evaluated using an *in* vivo assay. The oral administration of asiatic acid **1.27** (30 mg/kg/day)

decreased the growth of ectopic U-87 MG xenografts in nude mice. In mouse brains that had undergone implantation of U-87 MG cells, asiatic acid **1.27** administered orally also reduced the volume of U-87 MG xenografts by 60% compared with nontreated mice, suggesting that asiatic acid **1.27** has the ability to cross the BBB. No toxicity was observed after the oral administration of this compound.[233]

As summarized in this section and in Table 1.3, asiatic acid **1.27** induces cell-cycle arrest and apoptosis in several cell lines from different types of cancer. However, the effect of asiatic acid **1.27** on the cell cycle varies according to type of cancer; for example, in OVCAR3 and SKOV3 cells (Table 1.3, entries 7 and 8), asiatic acid **1.27** induced cell-cycle arrest at the G0/G1 phase, whereas in RPMI 8226 cells (Table 1.3, entry 13), it induced cell-cycle arrest at the G2/M phase. The molecular targets of asiatic acid **1.27** also are different according to type of cancer, suggesting that several molecular mechanisms mediate the anticancer effect of asiatic acid **1.27**. Nevertheless, it is important to note that some molecular targets are common among cell lines from different types of cancer. Asiatic acid **1.27** is a multifunctional compound and affects multiple signaling pathways to inhibit the proliferation of, and induce apoptosis in, cancer cells. Because of these anticancer properties, asiatic acid **1.27** is a valuable compound that could be used as a starting point for the development of effective drugs for prevention and treatment of cancer.

Table 1.3 Molecular targets and effects of asiatic acid **1.27**.

Entry	Tumor type	Cell Line	Proliferation	Cell cycle	Apoptosis	Molecular targets/Mechanism of action	Ref.
1	**Skin**	SK-MEL-2	✓	-	✓	↑ Intracellular ROS ↑Bax ↑ Caspase 3	207
2	**Liver**	HepG2	✓	-	✓	↑intracellular Ca^{2+} ↑ p53 ↑ $p21^{waf1/cip1}$	206,209
3	**Colon**	SW480	✓	-	✓	↓Bcl-2, Bcl-x_L Cytochrome *c* release	221
4		HT-29	✓	-	✓	↑ Caspases 3 and 9 Cleavage of PARP	220
5	**Breast**	MCF-7	✓	Arrest at S-G2/M	✓	↓CyclinB1, CyclinA ↓Cdc2, Cdc25 ↑$p21^{cip1/waf1}$ ↑ERK1/2, p38 MAPK	222
6		MDA-MB-231	✓	Arrest at S-G2/M	✓		
7	**Ovary**	SKOV3	✓	Arrest at G0/G1 phase	✓	↓PI3K/Akt/mTOR ↓ Cyclin D1, Cyclin E, CDK2, CDK4 and CDK6 ↑ $p21^{cip1/waf1}$, $p27^{kip1}$ ↑Caspases 9 and 3 Cleavage of PARP ↑Bax ↓Bcl-2	225
8		OVCAR3	✓	Arrest at G0/G1 phase	✓		
9	**Prostate**	PPC-1	-	-	✓	↑ Caspases 2, 3 and 8 ↑Intracellular Ca^{2+}	226
10	**Brain**	U-87 MG	✓	-	✓	↑ ER stress ↑ Intracellular Ca^{2+} ↓Mito. Memb. Potential ↓ Bid, Bcl-2 ↑Bax ↑Caspase 9, 8 and 3 ↓ survivin ↓ VEGF	231, 232, 233
11		LN18	✓				
12		U-118 MG	✓				
13	**Blood**	RPMI 8226	✓	Arrest at G2/M	-	↓ FAK ↓ pFAK	227

1.4.2 Semisynthetic derivatives of asiatic acid with anticancer activity

Small modifications in the backbone of triterpene compounds may have a significant impact on their biological activities. In light of this observation, several semisynthetic derivatives of asiatic acid **1.27** have been prepared by different research groups, to obtain novel compounds with improved anticancer properties compared with the parental compound. Modifications in the three hydroxyl groups located at positions 2, 3, and 23, in the position 11, and in the carboxylic acid located at position 28 of asiatic acid **1.27** are the most commonly reported.

Jew et al. prepared a panel of asiatic acid **1.27** derivatives containing a modified A-ring **1.31**–**1.39** (Fig. 1.15).[139] These new compounds were tested for their antiproliferative activities against lymphoid neoplasm (P388D1) and melanoma (Malme-3M) cancer cell lines and against a nontumor cell line (Detroit 551), to evaluate selectivity (Table 1.4).[139]

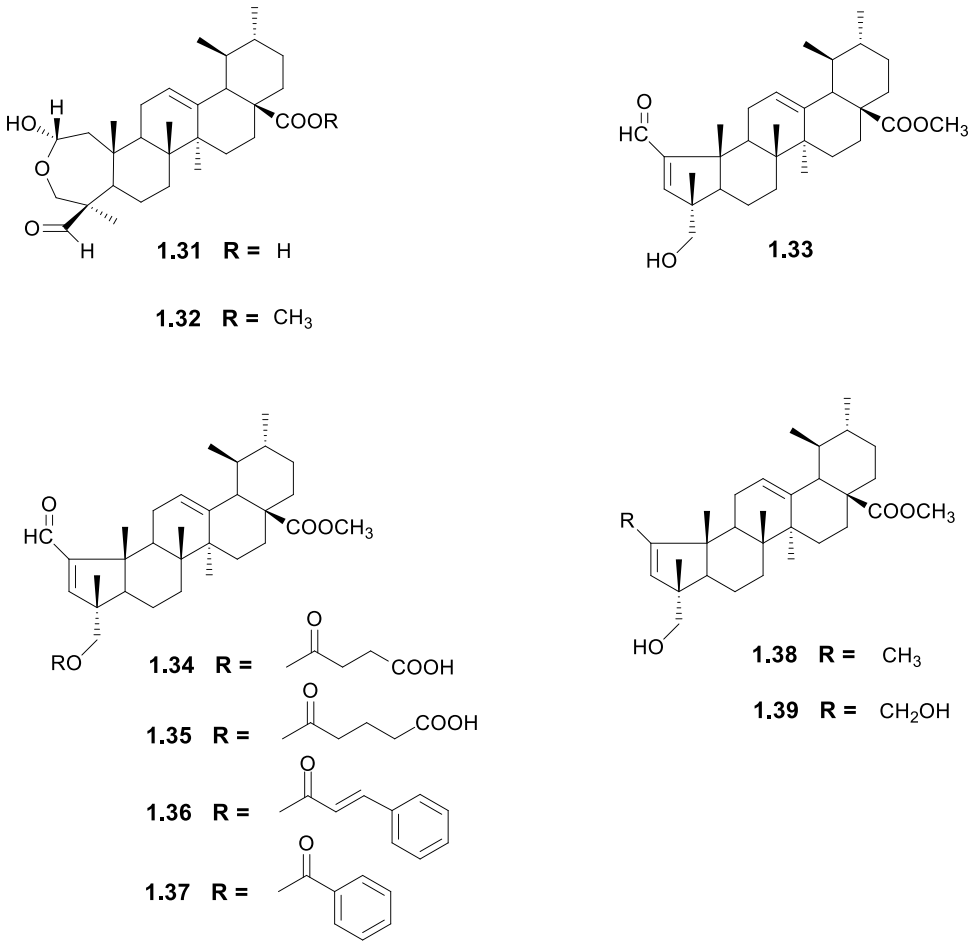

Figure 1.15 Asiatic acid derivatives **1.31**–**1.39**.

Compound **1.32** (Table 1.4, entry 2), with a lactol A-ring, showed antiproliferative activity against P388D1 and Malme-3M cells, with IC_{50} values of 8.6 and 18 μM, respectively, while it displayed a lower toxicity against the nontumor cell line Detroit 551 (about 6 and 3 times less toxic).[139]

Table 1.4 Cytotoxic activity, expressed as IC_{50} values, of derivatives **1.31**–**1.39** against the P388D1 and Malme-3M human cancer cell lines and a nontumor cell line (Detroit 551).[a] [139]

Entry	Compound	Cell line/ IC_{50} (μM) [b]		
		P388D1	**Malme-3M**	**Detroit 551**
1	**1.31**	14	-.	-
2	**1.32**	8.6	18	55.5
3	**1.33**	5	6	9.7
4	**1.34**	0.9	-	-
5	**1.35**	6.5	-	-
6	**1.36**	63	-	-
7	**1.37**	58.1	-	-
8	**1.38**	9.2	-	-
9	**1.39**	46.8	-	-

[a] Cells were treated with increasing concentrations of each compound for 24 h. Cell viability was determined using MTT.

[b] IC_{50} is the concentration of compound that inhibits 50% of cell growth.

The derivative **1.33** (Table 1.4, entry 3), bearing a vinyl aldehyde in a pentameric A-ring, showed significant antiproliferative activity against the P388D1 and Malme-3M cancer cell lines, with IC_{50} values of 5 and 6 μM, respectively. Compound **1.34** (Table 1.4, entry 4), bearing a succinic ester moiety at C23, was the most active compound of this panel of derivatives (**1.31**–**1.39**), displaying an IC_{50} value of 0.9 μM in PD388D1 cells.[139]

Compound **1.39** (Table 1.4, entry 9), with a hydroxymethyl at C2, was less active than compound **1.38** (Table 1.4, entry 8), with a methyl group at C2, and significantly less active than compound **1.33** (Table 1.4, entry 3), with an aldehyde group at C2.

A panel of C28-substituted asiatic acid **1.27** derivatives, **1.40**–**1.51**, was prepared (Fig. 1.16) and their cytotoxic activities were evaluated against human cervical (HeLa), hepatic (HepG2), gastric (BGC823), and ovary (SKOV3) cancer cell lines (Table 1.5).[215]

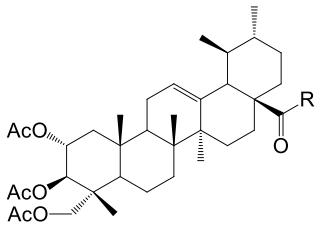

1.40 **R =** $O(C_6H_4)C(CH_3)_3$

1.41 **R =** $NHCH_2CH_2OH$

1.42 **R =** $NH(CH_2)_3OH$

1.43 **R =** $N(C_2H_5)_2$

1.44 **R =** $NHCH_2C_6H_5$

1.45 **R =** $NHC_6H_4(p\text{-}CH_3)$

1.46 **R =** $NHC_6H_3(o\text{-}F)(p\text{-}Cl)$

1.47 **R =** $NHC_6H_3(o\text{-}Cl)(p\text{-}Cl)$

1.48 **R =** $NHNHC_6H_5$

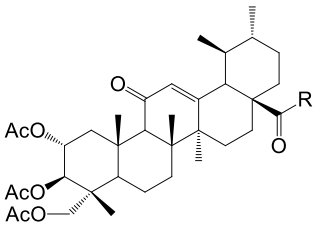

1.49 **R =** $N(C_2H_5)_2$

1.50 **R =** 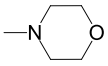

1.51 **R =** OCH_2CH_2OH

Figure 1.16 Asiatic acid derivatives **1.40–1.51**.

The ester derivative **1.40** (Table 1.5, entry 2) and asiatic acid **1.27** exhibited a similar cytotoxic activity against the HeLa and BGC823 cell lines, whereas the derivatives **1.41** and **1.42** (Table 1.5, entries 3 and 4), bearing amide moieties at C28, displayed a more potent antiproliferative activity compared with asiatic acid **1.27** against HeLa and BGC823 cells. The diethyl amide derivative **1.43** (Table 1.5, entry 5) was found to be the most active compound of this panel, with IC_{50} values of 0.65, 0.12, and 3.94 μM against HeLa, BGC823, and SKOV3 cells, respectively. The derivatives **1.44**–**1.46**, **1.48**, and **1.49** also displayed better antitumor activity than did asiatic acid **1.27** against HeLa, HepG2, and BGC823 cells. The introduction of an amide substituent at C28 increased antitumor activity.[215] The nature of the amide substituent also affected antitumor activity. The authors concluded that the introduction of a carbonyl group at C11 apparently was not essential for the cytotoxic activity of the compound.[215]

Table 1.5 Cytotoxic activities, expressed as IC_{50}, of derivatives **1.40**–**1.51** against the HeLa, HepG2, BGC823, and SKOV3 human cancer cell lines.[a] [215]

Entry	Compound	Cell line/ IC_{50} (μM) [b]			
		HeLa	**HepG2**	**BGC823**	**SKOV3**
1	Asiatic acid **1.27**	> 10	> 10	> 10	-
2	**1.40**	> 10	-	> 10	> 10
3	**1.41**	2.56	-	4.44	10.33
4	**1.42**	1.52	-	2.65	7.39
5	**1.43**	0.65	-	0.12	3.94
6	**1.44**	1.77	2.88	1.45	-
7	**1.45**	2.28	4.66	2.39	-
8	**1.46**	5.45	7.86	8.13	-
9	**1.47**	16.66	17.86	11.8	-
10	**1.48**	1.14	4.79	1.51	-
11	**1.49**	3.32	5.94	4.54	-
12	**1.50**	26.62	> 10	> 10	-
13	**1.51**	4.78	6.84	8.75	-

[a] Cells were treated with increasing concentrations of each compound for 48 h. Cell viability was determined using an MTT assay.

[b] IC_{50} is the concentration of compound that inhibits 50% of cell growth.

Derivatives **1.52**–**1.58** (Fig. 1.17), bearing a dihydroxyl group at C3 and C23 protected with acetonide and substituted at C2, were prepared and their antiproliferative activities were evaluated against several cancer cell lines.[212,213] An improvement in antiproliferative activity was observed for the acetonide derivative **1.52** (Table 1.6, entry 2) compared with asiatic acid **1.27** (Table 1.6, entry 1) against the tested cell lines. The conversion of the C28 carboxylic group to methyl ester in compound **1.53** (Table 1.6, entry 3) reduced the biological activity.[212,213]

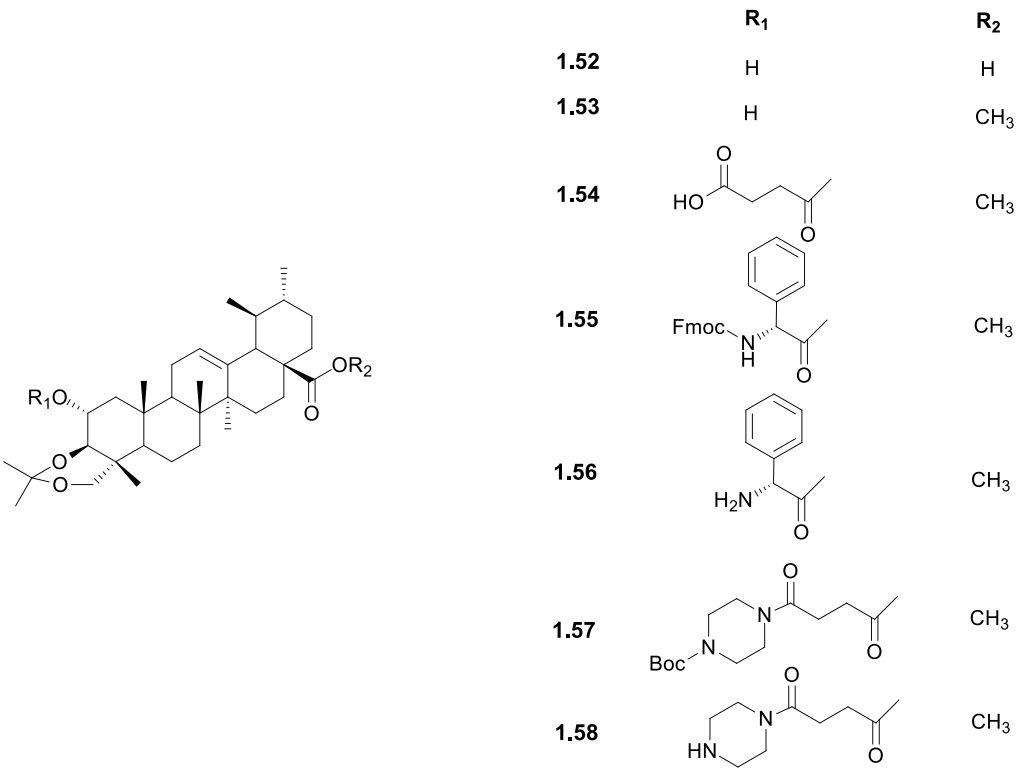

Figure 1.17 Chemical structures of asiatic acid derivatives **1.52**–**1.58**.

The derivative **1.54** (Table 1.6, entry 4), containing a succinic ester at C2, was significantly more active than was asiatic acid **1.27** against the non-small cell lung cancer cell lines A549 and PC9/G, displaying IC_{50} values of 26.03 and 25.57 μM, respectively. Derivative **1.55** (Table 1.6, entry 5) showed no activity against A549 or PC9/G cells, while compound **1.56** (Table 1.6, entry 6) was particularly active against PC9/G cells, displaying an IC_{50} value of 21.66 μM.[213]

Additional studies that were performed to clarify the mechanism underlying the antitumor effect of compound **1.55** against A549 and PC9/G cells revealed that the growth-inhibitory activity of this compound may be related to the downregulation of the Ras/Raf/MEK/ERK pathway and the arrest of the cell cycle at the G1/S and G2/M phases.[213]

Table 1.6 Cytotoxic activity, expressed as IC_{50}, of derivatives **1.52**–**1.58** against the A549, PC9/G, MCF-7, and HeLa human cancer cell lines.[a] [212,213]

Entry	Compound	Cell line/ IC_{50} (μM)[b]			
		A549	**PC9/G**	**MCF-7**	**HeLa**
1	Asiatic acid **1.27**	> 60	> 60	67.58	91.07
2	**1.52**	34.73	52.45	59.85	60.04
3	**1.53**	48.86	47.61	>100	>100
4	**1.54**	26.03	25.57	45.55	55.63
5	**1.55**	> 60	> 60	-	-
6	**1.56**	40.21	21.66	-	-
7	**1.57**	33.61	-	21.12	23.75
8	**1.58**	13.13	-	7.58	8.13

[a] Cells were treated with increasing concentrations of each compound for 48 h. Cell viability was determined using the Cell Counting Kit-8 (CCK-8).

[b] IC_{50} is the concentration of compound that inhibits 50% of cell growth.

Compounds **1.57** and **1.58** (Table 1.6, entries 7 and 8) showed increased growth-inhibitory activity against A549, MCF-7, and HeLa cells compared with asiatic acid **1.27**. The piperazine derivative **1.58** was the most active compound against these cell lines, with IC_{50} values of 13.13, 7.58, and 8.13 μM, respectively. The treatment of A549, MCF-7, and HeLa cells with **1.58** resulted in cell-cycle arrest, which may be related with the upregulation of $p16^{Ink4a}$ and $p21^{cip1/waf1}$ and the downregulation of cyclin D1, cyclin B, and CDK1.[212]

A panel of aniline derivatives of asiatic acid **1.27** was synthesized (Fig. 1.18) and tested against human gastric (MGC-803), lung (NCI-H460), liver (HepG2 and 7404), and cervix (HeLa) cancer cell lines. The growth-inhibitory activities of asiatic acid **1.27** derivatives were also evaluated against a nontumor cell line (HUVEC), to assess selectivity (Table 1.7).[214]

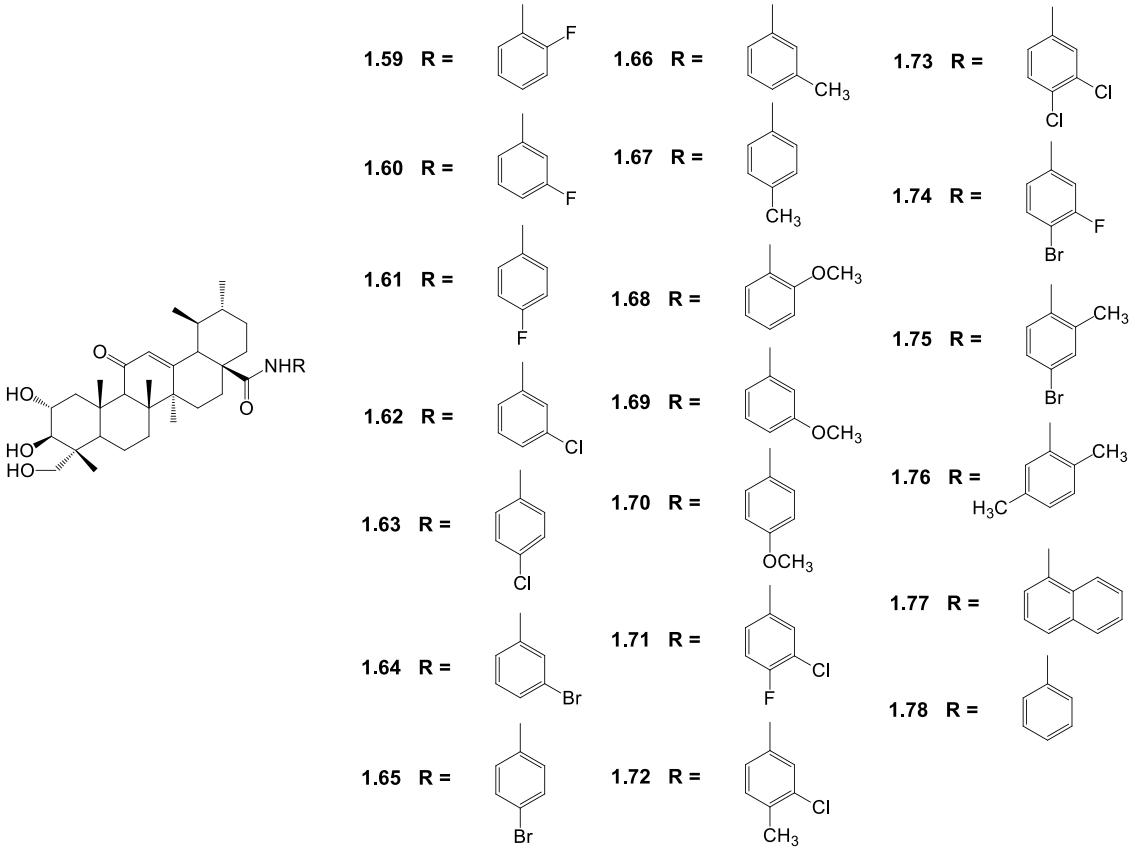

Figure 1.18 Chemical structures of aniline asiatic acid derivatives **1.59**–**1.78**.

The majority of the synthesized derivatives (**1.59–1.78**) displayed higher growth inhibitory activities against the tested cancer cell lines than did the parental compound asiatic acid **1.27** (Table 1.7**)**. Compounds **1.60** and **1.69** (Table 1.7, entries 3 and 12) were the most active compounds against the HepG2 cell line, displaying IC_{50} values of 5.97 and 8.89 μM, respectively.[214]

No obvious differences in antiproliferative activities were observed between the derivatives with a monosubstituted acyl phenyl ring (**1.59–1.70)** and the derivatives with a disubstituted acyl phenyl ring (**1.71–1.76**).[214]

The results of *in vitro* cytotoxicity experiments revealed that the introduction of a carbonyl group at C11 and an amide group at C28 had a positive impact anticancer activity.[214]

Compounds **1.59–1.78** displayed a much lower cytotoxic activity toward the HUVEC cell line (IC_{50}> 100 μM) than against cancer cell lines, which revealed that these compounds exhibit selectivity for cancer cell lines.[214]

Table 1.7 Cytotoxic activity, expressed as IC_{50}, of derivatives **1.59**–**1.78** against the MGC-803, NCI-H460, HepG2, HeLa, and 7404 human cancer cell lines and a nontumor cell line (HUVEC).[a 214]

Entry	Compound	Cell line/ IC_{50} (μM) [b]					
		MGC-803	NCI-H460	HepG2	HeLa	7404	HUVEC
1	Asiatic acid **1.27**	22.57	39.55	34.9	37.26	40.78	> 100
2	**1.59**	19.91	61.63	> 100	32.55	23.24	> 100
3	**1.60**	14.33	23.58	5.97	28.18	14.13	> 100
4	**1.61**	26.59	31.94	> 100	20.76	> 100	> 100
5	**1.62**	19.44	24.41	11.60	14.2	34.43	> 100
6	**1.63**	22.50	12.8	29.83	13.1	17.20	> 100
7	**1.64**	15.52	24.84	20.43	16.23	22.44	> 100
8	**1.65**	20.59	31.18	21.27	18.46	> 100	> 100
9	**1.66**	21.18	21.78	19.38	14.58	16.11	> 100
10	**1.67**	14.61	30.16	22.62	32.45	> 100	> 100
11	**1.68**	18.96	18.44	10.91	34.5	16.25	> 100
12	**1.69**	24.31	23.05	8.89	17.81	23.47	> 100
13	**1.70**	30.07	> 100	16.62	> 100	> 100	> 100
14	**1.71**	14.09	24.21	19.38	14.25	19.07	> 100
15	**1.72**	20.08	19.05	18.42	16.04	20.57	> 100
16	**1.73**	13.94	21.45	13.75	12.4	17.20	> 100
17	**1.74**	16.03	16.45	28.36	9.71	17.39	> 100
18	**1.75**	14.63	23.82	22.79	15.69	17.03	> 100
19	**1.76**	20.66	27.52	25.47	16.03	15.72	> 100
20	**1.77**	19.88	16.59	21.31	14.01	20.44	> 100
21	**1.78**	> 100	12.16	> 100	26.88	> 100	> 100

[a] Cells were treated with increasing concentrations of each compound for 48 h. Cell viability was determined using an MTT assay.

[b] IC_{50} is the concentration of compound that inhibits 50% of cell growth.

Mechanistic studies revealed that compound **1.60** induced cell-cycle arrest at the G1 phase and apoptosis in HepG2 cells. The proapoptotic effect of compound **1.60** was related to the generation of ROS and the activation of the intrinsic mitochondrial pathway.[214]

The asiatic acid **1.27** amino acid derivatives **1.79–1.93** (Fig. 1.19) were prepared and their anticancer effects were evaluated *in vitro* against lung (A549), cervix (HeLa), liver (HepG2), gastric (SGC7901), breast (MCF-7), and prostate (PC-3) human cancer cell lines and a melanoma (B16F10) mouse cell line (Table 1.8). The antiangiogenic activity of these derivatives was evaluated *in vivo* using a larval zebrafish model.[211]

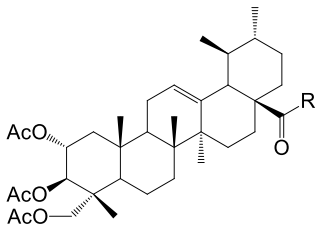

1.79 **R =** OH

1.80 **R =** HNCHCOOCH$_3$ (CH$_2$Ph)

1.81 **R =** HNCH$_2$COOCH$_3$

1.82 **R =** HNCHCOOCH$_3$ (CH$_3$)

1.83 **R =** HNCHCOOCH$_3$ (CHCH$_3$CH$_2$CH$_3$)

1.84 **R =** HNCHCOOCH$_3$ (CH$_2$CH(CH$_3$)$_2$)

1.85 **R =** HNCHCOOCH$_3$ (CH(CH$_3$)$_2$)

1.86 **R =** NH–CHCOOCH$_3$

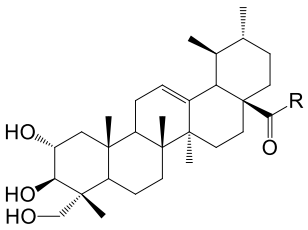

1.87 **R =** HNCHCOOH (CH$_2$Ph)

1.88 **R =** HNCH$_2$COOH

1.89 **R =** HNCHCOOH (CH$_3$)

1.90 **R =** HNCHCOOH (CHCH$_3$CH$_2$CH$_3$)

1.91 **R =** HNCHCOOH (CH$_2$CH(CH$_3$)$_2$)

1.92 **R =** HNCHCOOH (CH(CH$_3$)$_2$)

1.93 **R =** NH–CHCOOH

Figure 1.19 Chemical structures of asiatic acid amino acid derivatives **1.79**–**1.93**.

Compound **1.79** (Table 1.8, entry 2) exhibited lower antiproliferative activities than did asiatic acid **1.27** (Table 1.8, entry 1) against A549, B16-F10, and HepG2 cells. The triacetylated derivatives **1.80–1.86** (Table 1.8, entries 3–9) were more active than asiatic acid **1.27**, whereas the correspondent trihydroxy derivatives **1.87–1.93** (Table 1.8, entries 10–16)

were less actives than asiatic acid **1.27**. The acetylation of C2, C3, and C23 hydroxyl groups combined with the introduction of amino acid methyl ester moieties at C28 had a positive effect on anticancer activity.[211]

Table 1.8 Cytotoxic activity, expressed as IC_{50}, of derivatives **1.79**–**1.93** against the A549, HeLa, HepG2, SGC-7901, MCF-7, and PC-3 human cancer cell lines and a melanoma (B16F10) mouse cell line.[a 211]

Entry	Compound	Cell line/ IC_{50} (μM) [b]						
		A549	B16-F10	HeLa	HepG2	SGC-7901	MCF-7	PC-3
1	Asiatic acid **1.27**	18.8	20.4	55.1	4.0	36.8	32.8	53.6
2	**1.79**	21.1	> 50	24.2	10.2	-	-	17.5
3	**1.80**	5.7	2.9	9.2	0.3	14.2	12.1	10.9
4	**1.81**	7.4	5.8	11.0	1.8	4.5	5.6	> 10
5	**1.82**	3.1	4.4	5.1	0.3	9.2	3.9	10.1
6	**1.83**	2.0	17.1	4.2	1.7	4.7	> 50.0	> 10.0
7	**1.84**	33.9	3.8	32.3	1.4	-	17.0	10.2
8	**1.85**	2.4	11.3	3.7	4.1	9.6	12.8	> 10
9	**1.86**	2.4	4.2	4.8	0.9	4.6	4.5	9.2
10	**1.87**	-	-	-	14.0	-	-	> 50.0
11	**1.88**	30.2	> 50.0	-	18.7	-	> 50.0	> 50.0
12	**1.89**	21.8	> 50.0	19.2	20.5	-	17.1	-
13	**1.90**	25.4	> 50.0	13.8	-	-	-	-
14	**1.91**	-	-	-	16.5	-	-	> 50.0
15	**1.92**	25.0	24.2	-	-	-	-	-
16	**1.93**	-	-	21.3	-	-	-	-

[a] Cells were treated with increasing concentrations of each compound for 72 h. Cell viability was determined using CCK-8.

[b] IC_{50} is the concentration of compound that inhibits 50% of cell growth.

The L-proline methyl ester derivative **1.86** exhibited the best antiproliferative profile, displaying IC_{50} values of 2.4 and 0.9 μM against the A549 and HepG2 cell lines, respectively. Derivatives **1.80**–**1.87** were also found to possess stronger antiangiogenic activity than asiatic acid **1.27**. Stability studies revealed that compound **1.86** was stable at 37 °C and –20 °C over several days.[211]

Compound **1.86** also showed inhibitory activities against SGC-7901 and HGC-27 human gastric cancer cells, displaying IC_{50} values of 4.48 and 7.92 μM, respectively. Conversely, this compound did not show significant toxicity against human gastric mucosa epithelial cells (GES-1).[218] Additional mechanistic studies revealed that treatment of SGC-7901 and HGC-27 cells with compound **1.86** resulted in cell-cycle arrest at the G0/G1 phase and induction of apoptosis with downregulation of Bcl-2, caspase 3, and c-Myc and upregulation of Bax. This compound also suppressed the invasion and migration of both gastric cancer cells.[218]

As depicted in this section, chemical modifications of asiatic acid **1.27** to produce derivatives have been successful in improving its anticancer activity. However, the number of semisynthetic derivatives that have been synthesized and investigated with respect to their anticancer activity are still quite limited. Therefore, there is a great interest in the synthesis and evaluation of new asiatic acid **1.27** derivatives in order to found potential candidates for the development of effective drugs for prevention and treatment of cancer.

Chapter 2

General objectives

Each year, millions of people die from cancer and millions of new cancer cases are diagnosed. Moreover, the burden of cancer is expected to rise in the next few years. The current armamentarium against cancer has limitations, including the development of drug resistance by some types of cancer and the toxicity related with nonspecific effects. Thus, there is an urgent need for more-effective drugs for the prevention and treatment of cancer.

Asiatic acid **1.27** is a pentacyclic triterpenoid with recognized anticancer properties. This multifunctional compound targets various signaling pathways. Moreover, the anticancer activity and the pharmacokinetic properties of asiatic acid **1.27** can be modulated through structural modifications. Therefore, asiatic acid **1.27** is a promising candidate for the design of new leads for drug discovery in the field of cancer.

Given these considerations, the work presented in this thesis has the following general objectives:

2.1 Synthesis of new semisynthetic derivatives of asiatic acid

The preparation of new asiatic acid **1.27** derivatives was designed to follow three main synthetic strategies:

1. Introduction of fluorine into the asiatic acid **1.27** backbone;
2. Introduction of an α,β-unsaturated carbonyl group or a nitrile group in the structure of asiatic acid **1.27**;
3. Conversion of the C28 carboxylic acid into amides or hydroxamic acids in combination with additional modifications in the A-ring.

The structures of all new semisynthetic derivatives should be elucidated using several analytical techniques including IR, MS, ^{1}H NMR, and ^{13}C NMR.

2.2 Evaluation of the anticancer activity of the new derivatives prepared

To investigate the anticancer properties of the new derivatives, their antiproliferative activities should be evaluated in several human cancer cell lines and the IC_{50} values should be determined. A structure–activity relationship should be established based on the IC_{50} values.

The compounds with the best antiproliferative profiles against the cancer cell lines should also be tested against a nontumor cell line, to assess selectivity.

2.3 Preliminary investigation of the mechanism underlying the anticancer effect of the most active compounds.

The most active compounds of each panel of derivatives should be further investigated in order to shed some light on the mechanisms underlying their anticancer activities. Several assays should be used to investigate these mechanisms of action, including:

- **Cell-cycle flow cytometry assay:** to investigate the effect of the compounds on cell-cycle distribution;
- **Morphological analysis and annexin V-FITC/PI double staining assay:** to evaluate the ability of the compounds to induce apoptosis;
- **Western blotting:** to investigate some of the molecular targets of the compounds tested.

In addition to these assays, the existence of synergism between cisplatin (an anticancer agent that is widely used in clinical settings) and at least one of the new derivatives of asiatic acid **1.27** should also be investigated**.**

The final goal of this work is to select the best compounds for *in vivo* evaluation of their anticancer potential.

Chapter 3

Synthesis and anticancer evaluation of fluorinated asiatic acid derivatives

Synthesis and anticancer activity of novel fluorinated asiatic acid derivatives

Bruno M. F. Gonçalves, Jorge A. R. Salvador, Sílvia Marín and Marta Cascante

European Journal of Medicinal Chemistry, 114, (2016), 101–117.

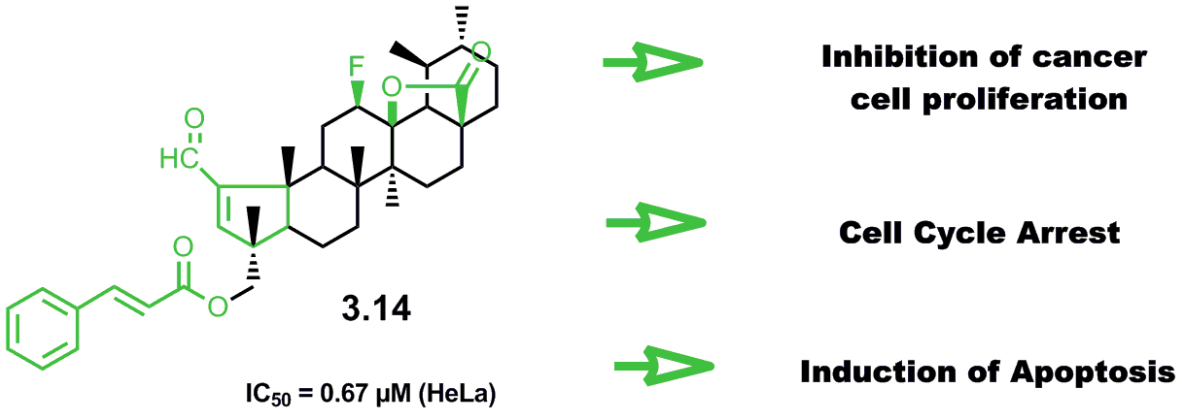

3.1 Introduction

Fluorine is a small and highly electronegative atom that, because of these unique properties, markedly affects the chemical, physical, and biological properties of organic molecules.[234,235] In the field of pharmaceuticals, the incorporation of fluorine into molecular structures may improve their metabolic and chemical stability, increase their lipid solubility and membrane permeability, and enhance the binding affinity of the drug to molecular targets.[234–237] As a consequence of the remarkable properties of organofluorine compounds, fluorine has gained an increasingly important role in the design and development of new drugs[237–240], which is reflected in the number of drugs currently in the market that contain fluorine atoms (20% of all pharmaceuticals).[241]

The enormous potential of fluorinated drugs in the field of cancer treatment started to be explored in 1957 by Heidelberger and coworkers, who prepared the well-known 5–fluorouracil compound, which has been used for the treatment of several solid tumors.[240] Since then, many other fluorinated antitumor agents have been successfully developed and approved for the clinical treatment of several types of cancer,[240] these include fludarabine (Fludara®), fulvestrant (Faslodex®; AstraZeneca), nilutamide (Nilandron®, Anandron®), and flutamide (Eulexin®), among others.[240]

Naturally occurring organofluorine compounds are very rare in nature,[240] and carbon–fluorine bond formation is a challenging chemical transformation.[242] Therefore, this growing use of fluorinated molecules was only possible because of advances in the field of fluorine chemistry, which led to the development of a wide variety of nucleophilic and electrophilic fluorinating agents. The nucleophilic fluorinating reagents used most widely are DAST and Deoxo-fluor® (Fig. 3.1).[243,244] These reagents, under mild conditions, fluorinate a hydroxyl or carbonyl group to afford the corresponding fluorinated derivatives in good yields and with high efficiency and selectivity.[244] The electrophilic fluorination was initially performed using elemental fluorine. However, the high toxicity and low selectivity of fluorine and the need for special equipment and care for safe handling limited the use of such method.[245] The need for safe, selective, and efficient methods of electrophilic fluorination led to the development of Selectfluor® (Fig. 3.1). This reagent proved to be remarkably stable, nontoxic, and easy to handle and has been found to be very effective for the fluorination of a wide variety of organic compounds.[246,247]

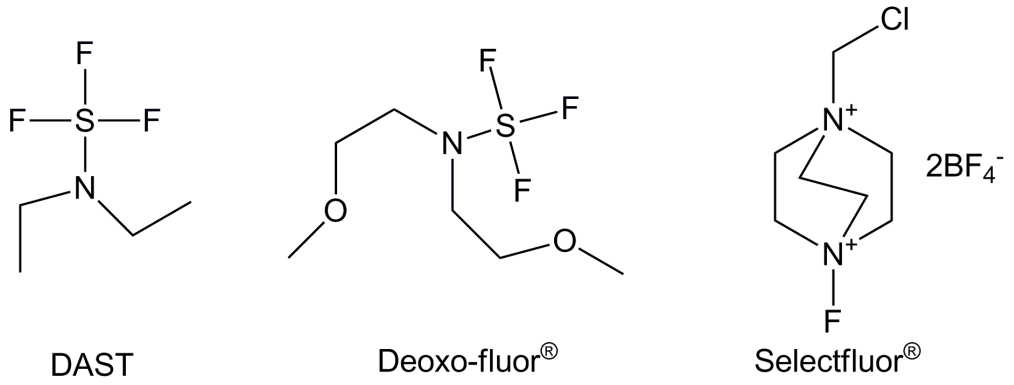

Figure 3.1 Chemical structures of the fluorinating reagents DAST, Deoxo-fluor® and Selectfluor®.

In the last few years, some fluorinating reagents have been used with relative success to prepare fluorinated derivatives of terpene-type compounds,[241,248] including triterpenoids.[249] Moreover, our group recently reported the synthesis of a series of ursolic acid fluorolactone derivatives that exhibited promising antiproliferative activities.[250] Taking into account our previous results and the fact that fluorination often imparts desirable properties to bioactive molecules,[234] a series of fluorolactone and fluorolactam derivatives of asiatic acid **1.27** was prepared using the electrophilic fluorinating reagent Selectfluor®, aiming to improve the anticancer properties of the parental compound asiatic acid **1.27**.

3.2 Results

3.2.1 Chemistry

3.2.1.1 Synthesis and structural elucidation

Asiatic acid **1.27** has three hydroxyl groups at C2, C3 and C23, an olefin group at C12 and a carboxylic acid group at C28. Structural modifications were carried out in these functional groups in order to obtain the semisynthetic derivatives and to study structure-activity relationships (SAR). The structures of all new synthesized derivatives were elucidated by infrared spectroscopy (IR), mass spectrometry (MS) and nuclear magnetic resonance

(NMR) spectroscopy. As shown in Scheme **3.1** the preparation of fluorinated asiatic acid **1.27** derivatives started with the treatment of asiatic acid **1.27** with Selectfluor® in a mixture of two inert solvents, nitromethane and dioxane, at 80 ºC[250], to afford the 12β-fluorolactone derivative **3.1** in 61% yield. Derivatives **3.2** and **3.3** were prepared in good yields by esterification of the three hydroxyl groups of compound **3.1** with acetic and butyric anhydrides respectively in tetrahydrofuran (THF) in the presence of 4-dimethylaminopyridine (DMAP) (Scheme **3.1**).

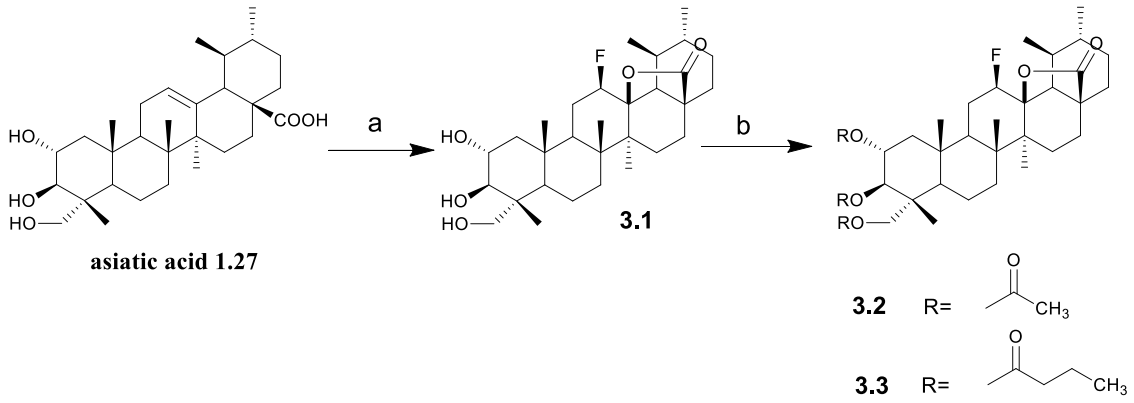

Scheme 3.1 Synthesis of derivatives **3.1**–**3.3**. *Reagents and conditions*: a) Selectfluor®, dioxane, nitromethane, 80 ºC; b) Acetic anhydride or butyric anhydride, DMAP, THF, rt.

The presence of the fluorolactone moiety in derivatives **3.1**–**3.17**, was confirmed by the presence in ^{1}H NMR of a double triplet or a double quartet at 4.85–5.00 ppm, with a coupling constant of around 45 Hz**,** typical of the germinal proton (H12) for the β-fluorine (Fig. **3.2**). In addition, the characteristic ^{13}C NMR signal for C12 was observed as a doublet ranging from 88.6 to 89.5 ppm, with a coupling constant of around 186 Hz. The ^{13}C signal for C13 also appeared as a doublet ranging from 91.5 to 92.0 ppm with a coupling constant of around 14 Hz (Fig. **3.3**). These ^{1}H NMR and ^{13}C NMR signals are typical of the β-fluorine isomer.[250]

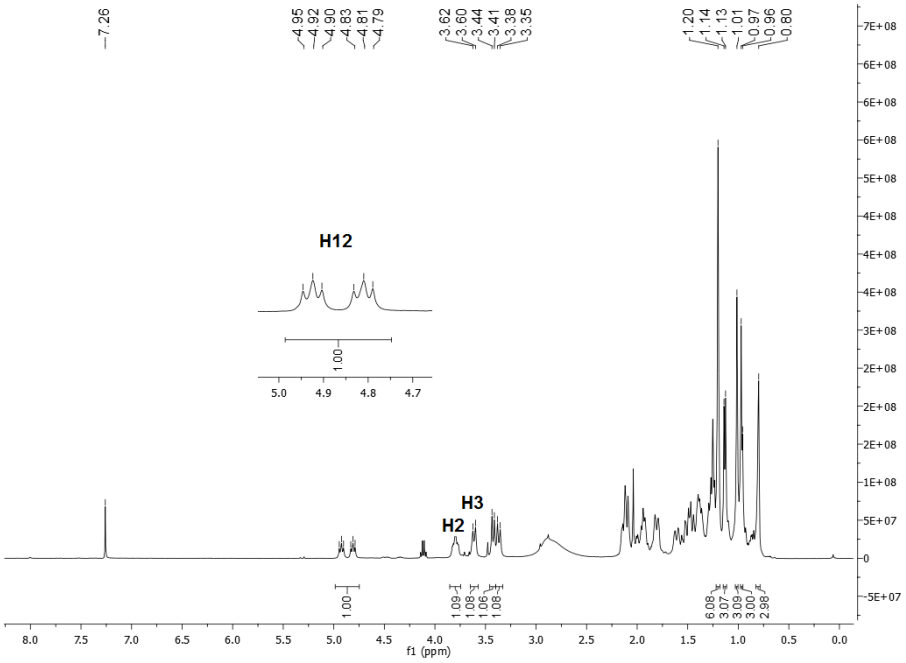

Figure 3.2 ^{1}H NMR spectrum of compound **3.1**.

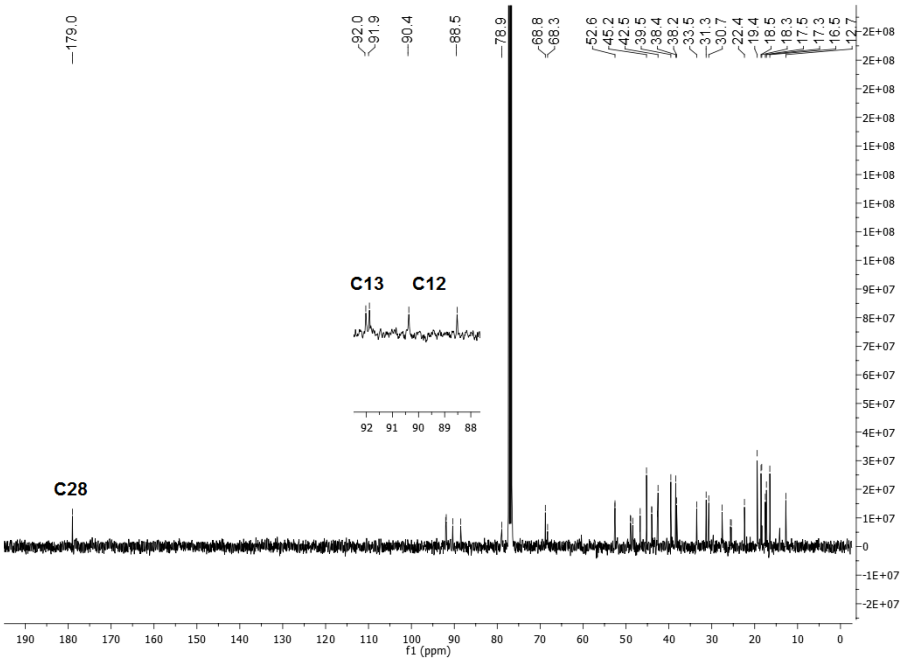

Figure 3.3 ^{13}C NMR spectrum of compound **3.1**.

Reaction of **3.1** with dry acetone and a catalytic amount of HCl in the presence of activated molecular sieves,[251] afforded the alcohol acetonide derivative **3.4** (Scheme 3.2), which was oxidized with pyridinium dichromate (PDC) in dichloromethane to give the 2-oxo derivative **3.5** in 39% yield. The deprotection of acetonide **3.5** with HCl 1 M, in THF, followed by acetylation of C3 and C23 hydroxyl groups with acetic anhydride, gave the diacetylated compound **3.7** (Scheme 3.2).

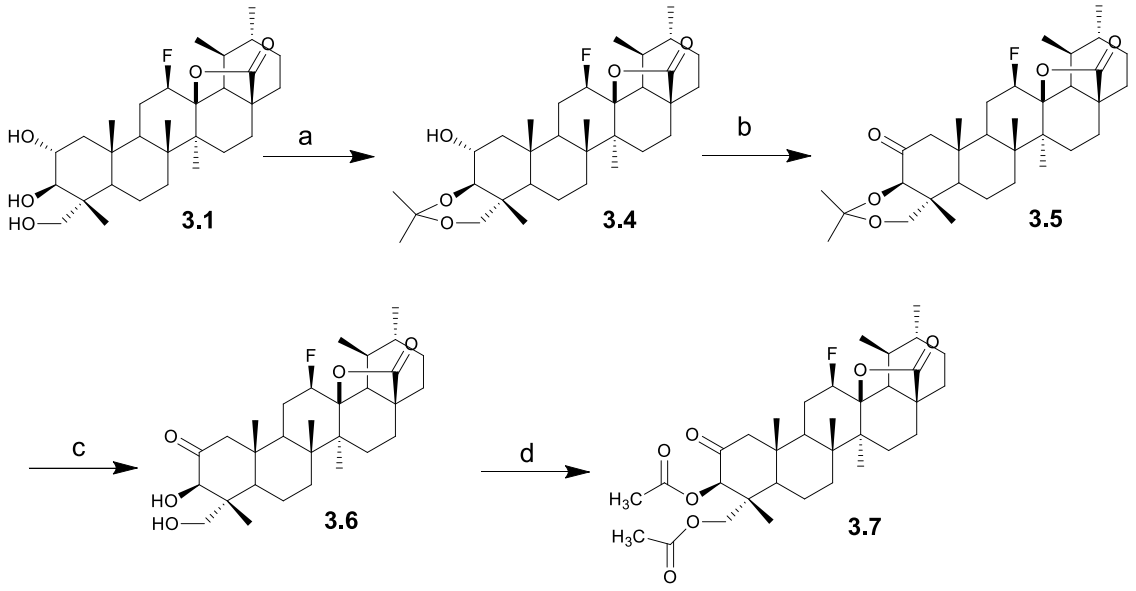

Scheme 3.2 Synthesis of derivatives **3.4**–**3.7**. *Reagents and conditions*: a) Dry acetone, molecular sieves 4 Å, HCl, rt; b) PDC, acetic anhydride, DCM, reflux; c) aq. HCl 1 M, THF, rt; d) Acetic anhydride, DMAP, THF, rt.

A known procedure was adapted for the synthesis of compounds **3.8** and **3.9**.[252] Oxidation of compound **3.1** with $NaIO_4$ in methanol/water gave the lactol derivative **3.8**, in 59% yield, which opened in the presence of catalytic amounts of piperidine and acetic acid in benzene at 60 ºC and underwent recyclization to give the α,β-unsaturated aldehyde derivative **3.9** in 62% yield (Scheme 3.3).

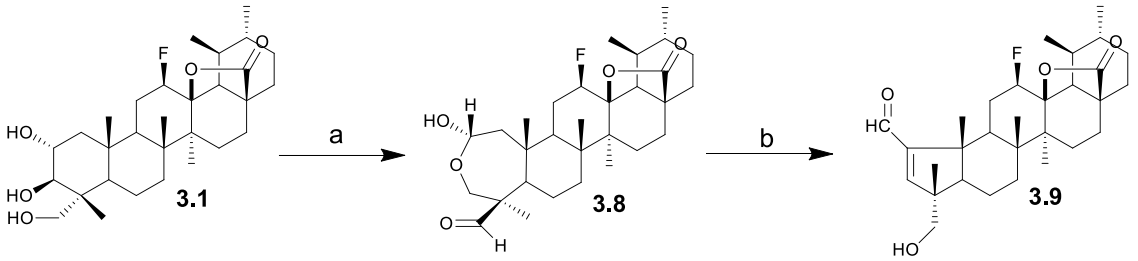

Scheme 3.3 Synthesis of derivatives **3.8** and **3.9**. *Reagents and conditions*: a) $NaIO_4$, $MeOH/H_2O$, rt; b) i- Acetic acid, piperidine, dry benzene, 60 ºC, N_2; ii- Anhydrous $MgSO_4$, 60 ºC, N_2.

The presence of the α,β-unsaturated aldehyde moiety in compound **3.9** was confirmed by the presence in the ^{1}H NMR spectrum of a signal at 9.71 ppm, corresponding to the CHO proton and a signal at 6.74 ppm, corresponding to the proton H3 (Fig. 3.4). The signals corresponding to the tertiary carbons CHO and C3 were found at 190.4 and 161.6 ppm, respectively, in the ^{13}C NMR spectrum (Fig. 3.5). The signals corresponding to the quaternary carbons C28 and C2 were observed at 179.1 and 159.0 ppm, respectively, as these signals were not present in the DEPT 135 spectrum (Fig. 3.6). These data were constant for all the derivatives containing an α,β-unsaturated aldehyde moiety (**3.9**–**3.16**).

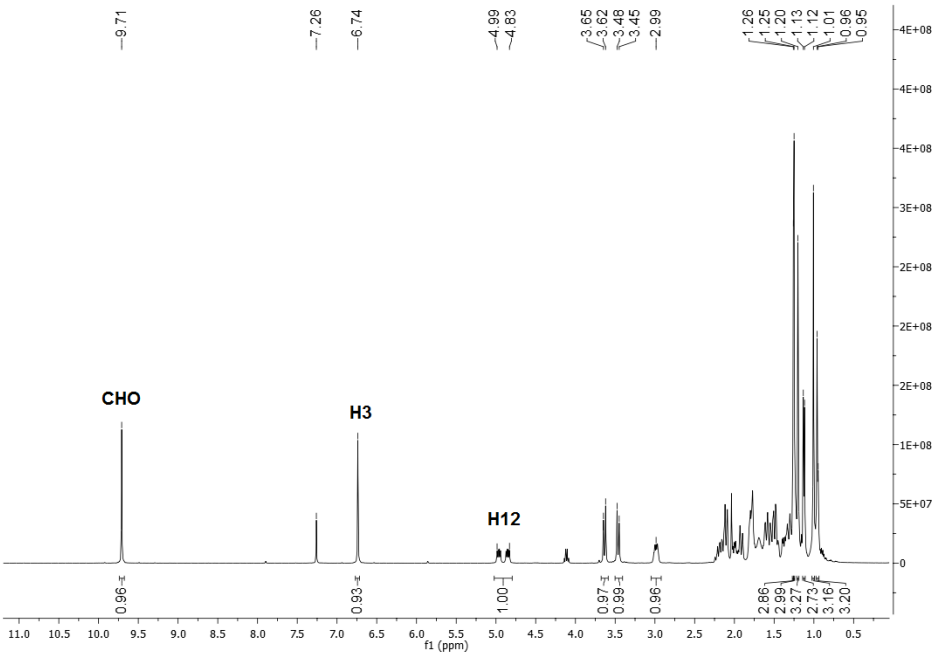

Figure 3.4 ^{1}H NMR spectrum of compound **3.9.**

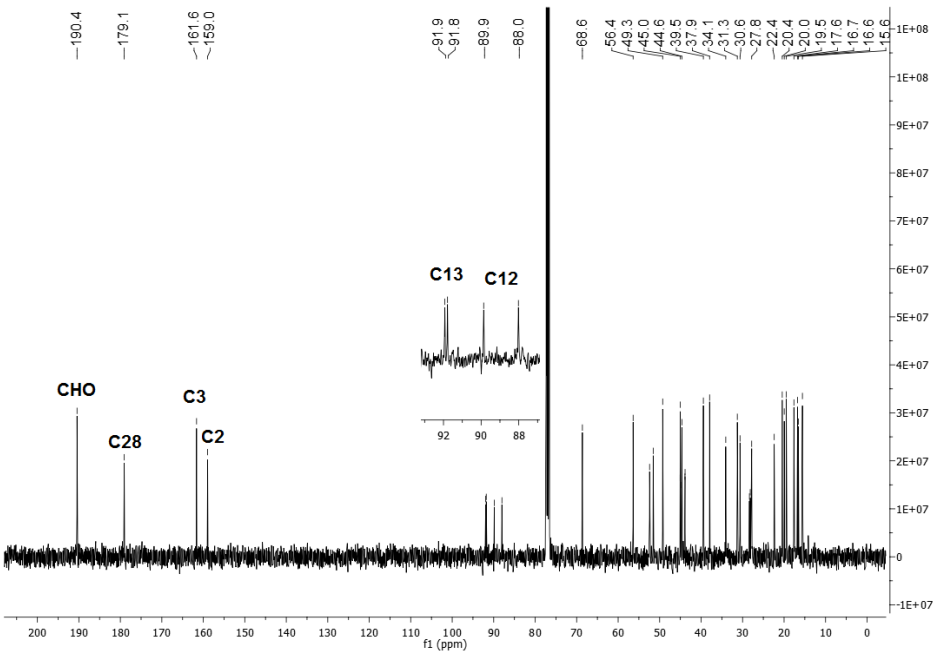

Figure 3.5 ^{13}C NMR spectrum of compound **3.9**.

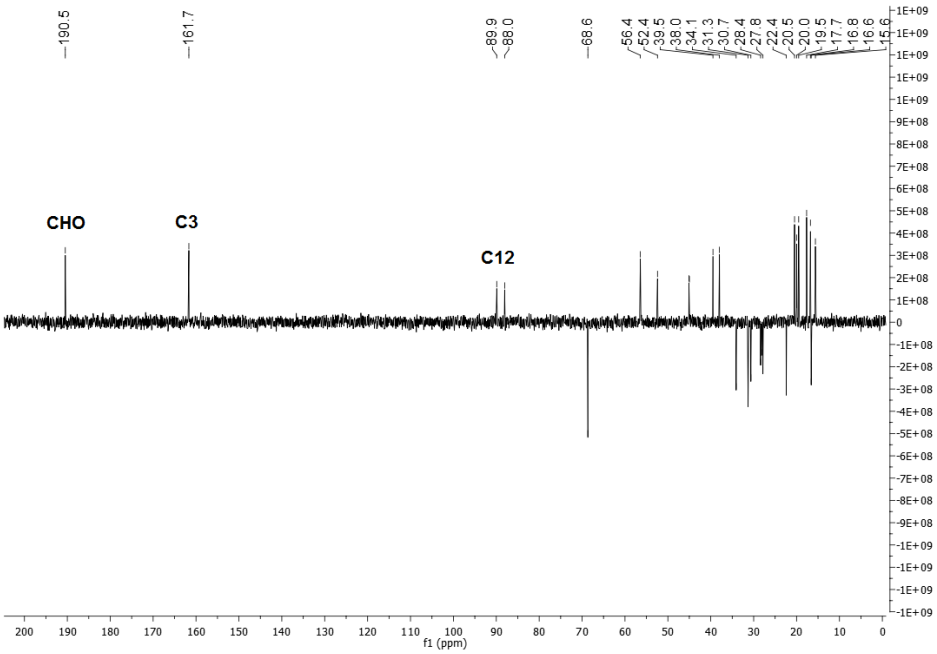

Figure 3.6 DEPT 135 spectrum of compound **3.9**.

The ester derivatives **3.10**–**3.13** were obtained in moderate to good yields through reaction of compound **3.9** with acetic, butyric, benzoic and succinic anhydrides respectively, as depicted in Scheme **3.4**. For the synthesis of cinnamic ester derivative **3.14**, compound **3.9**

was treated with cinnamoyl chloride in dry benzene at 60 ºC in the presence of DMAP affording the derivative **3.14** in 40% yield.[253]

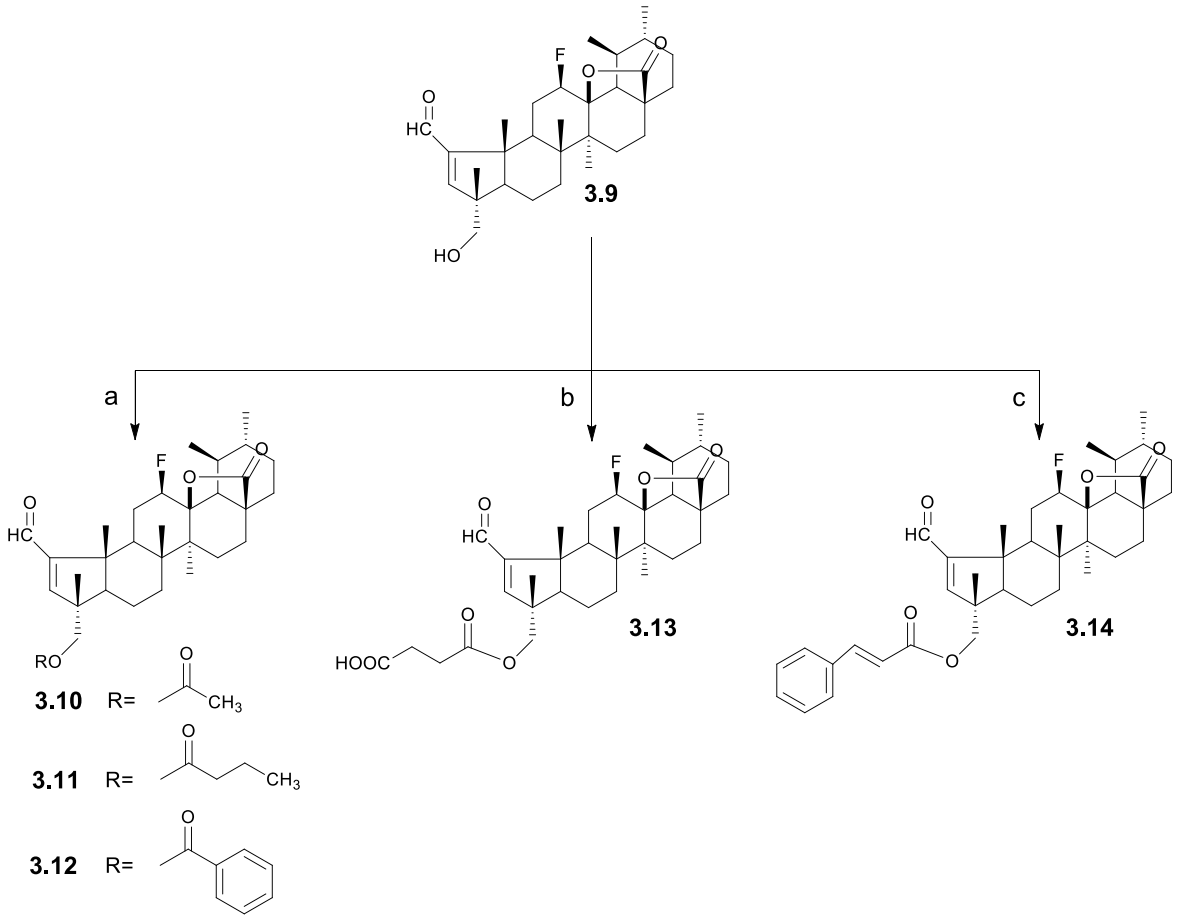

Scheme 3.4. Synthesis of derivatives **3.10–3.14**. *Reagents and conditions*: a) Acetic anhydride, butyric anhydride or benzoic anhydride, DMAP, THF, rt; b) Succinic anhydride, DMAP, DCM, rt; c) Cinnamoyl chloride, dry benzene, DMAP, 60 ºC, N_2.

Previous studies revealed that introduction of imidazole and methylimidazole rings in pentacyclic triterpene structures could improve the *in vitro* anticancer activity of the parental compounds.[250,254–258] Hence the imidazole carbamate derivative **3.15** and the methylimidazole carbamate derivative **3.16** were synthesized by reaction of compound **3.9** with 1,1′-carbonyldiimidzole (CDI) and 1,1′-carbonylbis-2′methlyimidazole (CBMI), respectively, in anhydrous THF at reflux temperature under inert atmosphere (N_2) (Scheme 3.5).[256,257]

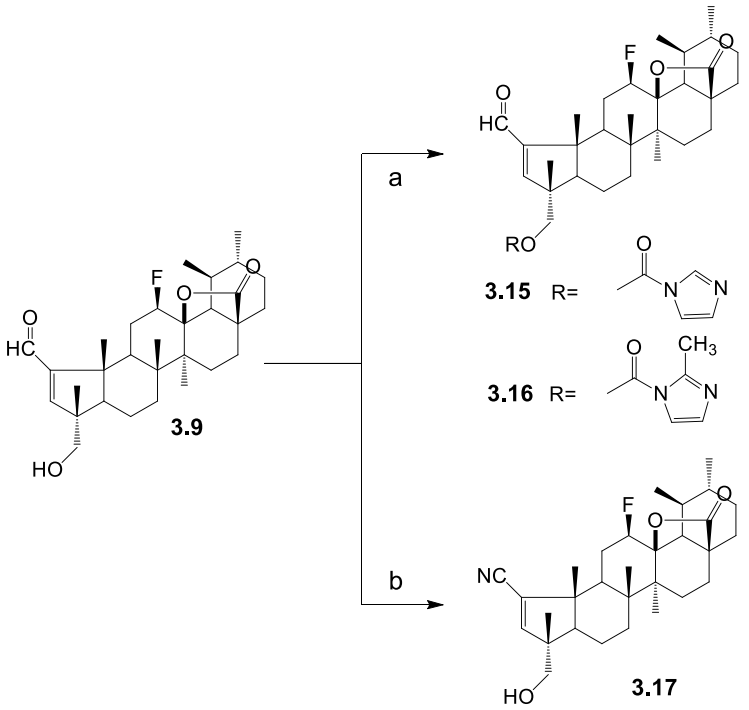

Scheme 3.5 Synthesis of derivatives **3.15**–**3.17**. *Reagents and conditions*: a) CDI or CBMI, THF, 70 ºC, N_2; b) I_2, aq. NH_3, THF, rt.

The formation of carbamate derivative **3.15** was confirmed by the presence of three signals in the ^{1}H NMR spectrum at 8.11, 7.40 and 7.10 ppm that are characteristic for the three protons of the imidazole ring (Fig. 3.7).[256] In the case of derivative **3.16**, only two signals that corresponded to the methylimidazole ring protons appeared in ^{1}H NMR spectrum at 7.29 and 6.87 ppm and an additional methyl signal was observed at 2.63 ppm (Fig. 3.8).[257]

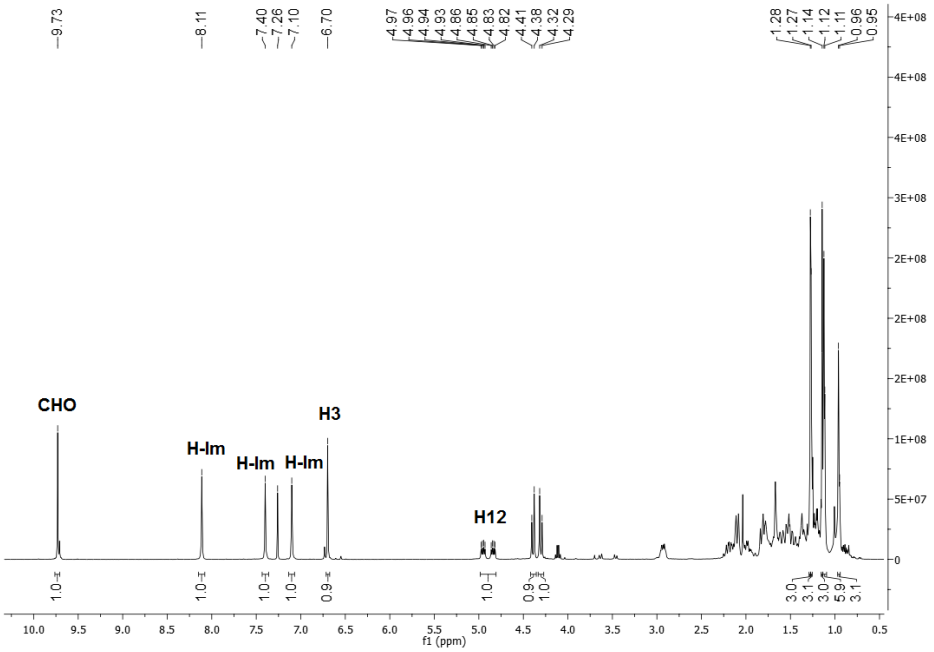

Figure 3.7 [1]H NMR spectrum of compound **3.15**.

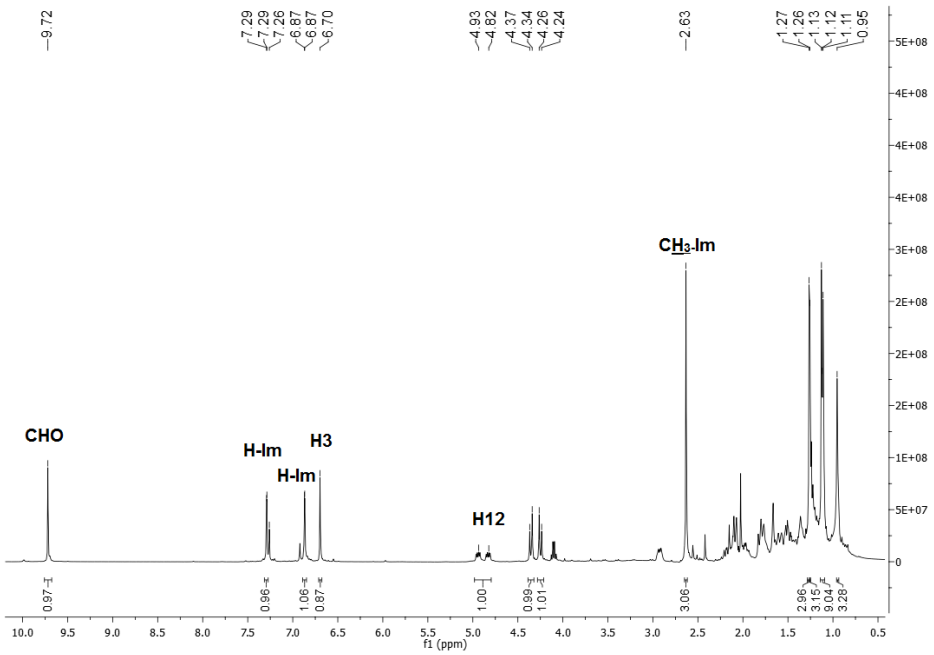

Figure 3.8 [1]H NMR spectrum of compound **3.16**.

Actually more than 30 nitrile containing drugs are used in clinic for diverse therapeutic indications, including treatment of cancer[259], which reveals the pharmaceutical importance of the presence of a nitrile group in organic molecules.[259,260] Thus, the α,β-unsaturated aldehyde **3.9** was treated with iodine in ammonia water at room temperature to afford the α,β-unsaturated nitrile derivative **3.17** (Scheme 3.5) in 57% yield.[261] The conversion of aldehyde into nitrile was confirmed by the presence of an absorption band at 2210 cm^{-1}, in the IR spectrum, corresponding to the C≡N stretching vibration (Fig. 3.9). In the ^{1}H NMR spectrum of compound **3.17**, the signal for the H3 proton was found at 6.54 ppm (which is slightly lower than that observed for compound **3.9**) (Fig. 3.10). Moreover, the signal for the quaternary carbon attached to the nitrogen was observed in the ^{13}C NMR spectrum at 117.2 ppm (this signal was not present in DEPT, and is characteristic of the CN carbon) (Fig. 3.11). The signal for the C2 carbon was found at 127.0 ppm, which was a lower value than that observed for C2 in compound **3.9** (which have the α,β-unsaturated aldehyde moiety). Carbon C28 appeared as a signal at 178.8 ppm in the ^{13}C NMR spectrum, and the tertiary carbon C3 was also present in DEPT 135 as a signal at 154.4 ppm (Fig. 3.12).

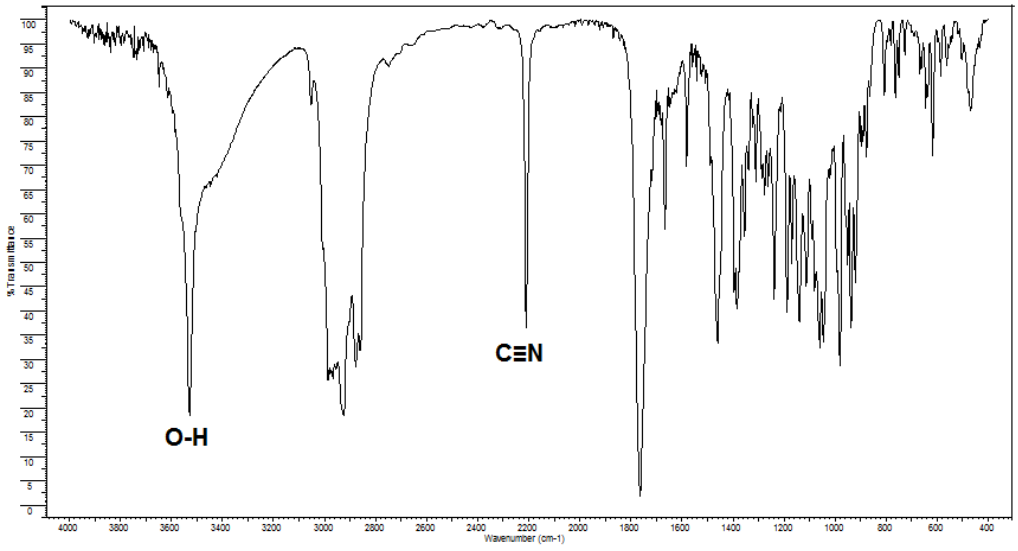

Figure 3.9 IR spectrum of compound **3.17**.

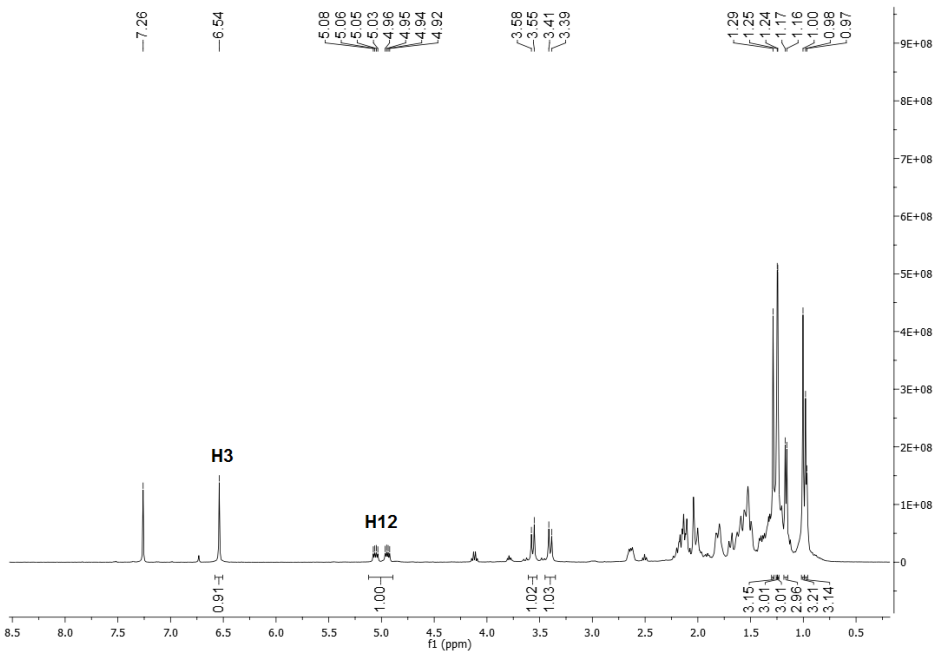

Figure 3.10 ^{1}H NMR spectrum of compound **3.17**.

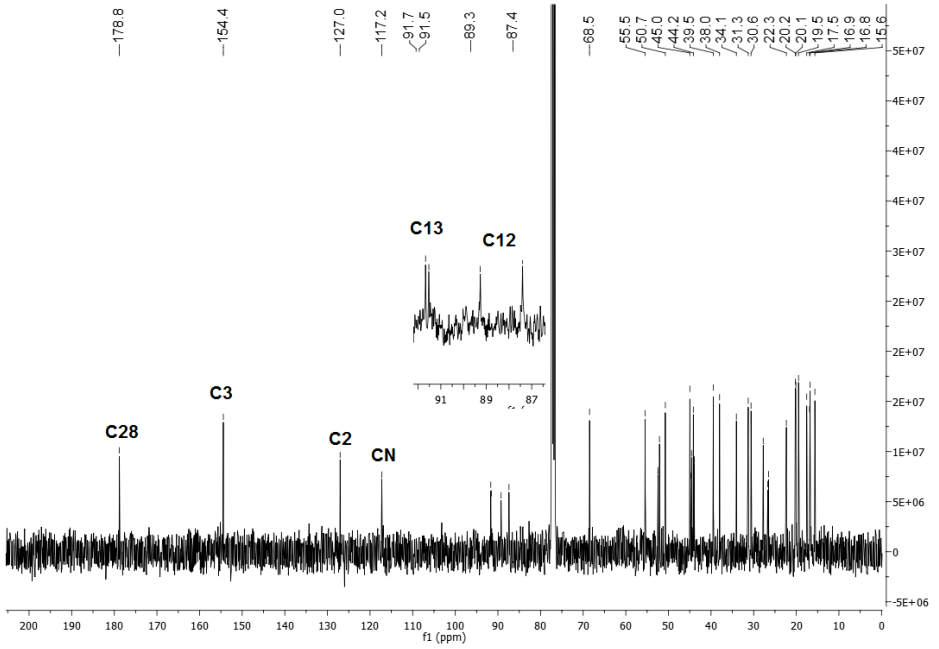

Figure 3.11 ^{13}C NMR spectrum of compound **3.17.**

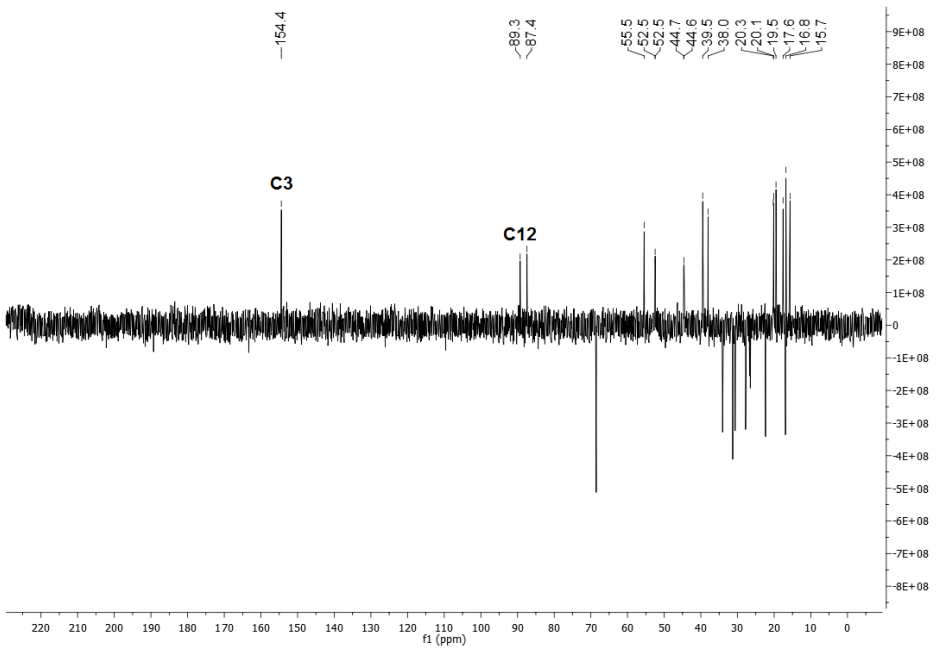

Figure 3.12 DEPT 135 spectrum of compound **3.17**.

As depicted in Scheme 3.6 the full acetylation of asiatic acid **1.27** with acetic anhydride in THF and in the presence of DMAP yielded the triacetate derivative **3.18**, quantitatively. Treatment of **3.18** with oxalyl chloride in dichloromethane, afforded the corresponding 28-acyl chloride, which reacted without purification with ammonia, methylamine or amino acids methyl ester hydrochloride to give the corresponding amide derivatives **3.19** and **3.20**, and amino acid derivatives **3.21** and **3.22**.[177,211] The amide derivatives **3.19**–**3.22** reacted with Selectfluor® in a mixture of two inert solvents, nitromethane and dioxane, at 80 ºC, to afford the corresponding fluorolactams **3.23**–**3.26**. In the absence of an external nucleophilic donor, the amide carries out a nucleophilic attack on C13, allowing the formation of the lactam and the introduction of fluorine at C12.

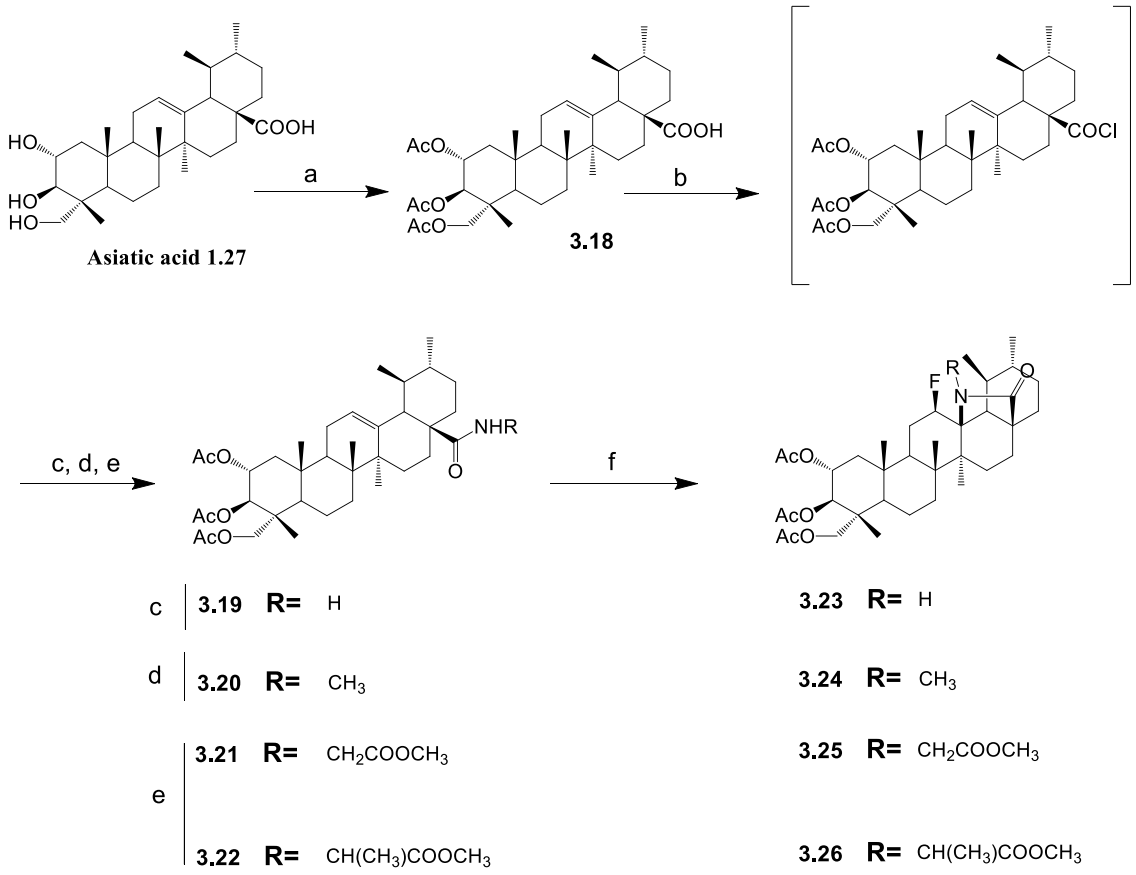

Scheme 3.6 Synthesis of derivatives **3.18**–**3.26**. *Reagents and conditions*: a) Acetic anhydride,THF, DMAP, rt; b) Oxalyl chloride, DCM, r.t.; c) $NH_3.H_2O$ 25%, THF, rt.; d) Methylamine, Et_3N, DCM, rt.; e) Glycine or L-alanine methyl ester, Et_3N, DCM, rt.; f) Selectfluor®, dioxane, nitromethane, 80 ºC.

In the IR spectrum, the amide derivatives **3.19**–**3.22** presented a band corresponding to the carbonyl stretching vibration of the amide at 1648.8–1671.9 cm^{-1}, a value that was lower than that observed for the carbonyl stretching vibration of carboxylic acid (1747.2 cm^{-1}). Moreover, the primary amide **3.19** presented a pair of N–H stretching bands at 3477.0 and 3367.1 cm^{-1} (Fig. 3.13), whereas in the IR spectra of secondary amides **3.20**–**3.22**, only one N–H stretching band was observed at around 3400 cm^{-1} (Fig. 3.14).

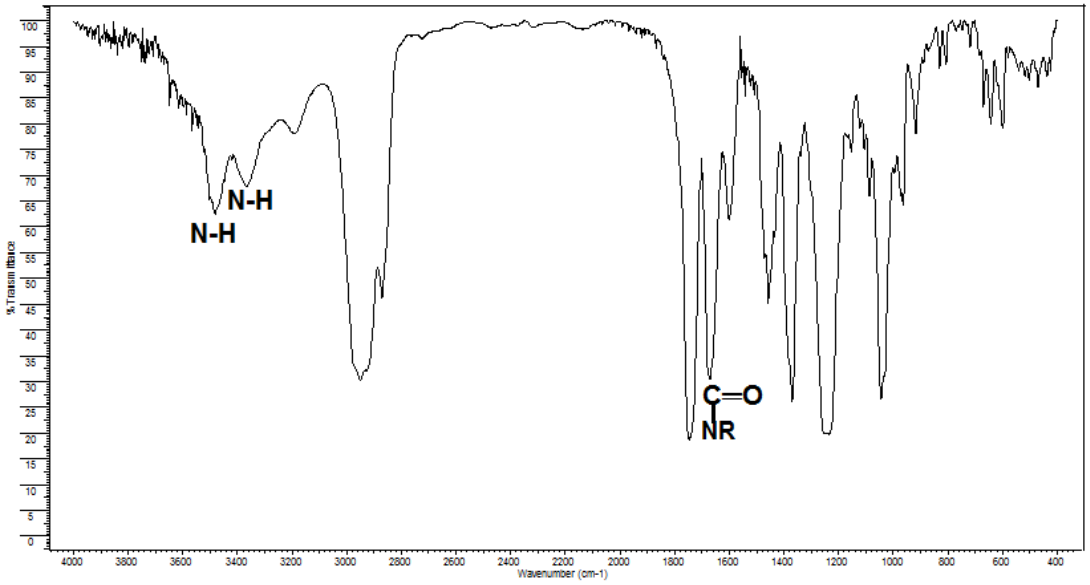

Figure 3.13 IR spectrum of compound **3.19**.

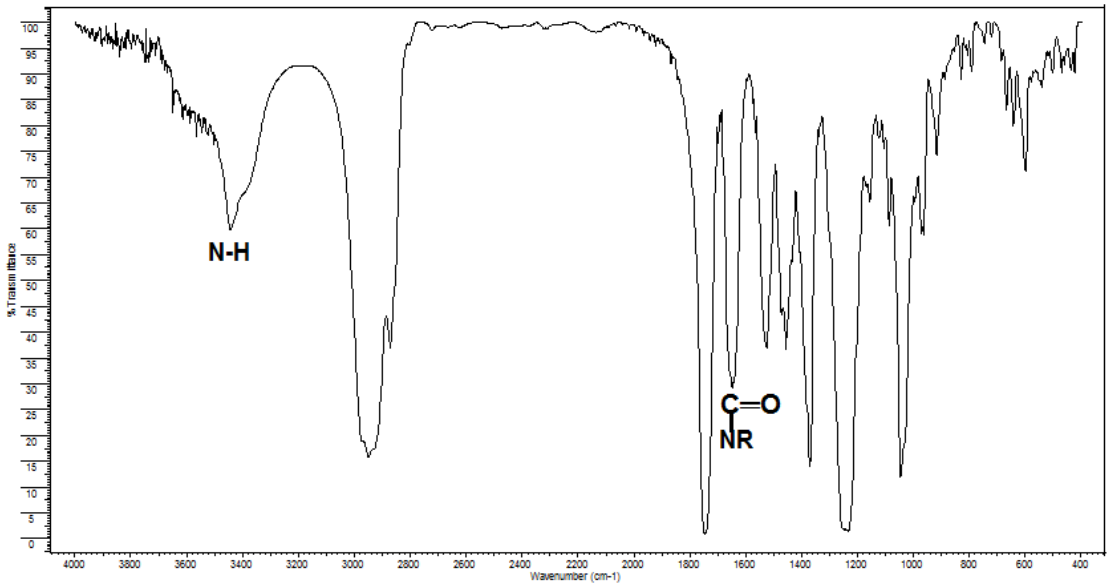

Figure 3.14 IR spectrum of compound **3.20**.

In the ^{1}H NMR spectrum of compound **3.19**, the signals for the NH_2 protons were found at 5.82 and 5.40 ppm, respectively (Fig. 3.15), whereas the NH proton in compounds **3.20**–**3.22** appeared as a signal between 5.86 and 6.60 ppm. The ^{13}C NMR signal for the C28 carbon in compounds bearing the amide moiety (**3.19–3.22**) was observed at 177.3–181.0 ppm (Fig. 3.16), which was a lower value than that observed for the C28 carbon in derivative **3.18** bearing the carboxylic acid moiety (183.1 ppm).

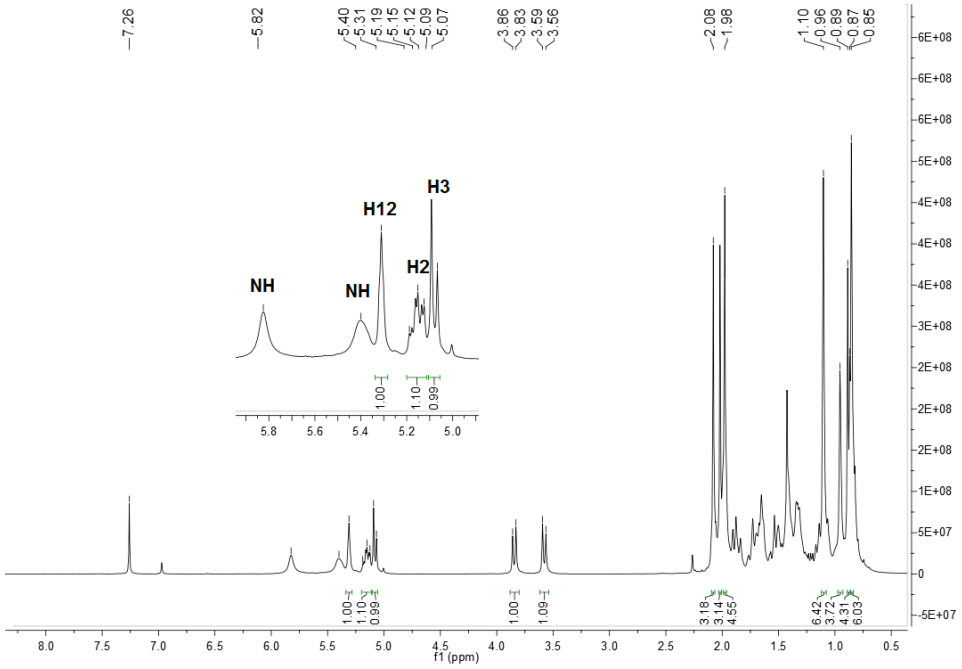

Figure 3.15 ^{1}H NMR spectrum of compound **3.19**.

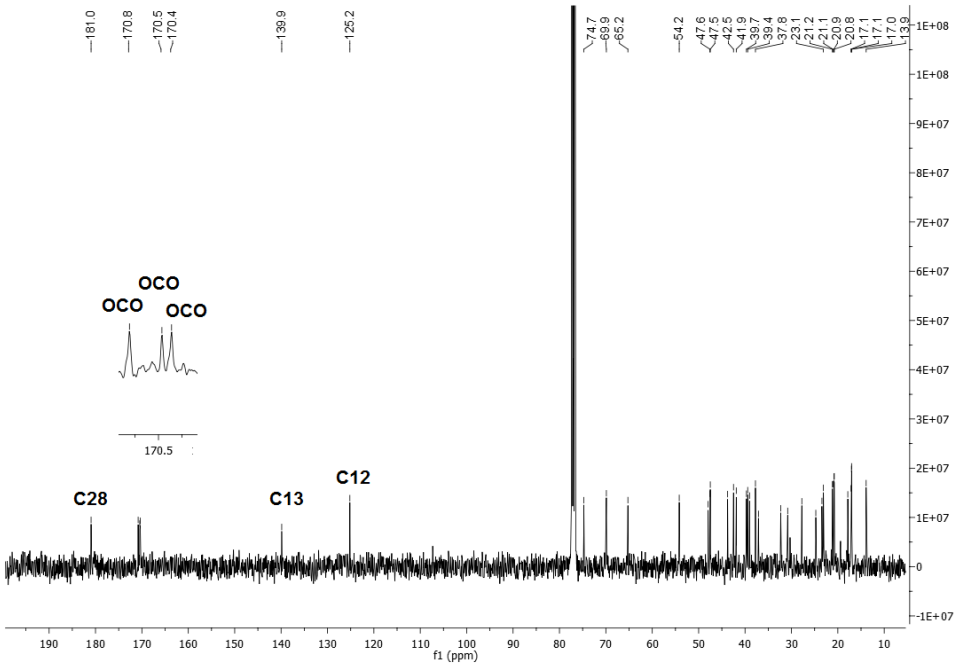

Figure 3.16 ^{13}C NMR spectrum of compound **3.19.**

The presence of fluorolactam moiety in derivatives **3.23**–**3.26** was confirmed by the signal for proton H12, which appeared in the ^{1}H NMR spectrum as a double quartet at 4.82–4.87 ppm with a coupling constant of around 45 Hz (Fig. 3.17). The ^{13}C NMR signal for carbon C12 was observed as a doublet ranging from 89.5 to 89.7 ppm with a coupling

constant of around 186 Hz. Another doublet signal was observed for carbon C13 ranging from 90.8 to 91.8 with a coupling constant of around 14 Hz (Fig. 3.18). These values are similar to those observed for the 12β-fluorolactones and they are characteristic of the β-isomer.[250] Selected ^{1}H NMR and ^{13}C NMR spectral data for the fluorolactam derivatives **3.23**–**3.26** are depicted in Table 3.1.

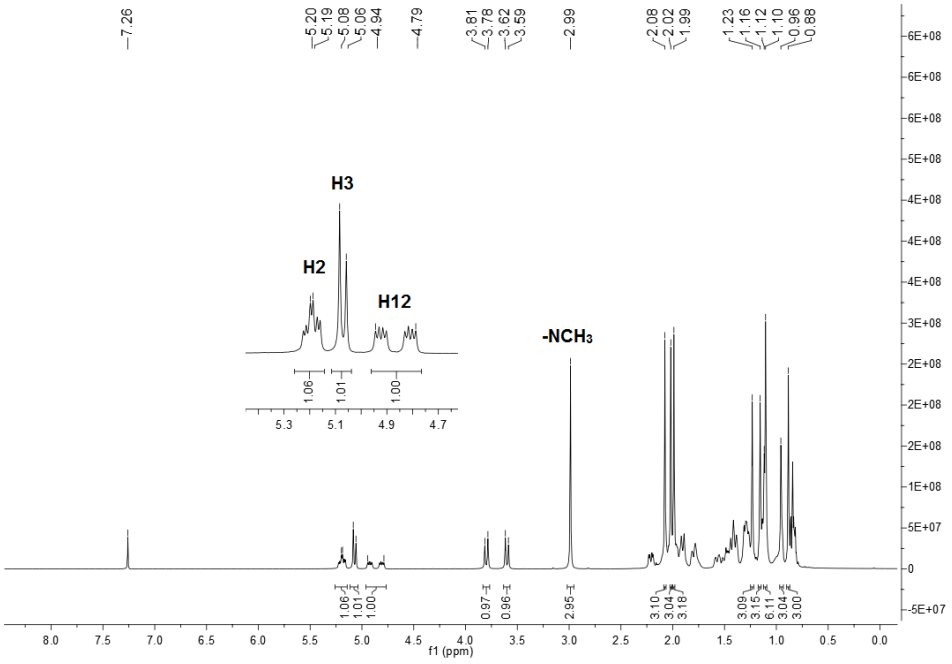

Figure 3.17 ^{1}H NMR spectrum of compound **3.24**.

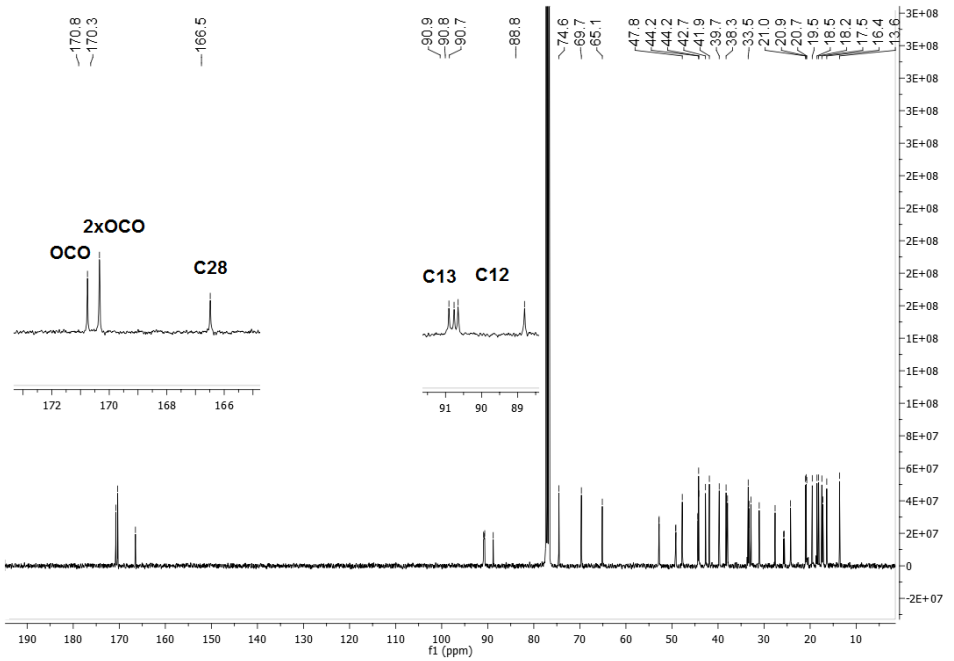

Figure 3.18 ^{13}C NMR spectrum of compound **3.24**.

Table 3.1 ^{1}H and ^{13}C NMR selected data for the compounds **3.23**, **3.25** and **3.26**.

Position	compound 3.23		compound 3.25		Compound 3.26	
	δH	**δC**	**δH**	**δC**	**δH**	**δC**
2	5.22–5.16 (m)	-	5.21–5.15 (m)	-	5.22–5.16 (m)	-
3	5.07 (d, J = 10.3 Hz)	-	5.06 (d, J = 10.3 Hz)	-	5.07 (d, J = 10.4 Hz)	-
12	4.85 (dq, J = 45.6 Hz)	89.5 (d, J = 185.9 Hz)	4.84 (dq, J = 45.8 Hz)	89.5 (d, J = 185.8 Hz)	4.82 (dq, J = 45.9 Hz)	89.5 (d, J = 186.0 Hz)
13	-	91.3 (d, J = 14.4 Hz)	-	91.8 (d, J = 14.2 Hz)	-	91.6 (d, J = 14.7 Hz)

3.2.2 Biological evaluation

3.2.2.1 Evaluation of the antiproliferative activity

Asiatic acid **1.27** and its fluorinated derivatives were screened for their *in vitro* antiproliferative activities against colon (HT-29) and cervical (HeLa) cancer cell lines, to obtain information about the anticancer potential of the newly synthesized compounds. Cisplatin was used as reference drug. Cell lines were treated with different concentrations of each compound for 72 h. The IC_{50} values (concentration that inhibits 50% of cell growth) for all compounds were determined by 3-(4,5-dimethylthiazol-2-yl)-2,5-diphenyltetrazolium bromide (MTT) or 2,3-bis-(2-methoxy-4-nitro-5-sulfophenyl)-2H-tetrazolium-5-carboxanilide (XTT) assays.

As shown in the Table **3.2**, all the tested derivatives exhibited improved antiproliferative activities in both cell lines compared to asiatic acid **1.27** with the exception of compound **3.1**. The identical inhibitory activity of asiatic acid **1.27** and compound **3.1** in both cell lines, as well as compound **3.2** and **3.18** against HeLa cell line, suggested that the formation of fluorolactone moiety was not critical for antiproliferative activity.

Table 3.2 Cytotoxic activity, expressed as IC_{50}, of asiatic acid **1.27**, its semisynthetic derivatives and cisplatin against breast (MCF-7) and colon (HT-29) cancer cell lines.[a]

Compound	Cell Line/ IC_{50} (μM ± SD)[b]	
	HT-29	HeLa
Asiatic acid 1.27	64.30 ± 3.21	52.47 ± 0.06
3.1	51.25 ± 1.77	60.17 ± 2.75
3.2	6.38 ± 0.18	4.43 ± 0.25
3.3	7.40 ± 0.69	5.05 ± 0.49
3.6	23.50 ± 0.71	24.50 ± 1.41
3.7	N.D.	11.70 ± 1.13
3.8	11.25 ± 0.35	7.40 ± 0.71
3.9	1.28 ± 0.08	1.08 ± 0.04
3.10	2.02 ± 0.19	1.40 ± 0.14
3.11	1.29 ± 0.09	0.95 ± 0.01
3.12	1.05 ± 0.05	0.80 ± 0.04
3.13	6.35 ± 0.64	3.48 ± 0.04
3.14	0.71 ± 0.02	0.67 ± 0.07
3.15	2.37 ± 0.23	1.62 ± 0.09
3.16	2.80 ± 0.14	1.63 ± 0.15
3.17	N.D.	7.50 ± 0.42
3.18	N.D.	6.1 ± 0.28
3.19	N.D.	1.65 ± 0.07
3.20	N.D.	1.1 ± 0.10
3.21	N.D.	0.98 ± 0.04
3.22	N.D.	1.07 ± 0.12
3.23	7.50 ± 0.57	2.37 ± 0.15
3.24	8.50 ± 0.71	2.95 ± 0.21
3.25	9.23 ± 0.75	2.72 ± 0.23
3.26	6.37 ± 0.47	3.97 ± 0.31
Cisplatin	6.11[262] [c]	2.28 ± 0.26

[a] HT-29 and HeLa cells were treated with crescent concentrations of each compound for 72 h. IC_{50} values were determined by MTT assay and are expressed as the mean ± SD of three independent experiments. N.D.- not determined.

[b] IC_{50} is the concentration of compound that inhibits 50% of cell growth.

[c] IC_{50} value obtained from literature, determined using the same experimental methodology and included here for comparison.

A considerable improvement in the antiproliferative activity in both cell lines was observed for compounds **3.2** and **3.3**. The oxidation of hydroxyl at C2 in derivative **3.6** resulted in an increase of the antiproliferative activity against HeLa and HT-29 cell lines, when compared with compound **3.1**. The diacetylated compound **3.7** was two-fold more active than its precursor compound **3.6** against HeLa cell line. These combined results suggested that free hydroxyl groups in A-ring were not essential for cytotoxic activity. Furthermore, esterification of A-ring hydroxyl groups with lipophilic substituents, significantly enhance the antiproliferative activity, possibly because it improves the cellular permeability.[263]

Compound **3.9** was 40 and 56 - fold more active than its hexameric analog **3.1** towards HT-29 and HeLa cell lines respectively. Compounds having a pentameric A-ring with an α,β-unsaturated carbonyl (**3.9**–**3.16**) proved to be significantly more active than asiatic acid **1.27**, being the most active compounds among all tested derivatives. In fact, these compounds presented lower IC_{50} values than reference drug cisplatin on HeLa cell line. These results are in good agreement with previous studies which suggested that the presence of an α,β-unsaturated carbonyl moiety in A-ring of some triterpenoids significantly enhance their biological activity.[264] The biological importance of α,β-unsaturated carbonyl was also confirmed by the reduction of antiproliferative activity observed when derivative **3.9** was converted into nitrile derivative **3.17**.

To explore the effects of substitution at C23-OH group of compound **3.9**, several C23-ester and C23-carbamate derivatives were synthesized. When compared with compound **3.9**, the butyrate ester **3.11**, benzyl ester **3.12** and cinnamic ester **3.14** derivatives showed increased antiproliferative activity against HeLa cells. On the other hand, the succinic ester derivative **3.13** presented a significant decrease of activity. These results indicated that esterification of C23-OH with lipophilic moieties slightly improve the anticancer activity, while hydrophilic moieties decrease it. The carbamate derivatives **3.15** and **3.16** exhibited a slight decrease in the antiproliferative activity compared with compound **3.9**.

Compounds **3.19–3.22** with introduction of amide moieties at C28 exhibited increased activity against HeLa cells compared to compound **3.18**. Finally, fluorolactam derivatives **3.23**–**3.26** showed decreased antiproliferative activity compared to the respective precursor amides **3.19–3.22**. These results suggested that the introduction of the fluorolactam moiety was not critical for the antiproliferative activity. The direct comparison of the antiproliferative effects of the compounds **3.2**, **3.18**, **3.19–3.22** and **3.23–3.26** against HeLa cell line revealed

that C28 amide derivatives show better activity than C28 carboxylic acid, fluorolactone and fluorolactam derivatives.

The analysis of the IC_{50} values obtained for the new compounds in HeLa cells led to the establishment of a structure–activity relationship (SAR), which is schematically represented in Figure 3.19.

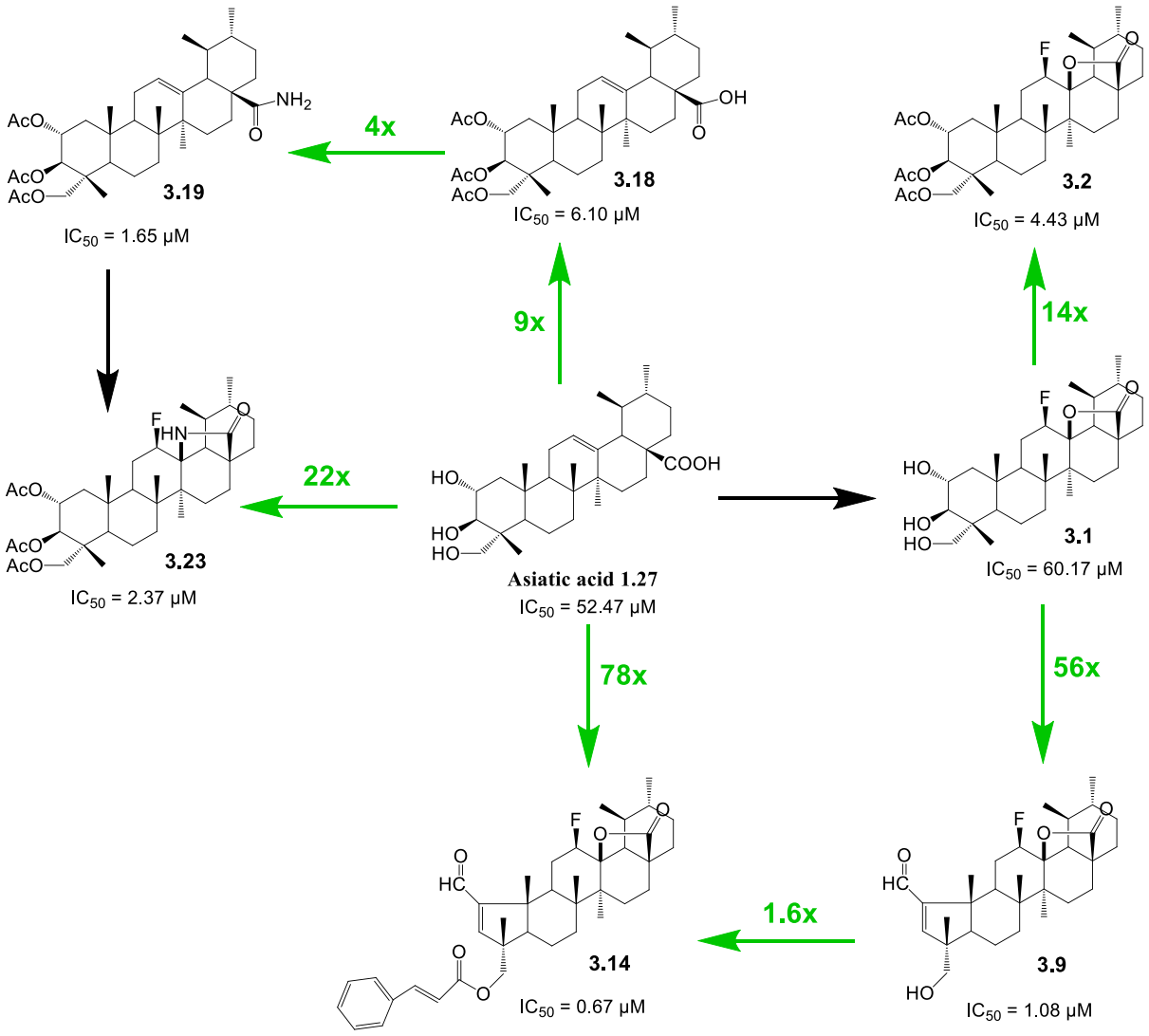

Figure 3.19 Schematic representation of the SAR for the antiproliferative activity of several semisynthetic derivatives of asiatic acid **1.27** against the HeLa cell line. The SAR was established based on IC_{50} values. In compounds with a hexameric A-ring, the esterification of C2, C3, and C23 hydroxyl groups with hydrophobic moieties improved antiproliferative activity: compound **3.18** was 9-fold more active than asiatic acid **1.27**, and compound **3.2** was 14-fold more active than compound **3.1**. The introduction of amide moieties at C28 increased antiproliferative activity: compound **3.19** was 4-fold more active than compound **3.18**. Fluorolactone and fluorolactam moieties were not critical for antiproliferative activity: compounds **3.1** and **3.23** were less active than their precursor compounds, asiatic acid **1.27** and compound **3.19**, respectively. The formation of the pentameric A-ring containing an α,β-unsaturated aldehyde significantly increased antiproliferative activity: compound **3.9** was 56-fold more active than compound **3.1**. The esterification of C23-OH with a cinnamic moiety afforded the most active compound **3.14**. Compound **3.14** was 78-fold more active than asiatic acid **1.27** and 1.6-fold more active than its precursor compound **3.9**.

The antiproliferative activity of the most active compounds: **3.11**, **3.12** and **3.14**, was then evaluated against additional cancer cell lines (MCF-7, Jurkat, PC-3, MIA PaCa-2 and A375) (Table 3.3). To evaluate the selectivity of these derivatives for cancer cell lines, they were also tested against a nontumor human fibroblast cell line (BJ). The obtained results showed that the tested derivatives were remarkably more active than asiatic acid **1.27** in all cancer cell lines. Furthermore, these compounds showed higher cytotoxicity toward tumor cell lines than toward a nontumor fibroblast cell line (BJ): the IC_{50} values of compounds **3.12** and **3.14** determined in HeLa cells were 2.8 and 2.9 times lower, respectively, than those determined in BJ cells (Table 3.3, Fig. 3.20).

Table 3.3 Cytotoxic activities, expressed as IC_{50}, of asiatic acid **1.27** compounds **3.11**, **3.12** and **3.14** and cisplatin against several cancer cell lines (MCF-7, Jurkat, PC-3, MIA PaCa-2 and A375) and nontumor human fibrobast cell line (BJ).[a]

Compound	**Cell Line/ IC_{50} (μM ± SD)[b]**					
	Jurkat	**PC-3**	**MCF-7**	**MIA PaCa-2**	**A-375**	**BJ**
Asiatic acid 1.27	37.17 ± 3.75	67.25 ± 0.35	68.5 ± 2.50	50.67 ± 1.15	50.33 ± 2.57	88.7 ± 0.58
3.11	N.D.	N.D.	1.40 ± 0.10	1.47 ± 0.07	1.02 ± 0.06	N.D.
3.12	N.D.	N.D.	0.88 ± 0.07	1.33 ± 0.30	0.96 ± 0.03	2.24 ± 0.01
3.14	0.68 ± 0.06	0.74 ± 0.02	0.84 ± 0.02	1.13 ± 0.09	0.72 ± 0.06	1.94 ± 0.15
Cisplatin	1.94 [265 c]	4.60 [266 c]	19.10 ± 4.50	5.00 ± 1.00 [267 c]	3.11 ± 0.98 [268 c]	10.10 ± 2.00

[a] The different cell lines were treated with crescent concentrations of each compound for 72 h. IC_{50} values were determined by XTT assay in Jurkat cell line and MTT assay in the other cell lines. IC_{50} values are expressed as the mean ± SD of three independent experiments. N.D.-not determined.

[b] IC_{50} is the concentration of compound that inhibits 50% of cell growth.

[c] IC_{50} value obtained from literature, determined using the same experimental methodology and included here for comparison.

Compound **3.14** proved to be the most active compound among all tested derivatives, with IC_{50} values ranging from 0.67 μM on HeLa cells to 1.13 μM on MIA PaCa-2 cells. This compound was 78 and 3.4-fold more potent than asiatic acid **1.27** and cisplatin, respectively, towards HeLa cells. Compound **3.14** was selected for a preliminary investigation on its anticancer mechanism.

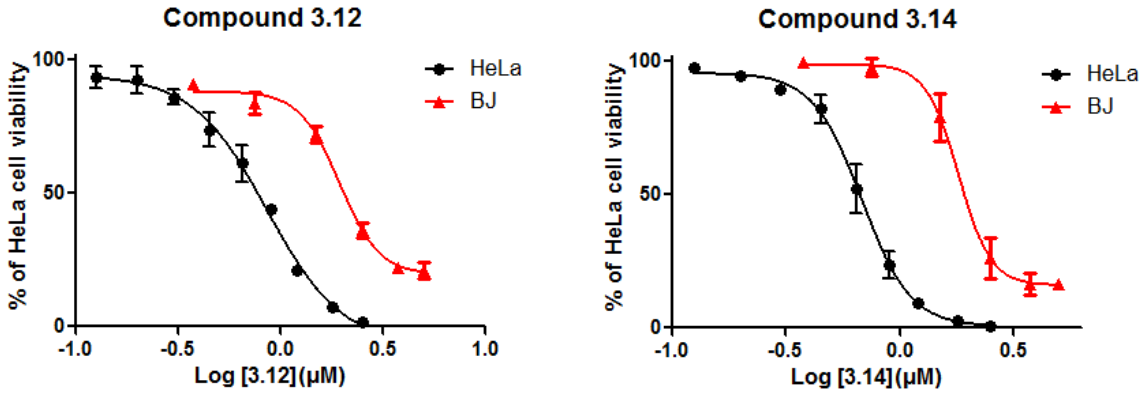

Figure 3.20 Dose-response curves of the antiproliferative effect of derivatives **3.12** and **3.14** against the cancer cell line HeLa and against the nontumor cell line BJ. Results are presented as the mean ± SD of three independent experiments.

3.2.2.2 Effects of compound 3.14 on cell cycle distribution

To shed some light on the antiproliferative mechanism of compound **3.14**, its effect on cell-cycle distribution in HeLa cells was evaluated. The cells were treated with different concentrations (0.67, 1.34, and 2.68 µM) of compound **3.14** for 24 and 48 h, stained with propidium iodide (PI) and analyzed by flow cytometry. Non treated cells were used as control. As shown in Figure 3.21, the incubation of HeLa cells with 1.34 and 2.68 µM of compound **3.14** for 24 h increased the percentage of cells at G0/G1 (from 51.41% in control to 67.26% at 1.34 µM and 72.72% at 2.68 µM). At same conditions, the percentage of cells in S phase was obviously decreased (from 35.72% in control to 22.55% and 11.05% in 1.34 µM and 2.68 µM treated cells, respectively). These results revealed that compound **3.14** arrested the cell cycle at the G0/G1 stage, leading to the inhibition of the cell proliferation.

When the treatment of HeLa cells with 1.34 µM compound **3.14** was prolonged for 48 h, the percentage of cells at G0/G1 phase of cell cycle increased substantially from 54.05% in control cells to 76.03% in treated cells, in accordance with the results gathered 24 h after treatment. Additionally, an expansion of 11.39% in the sub G0/G1 cell population, in 2.68 µM **3.14** treated cells, was also observed. The expansion of sub G0/G1 peak is associated with the existence of fragmented DNA, suggesting cell death. These data indicate that

antiproliferative activity of compound **3.14** is related with cell cycle arrest at G0/G1 phase and induction of cell death.

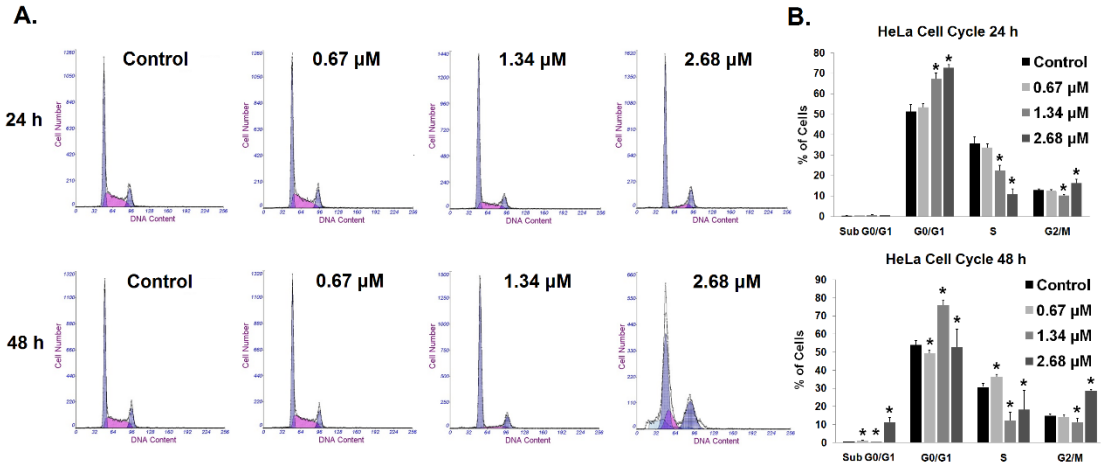

Figure 3.21 Cell-cycle distribution of HeLa cells untreated (control) or treated with the indicated concentrations of compound **3.14** for 24 h (upper part) or 48 h (lower part). After treatment with compound **3.14** for the indicated times, the harvested cells were stained with PI and their DNA content was analyzed by flow cytometry. **A.** Representative histograms obtained in the cell-cycle analysis. **B.** Graph bar summarizing the variation in the percentage of cells in each phase of the cell cycle. Results are presented as the mean ± SD of three independent experiments. Differences between treated and control groups were considered statistically significant at $p < 0.05$ (*).

3.2.2.3 Effect of compound 3.14 on the levels of cell cycle-related proteins

Since compound **3.14** arrested cell cycle at G0/G1 phase, its effect on the levels of some cell cycle regulatory proteins was evaluated. As depicted in Figure 3.22, treatment of HeLa cells with 1.34 µM or 2.68 µM of compound **3.14** for 48 h, clearly upregulated the levels of $p21^{cip1/waf1}$ and $p27^{kip1}$. A significant downregulation in the levels of cyclin D3, was also observed, in a dose dependent way. In the same conditions, compound **3.14** slightly decreased the levels of cyclin E. These observations are in accordance with cell cycle arrest at G0/G1 phase. Taken together, these results suggest that compound **3.14** upregulated the protein levels of $p21^{cip1/waf1}$ and $p27^{kip1}$ which can bind to and inhibit the cyclin E-Cdk2 and cyclin D3-Cdk 4/6 complexes, leading to cell cycle arrest at G0/G1 phase.

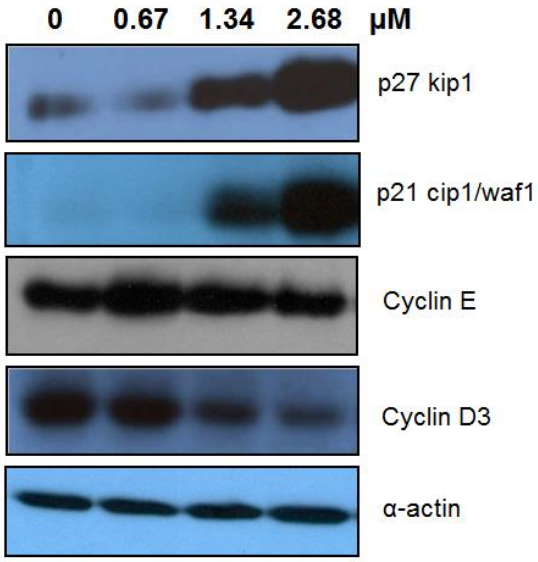

Figure 3.22 Effect of compound **3.14** on the levels of cell-cycle related proteins. HeLa cells were treated with compound **3.14** at the indicated concentrations for 48 h. The levels of the indicated proteins were analyzed by western blotting. α-Actin was used as a loading control.

3.2.2.4 Apoptosis-inducing effect of compound 3.14 evaluated by annexin V-FITC/PI flow cytometric assay

In the early stages of an apoptotic process, the disruption of membrane asymmetry and the translocation of phosphatidylserine (PS) from the inner to the outer cell membrane are observed. The externalized PS can be detected and quantified by Annexin V-FITC, a fluorescent labeled conjugate that binds with high affinity to PS.[269] In the later stages of apoptosis, cell membrane loses its integrity allowing the penetration of PI through cell membrane, which intercalates with DNA. FACS analysis of annexin V-FITC/PI double stained cell was used to differentiate live cells (annexin V^-/PI^-), from early apoptotic cells (annexin V^+/PI^-), late apoptotic cells (annexin V^+/PI^+) and necrotic cells (annexin V^-/PI^+). Therefore, apoptosis was quantified by flow cytometry after double staining of HeLa cells treated with different concentrations (0.67 μM, 1.34 μM and 2.68 μM) of compound **3.14** during 48 h with annexin V-FITC/PI. Untreated HeLa cells were used as control. As shown in Figure 3.23, treatment of HeLa cells with 2.68 μM of compound **3.14** decreased the percentage of live cells from 95.73% to 62.05%, and increased the percentage of apoptotic cells from 4.32% to 33.98%, being 11.20% earlier apoptotic cells and 22.78% late apoptotic cells. These results suggest that compound **3.14** induces apoptosis in HeLa cells.

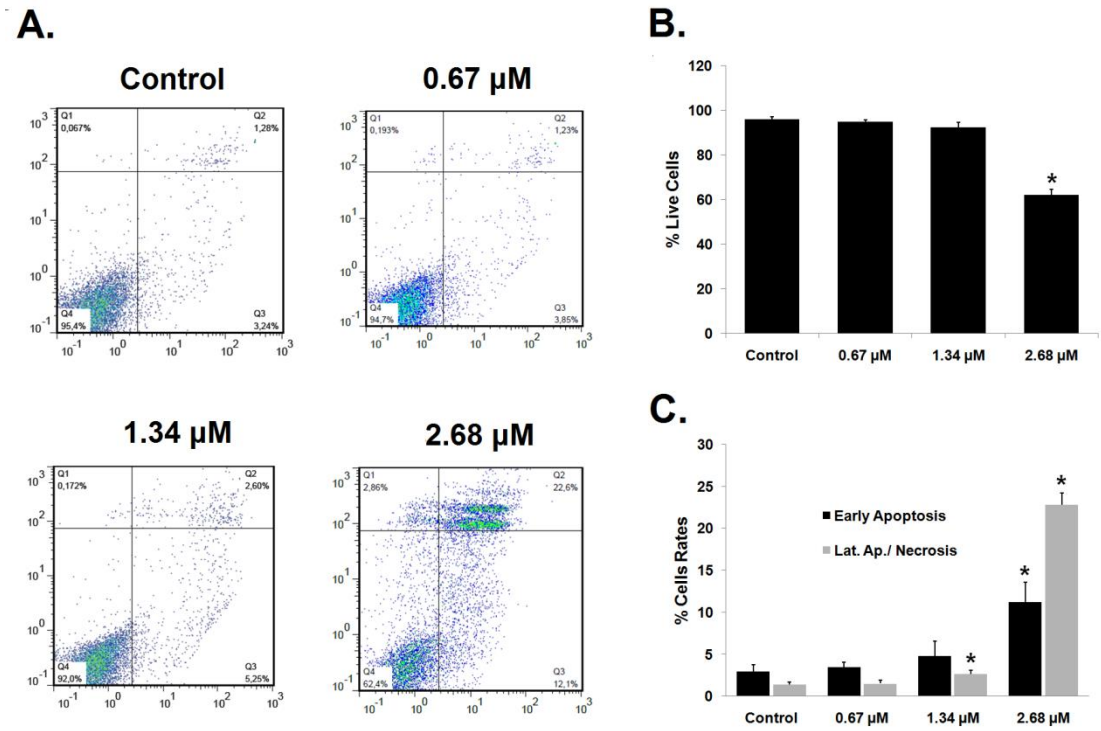

Figure 3.23 Annexin V-FITC/PI assay of HeLa cells untreated (control) or treated with compound **3.14** at the indicated concentrations for 48 h. **A.** Representative flow cytometric plots for the quantification of apoptosis are shown: the lower-left quadrant (annexin $V^-$and PI^-) represents nonapoptotic cells, the lower-right quadrant (annexin V^+ and PI^-) represents early apoptotic cells, the upper-right quadrant (annexin V^+ and PI^+) represents late apoptotic/necrotic cells and the upper-left quadrant (annexin V^- and PI^+) represents necrotic cells. **B.** The bar graph depicts the variation in the percentage of live cells. **C.** The bar graph depicts the variation in the percentage of cells that are in early apoptosis and in late apoptosis/necrosis. Results are presented as the mean ± SD of three independent experiments. Differences between treated and control groups were considered statistically significant at $p < 0.05$ (*).

3.2.2.5 Apoptosis-inducing effect of compound 3.14 evaluated by morphological analysis

It is well known that apoptotic cells are characterized by specific morphological features, such as cell volume reduction, chromatin condensation, nuclear membrane blebbing, and the formation of apoptotic bodies.[269] Some of these modifications were observed and analyzed using phase-contrast and fluorescence microscopy techniques.

3.2.2.5.1 Phase-contrast microscopy

HeLa cells untreated (control) or treated with compound **3.14** at 0.67, 1.34, and 2.68 µM were observed using a phase-contrast microscope and several images were captured. As depicted in Figure 3.24, after 48 h of exposure to compound **3.14,** a dose-dependent reduction in cell confluence, was evident. Moreover, control cells presented an intact appearance, whereas cells treated with 2.68 µM **3.14** exhibited obvious morphological changes, including a reduction in the cell volume, a rounded morphology, and detachment from the culture dishes. These observations are in good agreement with cell death by apoptosis.

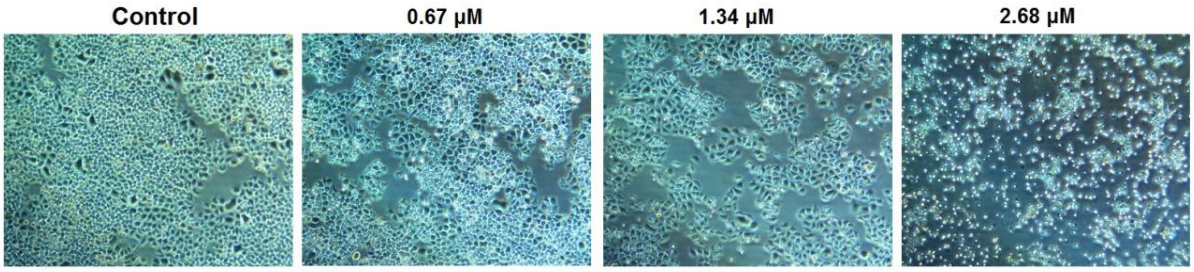

Figure 3.24 Representative phase-contrast images of HeLa cells untreated (control) or treated with compound **3.14** at the indicated concentrations for 48 h.

3.2.2.5.2 Fluorescence microscopy after Hoechst 33258 staining

Hoechst 33258 is a membrane permeable dye that binds to DNA and emits fluorescence allowing the visualization of nuclear morphological changes. Since cell cycle and Annexin V-FITC/PI results suggested that compound **3.14** has proapoptotic activity, we used fluorescence microscopy to observe the morphology of HeLa cells stained with Hoechst 33258, after treatment with 0.67, 1.34 and 2.68 µM of compound **3.14** during 48 h. Non treated cells were used as control.

The morphological analysis, depicted in Figure 3.25**,** showed that control cells were uniformly stained with Hoechst 33258 and presented round homogeneous nuclei, without morphological changes. HeLa cells exposed to 0.67 µM and 1.34 µM of compound **3.14** during 48 h presented remarkable morphological changes, such as cell shrinkage, chromatin condensation and an evident reduction in the number of cells. The rupture of cell membrane and the nuclear fragmentation were evident after treatment of HeLa cells with 2.68 µM of

compound **3.14**. HeLa cells acquired typical apoptotic morphology after being treated with compound **3.14**, which strongly support the proapoptotic effect of compound **3.14**.

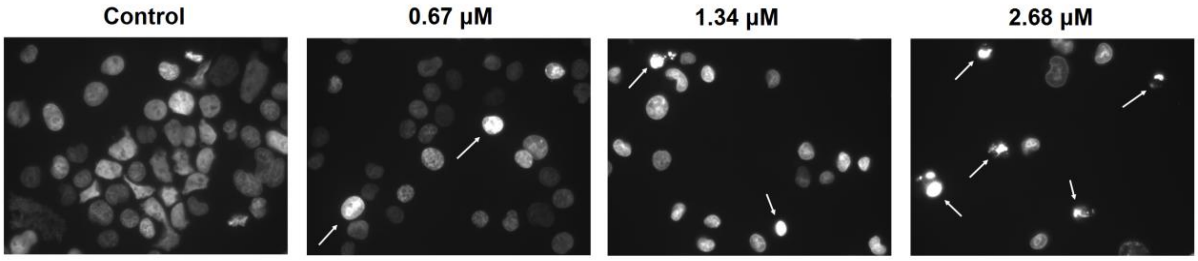

Figure 3.25 Representative fluorescence microscopic images of HeLa cells untreated (control) or treated with compound **3.14** at the indicated concentrations for 48 h. HeLa cells were stained with Hoechst 33258 before analysis by fluorescence microscopy. The white arrows indicate apoptotic cells.

3.2.2.6 Effects of compound 3.14 on the levels of apoptosis related proteins

To gain deeper insight into the mechanism of action of compound **3.14**, its effect on several molecular targets was investigated using western blot analysis. HeLa cells were treated with increasing concentrations of compound **3.14** (0–2.68 µM) for 48 h. Non treated cells were used as control.

Apoptosis is a cell death program regulated by a family of caspases through two major pathways: the extrinsic or death receptor pathway and the intrinsic or mitochondrial pathway.[270] The effects of compound **3.14** on the activation of caspase 3 and caspase 8 were investigated. Results showed that treatment of HeLa cells with 2.68 µM of compound **3.14** resulted in the proteolytic cleavage of pro-caspases 8 and 3 to their active forms (Fig. 3.26). In the same conditions an upregulation of cleaved Poly (ADP-ribose) polymerase (PARP) was also observed. Active caspase 3 cleave PARP, yielding an 85kDa fragment (cleaved PARP), whose presence is a marker of cells undergoing apoptosis.[271] These results clearly suggest that compound **3.14** induced cell death by caspase-dependent apoptosis. Furthermore, the activation of caspase 8 indicates that extrinsic pathway may be involved in the apoptotic process.

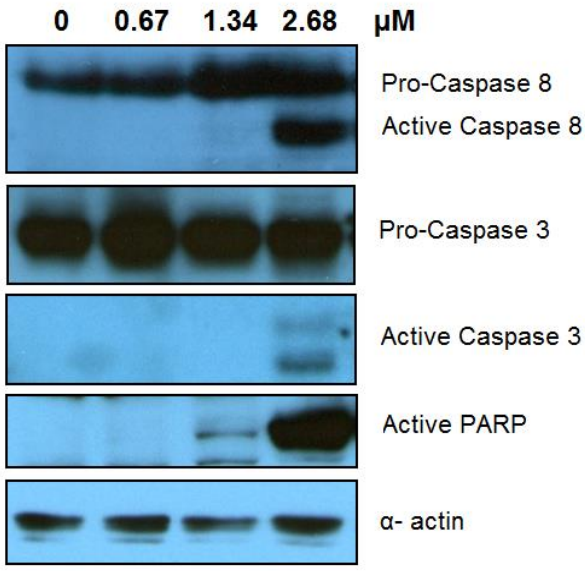

Figure 3.26 Effect of compound **3.14** on the levels of apoptosis-related proteins. HeLa cells were treated with the indicated concentrations of compound **3.14** for 48 h. The levels of the indicated proteins were assessed by western blot analysis. Compound **3.14** induced caspase 8 and caspase 3 activation and the cleavage of PARP.

Active caspase 8 can cleave Bid affording proapoptotic t-Bid, which in turn can establish the connection between the extrinsic and the intrinsic pathways.[272,273] Therefore, the effects of compound **3.14** on the levels of Bid were investigated (Fig. 3.27). It was found that compound **3.14** at 2.68 μM induced the cleavage of Bid (22 kDa) to yield the proapoptotic t-Bid (15 kDa fragment). The effects of compound **3.14** on the levels of Blc-2 and Bax proteins were also examined. In comparison with non treated cells, compound **3.14** induced the upregulation of proapoptotic Bax and the downregulation of antiapoptotic Bcl-2 in a concentration dependent manner (Fig. 3.27). The increase of the ratio of Bax to Bcl-2, suggests that compound **3.14** also activates the mitochondrial pathway.

All these findings suggest that compound **3.14** induces caspase-dependent apoptosis in a dose dependent manner in HeLa cells, and both pathways, extrinsic and intrinsic, are apparently involved in the apoptotic cell death. The cleavage of Bid suggested the convergence of extrinsic and intrinsic pathways at mitochondrial level, because t-Bid could interact with Bcl-2 and Bax proteins, leading to the activation of mitochondrial pathway, with subsequent caspase 3 activation.

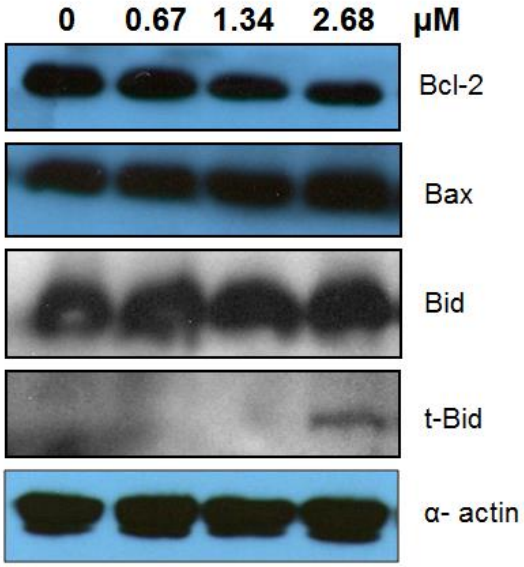

Figure 3.27 Effect of compound **3.14** on the levels of apoptosis-related proteins. HeLa cells were treated with the indicated concentrations of compound **3.14** for 48 h. The levels of the indicated proteins were assessed by western blot analysis. Compound **3.14** downregulated the levels of Bcl-2, upregulated the levels of Bax, and induced the cleavage of Bid into t-Bid.

3.3 Conclusions

A panel of new fluorinated asiatic acid **1.27** derivatives was successfully synthesized and the structures of new compounds were elucidated.

The vast majority of the new derivatives showed improved antiproliferative activity against several cancer cell lines, compared with the parental asiatic acid **1.27**.

Compound **3.14** proved to be the most active compound among all tested derivatives. Further investigation of its mechanism of action in the HeLa cell line revealed that compound **3.14** induced cell-cycle arrest at the G0/G1 phase, which led to cell-growth inhibition via the upregulation of $p21^{cip1/waf1}$ and $p27^{kip1}$ and the downregulation of cyclin E and cyclin D3. Compound **3.14** also induced apoptotic cell death with the activation of caspases 8 and 3 and the cleavage of PARP. The downregulation of Bcl-2, the upregulation of Bax, and the cleavage of Bid induced by compound **3.14** suggest that both intrinsic and extrinsic pathways were involved in apoptosis.

3.4 Experimental section

3.4.1 Chemistry

3.4.1.1 Reagents and solvents

Asiatic acid, Selectfluor®, acetic anhydride, butyric anhydride, 4-(dimethylamino)pyridine (DMAP), pyridinium dichromate (PDC), sodium periodate ($NaIO_4$), piperidine, magnesium sulfate ($MgSO_4$), benzoic anhydride, succinic anhydride, cinnamoyl chloride, 1,1′-carbonyldiimidazole (CDI), 1,1′-carbonylbis(2-methylimidazole) (CBMI), iodine, sodium thiosulfate ($Na_2S_2O_3$), oxalyl chloride, aqueous ammonia solution 25%, methylamine solution 33 wt. % in methanol, glycine methyl ester hydrochloride and *L*-alanine methyl ester hydrochloride, nitromethane and dioxane were purchased from Sigma-Aldrich Co. Tetrahydrofuran (THF), acetone, dichloromethane (DCM) and methanol were obtained from Merck. When necessary, the solvents used in reactions were purified and dried according to usual procedures described in the literature.[274] The solvents used in the workup procedures were purchased from VWR Portugal.

3.4.1.2 Chromatographic techniques

Thin layer chromatography (TLC) was used to monitor the progress of reactions. TLC was carried out in Kieselgel 60HF254/Kieselgel 60G plates, which were observed under UV light and revealed using a mixture of etanol/sulfuric acid (95:5) followed by heating at 120 ^{o}C.

The separation and purification of the synthesized compounds were performed by flash column chromatography (FCC), using Kieselgel 60 (230-400 mesh, Merck) with the appropriate eluent.

3.4.1.3 Analytical techniques and equipment

Melting points were recorded on a BUCHI melting point B-540 apparatus and were uncorrected.

Infrared (IR) spectra were recorded on a Fourier transform spectrometer. The IR measurements were performed using the KBr pellets method. To prepare the KBr pellets, about 2 mg of the solid compound was diluted with 198 mg of KBr. The mixture was ground to a fine powder and pressed at around 12000 psi for 5 min, to obtain a thin and transparent pellet.

NMR spectra were obtained using a Brucker Digital NMR–Avance 400 spectrometer. Deuterated chloroform ($CDCl_3$) was used as the solvent and as the internal standard. The chemical shifts (δ) are reported in parts per million (ppm), and coupling constants (*J*) are reported in hertz (Hz).

Mass spectra were recorded on a Quadrupole/Ion Trap Mass Spectrometer (QIT-MS) (LCQ Advantage MAX, THERMO FINNINGAN). High-resolution mass spectrometry (HRMS) was performed on a Fourier Transform Ion Cyclotron Resonance (FT-ICR) mass spectrometer (Bruker Apex Ultra with a 7 Tesla actively shielded magnet).

The elemental analysis was performed on an Analyzer Elemental Carlo Erba 1108 apparatus by chromatographic combustion.

3.4.1.4 Synthesis of asiatic acid derivatives

2*α*,3β,23-Trihydroxy-12β-fluoro-urs-13,28β-olide (3.1)

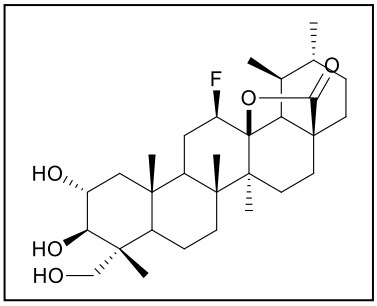

To a stirred solution of asiatic acid **1.27** (300 mg; 0.62 mmol) in nitromethane (14.30 mL) and dioxane (9.50 mL) at 80 ºC, Selectfluor® (650.40 mg, 1.84 mmol) was added. After 22 h, the reaction mixture was evaporated under reduced pressure to remove the organic phase and the crude obtained was dispersed with water (60 mL). The aqueous phase was extracted with ethyl acetate (3 × 60 mL) and the resulting organic phase was washed with 5% aqueous HCl (2 × 60 mL), 10% aqueous $NaHCO_3$ (2 × 60 mL), 10% aqueous Na_2SO_3 (60 mL), and water (60 mL), dried over Na_2SO_4, filtered, and concentrated under vacuum, to afford a light-yellow powder. The crude solid was purified by flash column chromatography (petroleum ether/ethyl acetate, 1:1 → 1:6), to afford **3.1** as a white solid (190.14 mg, 61%). Mp.: 312.1–314.5 ºC. IR (KBr): 3612.0, 3484.7, 3376.7, 2927.4, 2877.3, 1766.5, 1459.9, 1392.4, 1045.2 cm^{-1}. ^1H NMR (400 MHz, $CDCl_3$): δ = 4.86 (dt, J = 45.5 Hz, 1H, H-12), 3.83–

3.77 (m, 1H, H-2), 3.61 (d, *J* =10.7 Hz, 1H, H-3), 3.43 (d, *J* = 9.6 Hz, 1H, H-23), 3.37 (d, *J* =10.7 Hz, 1H, H-23),1.20 (s, 6H), 1.14 (d, *J* = 6.3 Hz, 3H), 1.01 (s, 3H), 0.97 (d, *J* = 5.7 Hz, 3H), 0.80 (s, 3H) ppm. ^{13}C NMR (100MHz, $CDCl_3$): δ = 179.0 (C28), 91.9 (d, *J* =13.8 Hz, C13), 89.5 (d, *J* =186.1 Hz, C12), 78.9, 68.8, 68.3, 55.6 (d, *J* = 2.4 Hz), 48.9 (d, *J* = 9.0 Hz), 48.4, 46.9, 45.2, 44.0 (d, *J* =2.6 Hz), 42.7, 42.5, 39.5, 38.4, 38.2, 33.5, 31.3, 30.7, 27.6, 25.6 (d, *J* = 18.3 Hz), 22.4, 19.4, 18.5, 18.4, 17.5, 17.3, 16.5, 12.7 ppm. DI-ESI-MS *m/z* $[M+H]^+$: 507.00. ESI-HRMS *m/z* calculated for $C_{30}H_{47}FO_5$ $[M + Na]^+$: 529.3305, found: 529.3299.

2*α*,3β,23-Triacetoxy-12β-fluoro-urs-13,28β-olide (3.2)

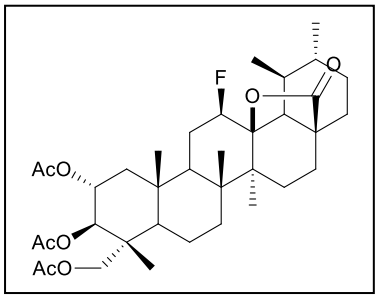

To a solution of **3.1** (100 mg, 0.20 mmol) in dry THF (3 mL), acetic anhydride (84.01 µl, 0.89 mmol) and a catalytic amount of DMAP (10 mg) were added. The mixture was stirred at room temperature in anhydrous conditions. After 2 h 15 min, the reaction mixture was evaporated under reduced pressure to remove the organic phase. The crude obtained was dispersed with water (40 mL) and aqueous phase was extracted with ethyl acetate (2 × 40 mL). The resulting organic phase was washed with 5% aqueous HCl (2 × 20 mL), 10% aqueous $NaHCO_3$ (2 ×20 mL), 10% aqueous Na_2SO_3 (20 mL), water (20 mL) and brine (20 mL), dried over Na_2SO_4, filtered, and concentrated under vacuum to afford compound **3.2** as a white powder (111.89 mg, 90% quantitative). Mp: 172.2–174.2 ºC. IR (KBr): 2956.3, 2875.3, 1778.1, 1747.2, 1459.9, 1369.2, 1236.2, 1043.3 cm^{-1}. ^{1}H NMR (400MHz, $CDCl_3$): δ = 5.21–5.14 (m, 1H, H-2), 5.06 (d, *J* = 10.3 Hz, 1H, H-3), 4.85 (dq, *J* = 45.6 Hz, 1H, H-12), 3.79 (d, *J* = 11.8 Hz, 1H, H-23), 3.60 (d, *J* = 11.8 Hz, 1H, H-23), 2.07 (s, 3H, C$\underline{H}_3$CO), 2.01 (s, 3H, C$\underline{H}_3$CO), 1.98 (s, 3H, C$\underline{H}_3$CO), 1.20 (s, 6H), 1.12 (d, *J* = 6.0 Hz, 3H), 1.09 (s, 3H), 0.96 (d, *J* = 5.0 Hz, 3H), 0.87 (s, 3H) ppm. ^{13}C NMR (100MHz, $CDCl_3$): δ = 178.6 (C28), 170.7 (O$\underline{C}$O), 170.3 (O$\underline{C}$O), 170.3 (O$\underline{C}$O), 91.6 (d, *J* = 14.4 Hz, C13), 89.2 (d, *J* = 186.0 Hz, C12), 74.5, 69.6, 65.1, 52.5 (d, *J* = 3.3 Hz), 49.1 (d, *J* = 9.4 Hz), 47.8, 45.1, 44.1, 43.9 (d, *J* = 2.6 Hz), 42.5, 41.9, 39.5, 38.4, 37.9, 33.5, 31.3, 30.7, 27.6, 25.6 (d, *J* = 19.6 Hz), 22.3, 21.0, 20.8, 20.7, 19.4, 18.4, 18.2, 17.2, 17.2, 16.4, 13.6 ppm. DI-ESI-MS *m/z* $[M+H]^+$: 632.95. ESI-HRMS *m/z* calculated for $C_{36}H_{53}FO_8$ $[M + Na]^+$: 655.3622, found: 655.3617.

2α,3β,23-Tributyroxy-12β-fluoro-urs-13,28β-olide (3.3)

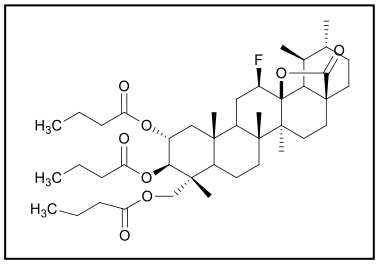

Prepared accordingly to the method described for **3.2** using: compound **3.1** (100 mg, 0.20 mmol), THF (3 mL), DMAP (10 mg) and butyric anhydride (145.39 µl; 0.89 mmol), at room temperature for 3 h, to afford compound **3.3** as a white solid (130.19 mg, 92%). Mp: 176.2–178.1 ºC. IR (KBr): 2964.1, 2875.3, 1774.2, 1739.5, 1459.9, 1180.2 cm^{-1}. ^{1}H NMR (400MHz, $CDCl_3$): δ = 5.21–5.16 (m, 1H, H-2), 5.11 (d, *J* =10.1 Hz, 1H, H-3), 4.86 (dq, *J* = 45.4 Hz, 1H, H-12), 3.84 (d, *J* = 11.9 Hz, 1H, H-23); 3.51 (d, *J* = 11.9 Hz, 1H, H-23), 1.21 (s, 3H), 1.19 (s, 3H), 1.13 (d, *J* = 5.6 Hz, 3H), 1.10 (s, 3H), 0.96–0.88 (m, 18H) ppm. ^{13}C NMR (100MHz, $CDCl_3$): δ = 178.6 (C28), 173.2 (O<u>C</u>O), 172.9 (O<u>C</u>O), 172.7 (O<u>C</u>O), 91.7 (d, *J* = 14.3 Hz, C13), 89.3 (d, *J* = 186.8 Hz, C12), 74.0, 69.4, 64.8, 52.5 (d, *J* = 3.1 Hz), 49.2 (d, *J* = 9.5 Hz), 47.8, 45.1, 44.3, 43.9 (d, *J* = 2.6 Hz), 42.5, 42.0, 39.5, 38.4, 38.0, 36.3, 36.2 (2C), 33.4, 31.3, 30.7, 27.6, 25.6 (d, *J* = 19.8 Hz), 22.3, 19.4, 18.5 (3C), 18.4, 18.1, 17.2, 17.1, 16.5, 13.7, 13.7 (2C), 13.7 ppm. DI-ESI-MS *m/z* $[M+H]^+$: 716.87. ESI-HRMS *m/z* calculated for $C_{42}H_{65}FO_8$ $[M + Na]^+$: 739.4561, found: 739.4556.

2α-Hydroxy-3β,23-isopropylidenedioxy-12β-fluoro-urs-13,28β-olide (3.4)

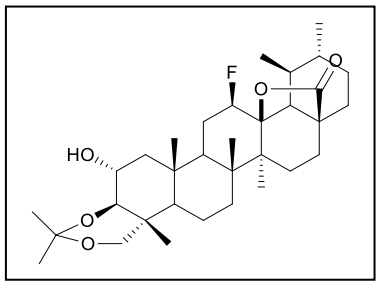

To a solution of **3.1** (305 mg, 0.60 mmol) in dry acetone (30.6 mL) at room temperature, activated molecular sieves, 4Å, and concentrated hydrochloric acid (HCl) in catalytic amounts were added. After 1 h 30 min the reaction mixture was filtered and concentrated under vacuum to afford a light yellow powder. The crude solid was purified by flash column chromatography (petroleum ether/ethyl acetate, 2:1) to afford **3.4** as a white solid (57.65 mg, 17%). Mp: 218.3–221.1 ºC. IR (KBr): 3445.3, 2933.5, 2874.6, 1774.4, 1457.3, 1046.3 cm^{-1}. ^{1}H NMR (400 MHz, $CDCl_3$): δ = 4.85 (dt, *J* = 45.6 Hz, 1H, H-12), 3.83–3.77 (m, 1H, H-2), 3.49 (d, *J* = 10.9 Hz, 1H, H-23), 3.44 (d, *J* =10.4 Hz, 1H, H-23), 3.29 (d, *J* =10.0 Hz, 1H, H-3), 1.43 (s, 6H), 1.21 (s, 3H), 1.18 (s, 3H), 1.13 (d, *J* = 6.3 Hz, 3H), 1.05 (s, 3H), 1.02 (s, 3H), 0.96 (d, *J* = 5.3 Hz, 3H) ppm. ^{13}C NMR (100MHz, $CDCl_3$): δ = 178.8 (C28), 99.6, 91.8 (d, *J* = 14.2 Hz, C13), 89.3 (d, *J* = 185.9 Hz, C12), 82.0, 72.5, 65.2, 52.5 (d, *J* = 3.1 Hz), 51.6, 49.1 (d, *J* = 9.3 Hz), 47.0, 45.1, 44.0 (d, *J* = 2.8 Hz), 42.6, 39.5, 38.4, 38.1, 36.8, 33.4, 31.3, 30.7, 29.7, 27.6, 25.4 (d, *J* = 19.5 Hz), 22.3, 19.4, 19.3, 19.2, 18.5, 17.3,

16.9, 16.5, 13.2 ppm. DI-ESI-MS *m/z* $[M+H]^+$:546.83. ESI-HRMS *m/z* calculated. for $C_{33}H_{51}FO_5$ $[M + H]^+$: 547.3799, found: 547.3793.

2-Oxo-3β,23-isopropylidenedioxy-12β-fluoro-urs-13,28β-olide (3.5)

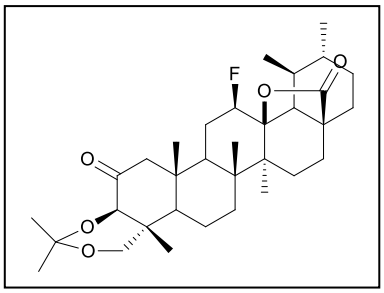

A solution of pyridinium dichromate (290 mg, 0.77 mmol) and acetic anhydride (268.8 µl, 2.85 mmol) in dry dichloromethane (35 mL) was stirred for 30 min at 20 ºC. Then, a solution of **3.4** (385 mg, 0.70 mmol) in dry dichloromethane (15 mL) was slowly added. The resultant mixture was stirred at reflux, in anhydrous conditions, for 8 h. The mixture was evaporated under reduced pressure. The resulting crude was dissolved in ethyl acetate (70 mL) and filtered through a celite pad. The filtered organic phase was washed with water (2 × 70 mL) and brine (70 mL), dried over Na_2SO_4, filtered and evaporated to the dryness to afford a brown powder. The crude solid was purified by flash column chromatography (petroleum ether/ethyl acetate, 3:1 → 2:1), to afford compound **3.5** as a white solid (149.63 mg, 39%). Mp: 213.1–215.9 ºC. IR (KBr): 2936.3, 2875.4, 1770.2, 1710.5, 1457.3, 1048.5 cm^{-1}. ^1H NMR (400 MHz, $CDCl_3$): δ = 4.86 (dq, *J* = 46.2 Hz, 1H, H-12), 4.38 (s, 1H, H-3), 3.67 (d, *J* = 10.5 Hz, 1H, H-23), 3.58 (d, *J* = 10.5 Hz, 1H, H-23), 1.51 (s, 3H), 1.44 (s, 3H), 1.26 (s, 3H), 1.21 (s, 3H), 1.14 (d, *J* = 6.2 Hz, 3H), 1.04 (s, 3H), 1.00 (s, 3H), 0.97 (d, *J* = 5.8 Hz, 3H) ppm. ^{13}C NMR (100MHz, $CDCl_3$): δ = 203.9 (C2), 178.5 (C28), 99.9, 91.5 (d, *J* = 14.3 Hz, C13), 89.0 (d, *J* = 186.2 Hz, C12), 81.6, 71.6, 54.8, 52.5 (d, *J* = 3.4 Hz), 51.6, 49.1 (d, *J* = 9.5 Hz), 45.1, 44.0 (d, *J* = 2.5 Hz), 43.7, 42.8, 42.2, 39.5, 38.4, 33.2, 31.3, 30.7, 29.5, 27.7, 25.4 (d, *J* = 20.0 Hz), 22.3, 19.4, 18.8, 18.6, 18.2, 17.3 (2C), 16.5, 13.1 ppm. DI-ESI-MS *m/z* $[M+H]^+$: 544.91. ESI-HRMS *m/z* calculated for $C_{33}H_{49}FO_5$ $[M + H]^+$: 545.3642, found: 545.3637.

2-Oxo-3β,23-dihydroxy-12β-fluoro-urs-13,28β-olide (3.6)

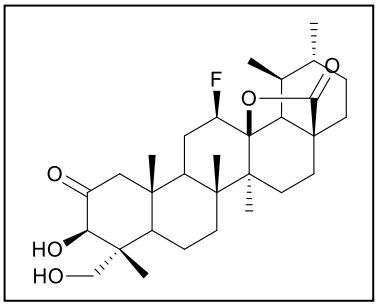

To a solution of **3.5** (100 mg, 0.18 mmol) in dry THF (3.30 mL), 1 M aqueous HCl (0.5 mL) was added. The mixture was stirred at room temperature for 2 h. Then, the reaction mixture was evaporated under reduced pressure to remove the organic phase and the crude obtained was dispersed with water (50 mL). The aqueous phase was extracted with ethyl acetate (3 × 50

mL) and the resultant organic phase was washed with water (2 × 50 mL) and brine (50 mL), dried over Na_2SO_4, filtered, and concentrated under vacuum to afford **3.6** as a white powder (quantitative). Mp: 293.7–296.8 ºC. IR (KBr): 3502.1, 3432.7, 2935.1, 2877.3, 1770.3, 1708.6, 1457.9, 1396.2, 1139.7, 1049.1 cm^{-1}. ^1H NMR (400MHz, $CDCl_3$): δ = 4.88 (dq, *J* = 45.6 Hz, 1H, H-12), 4.35 (s, 1H, H-3), 3.55 (d, *J* = 11.1 Hz, 1H, H-23), 3.49 (d, *J* = 11.1 Hz, 1H, H-23), 1.25 (s, 3H), 1.21 (s, 3H), 1.14 (d, *J* = 6.2 Hz, 3H), 0.97 (d, *J* = 5.3 Hz, 3H), 0.90 (s, 3H), 0.58 (s, 3H) ppm. ^{13}C NMR (100MHz, $CDCl_3$): δ = 211.0 (C2), 178.7 (C28), 91.7 (d, *J* = 14.2 Hz, C13), 89.2 (d, *J* =186.5 Hz, C12), 77.2, 65.4, 53.3, 52.6 (d, *J* = 3.2 Hz), 48.9, 48.8 (d, *J* = 9.5 Hz), 46.3, 45.5, 44.1 (d, *J* = 2.8 Hz), 43.2, 42.9, 39.5, 38.5, 33.3, 31.3, 30.7, 27.7, 25.6 (d, *J* = 19.8 Hz), 22.4, 19.4, 18.1, 18.1, 17.5, 17.3, 16.5, 12.6 ppm. DI-ESI-MS *m/z* $[M+H]^+$: 504.97. ESI-HRMS *m/z* calculated for $C_{30}H_{45}FO_5$ $[M + Na]^+$: 527.3149, found: 527.3143.

2-Oxo-3β,23-diacetoxy-12β-fluoro-urs-13,28β-olide (3.7)

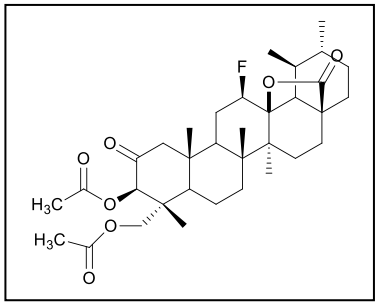

Accordingly to the method described for **3.2,** using compound **3.6** (325 mg, 0.64 mmol), THF (11 mL), acetic anhydride (188.70 µl, 1.99 mmol) and DMAP (32.50 mg). The crude solid was purified by flash column chromatography (petroleum ether/ethyl acetate, 2:1), to afford **3.7** as a white solid (224.67 mg, 60%). Mp: 258.8–261.7 ºC. IR (KBr): 2973.7, 2935.1, 2873.4, 1766.48, 1751.1, 1727.9, 1463.7, 1369.2, 1047.2 cm^{-1}. ^1H NMR (400MHz, $CDCl_3$): δ = 5.22 (s, 1H, H-3), 4.88 (dq, *J* = 45.4 Hz, 1H, H-12), 4.01 (d, *J* = 11.7 Hz, 1H, H-23), 3.78 (d, *J* = 11.7 Hz, 1H, H-23), 2.16 (s, 3H, C$\underline{H}_3$CO), 2.10 (s, 3H, C$\underline{H}_3$CO), 1.25 (s, 3H), 1.22 (s, 3H), 1.15 (d, *J* = 6.4 Hz, 3H), 0.98 (d, *J* = 5.9 Hz, 3H), 0.95 (s, 3H), 0.83 (s, 3H) ppm. ^{13}C NMR (100MHz, $CDCl_3$): δ = 203.0 (C2), 178.5 (C28), 170.5 (O$\underline{C}$O), 170.1 (O$\underline{C}$O), 91.5 (d, *J* = 14.4 Hz, C13), 89.1 (d, *J* = 186.6 Hz, C12), 78.2, 65.3, 54.1, 52.5 (d, *J* = 3.0 Hz), 48.9 (d, *J* = 9.3 Hz), 48.0, 45.6, 45.2, 44.0 (d, *J* = 2.8 Hz), 42.8, 42.3, 39.5, 38.5, 33.3, 31.3, 30.7, 27.7, 25.6 (d, *J* = 19.6 Hz), 22.3, 20.9, 20.6, 19.4, 18.2, 17.9, 17.6, 17.2, 16.5, 13.7 ppm. DI-ESI-MS *m/z* $[M+H]^+$: 588.90. ESI-HRMS *m/z* calculated for $C_{34}H_{49}FO_7$ $[M + Na]^+$: 611.3360, found: 611.3355.

2α,23-Lactol-3-formyl-12β-fluoro-urs-13,28β-olide (3.8)

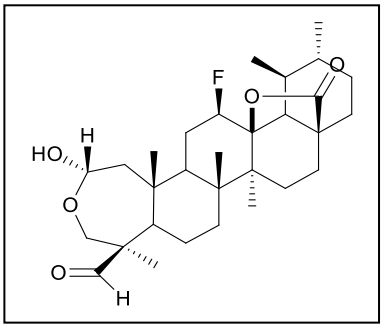

To a solution of **3.1** (650 mg, 1.28 mmol) in methanol / water (16.2 mL / 0.76 mL, 20:1), sodium periodate ($NaIO_4$) (417.05 mg; 1.95 mmol) was added and the mixture was stirred at room temperature. After 1 h, the reaction mixture was evaporated under reduced pressure to remove the organic phase and the crude obtained was dispersed with water (50 mL). The aqueous phase was extracted with ethyl acetate (3 × 50 mL). The resulting organic phase was washed with water (3 × 50 mL) and brine (60 mL), dried over Na_2SO_4, filtered, and concentrated under vacuum. The crude solid was purified by flash column chromatography (petroleum ether/ethyl acetate, 4:1 → 1:1), to afford **3.8** as a white solid (383.13 mg, 59%). Mp: 198.1–200.2 ºC. IR (KBr): 3446.2, 2977.6, 2931.3, 2875.3, 2744.2, 1770.3, 1716.3, 1457.9 cm^{-1}. ^1H NMR (400MHz, $CDCl_3$): δ = 9.94 (s, 1H, C<u>H</u>O), 5.16–5.13 (m, 1H, H-2), 4.83 (dq, *J* = 45.7 Hz, 1H, H-12), 3.95 (d, *J* = 13.5 Hz, 1H), 3.75 (d, *J* = 13.5 Hz. 1H), 1.30 (s, 3H), 1.19 (s, 3H), 1.13 (d, *J* = 6.0 Hz, 3H), 1.06 (s, 3H), 0.99 (s, 3H), 0.96 (d, *J* = 5.2 Hz, 3H) ppm. ^{13}C NMR (100MHz, $CDCl_3$): δ = 205.3 (<u>C</u>HO), 178.6 (C28), 93.4 , 92.0 (d, *J* = 14.5Hz, C13), 89.5 (d, *J* = 186.6, C12), 65.7, 61.2, 53.3, 52.7 (d, *J* = 3.0 Hz), 45.5, 45.2, 45.2 (d, *J* = 9.0 Hz), 44.1 (d, *J* = 2.4 Hz), 42.8, 40.3, 39.5, 38.5, 34.2, 31.2, 30.7, 27.4, 27.0 (d, *J* = 19.4 Hz), 22.2, 20.4, 19.8, 19.4, 18.9, 16.8, 16.5, 15.0 ppm. DI-ESI-MS *m/z* $[M+H]^+$: 505.00. ESI-HRMS *m/z* calculated for $C_{30}H_{45}FO_5$ $[M + Na]^+$: 527.3149, found: 527.3143.

2-Formyl-12β-fluoro-23-hydroxy-A(1)-norurs-2-en-13,28β-olide (3.9)

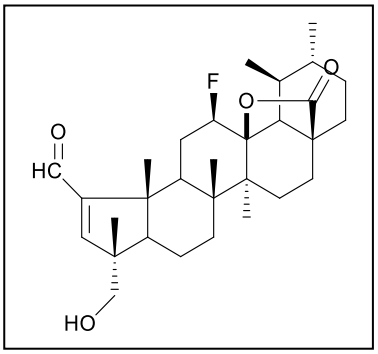

To a solution of **3.8** (300 mg, 0.59 mmol) in dry benzene (29.90 mL), piperidine (1.99 mL) and acetic acid (1.99 mL) were added. The resultant solution was heat at 60 ºC for about 1 h. Then, anhydrous magnesium sulfate was added and the reaction mixture was again heat at 60 ºC under nitrogen atmosphere for additional 6 h. The reaction mixture was evaporated under reduced pressure and the crude obtained was dispersed with water (60 mL). The aqueous phase was extracted with ethyl acetate (3 × 60 mL). The resulting organic phase was washed with water (4 × 50 mL) and brine (60 mL), dried over Na_2SO_4, filtered, and concentrated under vacuum to afford a dark yellow powder. The crude solid was purified by flash column chromatography (petroleum ether/ethyl acetate,

4:1 → 1:1), to afford **3.9** as a white solid (179.59 mg, 62%). Mp: 281.7–283.8 ºC. IR (KBr): 3563.8, 2987.2, 2919.7, 2829.1, 2744.2, 1764.55, 1666.2, 1573.6, 1457.9 cm^{-1}. ^{1}H NMR (400MHz, $CDCl_3$): δ = 9.71 (s, 1H, C<u>H</u>O), 6.74 (s, 1H, H-3), 4.93 (dq, *J* = 45.5 Hz, 1H, H-12), 3.64 (d, *J* = 10.5 Hz, 1H, H-23), 3.47 (d, *J* = 10.5 Hz, 1H, H-23), 1.26 (s, 3H), 1.25 (s, 3H), 1.20 (s, 3H), 1.13 (d, *J* = 6.2 Hz), 1.01 (s, 3H), 0.96 (d, *J* = 5.4 Hz) ppm. ^{13}C NMR (100MHz, $CDCl_3$): δ = 190.4 (<u>C</u>HO), 179.1 (C28), 161.6 (C3), 159.0 (C2), 91.9 (d, *J* = 14.6 Hz, C13), 89.0 (d, *J* = 186.3 Hz, C12), 68.6, 56.4, 52.4 (d, *J* = 2.9 Hz), 51.6, 49.3, 45.0, 45.0 (d, *J* = 10.6 Hz), 44.6, 43.9 (d, *J* = 2.9 Hz), 39.5, 38.0, 34.1, 31.3, 30.6, 28.3 (d, *J* = 20.0 Hz), 27.8, 22.4, 20.4, 20.0, 19.5, 17.6, 16.7, 16.6, 15.6 ppm. DI-ESI-MS *m/z* $[M+H]^+$: 486.98. Anal. Calcd. for $C_{30}H_{43}FO_4$: C, 74.04; H, 8.91. Found: C, 73.76; H, 9.21.

2-Formyl-12β-fluoro-23-acetoxy-A(1)-norurs-2-en-13,28β-olide (3.10)

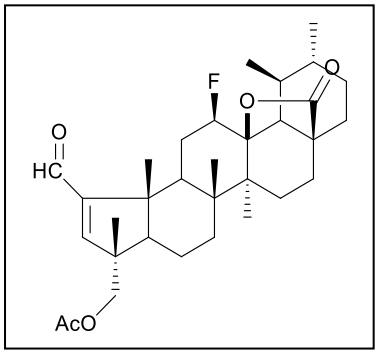

Accordingly to the method described for **3.2** using compound **3.9** (185 mg, 0.38 mmol), dry THF (5.6 mL), acetic anhydride (36.12 µl, 0.38 mmol) and DMAP (18.6 mg), at room temperature for 1 h to afford **3.10** as a white solid (170.4 mg, 85%). Mp: 204.1–207.3 ºC. IR (KBr): 2929.3, 2873.4, 2736.5, 1774.2, 1743.3, 1687.4, 1646.9, 1583.3, 1457.9, 1375.0 cm^{-1}. ^{1}H NMR (400MHz, $CDCl_3$): δ = 9.70 (s, 1H, C<u>H</u>O), 6.68 (s, 1H, H-3), 4.91 (dq, *J* = 45.4 Hz, 1H, H-12), 4.05 (d, *J* = 11.0 Hz, 1H, H-23), 3.95 (d, *J* = 11.0 Hz, 1H, H-23), 2.08 (s, 3H, C<u>H</u>$_3$CO), 1.25 (s, 3H), 1.24 (s, 3H), 1.18 (s, 3H), 1.14 (d, *J* = 6.3 Hz, 3H), 1.05 (s, 3H), 0.96 (d, *J* = 5.5 Hz, 3H) ppm. ^{13}C NMR (100MHz, $CDCl_3$): δ = 190.4 (<u>C</u>HO), 178.9 (C28), 170.9 (O<u>C</u>O), 160.0 (C3), 158.5 (C2), 91.7 (d, *J* = 14.4 Hz, C13), 88.9 (d, *J* = 186.1 Hz, C12), 69.8, 57.9, 52.4 (d, *J* = 3.2 Hz), 51.4, 47.4, 45.2 (d, *J* = 10.5 Hz), 45.0, 44.6, 43.8 (d, *J* = 2.8 Hz), 39.5, 37.9, 34.1, 31.3, 30.6, 28.2 (d, *J* = 20.2 Hz), 22.8, 22.4, 20.8, 20.5, 19.8, 19.5, 17.5, 16.8, 16.6, 15.7 ppm. DI-ESI-MS *m/z* $[M+H]^+$: 529.14. Anal. Calcd. for $C_{32}H_{45}FO_5$: C, 72.70; H, 8.58. Found: C, 72.38; H, 8.89.

2-Formyl-12β-fluoro-23-butyroxy-A(1)-norurs-2-en-13,28β-olide (3.11)

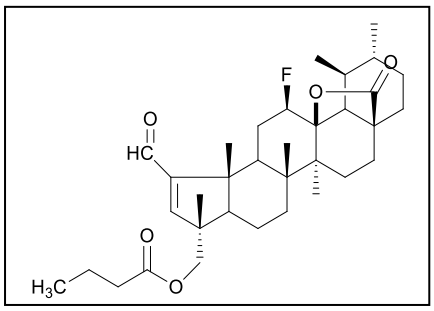

Accordingly to the method described for **3.2** using compound **3.9** (230 mg, 0.47 mmol), dry THF (9 mL), butyric anhydride (78 µl, 0.48 mmol) and DMAP (23.2 mg), at room temperature for 1 h to afford a light yellow solid. The crude solid was purified by flash column chromatography (petroleum ether/ethyl acetate, 4:1 → 2:1), to afford **3.11** as a white solid (131.57 mg, 50%)**.** Mp: 173.4–176.7 ºC. IR (KBr): 2967.9, 2875.3, 2819.4, 2732.6, 1766.5, 1735.6, 1689.3, 1581.3, 1457.9, 1178.3 cm^{-1}. ^{1}H NMR (400MHz, $CDCl_3$): δ = 9.70 (s, 1H, C<u>H</u>O), 6.68 (s, 1H, H-3), 4.91 (dq, *J* = 45.6 Hz, 1H, H-12), 4.06 (d, *J* = 10.7 Hz, 1H, H-23), 3.96 (d, *J* = 10.9 Hz, 1H, H-23), 1.25 (s, 3H), 1.24 (s, 3H), 1.17 (s, 3H), 1.13 (d, *J* = 6.1 Hz, 3H), 1.05 (s, 3H), 0.95 (m, 6H) ppm. ^{13}C NMR (100MHz, $CDCl_3$): δ = 190.4 (<u>C</u>HO), 178.9 (C28), 173.5 (O<u>C</u>O), 160.3 (C3), 158.5 (C2), 91.7 (d, *J* = 14.8 Hz, C13), 88.6 (d, *J* = 186.1 Hz, C12), 69.3, 57.7, 52.4 (d, *J* = 2.6 Hz), 51.4, 47.5, 45.2 (d, *J* = 10.6 Hz), 45.0, 44.6, 43.8 (d, *J* = 2.3 Hz), 39.5, 38.0, 36.2, 34.1, 31.3, 30.6, 28.2 (d, *J* = 19.7 Hz), 27.8, 22.4, 20.5, 19.8, 19.5, 18.5, 17.4, 16.8, 16.6, 15.8, 13.7 ppm. DI-ESI-MS *m/z* $[M+H]^+$: 556.93. Anal. Calcd. for $C_{34}H_{49}FO_5$: C, 73.35; H, 8.87. Found: C, 72.98; H, 9.20.

2-Formyl-12β-fluoro-23-benzoxy-A(1)-norurs-2-en-13,28β-olide (3.12)

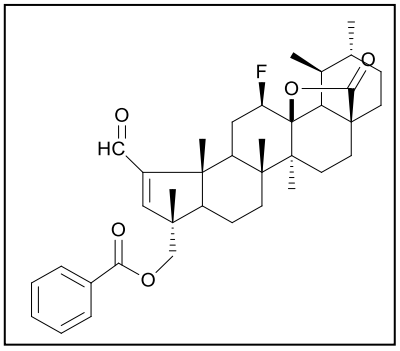

Accordingly to the method described for **3.2** using compound **3.9** (200 mg, 0.41 mmol), dry THF (8 mL), benzoic anhydride (102.30 mg, 0.45 mmol) and DMAP (20 mg), at room temperature for 2 h 30 min in anhydrous conditions to afford a yellow powder. The crude solid was purified by flash column chromatography (petroleum ether/ethyl acetate, 6:1 → 4:1), to afford **3.12** as a white solid (173.20 mg, 71%). Mp: 214.1–216.9 ºC. IR (KBr): 2977.6, 2929.3, 2873.4, 2742.3, 1770.3, 1724.1, 1685.5, 1600.6, 1583.3, 1452.1, 1270.8 cm^{-1}. ^{1}H NMR (400MHz, $CDCl_3$): δ = 9.73 (s, 1H, C<u>H</u>O), 8.02 (d, *J* = 7.3 Hz, 2H), 7.59 (t, *J* = 7.4 Hz, 1H), 7.46 (t, *J* = 7.8 Hz, 2H), 6.78 (s, 1H, H-3), 4.90 (dq, *J* = 44.9 Hz, 1H, H-12), 4.31 (d, *J* = 11.2 Hz, 1H, H-23). 4.23 (d, *J* = 11.2 Hz, 1H, H-23), 1.28 (s, 3H), 1.27 (s, 3H), 1.16 (s, 3H), 1.12 (m, 6H), 0.96 (d, *J* = 5.0 Hz, 3H) ppm. ^{13}C NMR (100MHz, $CDCl_3$): δ = 190.4 (<u>C</u>HO), 178.9 (C28), 166.3 (O<u>C</u>O), 160.1 (C3),

158.6 (C2), 133.3, 129.8, 129.5 (2C), 128.5 (2C), 91.7 (d, *J* = 14.5 Hz, C13), 88.8 (d, *J* = 185.0, C12), 70.0, 57.8, 52.4 (d, *J* = 3.0 Hz), 51.4, 47.9, 45.3 (d, *J* = 10.8 Hz), 45.0, 44.6, 43.8 (d, *J* = 2.8 Hz), 39.5, 37.9, 34.1, 31.3, 30.6, 28.2 (d, *J* = 20.2 Hz), 27.7, 22.4, 20.5, 19.7, 19.5, 17.2, 16.8, 16.2, 15.9 ppm. DI-ESI-MS *m/z* $[M+H]^+$: 590.88. Anal. Calcd. for $C_{37}H_{47}FO_5$: C, 75.22; H, 8.02. Found: C, 75.47; H, 8.38.

2-Formyl-12β-fluoro-23-succinoxy-A(1)-norurs-2-en-13,28β-olide (3.13)

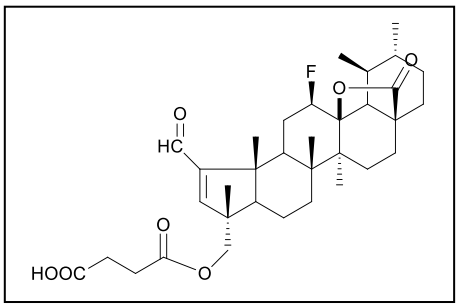

To a solution of **3.9** (250 mg, 0.51 mmol) in dry DCM (15 mL), succinic anhydride (102.80 mg; 1.03 mmol) and DMAP (94.13 mg, 0.77 mmol) were added. The mixture was stirred at room temperature, in anhydrous conditions until the reaction was completed as verified by TLC control. After 4 h, the reaction mixture was evaporated under reduced pressure to remove the organic phase and the crude obtained was dispersed with water (50 mL). Aqueous phase was extracted with ethyl acetate (3 × 50 mL). The resulting organic phase was washed with 5% aqueous HCl (2 × 50 mL), 10% aqueous $NaHCO_3$ (2 x 50 mL), 10% aqueous Na_2SO_3 (50 mL), water (50 mL) and brine (50 mL), dried over Na_2SO_4, filtered, and concentrated under vacuum to afford a yellow powder. The crude solid was purified by flash column chromatography (petroleum ether/ethyl acetate, 2:1 → 1:2), to afford **3.13** as a white solid (210.47 mg, 70%). Mp: 213.6–216.1 ºC. IR (KBr): 2965.9, 2931.3, 2877.3, 1762.6, 1731.8, 1687.4, 1650.8, 1573.6, 1457.9, 1170.6 cm^{-1}. ^1H NMR (400MHz, $CDCl_3$): δ = 9.68 (s, 1H, C<u>H</u>O), 6.65 (s, 1H, H-3), 4.95 (dq, *J* = 45.1 Hz, 1H, H-12), 4.10 (d, *J* = 11.0 Hz, 1H, H-23), 4.02 (d, *J* = 11.0 Hz, 1H, H-23), 2.67 (s, 4H), 1.25 (s, 3H), 1.24 (s, 3H), 1.19 (s, 3H), 1.14 (d, *J* = 6.3 Hz, 3H), 1.04 (s, 3H), 0.95 (d, *J* = 5.3 Hz, 3H) ppm. ^{13}C NMR (100MHz, $CDCl_3$): δ = 190.8 (<u>C</u>HO), 179.0 (C28), 177.3 (<u>C</u>OOH), 171.8 (O<u>C</u>O), 159.5 (C3), 158.5 (C2), 91.8 (d, *J* = 14.2 Hz, C13), 88.8 (d, *J* = 185.4 Hz, C12), 69.4, 57.2, 52.4 (d, *J* = 2.6 Hz), 51.3, 47.7, 45.1 (d, *J* = 9.0 Hz); 45.0, 44.6, 43.9 (d, *J* = 2.8 Hz), 39.5, 37.9, 34.1, 31.3, 30.6, 28.9, 28.7, 28.3 (d, *J* = 20.5 Hz), 27.8, 22.4, 20.4, 19.8, 19.5, 17.4, 16.8, 16.4, 15.7 ppm. DI-ESI-MS *m/z* $[M+H]^+$: 586.91. ESI-HRMS *m/z* calculated for $C_{34}H_{47}FO_7$ $[M + Na]^+$: 609.3204, found: 609.3198.

2-Formyl-12β-fluoro-23-cinnamoxy-A(1)-norurs-2-en-13,28β-olide (3.14)

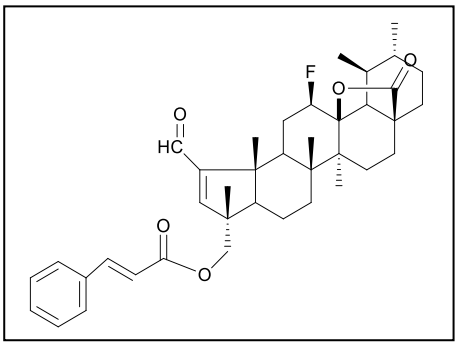

To a stirred solution of **3.9** (250 mg, 0.51 mmol) in dry benzene (15 mL), cinnamoyl chloride (246 mg, 1.54 mmol) and DMAP (187.9 mg, 1.54 mmol) were added. The mixture was stirred at 60 ºC under nitrogen atmosphere until the reaction was completed as verified by TLC control. After 1 h 30 min, the reaction mixture was evaporated under reduced pressure to remove the organic phase and the crude obtained was dispersed with water (50 mL). The aqueous phase was extracted with ethyl acetate (3 × 70 mL). The resulting organic phase was washed with water (4 × 50 mL) and brine (50 mL), dried over Na_2SO_4, filtered, and concentrated under vacuum to afford a light yellow powder. The crude solid was purified by flash column chromatography (petroleum ether/ethyl acetate, 5:1 → 1:1), to afford **3.14** as a white solid (127.59 mg, 40%). Mp: 247.5–249.9 ºC. IR (KBr): 3083.6, 3060.5, 3027.7, 2979.5, 2875.3, 2742.3, 1770.3, 1716.3, 1687.4, 1641.1, 1577.5, 1457.9, 1170.6 cm^{-1}. ^{1}H NMR (400MHz, $CDCl_3$): δ = 9.73 (s, 1H, C<u>H</u>O), 7.70 (d, *J* =16.0 Hz, 1H), 7.54–7.52 (m, 2H), 7.41–7.40 (m, 3H), 6.75 (s, 1H, H-3), 6.45 (d, *J* = 15.9 Hz, 1H), 4.90 (dq, *J* = 45.1 Hz, 1H, H-12), 4.18 (d, *J* = 11.1 Hz, 1H, H-23), 4.13 (d, *J* = 11.0 Hz, 1H, H-23), 1.26 (s, 6H), 1.15 (s, 3H), 1.11 (s, 3H), 1.10 (d, *J* = 6.5 Hz, 3H), 0.95 (d, *J* = 5.2 Hz) ppm. ^{13}C NMR (100MHz, $CDCl_3$): δ = 190.4 (<u>C</u>HO), 178.9 (C28), 166.8 (O<u>C</u>O), 160.2 (C3), 158.5 (C2), 145.5, 134.1, 130.6, 128.9 (2C), 128.1 (2C), 117.4, 91.7 (d, *J* = 14.9 Hz, C13), 88.9 (d, *J* = 186.0 Hz, C12), 69.7, 57.8, 52.4 (d, *J* = 3.2 Hz), 51.4, 47.7, 45.3 (d, *J* = 10.4 Hz), 45.0, 44.6, 43.8 (d, *J* = 2.8 Hz), 39.4, 37.9, 34.1, 31.3, 30.6, 28.2 (d, *J* = 20.1 Hz), 27.8, 22.4, 20.5, 19.8, 19.6, 17.5, 16.8, 16.6, 15.8 ppm. DI-ESI-MS *m/z* $[M+H]^+$: 616.97. Anal. Calcd. for $C_{39}H_{49}FO_5$: C, 75.94; H, 8.01. Found: C, 75.85; H, 8.14.

2-Formyl-12β-fluoro-23-(1H-imidazole-1-carbonyloxy)-A(1)-norurs-2-en-13,28β-olide (3.15)

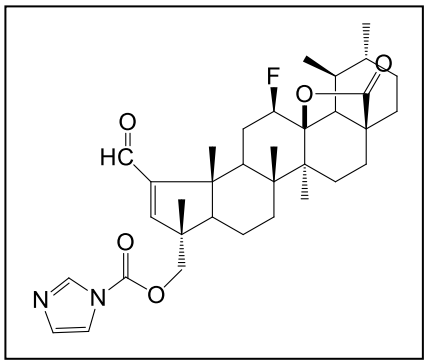

To a solution of compound **3.9** (200 mg, 0.41 mmol) in anhydrous THF (8 mL), CDI (133.28 mg, 0.82 mmol) was added. The reaction mixture was stirred at reflux temperature and N_2 atmosphere. After 1 h 50 min, the reaction mixture was evaporated under reduced pressure to remove the organic phase and the crude obtained was dispersed with water (60 mL). The aqueous phase was extracted with diethyl ether (3 × 60 mL). The combined organic phases were washed with water (4 × 50 mL) and brine (60 mL), dried over Na_2SO_4, filtered, and concentrated under vacuum to afford a yellowish powder. The crude solid was purified by flash column chromatography (petroleum ether/ethyl acetate, 1:1 → 1:2), to afford **3.15** as a white solid (168.19 mg, 70%). Mp: 210.2–212.8 ºC. IR (KBr): 3139.5, 3114.5, 2979.5, 2933.2, 2873.4, 2757.7, 1770.3, 1681.6, 1581.3, 1471.4 cm^{-1}. ^1H NMR (400MHz, $CDCl_3$): δ = 9.73 (s, 1H, C<u>H</u>O), 8.11 (s, 1H), 7.40 (t, *J* = 1.2 Hz, 1H), 7.10 (s, 1H), 6.70 (s, 1H, H-3), 4.90 (dq, *J* = 45.0 Hz, 1H, H-12), 4.40 (d, *J* = 10.9 Hz, 1H, H-23), 4.31 (d, *J* = 10.9 Hz, 1H, H-23), 1.28 (s, 3H), 1.27 (s, 3H), 1.14 (s, 3H), 1.12 (m, 6H), 0.96 (d, *J* = 5.2 Hz) ppm. ^{13}C NMR (100MHz, $CDCl_3$): δ = 190.4 (<u>C</u>HO), 179.2 (C28), 159.6, 158.3, 148.9, 137.3, 131.4, 117.3, 91.9 (d, *J* = 14.6 Hz, C13), 89.0 (d, *J* = 186.0, C12), 73.2, 58.1, 52.8 (d, *J* = 2.9 Hz), 51.8, 48.1, 45.7 (d, *J* = 10.9 Hz), 45.3, 44.9, 42.2 (d, *J* = 2.9 Hz), 39.8, 38.3, 35.0, 31.6, 31.0, 28.6 (d, *J* = 20.7 Hz), 28.1, 22.7, 20.8, 20.1, 19.8, 17.7, 17.2, 17.0, 16.1 ppm. DI-ESI-MS *m/z* $[M+H]^+$: 581.20. ESI-HRMS *m/z* calculated for $C_{34}H_{45}FN_2O_5$ $[M + H]^+$: 581.3391, found: 581.3385.

2-Formyl-12β-fluoro-23-(2′-methyl-1H-imidazole-carbonyloxy)-A(1)-norurs-2-en-13,28β-olide (3.16)

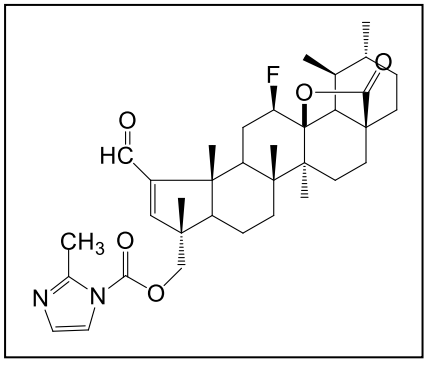

To a solution of compound **3.9** (230 mg, 0.47 mmol) in anhydrous THF (9 mL), CBMI (224.73 mg, 1.18 mmol) was added. The reaction mixture was stirred at reflux temperature and N_2 atmosphere. After 6 h, the reaction mixture was evaporated under reduced pressure to remove the organic phase and the crude obtained was dispersed with water (60 mL). The

aqueous phase was extracted with diethyl ether (3 × 60 mL). The combined organic phases were washed with water (4 × 50 mL) and brine (60 mL), dried over Na_2SO_4, filtered, and concentrated under vacuum to afford **3.16** as a yellowish powder (256.4 mg, 91%). Mp: 226.5–229.3 ºC. IR (KBr): 3147.3, 3114.5, 2979.5, 2873.4, 2751.9, 1770.3, 1681.6, 1457.9 cm^{-1}. ^1H NMR (400MHz, $CDCl_3$): δ = 9.72 (s, 1H, CHO), 7.29 (d, *J* = 1.6 Hz, 1H), 6.87 (d, *J* = 1.5 Hz, 1H), 6.70 (s, 1H, H-3), 4.89 (dq, *J* = 45.1 Hz, 1H, H-12), 4.36 (d, *J* = 11.0 Hz, 1H, H-23), 4.25 (d, *J* = 10.9 Hz, 1H, H-23), 2.63 (s, 3H), 1.27 (s, 3H), 1.26 (s, 3H), 1.13–1.11 (m, 9H), 0.95 (d, *J* = 5.1 Hz, 3H) ppm. ^{13}C NMR (100MHz, $CDCl_3$): δ = 190.0 (CHO), 178.8 (C28), 159.1, 158.3, 149.4, 147.9, 128.3, 117.7, 91.6 (d, *J* = 14.2 Hz, C13), 88.7 (d, *J* = 186.5 Hz, C12), 72.4, 57.5, 52.4 (d, *J* = 3.1 Hz), 51.4, 47.7, 45.3 (d, *J* = 10.5 Hz), 44.9, 44.6, 43.8 (d, *J* = 3.0 Hz), 39.4, 37.9, 34.1, 31.2, 30.6, 28.2 (d, *J* = 20.4 Hz), 27.7, 22.3, 20.4, 19.8, 19.4, 17.3, 16.8, 16.8, 16.5, 15.7 ppm. DI-ESI-MS *m/z* $[M+H]^+$: 595.75. ESI-HRMS *m/z* calculated for $C_{35}H_{47}FN_2O_5$ $[M + H]^+$: 595.3547, found: 595.3542.

2-Cyano-12β-fluoro-23-hydroxy-A(1)-norurs-2-en-13,28β-olide (3.17)

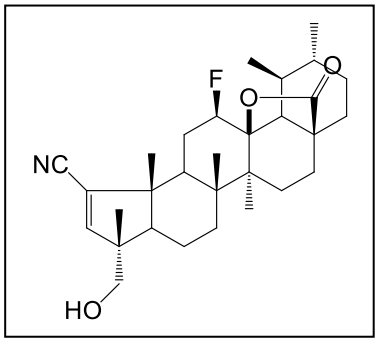

To a solution of **3.9** (270 mg, 0.55 mmol) in THF (4 mL), 25% aqueous ammonium solution (12.5 mL) and iodine (322.69 mg, 1.27 mmol) were added. The mixture was stirred at room temperature until the reaction was completed (the dark solution became colorless) as verified by TLC control. After 6 h 30 min the reaction mixture was charged with 5% aqueous $Na_2S_2O_3$ (50 mL) and extracted with ethyl acetate (3 × 60 mL). The resulting organic phases were washed with water (50 mL) and brine (50 mL), dried over Na_2SO_4, filtered, and concentrated under vacuum to afford a yellow powder. The crude solid was purified by flash column chromatography (petroleum ether/ethyl acetate, 2:1 → 1:2), to afford **3.17** as a light yellow solid (151.71 mg, 57%). Mp: 338.0–340.7 ºC. IR (KBr): 3529.1, 2987.2, 2925.5, 2877.3, 2210.0, 1762.62, 1668.1, 1581.3, 1459.9 cm^{-1}. ^1H NMR (400MHz, $CDCl_3$): δ = 6.54 (s, 1H, H-3), 5.00 (dq, *J* = 45.4 Hz, 1H, H-12), 3.57 (d, *J* = 10.6 Hz, 1H, H-23), 3.40 (d, *J* = 10.9 Hz, 1H, H-23), 1.29 (s, 3H), 1.25 (s, 3H), 1.24 (s, 3H), 1.17 (d, *J* = 6.3 Hz, 3H), 1.00 (s, 3H), 0.98 (d, *J* = 5.6 Hz, 3H) ppm. ^{13}C NMR (100MHz, $CDCl_3$): δ = 178.8 (C28), 154.4 (C3), 127.0 (C2), 117.2 (CN), 91.6 (d, *J* = 14.2 Hz, C13), 88.3 (d, *J* = 186.9 Hz, C12), 68.5, 55.5, 52.5 (d, *J* = 3.2 Hz), 52.1, 50.7, 45.0, 44.6 (d, *J* = 10.3 Hz), 44.2, 44.0 (d, *J* = 2.7 Hz), 39.5, 38.0, 34.1, 31.3, 30.6, 27.8, 26.6 (d, *J* = 20.1 Hz), 22.3,

20.2, 20.1, 19.5, 17.6, 16.9, 16.8, 15.6 ppm. DI-ESI-MS *m/z* $[M+H]^+$: 484.34. ESI-HRMS *m/z* calculated for $C_{30}H_{42}FNO_3$ $[M + Na]^+$: 506.3046, found: 506.3041.

2*α*,3β,23-Triacetoxyurs-12-en-28-oic acid (3.18)

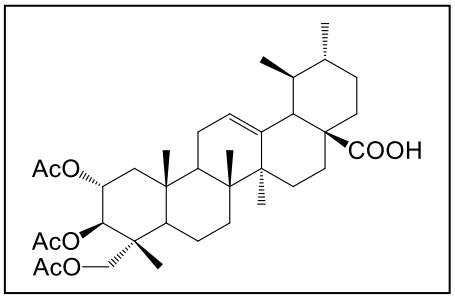

Prepared accordingly to the method described for **3.2** using asiatic acid **1.27** (1000 mg, 2.05 mmol), dry THF (30 mL), acetic anhydride (1.16 mL, 12.28 mmol) and DMAP (100 mg), at room temperature for 4 h in anhydrous conditions to afford **3.18** as a white powder (quantitative). Mp: 150.0–152.0 ºC. IR (KBr): 3463.53, 2948.63, 2871.49, 1816.62, 1747.19, 1455.99, 1369.21, 1236.15, 1045.23 cm^{-1}. ^1H NMR (400MHz, $CDCl_3$): δ = 5.23 (t, *J* = 3.2 Hz, 1H, H-12), 5.19–5.13 (m, 1H, H-2), 5.08 (d, *J* = 10.3 Hz, 1H, H-3), 3.85 (d, *J* = 11.9 Hz, 1H, H-23), 3.58 (d, *J* = 11.9 Hz, 1H, H-23), 2.08 (s, 3H, C$\underline{H}_3$CO), 2.02 (s, 3H, C$\underline{H}_3$CO), 1.97 (s, 3H, C$\underline{H}_3$CO), 1.10 (s, 3H), 1.07 (s, 3H), 0.94 (d, *J* = 5.3 Hz, 3H), 0.87 (s, 3H), 0.85 (d, *J* = 5.4 Hz, 3H), 0.76 (s, 3H) ppm. ^{13}C NMR (100MHz, $CDCl_3$): δ = 183.1 (C28), 170.9 (O$\underline{C}$O), 170.5 (O$\underline{C}$O), 170.4 (O$\underline{C}$O), 138.0, 125.3, 74.8, 69.9, 65.3, 52.5, 47.9, 47.6, 47.8, 43.7, 42.0, 41.9, 39.5, 39.0, 38.8, 37.8, 36.6, 32.4, 30.5, 27.9, 24.0, 23.4, 23.3, 21.1, 21.1, 20.9, 20.8, 17.9, 17.0, 16.9, 16.9, 13.9 ppm. DI-ESI-MS *m/z* $[M+H]^+$: 615.10. ESI-HRMS *m/z* calculated for $C_{36}H_{54}O_8$ $[M + Na]^+$: 637.3716, found: 637.3711.

2*α*,3β,23-Triacetoxyurs-12-en-28-amide (3.19)

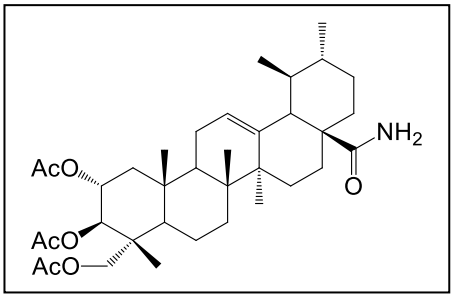

To a solution of **3.18** (660 mg, 1.07 mmol), in dry DCM (33 mL), oxalyl chloride (462.43 µl, 5.39 mmol) was slowly added. The resultant mixture was stirred at room temperature for 24 h. The solvent was removed by evaporation under reduced pressure, and petroleum ether (2 mL) was added to the residue and concentrated to dryness to give the acyl chloride derivative, which, without purification, was dissolved in THF (70 mL). Then, aqueous ammonia solution 25% (35 mL) was added and the resultant mixture was stirred at room temperature for 3 hours. The mixture was concentrated under vacuum to remove the solvent and the crude obtained was dispersed with water (60 mL). Aqueous phase was extracted with ethyl acetate (3 × 60 mL). The combined organic phase was washed with 5% aqueous HCl (2 × 60 mL), 10% aqueous $NaHCO_3$ (2 × 60 mL),

water (60 mL), dried over Na_2SO_4, filtered, and concentrated under vacuum to afford **3.19** as a light yellow powder (636.75 mg, 97%). Mp: 143.2–146.4 ºC. IR (KBr): 3477.0, 3367.1, 2950.6, 1747.2, 1671.9, 1600.6, 1455.9, 1234.2 cm^{-1}. ^1H NMR (400MHz, $CDCl_3$): δ = 5.82 (br s, 1H), 5.43 (br s, 1H), 5.31 (t, *J* = 3.1 Hz, 1H, H-12), 5.19–5.13 (m, 1H, H-2), 5.08 (d, *J* = 10.2 Hz, 1H, H-3), 3.85 (d, *J* = 11.7 Hz, 1H, H-23), 3.58 (d, *J* = 11.9 Hz, 1H, H-23), 2.08 (s, 3H, C$\underline{H}_3$CO), 2.02 (s, 3H, C$\underline{H}_3$CO), 1.98 (s, 3H, C$\underline{H}_3$CO), 1.10 (s, 6H), 0.96 (s, 3H), 0.88 (d, *J* = 6.9 Hz, 3H), 0.85 (s, 6H) ppm. ^{13}C NMR (100MHz, $CDCl_3$): δ = 181.0 (C28), 170.8 (O$\underline{C}$O), 170.5 (O$\underline{C}$O), 170.4 (O$\underline{C}$O), 139.9 (C13), 125.2 (C12), 74.7, 69.9, 62.3, 54.2, 48.0, 47.6, 47.5, 43.8, 42.5, 41.9, 39.7, 39.4, 39.0, 37.8, 37.1, 32.3, 30.8, 27.8, 24.8, 23.4, 23.1, 21.2, 21.1, 20.9, 20.8, 17.9, 17.2, 17.1, 17.0, 13.9 ppm. DI-ESI-MS *m/z* $[M+H]^+$: 613.96. ESI-HRMS *m/z* calculated for $C_{36}H_{55}NO_7$ $[M + Na]^+$: 636.3876, found: 636.3871.

N-(2α,3β,23-triacetoxyurs-12-en-28- oyl)methyl amine (3.20)

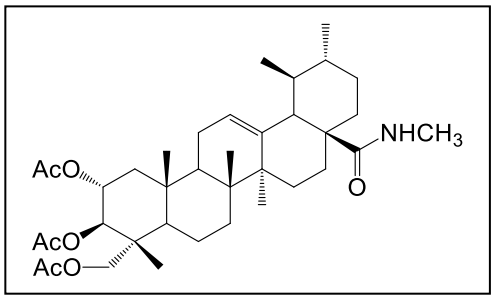

To a solution of **3.18** (500 mg, 0.81 mmol), in dry DCM (25 mL), oxalyl chloride (349.92 µl, 4.07 mmol) was slowly added. The resultant mixture was stirred at room temperature for 19 h. The solvent was removed by evaporation under reduced pressure, and petroleum ether (2 mL) was added to the residue, concentrated to dryness to give the acyl chloride. The acyl chloride was dissolved in dry dichloromethane (25 mL), basified to pH 8–9 with triethylamine (aprox. 300 µl), and methylamine (sol. 33% w/v in ethanol) (306.08 µl, 3.25 mmol) was added. The resultant mixture was stirred at room temperature for 4 h. The solvent was removed by evaporation under reduced pressure. The residue resultant was dispersed with water, acidified to pH 3–4 with aqueous HCl 1 M (aprox. 0,3 mL). The crude was diluted with water (40 mL), and extracted with ethyl acetate (3 × 40 mL). The combined organic phase was washed with 5% aqueous HCl (2 × 50 mL), 10% aqueous $NaHCO_3$ (2 × 50 mL), water (50 mL), dried over Na_2SO_4, filtered, and concentrated under vacuum to afford **3.20** as a white solid (470 mg, 92%). Mp: 122.4–125.1 ºC. IR (KBr): 3440.4, 2948.6, 2871.5, 1747.2, 1648.8, 1234.2 cm^{-1}. ^1H NMR (400MHz, $CDCl_3$): δ = 5.89–5.86 (m, 1H, N$\underline{H}$CH_3), 5.31 (t, *J* = 3.0 Hz, 1H, H-12), 5.19–5.12 (m, 1H, H-2), 5.08 (d, *J* = 10.3 Hz, 1H, H-3), 3.84 (d, *J* = 11.8 Hz, 1H, H-23), 3.58 (d, *J* = 12.0 Hz, 1H, H-23), 2.72 (d, *J* = 4.4 Hz, 2H, NHC$\underline{H}_3$) 2.07 (s, 3H, C$\underline{H}_3$CO), 2.02 (s, 3H, C$\underline{H}_3$CO), 1.98 (s, 3H, C$\underline{H}_3$CO), 1.10 (s, 3H), 1.08 (s, 3H), 0.94 (s, 3H), 0.89 (s, 3H), 0.86

(d, *J* = 6.5 Hz, 3H), 0.76 (s, 3H) ppm. ^{13}C NMR (100MHz, $CDCl_3$): δ = 178.6 (C28), 170.8 (O<u>C</u>O), 170.5 (O<u>C</u>O), 170.4 (O<u>C</u>O), 140.3 (C13), 125.0 (C12), 74.7, 69.9, 65.2, 53.7, 47.6, 47.6, 47.4, 43.7, 42.4, 41.9, 39.7, 39.5, 39.1, 37.7, 36.9, 32.1, 30.8, 27.7, 26.2, 24.9, 23.4, 23.2, 21.2, 21.1, 20.8, 20.8, 17.8, 17.2, 17.0, 16.6, 13.9 ppm. DI-ESI-MS *m/z* $[M+H]^+$: 628.23. ESI-HRMS *m/z* calculated for $C_{37}H_{57}NO_7$ $[M + H]^+$: 628.4213, found: 628.4208.

Methyl N-(2*α*,3β,23-triacetoxyurs-12-en-28-oyl)glycinate (3.21)

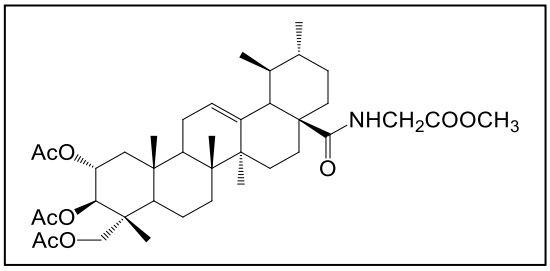

Prepared from **3.18** (600 mg, 0.98 mmol) accordingly to a previous reported method[211] to afford compound **3.21** as a light yellow powder (624.8 mg, 93%)**.** Mp: 174.9–177.8 ºC. IR (KBr): 3421.1, 2950.5, 2927.4, 2871.5, 1745.3, 1654.6, 1369.21, 1234.2, 1043.30 cm^{-1}. ^{1}H NMR (400MHz, $CDCl_3$): δ = 6.47 (m, 1H, N<u>H</u>CH_2COOCH_3), 5.40 (t, *J* = 3.1 Hz, 1H, H-12), 5.19–5.12 (m, 1H, H-2), 5.08 (d, *J* = 10.3 Hz, 1H, H-3), 4.11–4.05 (m, 1H, NHC<u>H</u>$_2COOCH_3$), 3.87–3.82 (m, 1H, NHC<u>H</u>$_2COOCH_3$), 3.84 (d, *J* = 12.3 Hz, 1H, H-23), 3.76 (s, 3H, $NHCH_2COOC$<u>H</u>$_3$), 3.58 (d, *J* = 11.7 Hz, 1H, H-23), 2.08 (s, 3H, C<u>H</u>$_3$CO), 2.02 (s, 3H, C<u>H</u>$_3$CO), 1.98 (s, 3H, C<u>H</u>$_3$CO), 1.09 (s, 6H), 0.96 (s, 3H), 0.88 (s, 3H), 0.86 (d, *J* = 6.9 Hz, 3H), 0.72 (s, 3H) ppm. ^{13}C NMR (100MHz, $CDCl_3$): δ = 178.0, 170.8, 170.6, 170.5, 170.4, 139.2, 125.7, 74.8, 69.9, 65.3, 53.6, 52.3, 47.7, 47.6, 47.5, 43.8, 42.3, 41.9, 41.5, 39.7, 39.6, 39.0, 37.7, 36.9, 32.2, 30.8, 27.7, 24.8, 23.5, 23.2, 21.2, 21.0, 20.9, 20.8, 17.8, 17.1, 17.1, 16.5, 13.9 ppm. DI-ESI-MS *m/z* $[M+H]^+$:686.4. ESI-HRMS *m/z* calculated for $C_{39}H_{59}NO_9$ $[M + H]^+$: 686.4268, found: 686.4263.

Methyl N-(2*α*,3β,23-triacetoxyurs-12-en-28-oyl)alaninate (3.22)

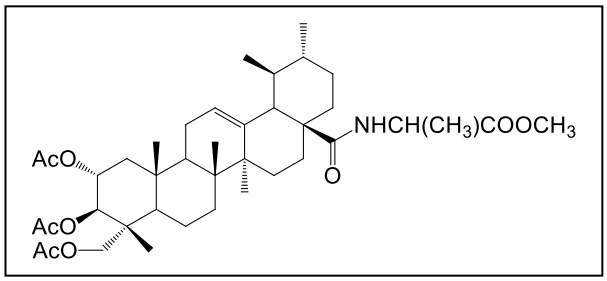

Prepared from **3.18** (400 mg, 0.65 mmol) accordingly to a previous reported method[211] to afford compound **3.22** as a light yellow powder (426 mg, 94%). Mp: 219.2–222.4 ºC. IR (KBr): 2973.7, 2950.6, 2871.5, 1747.2, 1656.6, 1455.9, 1371.1, 1236.2 cm^{-1}. ^{1}H NMR (400MHz, $CDCl_3$): δ = 6.60 (d, *J* = 5.8 Hz, 1H, N<u>H</u>$CH(CH_3)COOCH_3$), 5.39 (t, *J* = 3.1 Hz, 1H, H-12), 5.18–5.12 (m, 1H, H-2), 5.07 (d, *J* = 10.4 Hz, 1H, H-3), 4.49–4.41 (m, 1HNHC<u>H</u>$(CH_3)COOCH_3$), 3.84 (d, *J* = 11.8 Hz, 1H, H-23), 3.73 (s, 3H, $NHCH(CH_3)COOC$<u>H</u>$_3$) 3.58 (d, *J* = 11.8 Hz, 1H, H-23), 2.08

(s, 3H, C<u>H</u>$_3$CO), 2.02 (s, 3H, C<u>H</u>$_3$CO), 1.98 (s, 3H, C<u>H</u>$_3$CO), 1.36 (d, *J* = 7.0 Hz, 3H, NHCH(C<u>H</u>$_3$)COOCH$_3$), 1.08 (s, 6H), 0.95 (s, 3H), 0.87 (s, 6H), 0.69 (s, 3H) ppm. ^{13}C NMR (100MHz, $CDCl_3$): δ = 177.3, 173.7, 170.9, 170.5, 170.4, 138.5, 125.9, 74.8, 69.9, 65.3, 53.5, 52.4, 48.2, 47.6, 47.5, 43.7, 42.3, 41.9, 39.6, 39.6, 39.0, 37.7, 37.2, 32.4, 30.8, 27.7, 24.6, 23.4, 23.2, 21.2, 21.1, 20.9, 20.8, 18.7, 17.8, 17.1, 17.0, 16.5, 13.9 ppm. DI-ESI-MS *m/z* $[M+H]^+$:700.5. ESI-HRMS *m/z* calculated for $C_{40}H_{61}NO_9$ $[M + H]^+$: 700.4425, found: 700.4419.

2*α*,3β,23-Triacetoxy-12β-fluoro-ursa-13,28β-lactam (3.23)

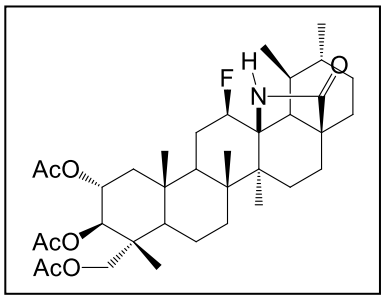

To stirred solution of **3.19** (610 mg, 0.99 mmol) in nitromethane (18.30 mL) and dioxane (12.20 mL) at 80 ºC, Selectfluor® (1057.89 mg, 2.99 mmol) was added. The mixture was stirred at 80 ºC, in anhydrous conditions, until the reaction was completed as verified by TLC control. After 25 h, the solvent was removed by evaporation under reduced pressure and the crude obtained was dispersed with water (50 mL). Aqueous phase was extracted with ethyl acetate (3 × 50 mL). The combined organic phase was washed with water (4 × 50 mL), dried over Na_2SO_4, filtered, and concentrated under vacuum to afford a light yellow solid. The crude solid was purified by flash column chromatography (petroleum ether/ethyl acetate, 1:1 → 1:4), to afford **3.23** as a white solid (268.4 mg, 43%). Mp: 202.7–205.6 ºC. IR (KBr): 2981.4, 2937.1, 2869.6, 1766.5, 1739.5, 1457.9, 1369.2, 1238.1, 1041.4 cm^{-1}. ^{1}H NMR (400MHz, $CDCl_3$): δ = 5.22–5.16 (m, 1H, H-2), 5.07 (d, *J* = 10.3 Hz, 1H, H-3), 4.85 (dq, *J* = 45.6 Hz, 1H, H-12), 3.81 (d, *J* = 11.7 Hz, 1H, H-23), 3.61 (d, *J* = 11.9 Hz, 1H, H-23), 2.08 (s, 3H, C<u>H</u>$_3$CO), 2.02 (s, 3H, C<u>H</u>$_3$CO), 1.99 (s, 3H, C<u>H</u>$_3$CO), 1.21 (s, 3H), 1.16 (s, 3H), 1.12 (d, *J* = 6.4 Hz, 3H), 1.10 (s, 3H), 0.97 (d, *J* = 5.1 Hz, 3H), 0.89 (s, 3H) ppm. ^{13}C NMR (100MHz, $CDCl_3$): δ = 175.4 (C28), 170.8 (O<u>C</u>O), 170.3 (2C, 2 × O<u>C</u>O), 91.3 (d, *J* = 14.4 Hz, C13), 89.54 (d, *J* = 185.9 Hz, C12), 74.6, 69.7, 65.2, 59.9 (d, *J* = 2.9 Hz), 49.2 (d, *J* = 9.7 Hz), 47.8, 44.5, 44.4 (d, *J* = 3.0 Hz), 44.2, 42.5, 41.9, 39.5, 38.3, 38.0, 33.5, 32.7, 30.9, 27.6, 25.7 (d, *J* = 19.6 Hz), 24.0, 21.0, 20.9, 20.7, 19.5, 18.4, 18.2, 17.5, 17.3, 16.4, 13.6 ppm. DI-ESI-MS *m/z* $[M+H]^+$: 632.32. Anal. Calcd. for $C_{36}H_{54}FNO_7$: C, 68.44; H, 8.61; N, 2.22. Found: C, 68.08; H, 8.54; N, 1.90.

Methyl N-(2α,3β,23-triacetoxy-12β-fluoro-ursa-13,28β-lactam) (3.24)

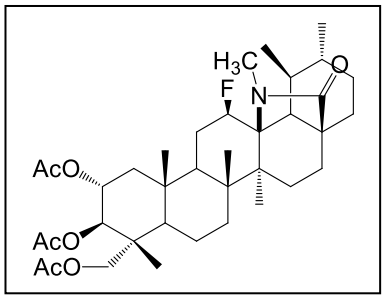

Prepared accordingly to the method described for **3.23** using compound **3.20** (420 mg, 0.67 mmol), nitromethane (16.76 mL), dioxane (10.90 mL) and Selectfluor® (709.08 mg, 2 mmol) at 80 ºC, in anhydrous conditions, for 46 h. The crude solid was purified by flash column chromatography (petroleum ether/ethyl acetate, 1:3 → 1:4) to afford **3.24** as a white solid (322,21 mg, 75%). Mp: 160.2–163.1 ºC. IR (KBr): 2956.34, 2873.42, 1749.12, 1716.34, 1461.78, 1369.21, 1035.59 cm^{-1}. ^{1}H NMR (400MHz, $CDCl_3$): δ = 5.22–5.16 (m, 1H, H-2), 5.07 (d, *J* = 10.6 Hz, 1H, H-3), 4.87 (dq, *J* = 45.9 Hz, 1H, H-12), 3.80 (d, *J* = 11.74 Hz, 1H, H-23), 3.61 (d, *J* = 11.8 Hz, 1H, H-23), 2.99 (s, 3H), 2.08 (s, 3H, C$\underline{H}_3$CO), 2.02 (s, 3H, C$\underline{H}_3$CO), 1.99 (s, 3H, C$\underline{H}_3$CO), 1.23 (s, 3H), 1.16 (s, 3H), 1.12–1.10 (m, 6H), 0.96 (d, *J* = 5.1 Hz, 3H), 0.88 (s, 3H) ppm. ^{13}C NMR (100MHz, $CDCl_3$): δ = 170.8 (O$\underline{C}$O), 170.3 (2C, 2 × O$\underline{C}$O), 166.5 (C28), 90.8 (d, *J* = 14.8 Hz, C13), 89.7 (d, *J* = 185.4 Hz, C12), 74.6, 69.7, 65.1, 52.8 (d, *J* = 3.0 Hz), 49.2 (d, *J* = 9.5 Hz), 47.8, 44.4 (d, *J* = 2.9 Hz), 44.2, 44.2, 42.7, 41.9, 39.7, 38.3, 37.9, 33.5, 33.3, 32.9, 31.1, 27.6, 25.7 (d, *J* = 19.7 Hz), 24.3, 21.0, 20.9, 20.7, 19.5, 18.5, 18.2, 17.5, 17.2, 16.4, 13.6 ppm. DI-ESI-MS *m/z* $[M+H]^+$: 646.38. ESI-HRMS *m/z* calculated for $C_{37}H_{56}FNO_7$ $[M + H]^+$: 646.4119, found: 646.4114.

Methyl N-(2α,3β,23-triacetoxy-12β-fluoro-ursa-13,28β-lactam)glycinate (3.25)

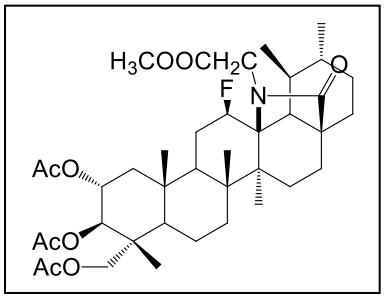

Prepared accordingly to the method described for **3.23** using **3.21** (625 mg, 0.91 mmol), nitromethane (18.7 mL), dioxane (12.5 mL) and Selectfluor® (968.43 mg, 2.73 mmol) at 80 ºC for 24 h to afford a light yellow solid. The crude solid was purified by flash column chromatography (petroleum ether/ethyl acetate, 1:1 → 1:2), to afford **3.25** as a white solid (363.46 mg, 57%). Mp: 148.2–150.9 ºC. IR (KBr): 2979.5, 2935.1, 2877.3, 1747.2, 1712.5, 1457.9, 1236.9, 1033.7 cm^{-1}. ^{1}H NMR (400MHz, $CDCl_3$): δ = 5.21–5.15 (m, 1H, H-2), 5.06 (d, *J* = 10.30 Hz, 1H, H-3), 4.84 (dq, *J* = 45.8 Hz, 1H, H-12), 4.18 (d, *J* = 17.5 Hz, 1H, NC$\underline{H}_2$COOCH$_3$), 4.12 (d, *J* = 17.5 Hz, 1H, NC$\underline{H}_2$COOCH$_3$), 3.79 (d, *J* = 11.9 Hz, 1H, H-23), 3.70 (s, 3H, -NCH$_2$COOC$\underline{H}_3$), 3.60 (d, *J* = 11.8 Hz, 1H, H-23), 2.07 (s, 3H, C$\underline{H}_3$CO), 2.01 (s, 3H, C$\underline{H}_3$CO), 1.98 (s, 3H, C$\underline{H}_3$CO), 1.15 (s, 3H), 1.13 (s, 3H), 1.10 (d, *J* = 6.5 Hz, 3H), 1.08 (s, 3H), 0.95 (d, *J* = 5.2 Hz, 3H), 0.87 (s, 3H) ppm. ^{13}C NMR (100MHz,

$CDCl_3$): δ = 171.9, 170.7 (O<u>C</u>O), 170.3 (2C, 2 × O<u>C</u>O), 168.1, 91.8 (d, *J* = 14.2 Hz, C13), 89.5 (d, *J* = 185.8 Hz, C12), 74.5, 69.6, 65.1, 52.8 (d, *J* = 3.4 Hz), 51.8, 49.1 (d, *J* = 9.2 Hz), 48.4, 47.7, 44.4, 44.3 (d, *J* = 2.7 Hz), 44.1, 42.7, 41.9, 39.7, 38.3, 37.9, 33.2, 32.6, 31.0, 27.5, 25.6 (d, *J* = 19.9 Hz), 24.0, 21.0, 20.8, 20.7, 19.5, 18.3, 18.1, 17.4, 17.2, 16.4, 13.6 ppm. DI-ESI-MS *m/z* $[M+H]^+$: 704.33. Anal. Calcd. for $C_{39}H_{58}FNO_9$: C, 66.55; H, 8.31; N, 1.99 . Found: C, 66.16; H, 8.39; N, 2.00.

Methyl N-(2*α*,3β,23-triacetoxy-12β-fluoro-ursa-13,28β-lactam)alaninate (3.26)

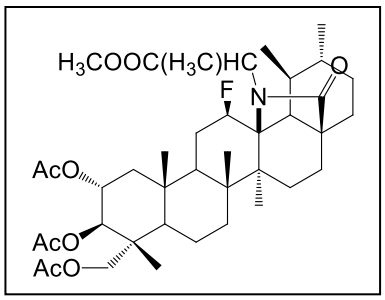

Prepared accordingly to the method described for **3.23** using **3.22** (275 mg, 0.39 mmol), nitromethane (11.0 mL), dioxane (7.15 mL) and Selectfluor® (417.57 mg, 1.18 mmol) at 80 ºC for 30 h to afford a light yellow solid which was purified by flash column chromatography (petroleum ether/ethyl acetate, 2:1), to afford compound **3.26** as a white solid (159.37 mg, 57%). Mp: 145.8–148.0 ºC. IR (KBr): 2981.4, 2935.1, 2875.3, 1754.9, 1704.8, 1457.9, 1369.2, 1236.2 cm^{-1}. ^1H NMR (400MHz, $CDCl_3$): δ = 5.22–5.16 (m, 1H, H-2), 5.07 (d, *J* = 10.4 Hz, 1H, H-3), 4.82 (dq, *J* = 45.9 Hz, 1H, H-12), 4.47 (q, *J* = 7.0 Hz, 1H, NC<u>H</u>(CH_3)$COOCH_3$), 3.81 (d, *J* = 11.8 Hz, 1H, H-23), 3.60 (d, *J* = 11.8 Hz, 1H, H-23), 3.68 (s, 3H, NCH(CH_3)$COOC\underline{H}_3$), 2.07 (s, 3H, $C\underline{H}_3CO$) 2.02 (s, 3H, $C\underline{H}_3CO$), 1.99 (s, 3H, $C\underline{H}_3CO$), 1.40 (d, *J* = 7.1 Hz, 3H, NCH($C\underline{H}_3$)$COOCH_3$), 1.20 (s, 3H), 1.16 (s, 3H), 1.10 (m, 6H), 0.95 (d, *J* = 5.9 Hz, 3H), 0.88 (s, 3H) ppm. ^{13}C NMR (100MHz, $CDCl_3$): δ = 174.6, 170.8 (O<u>C</u>O), 170.3 (2C, 2 × O<u>C</u>O), 166.6, 91.6 (d, *J* = 14.7 Hz, C13), 89.5 (d, *J* = 186.0 Hz, C12), 74.5, 69.7, 61.5, 54.0, 52.8 (d, *J* = 3.2 Hz), 51.9, 49.2 (d, *J* = 9.7 Hz), 47.7, 44.4 (d, *J* = 2.6 Hz), 44.2, 44.2, 42.7, 41.9, 39.6, 38.4, 37.9, 33.3, 32.6, 31.0, 27.6, 25.6 (d, *J* = 19.8 Hz), 23.9, 21.0, 20.9, 20.7, 20.2, 19.6, 18.5, 18.2, 17.4, 17.2, 16.4, 13.6 ppm. DI-ESI-MS *m/z* $[M+H]^+$: 718.37. ESI-HRMS *m/z* calculated for $C_{40}H_{60}FNO_9$ $[M + H]^+$: 718.4330, found: 718.4325.

3.4.2 Biology

3.4.2.1 Cells and reagents

Human cervical adenocarcinoma (**HeLa**), human colorectal adenocarcinoma (**HT-29**), human breast adenocarcinoma (**MCF-7**), human leukemic T (**Jurkat**), human prostate adenocarcinoma (**PC-3**), human melanoma (**A-375**), and human pancreatic carcinoma (**MiaPaca-2**) cell lines, as well as a nontumor human skin fibroblast (**BJ**) cell lines were obtained from the American Type Culture Collection (USA).

Dulbecco's Modified Eagle Medium (DMEM), RPMI 1640 Medium, Dulbecco's Phosphate Buffered Saline (DPBS) and L-glutamine were obtained from Biowest. Minimum Essential Medium (MEM), a penicilin/streptomicin solution and Fetal Bovine Serum (FBS) were obtained from Gibco. A 3-(4,5-dimethylthiazol-2-yl)-2,5-diphenyltetrazolium bromide (MTT) powder and the XTT cell proliferation kit were purchased from Applichem Panreac. A sodium pyruvate solution (100 mM) and Trypsin/EDTA were obtained from Biological Industries. A sodium bicarbonate solution (7.5%) and glucose solution (45%) were purchased from Sigma-Aldrich Co.

Primary antibodies against $p21^{cip1/waf1}$ (sc-397), Bcl-2 (sc-509), Bax (sc-493), cyclin E (sc-247) and cyclin D_3 (sc-182) were obtained from Santa Cruz Biotechnology, Inc. Primary antibodies against $p27^{kip1}$ (#610242), Bid (#550365) and PARP (#556493) were obtained from BD Biosciences. Primary antibodies against caspase 3 (#9662) and caspase 8 (#9746S) were purchased from Cell Signaling. The primary antibody against α-actin (#69100) was obtained from MP Biomedicals. Secondary antibodies (anti-mouse (P0260) and anti-rabbit (NA934)) were obtained from Dako and from Amersham Biosciences, respectively.

Cisplatin was obtained from Sigma-Aldrich Co.

3.4.2.2 Preparation and storage of the stock solutions

Asiatic acid **1.27** and its derivatives were suspended in DMSO at 20 mM as stock solutions that were stored at –80 °C. The working solutions were prepared freshly on the day of testing. To obtain final assay concentrations, the stock solutions were diluted in culture medium. The final concentration of DMSO in working solutions was always equal or lower than 0.5%.

3.4.2.3 Cell culture

HT-29, PC-3, A375, MIA PaCa-2 and HeLa cells were routinely maintained in DMEM supplemented with 10% heat-inactivated fetal bovine serum (FBS) and 1% penicillin/streptomycin. MCF-7 cells were maintained in MEM supplemented with 10% heat-inactivated FBS, 0.1% penicillin/streptomycin, 2 mM L-glutamine, 1 mM sodium pyruvate, 0.01 mg/mL of insulin, 10 mM glucose and 1× MEM-EAGLE Non Essential Aminoacids. BJ cells were routinely maintained in DMEM supplemented with 10% heat-inactivated FBS, 110 mg/L of sodium pyruvate, 1% penicillin/streptomycin and 1.5 g/L sodium bicarbonate. Jurkat cells were cultured in RPMI 1640 supplemented with 10% FBS, 1% penicillin/streptomycin and 2 mM L-glutamine. All cell lines were incubated in a 5% CO_2 humidified atmosphere at 37 °C.

3.4.2.4 Cell viability assay

The antiproliferative activities of the test compounds against the MCF-7, HT-29, PC-3, A375, MIA PaCa-2, HeLa and BJ cell lines were evaluated via a modified procedure of 3-(4,5-dimethylthiazol-2-yl)-2,5-diphenyltetrazolium bromide (MTT) assay, as described by Mosmann.[275] Briefly, 8×10^2 to 1×10^4 cells per well were plated in 96-well plates in 200 µl of medium and were left to grow. After 24 h of culture, the culture medium was removed and replaced by new medium (200 µl) containing the tested compounds at different concentrations, in triplicate. After 72 h of incubation, 100 µl of MTT solution (0.5 mg/mL) were used to replace the supernatant in each well. After 1 h of incubation, the MTT solution was removed and the resulting formazan crystals were dissolved with 100 µl of DMSO. Relative cell viability was measured by absorbance at 550 nm on an ELISA plate reader (Tecan Sunrise MR20-301, TECAN, Salzburg, Austria). Non treated cells were used as the control.

The antiproliferative activities of the compounds against Jurkat cells were determined using the XTT assay. Jurkat cells were seeded at a density of 4×10^3 cells per well in 96-well plates in 100 µl of medium. After 24 h of incubation, 100 µl of medium containing the tested compounds at different concentrations, in triplicate, were added. After 72 h of incubation, 100 µl of XTT solution were added to each well and the plates were incubated for an additional 4 h at 37 °C. Relative cell viability, compared to with the viability of nontreated cell, was

measured by absorbance at 450 nm on an ELISA plate reader (Tecan Sunrise MR20-301, TECAN, Salzburg, Austria).

IC_{50} values represent the concentration of each compound that inhibited the cell growth by 50%, compared with nontreated cells. The IC_{50} values were estimated from the dose-response curves using 9 different concentrations in triplicate. Each IC_{50} value was expressed as the mean IC_{50} ± standard deviation (SD) of three independent experiments.

3.4.2.5 Cell-cycle assay

The cell cycle was analyzed by flow cytometry using a fluorescence activated cell sorting (FACS). Briefly, 1×10^5 HeLa cells were seeded per well on 6-well pates, with 2 mL of medium. After 24 h of culture, cells were treated with compound **3.14** at the indicated concentrations. Control cells were treated with culture medium containing 0.5% DMSO. After 24 and 48 h of incubation, cells were harvested by mild trypsinization, collected by centrifugation, and resuspended in Tris-buffered saline (TBS) containing 50 mg/mL of PI, 10 mg/mL of Rnase-free Dnase, and 0.1% Igepal CA-630 (Sigma-Aldrich). The cells were stained for 1 h at 4 ºC and protected from light. FACS analysis was performed at 488 nm on an Epics XL flow cytometer (Coulter Corporation, Hialeah, FL). Data from 1×10^4 cells were collected and analyzed using the Multicycle software (Phoenix Flow Systems, San Diego, CA). Experiments were performed in triplicate, with two replicates per experiment.

3.4.2.6 Annexin V-FITC/PI flow cytometric assay

HeLa cells were seeded at a concentration of 1×10^5 cells per well on 6-well pates, with 2 mL of medium. After 24 h of culture, cells were treated with compound **3.14** at the specified concentrations and the plates were incubated for 48 h. Subsequently, cells were harvested, centrifuged, and resuspended in 95 µl of binding buffer (10 mM HEPES/NaOH, pH 7.4, 140 mM NaCl, 2.5 mM $CaCl_2$) at a maximum density of 8×10^5 cells/mL. The annexin V-FITC conjugate (1 µg/mL) was added and cells were incubated for 30 min at room temperature in the dark. Just before FACS analysis, 500 µl of binding buffer was added to each vial and cells were stained with 20 µl of a 1 mg/ml PI solution. Approximately 1×10^4

cells were analyzed for each histogram. Experiments were performed in triplicate, with two replicates per experiment.

3.4.2.7 Morphological analysis using phase–contrast microscopy

In this experiment, 1×10^5 HeLa cells per well were seeded in 6-well plates containing 2 mL of medium and incubated at 37 °C for 24 h. Cells were then treated with compound **3.14** at the specified concentrations for 48 h. Morphological changes were observed using an inverted phase–contrast microscope (Olympus IMT-2) with a 40× objective and a digital camera [*Fujifilm* A2O5S (*Fuji Foto Film*, CO. LTD)].

3.4.2.8 Hoechst 33258 staining

Nuclear morphological modifications were analyzed by fluorescence microscopy using Hoechst 33258 staining. In this experiment, 1×10^5 HeLa cells per well were seeded on 6-well plates containing 2 mL of medium. After 24 h of incubation, compound **3.14** was added at the indicated concentrations and cells were incubated again for a period of 48 h. Cells were harvested by mild trypsinization, collected by centrifugation, and washed twice with PBS. Cells were then stained with 500 µl of Hoechst 33258 solution (2 µg/mL in PBS) for 15 min at room temperature in the dark. After incubation, cells were washed with PBS, mounted on a slide, and observed under a fluorescence microscope (DMRB, Leica Microssystems, Wetzlar, Germany) using a DAPI filter.

3.4.2.9 Preparation of total protein extracts

HeLa cells (5.6×10^4) were seeded in 100 mm plates containing 10 mL of culture medium for 24 h. Cells were then treated with compound **3.14** at the specified concentrations for 48 h. After the incubation, cells were washed twice with ice-cold PBS and resuspended in ice-cold lysis buffer [20 mM Tris/acetate (pH 7.5), 270 mM sucrose, 1 mM EDTA (pH 8.8), 1 mM EGTA (pH 8.8), 1% Triton X-100, and 1% protease inhibitor cocktail (Sigma-Aldrich)]. The samples were sonicated, incubated on ice for 15 min, and centrifuged at 12000 rpm for 5 min at 4 ºC. The pellets were discarded and protein content was quantified in the supernatants

using a bicinchoninic acid (BCA) kit (Pierce Biotechnology, Rockford). After quantification, the supernatants were stored at –80 °C.

3.4.2.10 Western blotting

Equal amounts of protein were loaded and size-separated on 10% or 15% SDS–polyacrilamide gels according to the method described by Laemmli.[276] After electrophoresis, separated proteins were transferred to polyvinyl nitrocellulose membranes (BioRad Laboratories, Richmond). Membranes were blocked by incubation in TBS buffer [20 mM Tris (pH 7.5) and 132 mM NaCl] containing 0.1% Tween and 5% BSA or nonfat dry milk for 1 h at room temperature. Subsequently, membranes were blotted with primary specific antibodies overnight at 4 ºC. After incubation, blots were washed five times (5 min each time) with TBS-0.1% Tween and incubated with the appropriate secondary antibodies for 1 h at room temperature. After secondary antibody incubation, the membranes were washed five times (5 min each time) with TBS-0.1% Tween. Protein detection was performed by treating all blots with Immobilon ECL Western Blotting Detection Kit Reagent (Millipore). The blots were developed after exposure to an autoradiography film in a film cassette.

Chapter 4

Synthesis and anticancer evaluation of A-nor asiatic acid derivatives

Synthesis and biological evaluation of novel asiatic acid derivatives with anticancer activity

Bruno M. F. Gonçalves, Jorge A. R. Salvador, Sílvia Marín and Marta Cascante

RSC Advances, 2016, 6, 3967–3985.

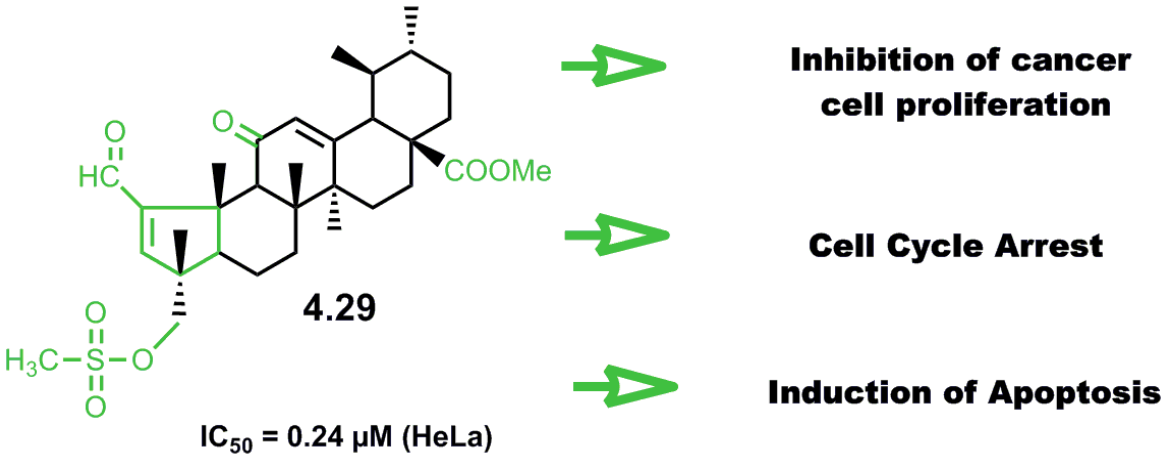

4.1 Introduction

The conversion of the hexameric A-ring of asiatic acid **1.27** containing the 2,3-vicinal diols into a pentameric A-ring containing an α,β-unsaturated carbonyl group was reported previously.[252] Information obtained from scientific the literature regarding structure–activity relationships, indicates that the introduction of an α,β-unsaturated carbonyl group in the A-ring of pentacyclic triterpenoids has a significant effect on their biological activity.[119,264] The transformations performed in the A-ring of asiatic acid had not been thoroughly explored. Taking all that into account, a series of new asiatic acid **1.27** derivatives containing a pentameric A-ring with an α,β-unsaturated carbonyl moiety, combined with additional modifications at C23, C11, and C28 was designed and synthesized, to obtain derivatives with improved anticancer activity.

Nitrile group has been gaining great importance in the design and development of new drugs[277,278], which is reflected in the more than 30 nitrile-containing pharmaceutical compounds currently in use for diverse therapeutic indications, and in the more than 20 nitrile-containing leads that are in clinical evaluation.[279] Because of its versatility, the presence of the nitrile functionality in organic molecules plays several biologically important roles.[277,278,280–283] This functional group proved to be a strong hydrogen acceptor and may work as a hydroxyl and carboxyl surrogate.[277,279] Furthermore, nitriles are precursors in organic synthesis and can be converted into amides, amines, triazines, thiazoles, 2-oxazolines, tetrazoles, imidazoles, triazoles, and other nitrogen-containing functional moieties that possess a broad spectrum of biological activities.[284,285]

Several methods exist for the preparation of nitriles from the corresponding aldehydes, including methods based on the dehydration of aldoximes and oxidation of aldimines, or those that use reagents such as sodium azide (NaN_3) and triflic acid (TfOH), among others.[286–289] Other methods are based on the use of ammonia combined with other reagents, such as iodosobenzene diacetate,[284] [bis(trifluoroacetoxy)iodo]benzene,[290] sodium periodate ($NaIO_4$), potassium iodide (KI),[291] and Copper/TEMPO using air as oxidant.[292]

Taking into account the potential importance of nitrile in the biological activity of our compounds, a panel of A-nor derivatives of asiatic acid **1.27** containing a nitrile group in ring A was designed and prepared. The introduction of the nitrile group in the A-ring was achieved by the direct conversion of the aldehyde group into nitrile using a method based on

ammonia/water combined with iodine, which was reported to be applicable for aromatic, heterocyclic and aliphatic aldehydes.[261,293,294]

4.2 Results

4.2.1 Chemistry

4.2.1.1 Synthesis and structural elucidation

The synthesis started with treatment of asiatic acid **1.27** with anhydrous potassium carbonate (K_2CO_3) and methyl iodide or ethyl iodide in DMF, to give the methyl ester derivative **4.1** and the ethyl ester derivative **4.2**, respectively, in almost quantitative yields (Scheme 4.1). Asiatic acid **1.27** and ester derivatives **4.1**, and **4.2,** were then oxidized with sodium periodate ($NaIO_4$) in methanol/water[252] affording the heptameric A-ring lactol derivatives **4.3**, **4.4** and **4.5**, respectively. Further treatment of compounds **4.3**, **4.4**, and **4.5** with catalytic amounts of piperidine and acetic acid in dry benzene at 60 °C afforded the pentameric A-ring derivatives **4.6**, **4.7**, and **4.8**, respectively.[252]

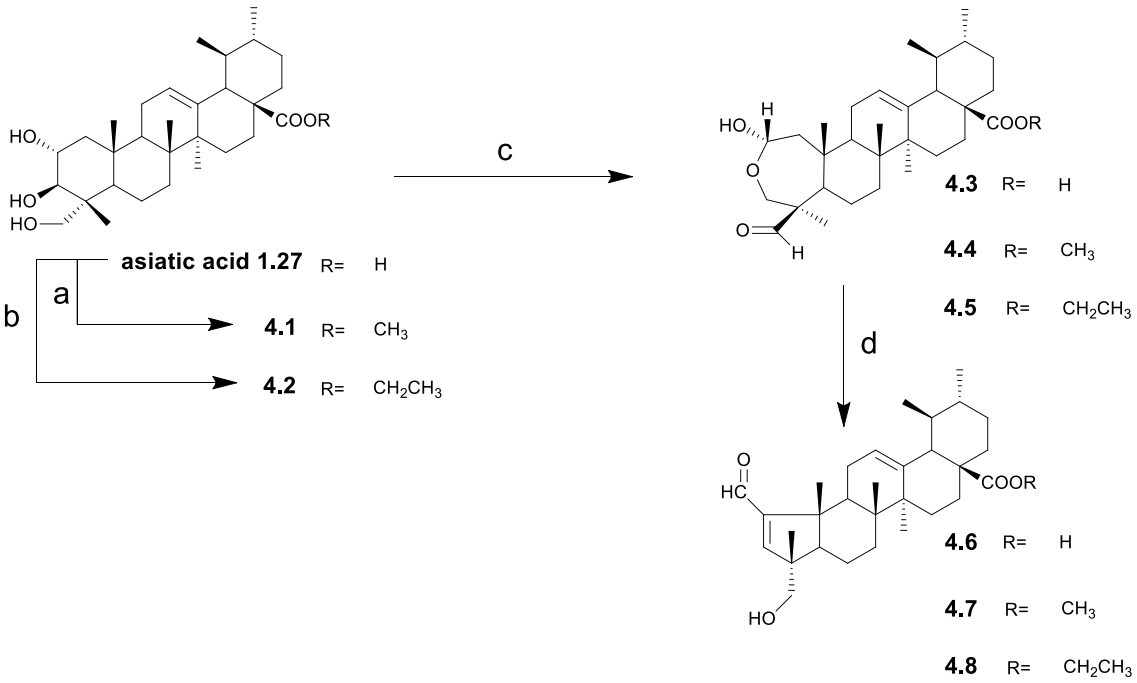

Scheme 4.1 Synthesis of derivatives **4.1**–**4.8**. *Reagents and conditions:* a) CH_3I, K_2CO_3, DMF, rt.; b) CH_3CH_2I, K_2CO_3, DMF, rt.; c) $NaIO_4$, MeOH / H_2O, rt; d) i- Acetic acid, piperidine, dry benzene, 60°C, N_2; ii -Anhydrous $MgSO_4$, 60 °C, N_2.

The elucidation of the structures of all newly synthesized derivatives was achieved using different techniques, including IR, ^{1}H and ^{13}C NMR and MS. For the identification of the intermediary compounds were also used the data reported in the literature.

The derivatives **4.3–4.5** and **4.12**, with a heptameric lactol A-ring, exhibited a broad band on the IR spectrum, at 3421–3444 cm^{-1}, corresponding to the hydroxyl group at C2. In the ^{1}H NMR spectrum, the proton of the CHO group appeared as a singlet at 9.94 ppm (Fig. 4.1). In the ^{13}C NMR spectrum, the signal corresponding to the CHO carbon was observed at around 206 ppm (Fig. 4.2).

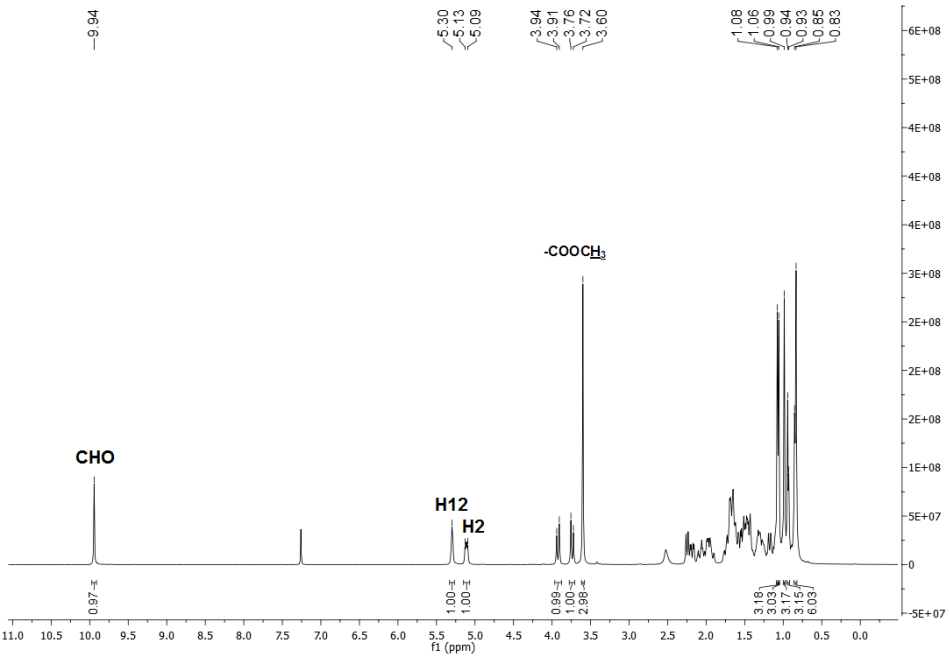

Figure 4.1 ^{1}H NMR spectrum of compound **4.4**.

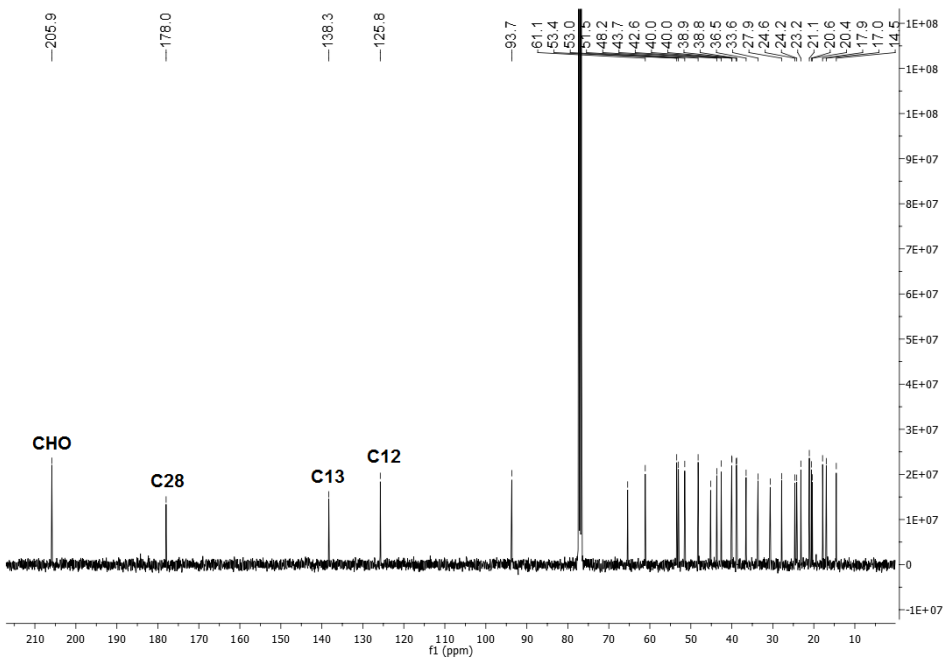

Figure 4.2 ^{13}C NMR spectrum of compound **4.4**.

In the IR spectrum of compounds **4.6**–**4.8**, the characteristic IR bands for the C=O and C=C stretching vibrations of the α,β-unsaturated aldehydes were observed at 1687–1689 cm^{-1} and 1581 cm^{-1}, respectively (as example see IR spectrum of compound **4.8**, Fig. 4.3). The signals of the aldehyde and H3 protons in the A ring were consistently observed as two singlet signals at 9.72 ppm and δ 6.66 ppm, respectively, in the ^{1}H NMR spectrum (Fig. 4.4). The ^{13}C NMR signal for the CHO carbon was observed at 190.8 ppm, whereas the signals for the carbons C2 and C3 of the A ring double bond appeared at around 158.9 ppm and 159.3 ppm, respectively (Fig. 4.5).

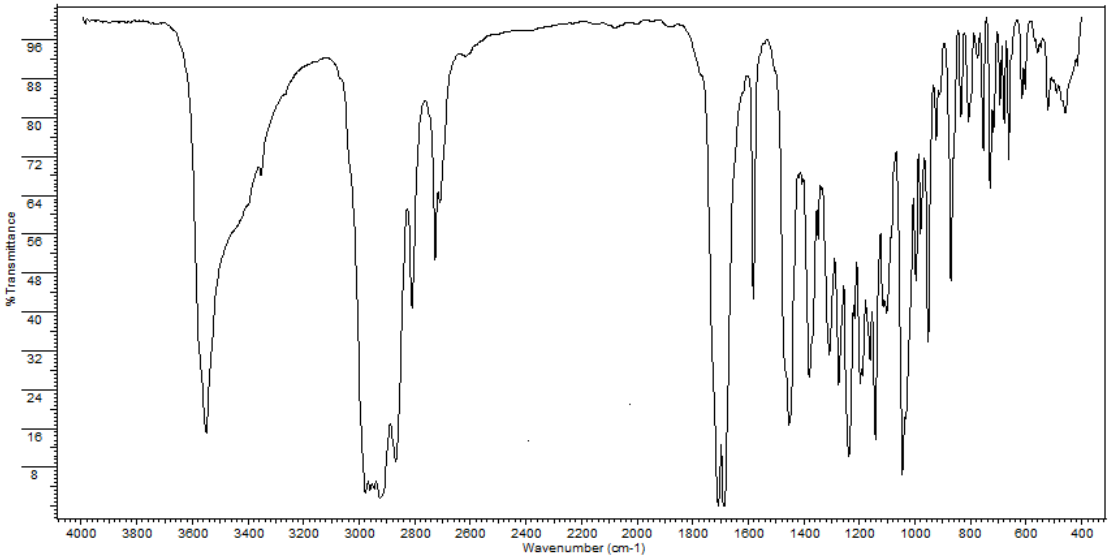

Figure 4.3 IR spectrum of compound **4.8**.

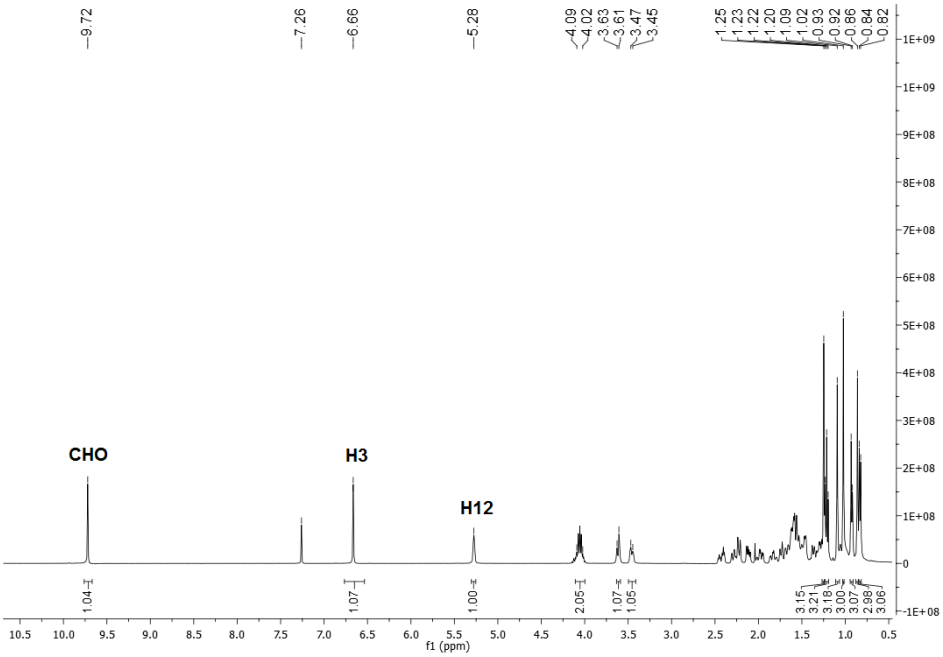

Figure 4.4 [1]H NMR spectrum of compound **4.8**.

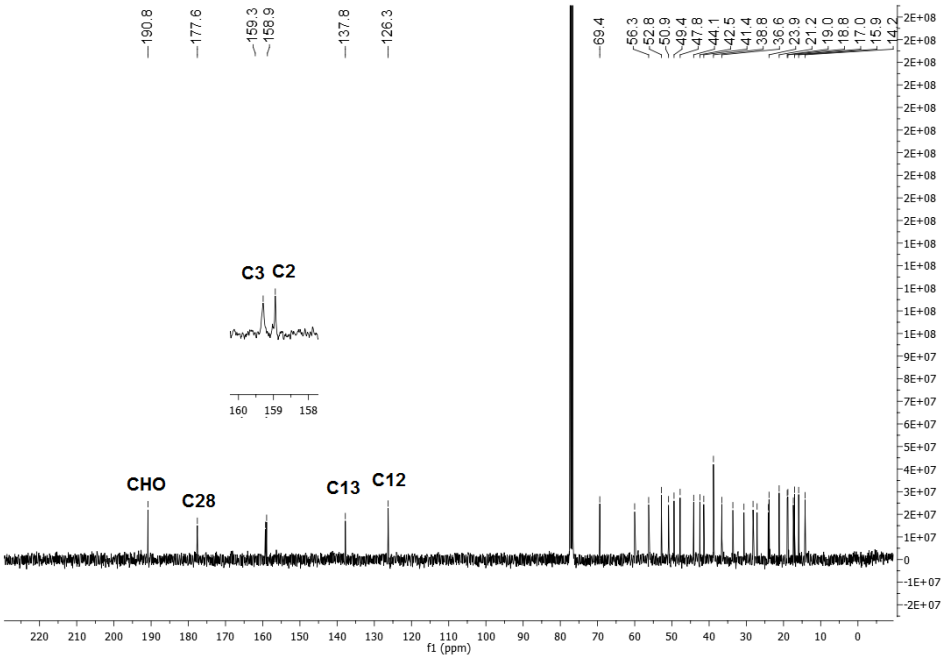

Figure 4.5 [13]C NMR spectrum of compound **4.8**.

To study the impact of the introduction of a carbonyl group at C11 on the anticancer activity, several asiatic acid **1.27** derivatives with an α,β-unsaturated ketone in the C-ring were prepared. As shown in Scheme 4.2, the reaction of compound **4.1** with acetic anhydride in the presence of DMAP in THF at room temperature gave compound **4.9**, which was further oxidized with a mixture of potassium permanganate and iron sulfate, to afford the 11-oxo-12-ene derivative **4.10** in 95% yield.[255,295] Compound **4.10** was then deacetylated with potassium hydroxide (KOH) in methanol, to afford the trihydroxy intermediate **4.11**. The lactol derivative **4.12** was prepared by reaction of compound **4.11** with sodium periodate ($NaIO_4$) in methanol/water at room temperature. The α,β-unsaturated aldehyde **4.13** was obtained from **4.12** using the procedure described previously for the preparation of compounds **4.6–4.8**.

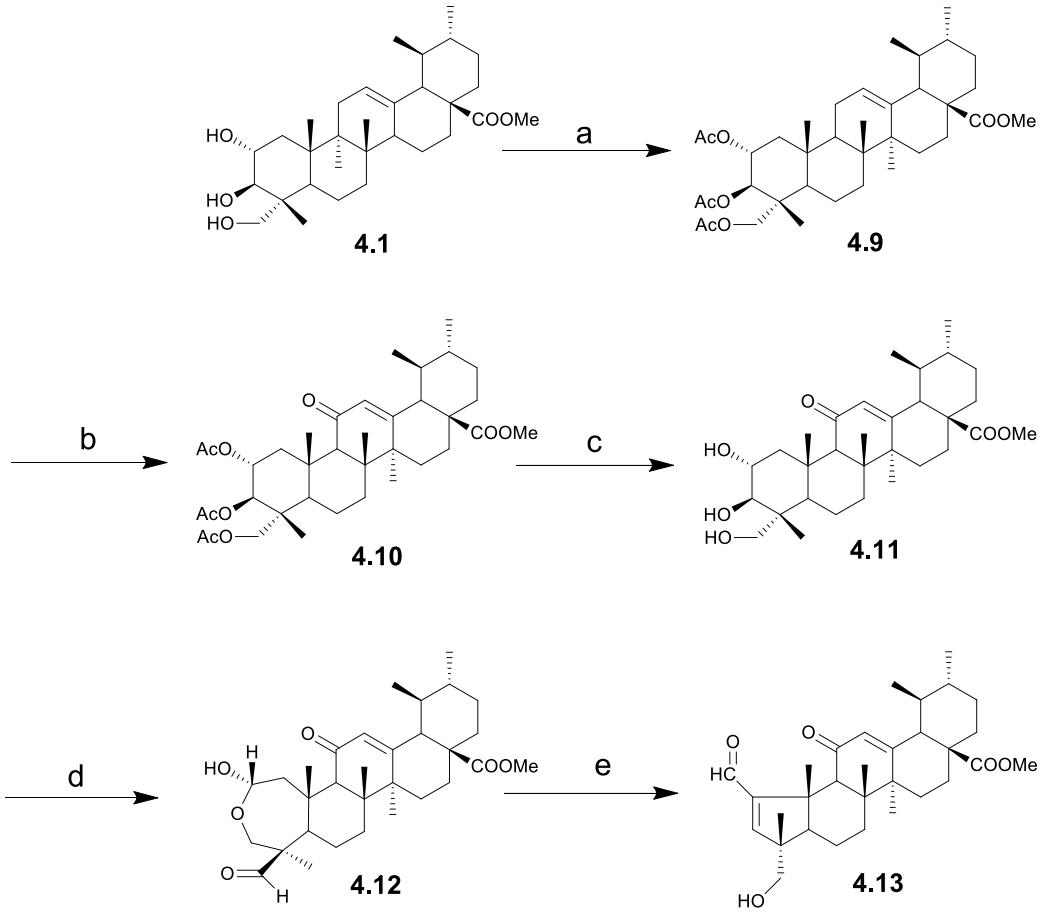

Scheme 4.2 Synthesis of derivatives **4.9**–**4.13**. *Reagents and conditions:* a) acetic anhydride, DMAP, THF, rt.; b) $KMnO_4$, $Fe_2(SO_4)_3.nH_2O$, t-BuOH, H_2O, CH_2Cl_2, rt.; c) KOH, MeOH, reflux; d) $NaIO_4$, MeOH / H_2O, rt.; e) i-acetic acid, piperidine, dry benzene, 60 °C, N_2; ii -anhydrous $MgSO_4$, 60 °C, N_2.

In the ^1H NMR spectrum of compound **4.10**, the signal for proton H12 was observed at 5.62 ppm; this was a higher value than that observed for proton H12 of compound **4.9** (5.24

ppm), which had no carbonyl at C11. Moreover, in the ^{13}C NMR spectrum, the signal for C11 appeared at 198.8 ppm. The signals for C12 and C13 appeared at 130.4 and 163.3 ppm, respectively, which are higher values than those observed in compound **4.9** (125.0 ppm for C12 and 138.3 ppm for C13).[255]

The synthesis of nitrile-containing A-nor asiatic acid derivatives was achieved via the direct conversion of the A-ring aldehyde group into nitrile. The aldehyde derivatives **4.6**, **4.7**, and **4.13** were dissolved in THF and treated with 25% aqueous ammonium solution and iodine at room temperature,[261] to afford the nitrile-containing derivatives **4.14**, **4.15**, and **4.16**, in 56%, 50%, and 48% yields, respectively (Scheme 4.3). After the addition of iodine, the reaction mixture acquired a dark color. Over the course of the reaction, the reaction mixture became colorless because of the consumption of iodine, which usually indicates that the reaction is complete.

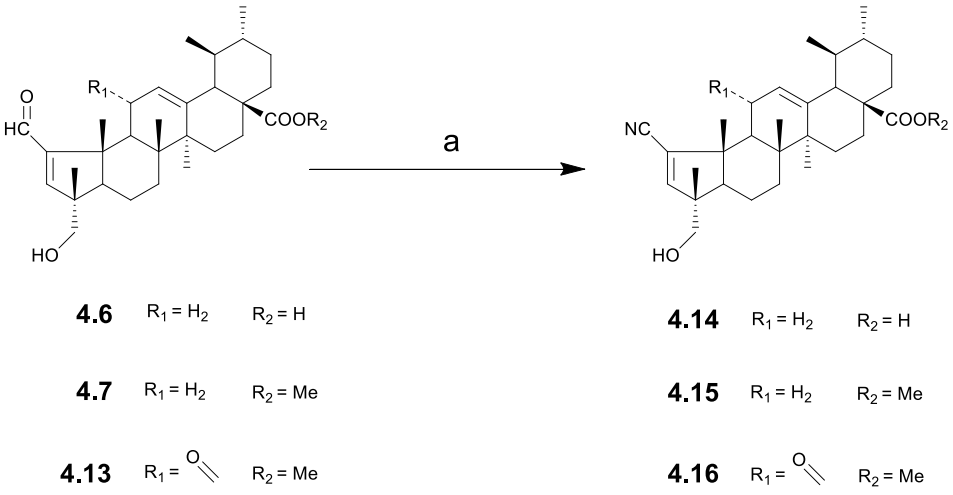

Scheme 4.3 Synthesis of derivatives **4.14-4.16.** *Reagents and conditions:* a) I_2, aq. NH_3, THF, rt.

According to previous studies, the conversion of aldehyde into nitrile presumably proceeds via the oxidation of aldimine with iodine, to afford an N-iodo aldimine intermediate, which eliminates hydrogen iodide in ammonia solution, affording the nitrile derivatives (Fig. 4.6).[261,286,293]

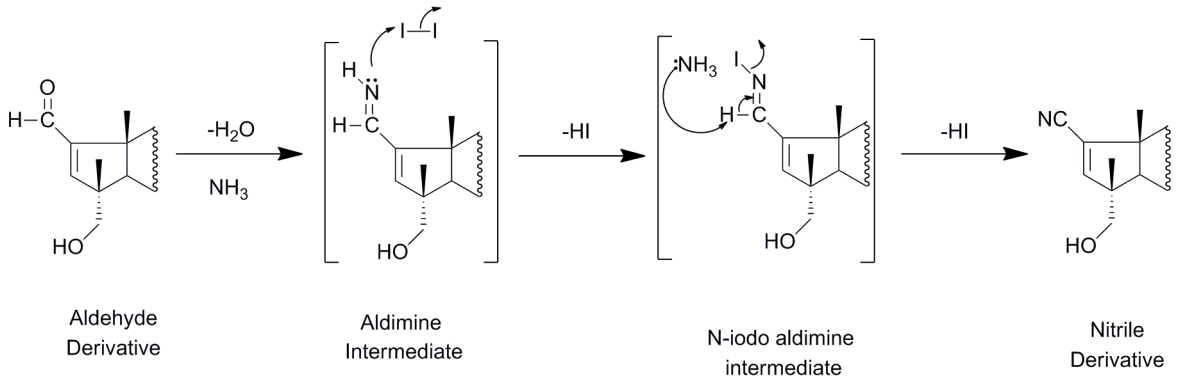

Figure 4.6 Proposed mechanism for the conversion of aldehyde intro nitrile.

The direct conversion of aldehyde into nitrile was confirmed by the IR absorption band for C≡N stretching vibration observed at 2215.8–2217.7 cm^{-1} (Fig. 4.7). In the ^{13}C NMR spectrum, the signal for the CN carbon appeared at around 117 ppm (Fig. 4.9). These structural data were consistent for all nitrile containing derivatives **(4.14**–**4.16** and **4.22**–**4.27** and **4.30)**.

Considering compound **4.15**, in its ^{1}H NMR spectrum, proton H3 appeared as a singlet at 6.48 ppm, and proton H12 appeared as a triplet at 5.26 ppm (Fig. 4.8).

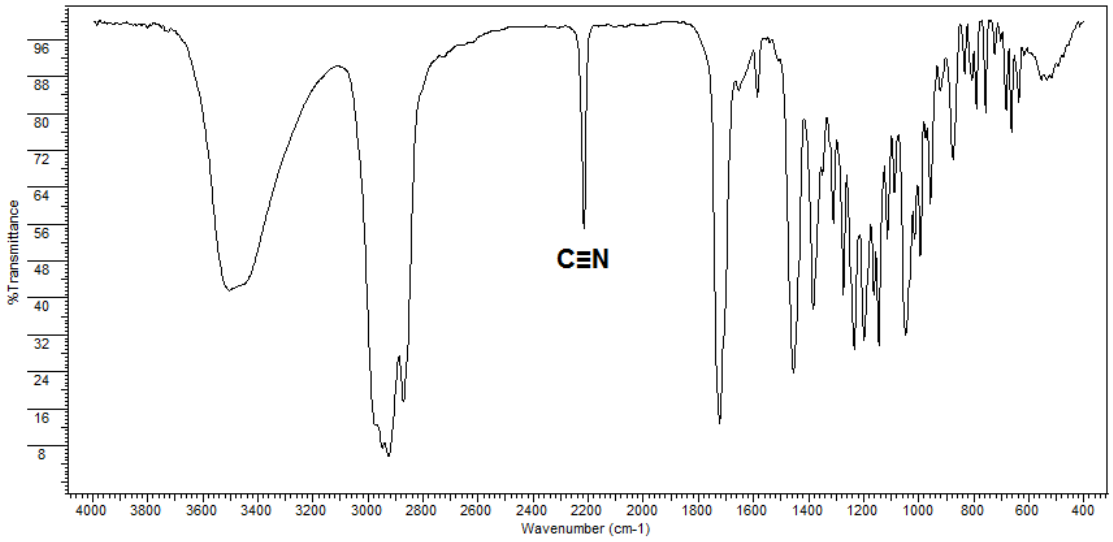

Figure 4.7 IR spectrum of compound **4.15**.

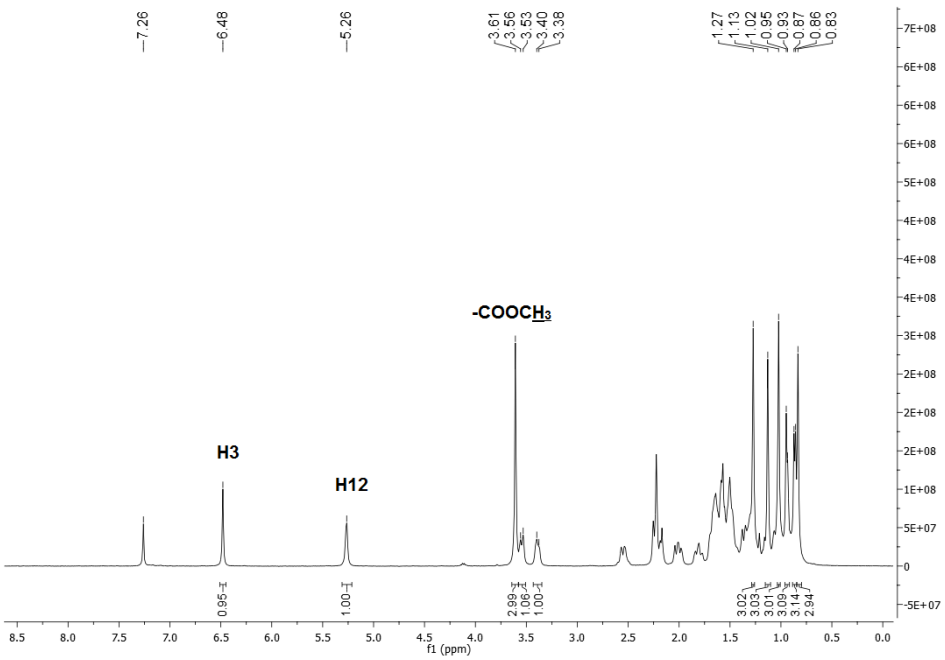

Figure 4.8 ^{1}H NMR spectrum of compound **4.15**.

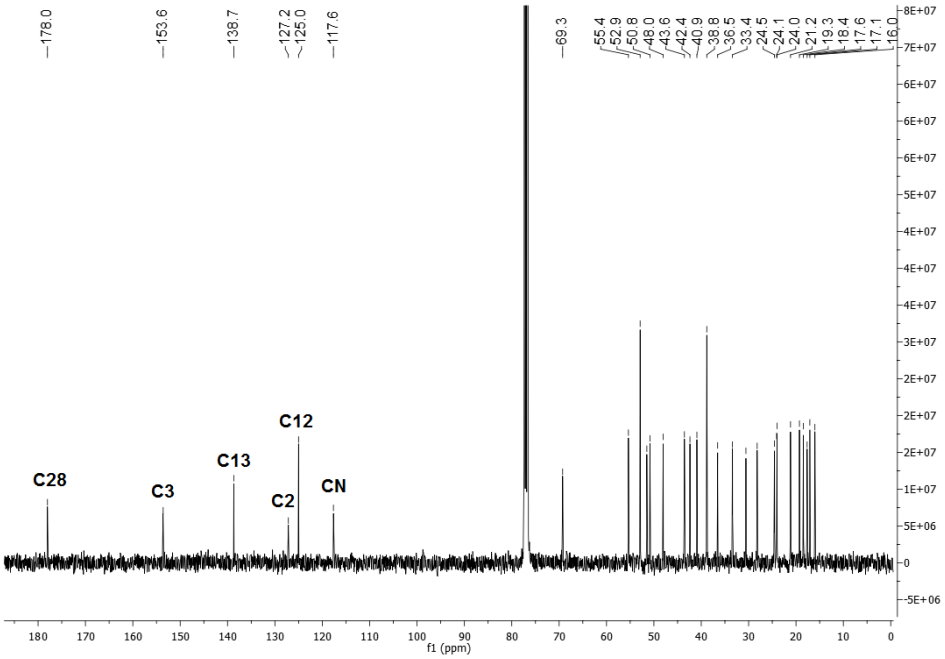

Figure 4.9 ^{13}C NMR spectrum of compound **4.15**.

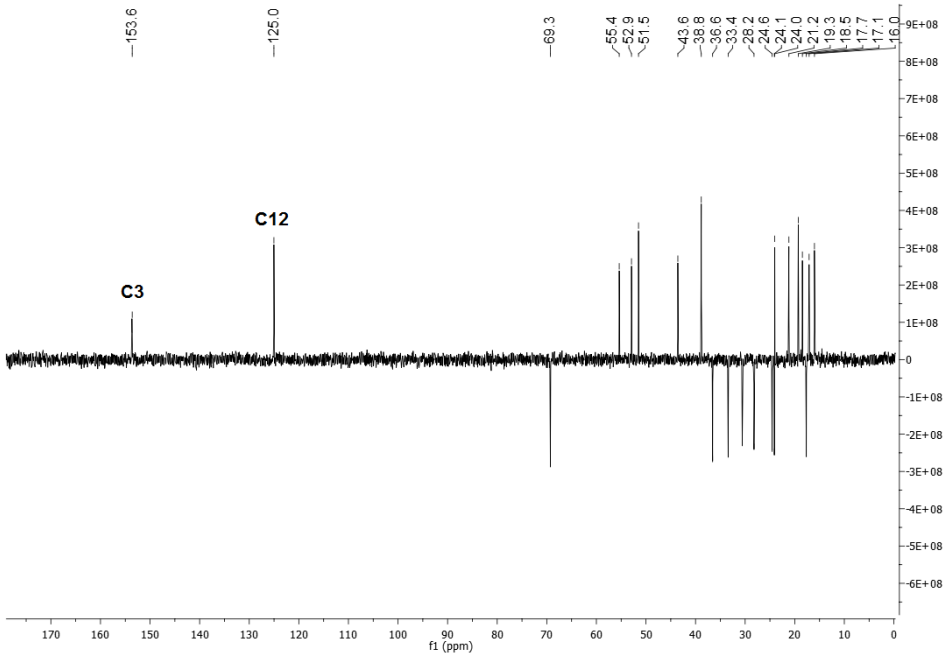

Figure 4.10 DEPT 135 spectrum of compound **4.15**.

To investigate the effect of C23-hydroxyl substitution on anticancer activity, compounds **4.13** and **4.15** were used as the starting materials for the preparation of a panel of C23-substituted ester (Schemes 4.4 and 4.5), carbamate (Schemes 4.4 and 4.5), and methanesulfonyloxy (Scheme 4.6) derivatives. The ester derivatives **4.17**, **4.18** and **4.23–4.26** were prepared in moderate-to-good yields via the reaction of compound **4.13** or compound **4.15** with the corresponding anhydrides in the presence of DMAP at room temperature. The treatment of compounds **4.13** or **4.15** with cinamoyl chloride and DMAP in dry benzene at 60 °C afforded the 23-cinnamic ester derivatives **4.19** and **4.27**, respectively.

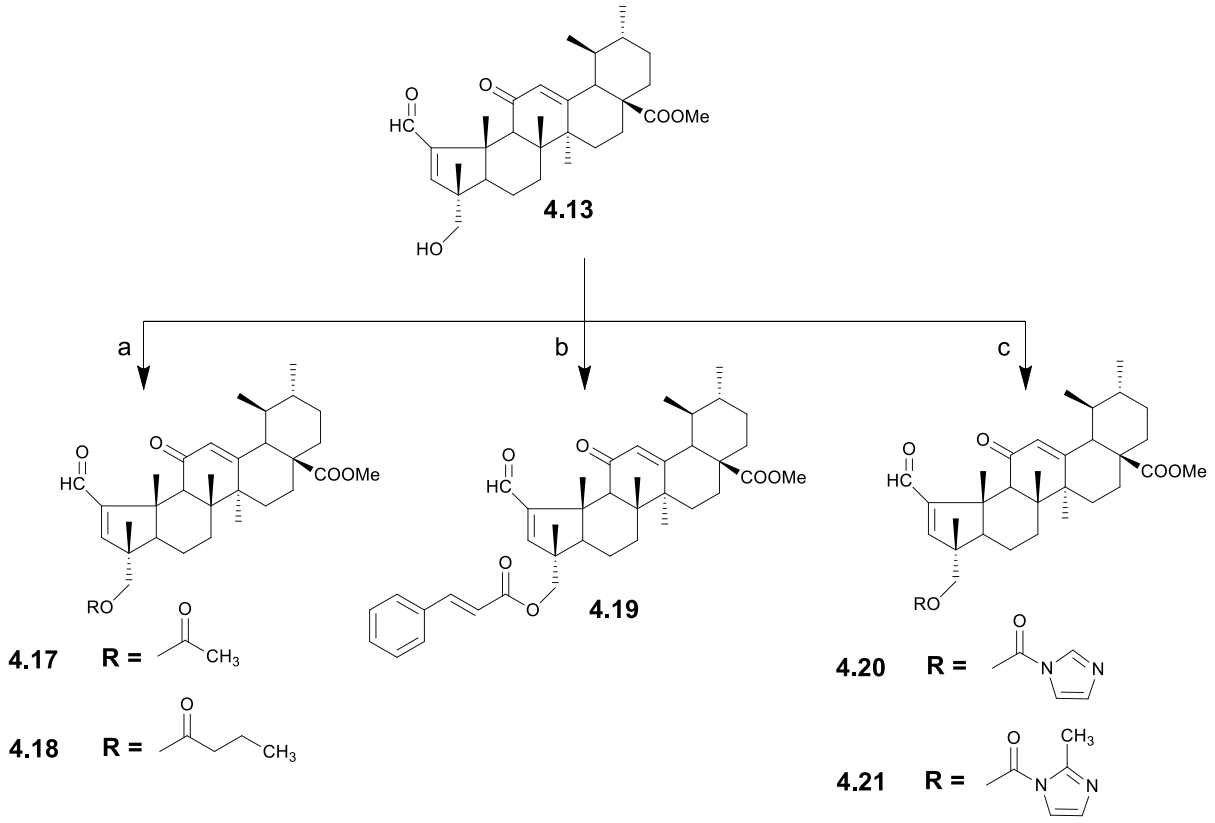

Scheme 4.4 Synthesis of derivatives **4.17**–**4.21.** *Reagents and conditions:* a) Acetic anhydride or butyric anhydride, DMAP, THF, rt.; b) Cinnamoyl chloride, dry benzene, DMAP, 60 °C, N_2; c) CDI or CBMI, THF, 70 °C, N_2.

In previous studies, our group found that the introduction of imidazole and 2′-methylimidazole rings into the structure of triterpenoid compounds increases the cytotoxic activity of the parental compounds.[254,256,257] Under this perspective, imidazole and 2′-methylimidazole rings were introduced into compounds **4.13** and **4.15** via the reaction of C23-OH with CDI or CBMI in THF at reflux under inert atmosphere, to afford the carbamate derivatives **4.20** and **4.21** in 12% and 33% yield (Scheme 4.4) and the carbamate derivative **4.22** in 59% yield (Scheme 4.5).

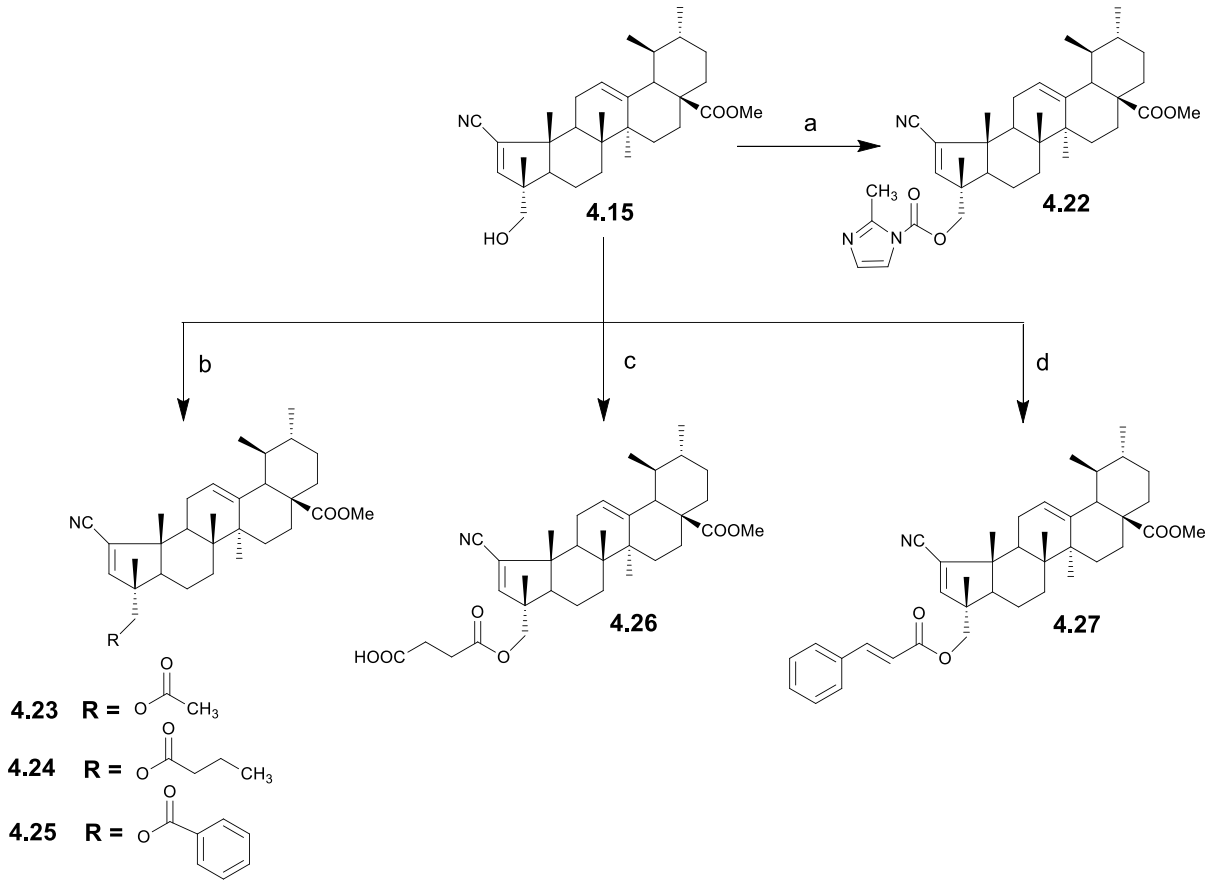

Scheme 4.5 Synthesis of derivatives **4.22**–**4.27.** *Reagents and conditions:* a) CBMI, THF, 70 °C, N_2; b) Acetic or butyric or benzoic anhydride, DMAP, THF, rt.; c) Succinic anhydride, DMAP, CH_2Cl_2, r.t.; d) Cinnamoyl chloride, dry benzene, DMAP, 60 °C, N_2.

In the ^{1}H NMR spectrum of compounds **4.21** and **4.22**, the two protons of the methylimidazole ring appeared as two signals at 7.27–7.28 ppm and 6.84–6.87 ppm (as example see ^{1}H NMR spectrum of compound **4.21**, Fig. 4.11). In the case of the derivative **4.20**, the imidazole ring protons appeared as three singlets at 8.09, 7.36, and 7.06 ppm.[256,257]

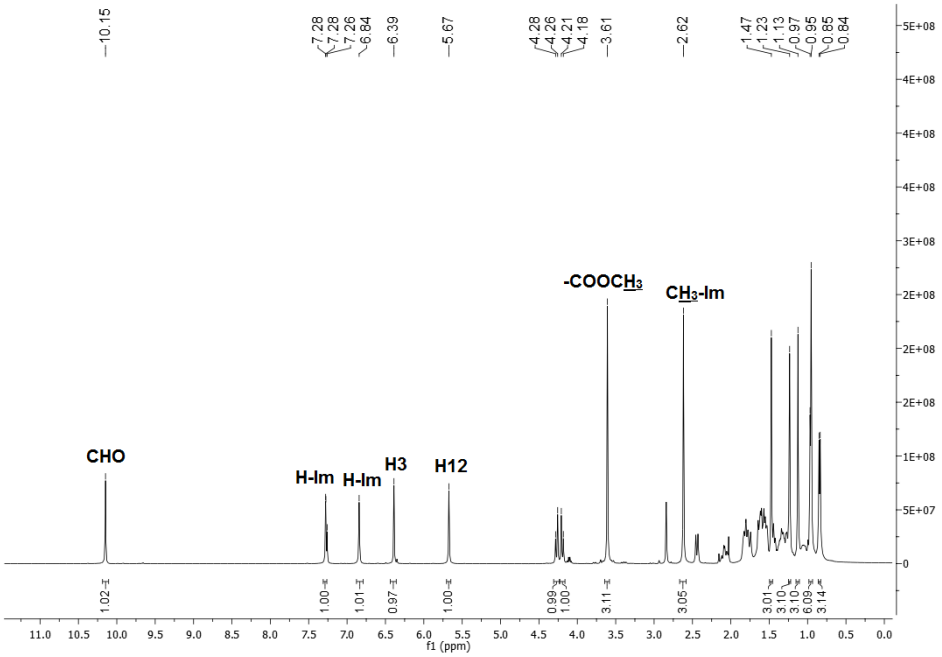

Figure 4.11 ^{1}H NMR spectrum of compound **4.21**.

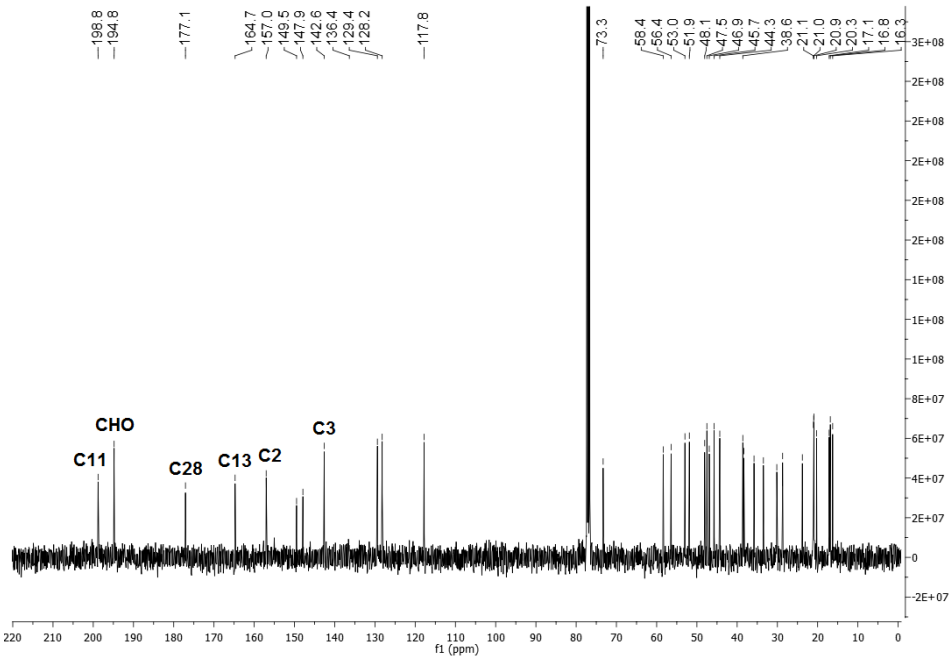

Figure 4.12 ^{13}C NMR spectrum of compound **4.21.**

Finally, the 23-methanesulfonyloxy derivatives **4.28**, **4.29** and **4.30** were obtained in moderate yields via the reaction of compounds **4.7**, **4.13** and **4.15,** respectively, with methanesulfonyl chloride and triethylamine in dry dichloromethane at room temperature (Scheme 4.6).

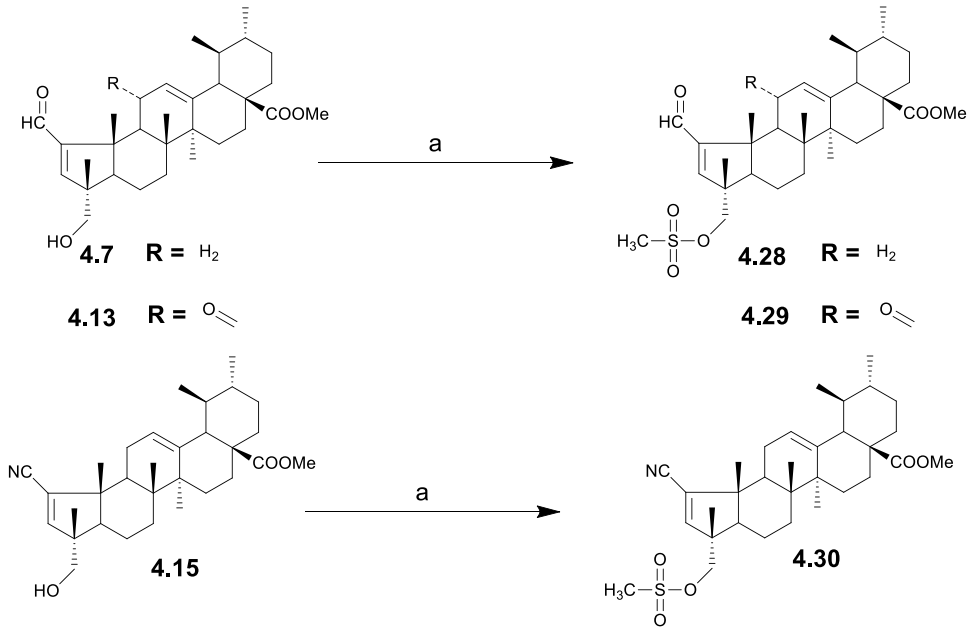

Scheme 4.6 Synthesis of derivatives **4.28**–**4.30.** *Reagents and conditions:* a) Methanesulfonyl chloride, triethylamine, dry CH_2Cl_2, rt.

The successful preparation of the 23-methanesulfonyloxy derivatives **4.28**, **4.29**, and **4.30** was confirmed by the IR absorption bands for the asymmetric and symmetric S=O stretching vibrations observed around 1355–1359 cm^{-1} and 1174–1176 cm^{-1}, respectively. In addition, the ^{1}H NMR signal for the protons from the mesylate methyl group was observed as a singlet at 3.01–3.03 ppm. A more detailed analysis of compound **4.29** showed that its ^{1}H NMR spectrum contained a singlet signal at 10.15 ppm corresponding to the CHO proton, a singlet signal at 6.30 ppm corresponding to the proton H3 on ring A, and a signal at 5.68 ppm corresponding to proton H12. The ^{1}H NMR signals for the geminal protons at C23 appeared as two doublets at 4.07 ppm and 4.04 ppm, with a coupling constant of J = 10.05 Hz. The signal observed at 3.01 ppm was assigned to the methyl group protons of the methanesulfonyloxy moiety (Fig. 4.13). Data from the literature combined with the analysis of data from ^{13}C NMR and DEPT 135 spectra allowed the attribution of several signals to the carbons of compound **4.29**.[139] In the ^{13}C NMR spectrum of compound **4.29,** 7 signals greater than 100 ppm were observed, that corresponded to the CHO carbon, C2, C3, C11, C12, C13, and C28. The ^{13}C NMR signal observed at 199.0 ppm corresponded to a quaternary carbon, as this signal was not present in DEPT, and was attributed to the carbonyl carbon C11 (Figs. 4.14 and 4.15). The signals for the CHO carbon and for C28 were observed at 194.9 and 177.1 ppm, respectively. The quaternary carbon observed at 164.9 ppm and the carbon

detected at 129.4 ppm were attributed to C13 and C12, respectively. The ^{13}C NMR signal for the quaternary C2 appeared at 157.2 ppm, and the signal for C3 was observed at 142.0 ppm (Fig. 4.14).

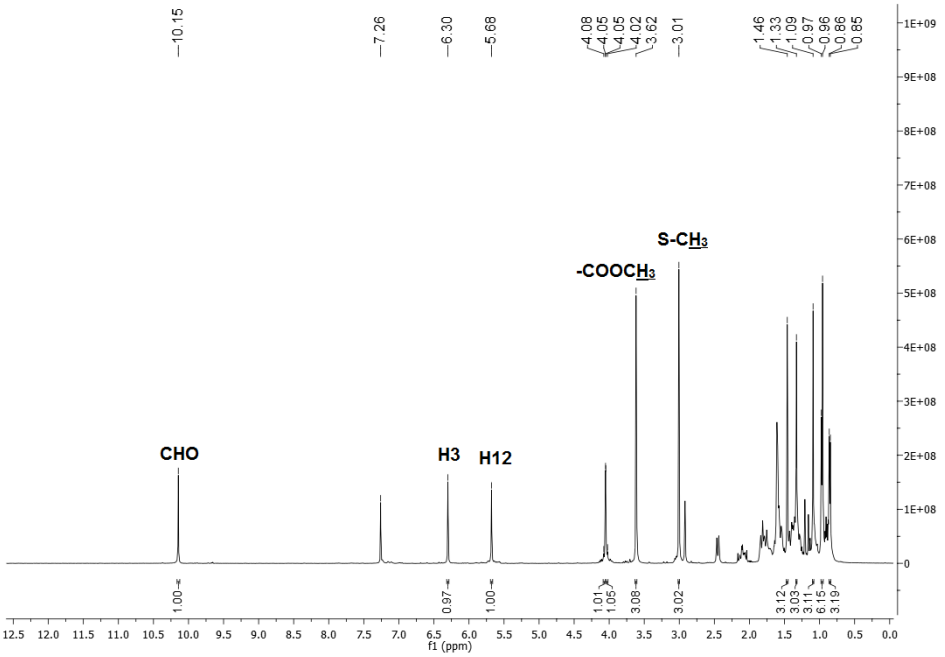

Figure 4.13 ^{1}H NMR spectrum of compound **4.29**.

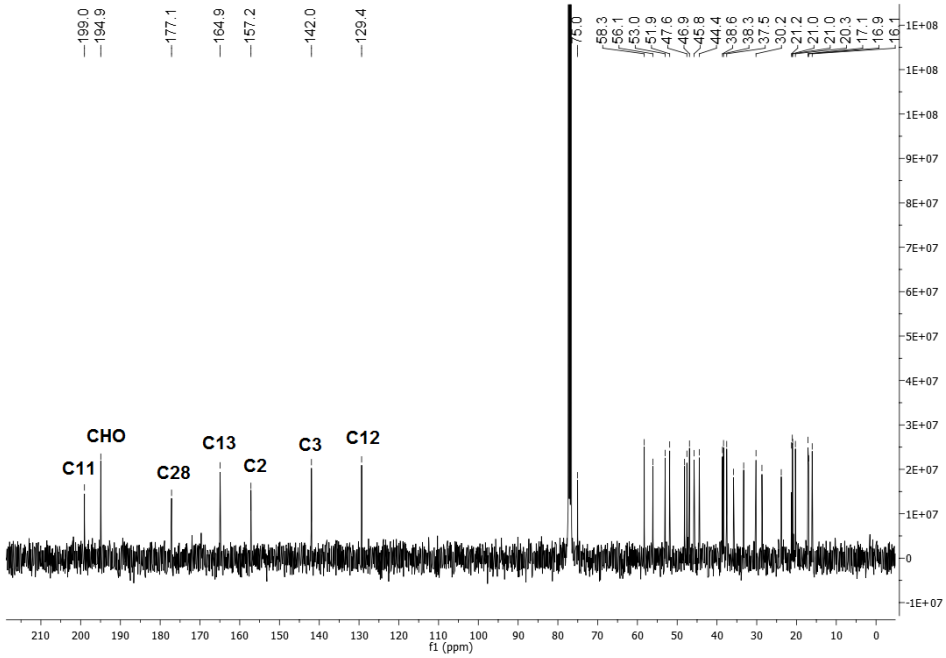

Figure 4.14 ^{13}C NMR spectrum of compound **4.29**.

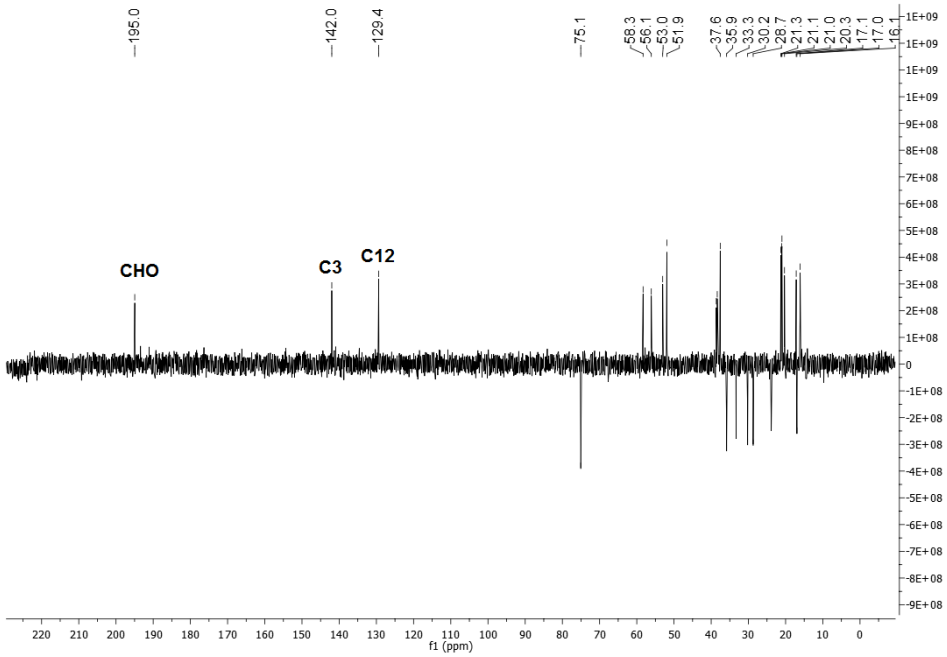

Figure 4.15 DEPT 135 spectrum of compound **4.29**.

4.2.2 Biological evaluation

4.2.2.1 Evaluation of the antiproliferative activity

The antiproliferative activity of asiatic acid **1.27** and of all the newly synthesized derivatives was evaluated against human breast adenocarcinoma (MCF-7), human colon adenocarcinoma (HT-29), and human cervix adenocarcinoma (HeLa) cell lines by MTT assay. The intermediates (**4.1**, **4.3**, **4.4**, **4.6**, **4.7**, **4.9**, **4.10** and **4.11**) and the control drug cisplatin were tested against the HeLa cell line. The IC_{50} values were determined after 72 h of incubation and are depicted in Table 4.1.

It was found that the great majority of the new derivatives showed better antiproliferative activities than parental asiatic acid **1.27** against the tested cell lines (Table 4.1). These new derivatives were particularly active against the HeLa cell line, with the exception of compound **4.27**. Therefore, a SAR was established based on their IC_{50} values obtained on HeLa cells (Fig. 4.2).

Table 4.1 Cytotoxic activity, expressed as IC_{50}, of asiatic acid **1.27**, its derivatives and cisplatin against breast (MCF-7), colon (HT-29) and cervix (HeLa) cancer cell lines.[a]

Compound	IC_{50} (µM ± SD) [b]		
	MCF-7	**HT-29**	**HeLa**
Asiatic acid 1.27	68.50 ± 2.12	64.33 ± 3.21	52.47 ± 0.06
4.1	N.D.	N.D.	27.50 ± 2.50
4.2	N.D.	N.D.	20.67 ± 1.53
4.3	N.D.	N.D.	21.67 ± 1.04
4.4	N.D.	N.D.	4.70 ± 0.40
4.5	4.00 ± 0.02	5.70 ± 0.46	4.75 ± 0.21
4.6	N.D.	N.D.	5.30 ± 0.2
4.7	N.D.	N.D.	0.60 ± 0.07
4.8	0.70 ± 0.05	0.64 ± 0.05	0.51 ± 0.03
4.9	N.D.	N.D.	0.60 ± 0.04
4.10	N.D.	N.D.	3.13 ± 0.32
4.11	N.D.	N.D.	37.17 ± 2.57
4.12	12.03 ± 0.40	12.20 ± 0.26	8.48 ± 1.31
4.13	0.74 ± 0.05	0.59 ± 0.04	0.30 ± 0.02
4.14	>60	>60	43.17 ± 3.55
4.15	14.33 ± 1.53	10.27 ± 1.55	8.90.± 0.53
4.16	16.10 ± 1.40	17.00 ± 1.32	14.60 ± 1.65
4.17	1.02 ± 0.11	0.97 ± 0.09	0.60 ± 0.05
4.18	0.88 ± 0.07	0.77 ± 0.03	0.49 ± 0.00
4.19	1.03 ± 0.04	0.84 ± 0.05	0.53 ± 0.01
4.20	1.20 ± 0.05	0.73 ± 0.02	0.53 ± 0.03
4.21	0.98 ± 0.02	0.66 ± 0.05	0.54 ± 0.02
4.22	7.00 ± 0.00	6.13 ± 0.32	6.33 ± 0.15
4.23	11.50 ± 1.32	12.20 ± 1.04	10.75 ± 0.35
4.24	>30	>60	12.00 ± 1.41
4.25	>60	>60	15.50 ± 0.71
4.26	30.00 ± 1.41	>30	26.80 ± 2.34
4.27	>60	>60	>60
4.28	0.47 ± 0.02	0.45 ± 0.05	0.30 ± 0.02
4.29	0.65 ± 0.04	0.59 ± 0.02	0.24 ± 0.02
4.30	19.50 ± 2.12	9.77 ± 0.23	7.27 ± 0.91
Cisplatin	19.10 ± 4.50	6.11[262] [c]	2.28 ± 0.26

[a] The cell lines were treated with increasing concentrations of each compound for 72 h. IC_{50} Values were determined by MTT assay and are expressed as means ± SD (standard deviation) of three independent experiments. N.D. not determined.

[b] IC_{50} is the concentration of compound that inhibits 50% of cell growth.

[c] IC_{50} value obtained from literature, determined using the same experimental methodology and included here for comparison.

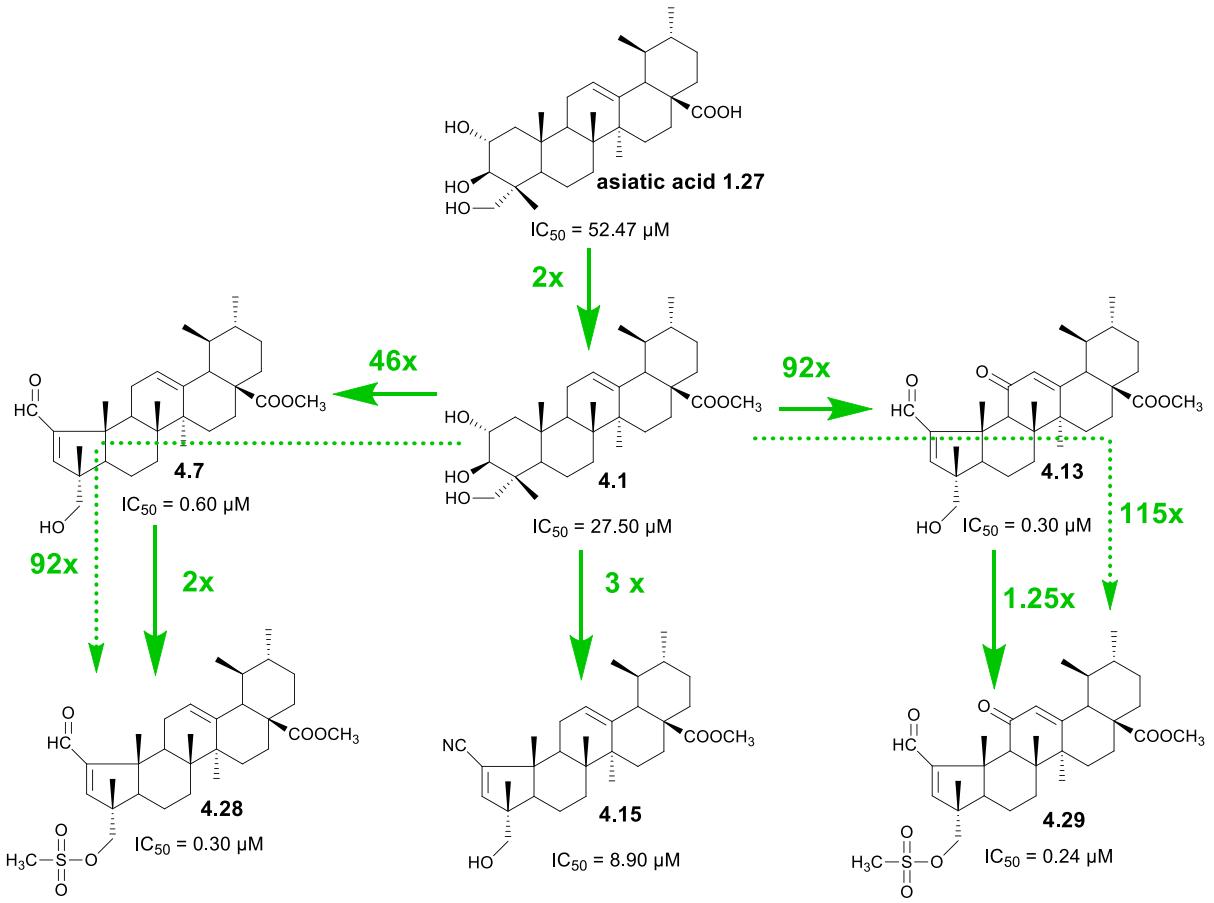

Figure 4.16 Schematic representation of the SAR for the antiproliferative activity of several semisynthetic derivatives of asiatic acid **1.27** against the HeLa cell line. The SAR was established based on IC_{50} values. The introduction of small ester moieties at C28 increased antiproliferative activity. Compound **4.1** was 2-fold more active than asiatic acid **1.27**. The conversion of the hexameric A-ring into a pentameric A-ring containing an α,β-unsaturated aldehyde moiety was critical for antiproliferative activity. Compounds **4.7** and **4.13** were 46- and 92-fold more active than compound **4.1**. The introduction of the methanesulfonyloxy moiety at C23 increased antiproliferative activity: Compounds **4.28** and **4.29** were 2- and 1.25-fold more active than compounds **4.7** and **4.13** respectively.

The methyl ester derivatives **4.1**, **4.4**, and **4.7** and the ethyl ester derivatives **4.2**, **4.5**, and **4.8** exhibited increased cytotoxic activity compared with the corresponding compounds with a free carboxylic acid group (asiatic acid **1.27**, **4.3**, and **4.6**, respectively). These results are in agreement with previous studies, in which the short chain ester derivatives at C28 of ursane-type triterpenoids increase cytotoxic activity.[263,296]

The direct comparison of the antiproliferative activities (against the HeLa cell line) of compounds **4.7** vs **4.13**, as well as compounds **4.28** vs **4.29**, indicated that the introduction of a keto group at position 11 improves antiproliferative activity. However, an opposite effect was observed when the activity of the following pairs of compounds: **4.1** vs **4.11**, **4.9** vs **4.10**, and **4.4** vs **4.12** was compared. These results suggest that there is no direct relationship between the introduction of a keto group at C11 and the antiproliferative activity of the compound, which is in accordance with the results of a previous study.[297]

The conversion of hexameric ring A into the corresponding heptameric lactol ring substantially improved the growth inhibitory activity in all tested cell lines. The lactol derivatives (**4.3**, **4.4**, **4.5**, and **4.12**) showed IC_{50} values ranging from 4.70 μM (**4.4**) to 8.48 μM (**4.12**), which was 6–11 times lower than the IC_{50} of asiatic acid **1.27** (52.47 μM) against the HeLa cell line.

The group of derivatives that had a pentameric A-ring with an α,β-unsaturated carbonyl moiety (**4.6**–**4.8**, **4.13**, **4.17**–**4.21**, **4.28** and **4.29**) proved to be the most active among all tested derivatives in all tested cancer cell lines. These compounds presented IC_{50} values ranging from 0.24 μM (compound **4.29**) to 5.30 μM (compound **4.6**) against the HeLa cell line. Moreover, with the exception of compound **4.6**, all derivatives of this group were more active than cisplatin (in HeLa cell line). These results indicate that the α,β-unsaturated carbonyl moiety in ring A is essential for the antiproliferative activity of these compounds against cancer cell lines.

The conversion of the aldehydes intro nitrile to afford derivatives **4.14**, **4.15**, and **4.16**, having a pentameric A-ring with an α,β-unsaturated nitrile resulted in a decrease of the activity, compared with precursor compounds **4.6**, **4.7** and **4.13**, respectively. However, compounds **4.14**, **4.15** and **4.16** were 1.2-, 5.9-, and 3.6-fold more potent than was asiatic acid **1.27**, respectively, against the HeLa cell line.

The effect of different substituents at the C23 of compounds **4.13** and **4.15** on their antiproliferative activities was also investigated. It was found that, with the exception of compound **4.22**, only the introduction of the methanesulfonyloxy group at C23 (compounds **4.28**, **4.29**, and **4.30**) resulted in a marked increase in antiproliferative activity. In fact, compounds **4.28** and **4.29** were the most active compounds among all the synthesized derivatives, as they were approximately 175- and 218-fold more active than asiatic acid **1.27**, respectively, against the HeLa cell line.

The most active compounds **4.8**, **4.13**, **4.28**, and **4.29**, were selected and their antiproliferative activity was further evaluated against a panel of other four cancer cell lines (Jurkat, PC-3, MIA PaCa-2, and A-375). As depicted in Table 4.2, the selected compounds markedly inhibited the proliferation of all tested cancer cell lines, with IC_{50s} lower than 1 μM.

Table 4.2 Cytotoxic activities, expressed as IC_{50}, of asiatic acid **1.27**, derivatives **4.8**, **4.13**, **4.28**, **4.29** and cisplatin against leukemia (Jurkat), prostate (PC-3), pancreas (MIA PaCa-2), melanoma (A375) cancer cell lines and nontumor fibroblast cell line (BJ).[a]

Compound	IC_{50} (μM ± SD) [b]				
	Jurkat	**PC-3**	**MiaPaca-2**	**A-375**	**BJ**
Asiatic acid 1.27	37.18 ± 3.75	67.25 ± 0.35	50.67 ± 1.15	50.33 ± 2.57	88.70 ± 0.58
4.8	0.45 ± 0.04	0.57 ± 0.04	0.83 ± 0.04	0.63 ± 0.05	N.D.
4.13	0.18 ± 0.02	0.60 ± 0.05	0.60 ± 0.06	0.38 ± 0.01	3.33 ± 0.25
4.28	0.27 ± 0.01	0.41 ± 0.02	0.60 ± 0.06	0.36 ± 0.03	1.94 ± 0.08
4.29	0.11 ± 0.01	0.42 ± 0.02	0.46 ± 0.04	0.25 ± 0.01	2.43 ± 0.11
Cisplatin	1.94[265 c]	4.60[266 c]	5.00 ± 1.00[267 c]	3.11 ± 0.98[268 c]	10.10 ± 2.00

[a] The cell lines were treated with increasing concentrations of each compound for 72h. IC_{50} Values were determined by MTT assay in PC-3, MIA PaCa-2, A375 and BJ cell lines and by XTT assay in Jurkat cell line. The results shown are expressed as means ± SD of three independent experiments. N.D. not determined.

[b] IC_{50} is the concentration of compound that inhibits 50% of cell growth.

[c] IC_{50} value obtained from literature, determined using the same experimental methodology and included here for comparison.

To evaluate the selectivity of compounds **4.13**, **4.28**, and **4.29**, their cytotoxic activity was also evaluated in a nontumor fibroblast cell line (BJ) (Table 4.2, Fig. 4.17). The results of this analysis revealed that compounds **4.13**, **4.28**, and **4.29** exhibited a decreased toxicity for the normal fibroblast cell line BJ compared with the cancer cell lines. The analysis of the selectivity index (IC_{50} in the BJ cell line/IC_{50} in the cancer cell line) values revealed that compound **4.13** was 4.5- to 18.5-fold more active against cancer cells than against nontumor BJ cells; compound **4.28** was 3.2- to 7.2-fold more active against cancer cells than against

nontumor BJ cells; and compound **4.29** was 3.7- to 22.1-fold more active against cancer cells than against nontumor BJ cells.

Compound **4.29** presented the best antiproliferative profile, and was especially active against the HeLa and Jurkat cell lines, with IC_{50} values of 0.24 μM and 0.11 μM, respectively. Thus, this compound was selected for further studies aimed at exploring the mechanism underlying its antiproliferative effect against the HeLa cell line.

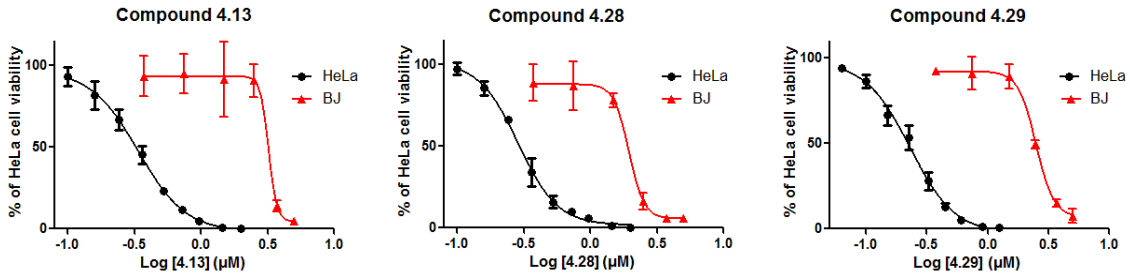

Figure 4.17 Dose-response curves of the antiproliferative effect of derivatives **4.13**, **4.28**, and **4.29** against the HeLa cancer cell line and the nontumor BJ cell line. Results are presented as the mean ± SD of three independent experiments.

4.2.2.2 Effects of compound 4.29 on the cell cycle distribution

The cell cycle consists in an organized set of events that culminate in proper division of the cell into two daughter cells.[23,25] To shed some light into the possible mechanism of action of compound **4.29**, its effect on the cell-cycle distribution of HeLa cells was investigated. Cells were treated with increasing concentrations of **4.29** (0.24, 0.48, 0.96 and 1.44 μM) for 24 h and the cell cycle distribution was assessed by FACS analysis after staining the cells with PI. As observed in Figure 4.18, treatment of HeLa cells with 0.96 μM of compound **4.29** increased the percentage of cells in the G0/G1phase, from 50.53% in control cells (non treated cells) to 68.65% in treated cells. Concomitantly, the percentage of cells in the S phase decreased from 36.24% in control cells to 12.89% in treated cells. These results suggest that compound **4.29** inhibits the proliferation of HeLa cells via cell-cycle arrest at the G0/G1 phase.

The population of cells at sub-G0/G1 phase increased around 17% after treatment of HeLa cells with 1.44 μM of compound **4.29**, which suggests that this compound has the ability to induce cell death in a dose-dependent manner.

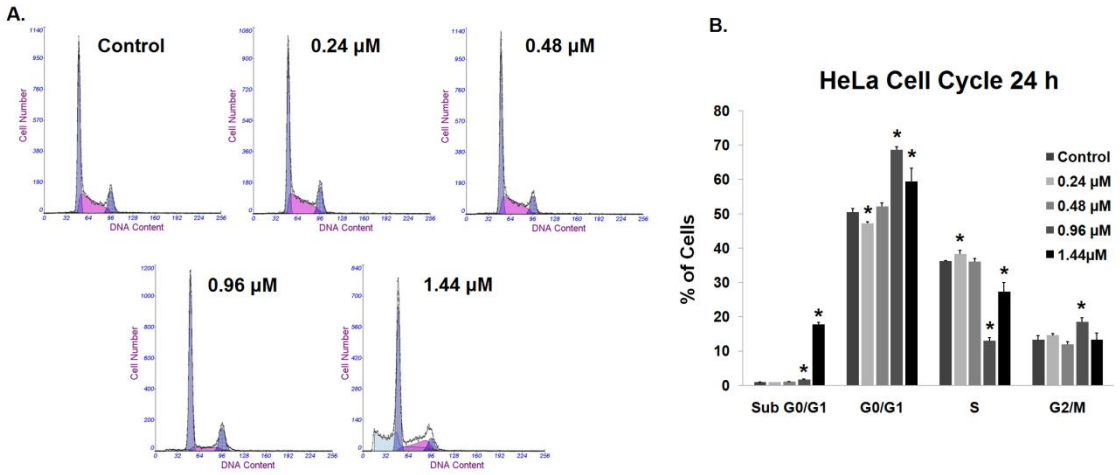

Figure 4.18 Cell-cycle distribution of HeLa cells untreated (control) or treated with the indicated concentrations of compound **4.29** for 24 h. The cell-cycle analysis was performed after propidium iodine staining. **A.** Representative histograms obtained for the cell-cycle analysis. **B.** Graph bar summarizing the variation in the percentage of cells in each phase of the cell cycle. Results are presented as the mean ± SD of three independent experiments. Differences between treated and control groups were considered statistically significant at $p < 0.05$ (*).

4.2.2.3 Effect of compound 4.29 on the levels of cell cycle-related proteins

Cell cycle dysregulation is one of the hallmarks of cancer; thus, proteins that regulate critical events of the cell cycle may be useful targets for the development of new anticancer drugs.[25,298] The experiment described above indicated that compound **4.29** arrested the cell cycle at the G0/G1 phase. Therefore, the effects of this compound on the levels of some cell-cycle-regulatory proteins were explored using western blot analysis. As shown in Figure 4.19, treatment of HeLa cells with compound **4.29** at 0.96 µM significantly increased the levels of $p27^{kip1}$, which was in agreement with the observation of cell-cycle arrest at the G0/G1 phase. Upregulation of $p21^{cip1/waf1}$ was also observed after treatment with 1.44 µM compound **4.29**. These data suggest that **4.29** preferably targets $p27^{kip1}$. Compound **4.29** also decreased the levels of cyclin D_3 in a concentration-dependent manner, but did not affect the levels of CDK4.

Considering that activated cyclin D/CDK4 complexes promote the progression of the G1 phase of the cell cycle and that the CDKIs $p21^{cip1/waf1}$ and $p27^{kip1}$ inhibit the kinase activity of such complexes, our results suggest that the upregulation of $p27^{kip1}$ and $p21^{cip1/waf1}$ and the downregulation of cyclin D3 induced by compound **4.29** lead to cell-cycle arrest at the G0/G1 phase, with the consequent inhibition of cell proliferation.

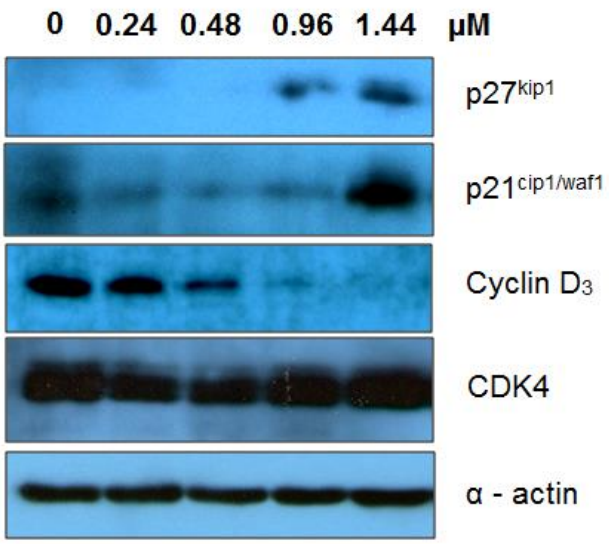

Figure 4.19 Effect of compound **4.29** on the levels of cell-cycle-related proteins. HeLa cells were treated with compound **4.29** at the indicated concentrations during 24 h. Protein levels were analyzed by western blot. α – Actin was used as loading control.

4.2.2.4 Apoptosis-inducing effect of compound 4.29 evaluated by annexin V-FITC/PI flow cytometric assay

The possibility of compound **4.29** to induce apoptosis in HeLa cells was explored. In the early stages of the apoptotic process, the membrane loses its symmetry and the phosphatidylserine (PS) is exposed to the external environment of the cell surface. Annexin V-FITC conjugate specifically binds to externalized PS, thus allowing the quantitative assessment of apoptosis.[299] In the late stages of apoptosis, the membrane loses its integrity and PI can enter the cell to access the nucleus and to intercalate between DNA bases.[299] Untreated (control) or treated HeLa cells with compound **4.29** at concentrations of 0.24, 0.48, 0.96 and 1.44 μM for 24 h, were double stained with Annexin V-FITC/PI and analyzed by flow cytometry.

It was observed that treatment of HeLa cells with 1.44 μM of compound **4.29** led to an increase in the number of apoptotic cells, from 2.9% in control cells to 19.17% in treated cells (i.e., 7.53% of early apoptotic cells and 11.64% of late apoptotic cells) (Fig. 4.20 C). Concomitantly, the percentage of live cells decreased from 96.53% in the control to 78.61% in treated cells (Fig. 20 B). Treatment with 0.24 μM or 0.48 μM of compound **4.29** did not

change the apoptotic rates significantly. These results suggest that compound **4.29** at 1.44 μM induces apoptosis in HeLa cells.

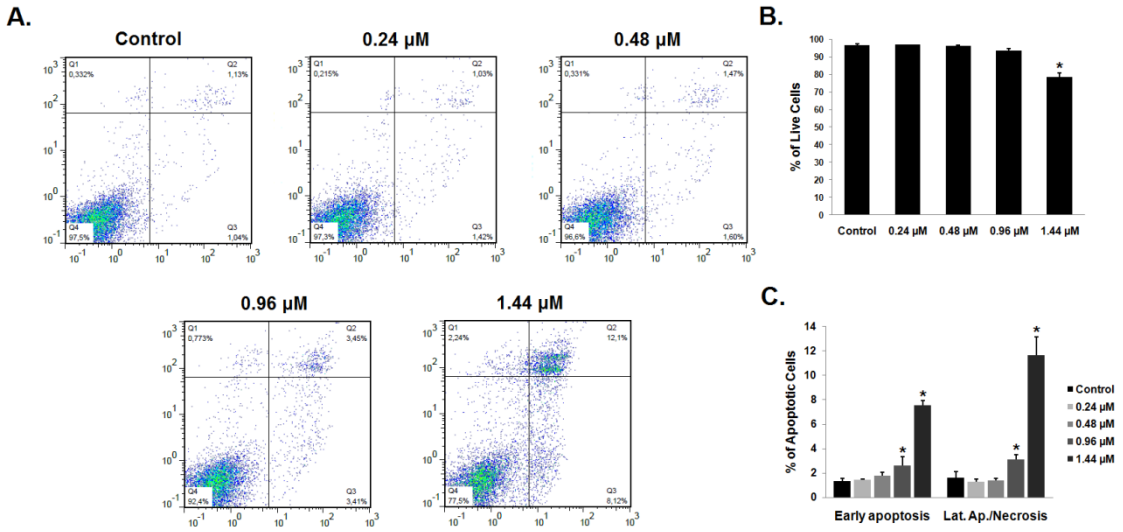

Figure 4.20 Annexin V-FITC/PI assay of HeLa cells untreated (control) or treated with the indicated concentrations of compound **4.29** for 24 h. **A.** Representative flow cytometric histograms that depict the variation in the percentage of cells that are alive (lower-left quadrant), in early apoptosis (lower-right quadrant), and in late apoptosis/necrosis (upper-left and upper-right quadrants). **B.** The bar graph depicts the variation in the percentage of live cells. **C.** The bar graph depicts the variation in the percentage of cells that are in early apoptosis and in late apoptosis/necrosis. Results are presented as the mean ± SD of three independent experiments. Differences between treated and control groups were considered statistically significant at $p < 0.05$ (*).

4.2.2.5 Apoptosis-inducing effect of compound 4.29 evaluated by morphological analysis

Apoptosis is characterized by typical morphological features.[42,300] Therefore, the morphology of HeLa cells untreated or treated with compound **4.29** at 0.96 μM and 1.44 μM for 24 h was analyzed using microscopic observation, to further evaluate the proapoptotic effect of compound **4.29**.

4.2.2.5.1 Phase-contrast microscopy

As shown in the phase-contrast microscopic pictures (Fig. 4.21), treatment of HeLa cells with compound **4.29** reduced the cell density and induced remarkable morphological

changes. Compared with control cells, treated cells became smaller and nonadherent and acquired a rounded morphology.

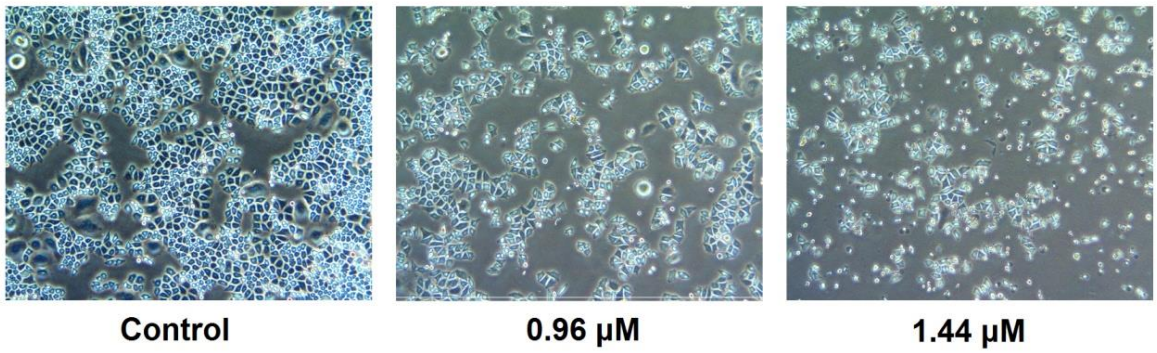

Figure 4.21 Representative phase-contrast images of HeLa cells untreated (control) or treated with compound **4.29** at the specified concentrations for 24 h.

4.2.2.5.2 Fluorescence microscopy after Hoechst 33258 staining

To assess the nuclear morphological changes in greater detail, HeLa cells were stained with Hoechst 33258 after treatment with compound **4.29** and were analyzed by fluorescence microscopy. As shown in Figure 4.22, control cells were uniformly stained and presented a normal morphology. Conversely, HeLa cells treated with 0.96 μM of compound **4.29** exhibited typical apoptotic morphological changes, such as chromatin condensation and cell shrinkage. Nuclear fragmentation and membrane blebbing were evident after treatment with 1.44 μM of compound **4.29**. A decrease in the number of cells with increasing drug concentrations was also observed. The morphological changes induced by compound **4.29** were consistent with an apoptotic cell death process.

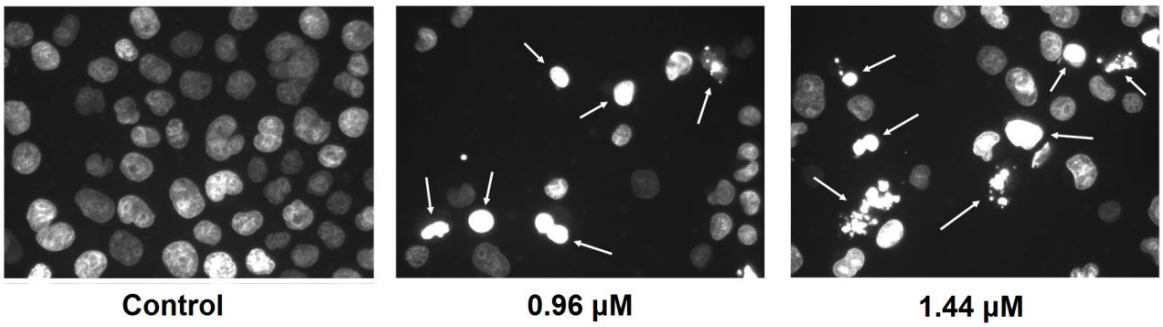

Figure 4.22 Representative fluorescence microscopic images of HeLa cells untreated (control) or treated with compound **4.29** at specified concentrations for 24 h. HeLa cells were stained with Hoechst 33258 before analysis by fluorescence microscopy. White arrows represent apoptotic cells.

4.2.2.6 Effects of compound 4.29 on the levels of apoptosis related proteins

To gain deeper insight into the mechanism via which compound **4.29** induces apoptosis in HeLa cells, we investigated the effects of this compound (0–1.44 μM over 24 h) on the levels of some apoptosis-related proteins using western blot analysis (Fig. 4.23). The activation of caspases is one of the most important mechanisms underlying the execution of apoptosis.[35,46,301] Therefore, the effect of compound **4.29** on the levels of caspase 9, caspase 8, caspase 3, and cleaved PARP was investigated. Cleaved PARP is an 85 kDa fragment that is generated during apoptosis from the full length PARP via the proteolytic action of active caspase 3 and is considered a biomarker of apoptosis.[271] As shown in Fig. 4.23, treatment of HeLa cells with 1.44 μM of compound **4.29** led to the cleavage of pro-caspase 8 and pro-caspase 3 into their active forms, and to increased levels of cleaved caspase 9 (active form of caspase 9). Compound **4.29** also induced a significant increase in the levels of cleaved PARP. The activation of caspases 8 and 9 suggest that compound **4.29** induces apoptosis in HeLa cells *via* a caspase-driven mechanism with activation of both extrinsic and intrinsic pathways.

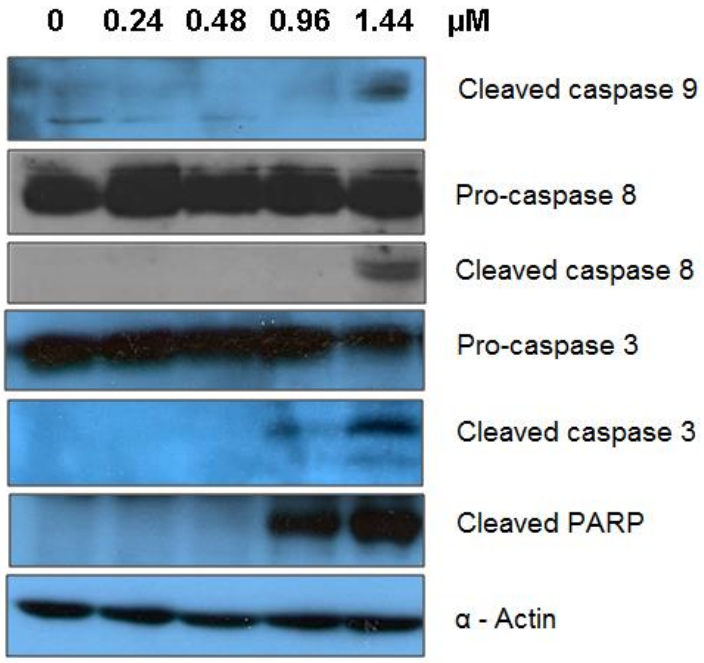

Figure 4.23 Effect of compound **4.29** on the levels of apoptosis-related proteins. HeLa cells were treated with the indicated concentrations of compound **4.29** for 24 h. The levels of the indicated proteins were assessed by western blot analysis. α–actin was used as loading control. Compound **4.29** induced caspase 9, caspase 8 and caspase 3 activation and the cleavage of PARP.

Subsequently, the effect of compound **4.29** on the levels of Bcl-2 protein family members, such as Bcl-2 (antiapoptotic), Bax (proapoptotic), and Bid (proapoptotic) was explored. As depicted in Figure 4.24 A and 4.24 B, the treatment of HeLa cells with compound **4.29** caused a downregulation of Bcl-2 and an upregulation of Bax in a concentration-dependent manner. These data suggest that the mitochondrial pathway is involved in compound **4.29**-induced apoptosis. Compound **4.29** also downregulated the levels of Bid, suggesting the activation of Bid into t-Bid. However, bands corresponding to t-Bid were not detected on western blots, which can be justified by the short half-life and small size of t-Bid. Further studies are needed to confirm and understand better the role of the intrinsic and extrinsic pathways in this possible apoptotic mechanism.

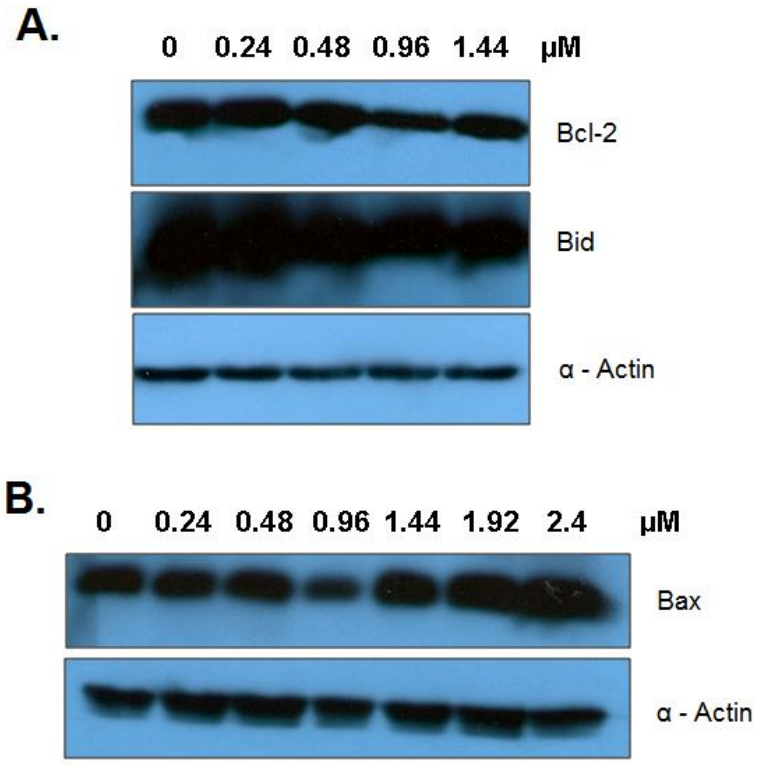

Figure 4.24 Effect of compound **4.29** on the levels of Bcl-2, Bid and Bax proteins. HeLa cells were treated with the indicated concentrations of compound **4.29** for 24 h. The levels of the indicated proteins were assessed by western blot analysis. α–actin was used as loading control. **A.** Compound **4.29** downregulated the levels of Bcl-2 and Bid. **B.** Compound **4.29** upregulated the levels of Bax.

4.3 Conclusions

In conclusion, a panel of new pentameric A-ring asiatic **1.27** acid derivatives was successfully synthesized and the structures of the new compounds were fully characterized using NMR, MS, and IR techniques.

Our results showed that the conversion of the hexameric A-ring of asiatic acid **1.27** into a pentameric A-ring with α,β-unsaturated carbonyl or α,β-unsaturated nitrile moieties significantly improved the antiproliferative activity of the parental compound (asiatic acid **1.27**).

Compound **4.29** displayed the best antiproliferative profile, with IC_{50} values ranging from 0.11 to 0.65 μM against human cancer cell lines. This compound arrested the cell cycle at the G0/G1 phase and induced apoptosis in HeLa cells via the activation of caspases 9, 8, and 3, cleavage of PARP, and modulation of the ratio of Bax/Bcl-2.

4.4. Experimental section

4.4.1 Chemistry

4.4.1.1 Reagents and solvents

Asiatic acid, potassium carbonate (K_2CO_3), methyl iodide, ethyl iodide, sodium periodate ($NaIO_4$), piperidine, acetic acid, magnesium sulfate ($MgSO_4$), acetic anhydride, 4-(dimethylamino)pyridine (DMAP), potassium permanganate ($KMNO_4$), iron(III) sulfate hydrate [$Fe_2(SO_4)_3.nH_2O$], *t*-butanol, potassium hydroxide (KOH), triethylamine, methanesulfonyl chloride, aqueous ammonia solution 25%, iodine, sodium tiosulfate ($Na_2S_2O_3$), acetic anhydride, butyric anhydride, benzoic anhydride, succinic anhydride, cinnamoyl chloride, 1,1'-carbonyldiimidazole (CDI), 1,1′-carbonylbis(2’-methylimidazole) (CBMI), hydrochloridric acid (HCl), sodium bicarbonate ($NaHCO_3$), sodium sulfate (Na_2SO_4) and sodium sulfite (Na_2SO_3) were purchased from Sigma-Aldrich Co. The solvents used in the reactions were obtained from Merck Co. These solvents were of analytical grade and if necessary they were purified and dried according to usual procedures described in the

literature.[274] The solvents used in the workup procedures were purchased from VWR Portugal.

4.4.1.2 Chromatographic techniques

Thin layer chromatography (TLC) was carried out in Kieselgel 60HF254/Kieselgel 60G. The plates were observed under UV light and revealed using a mixture of etanol/sulfuric acid (95:5) followed by heating at 120 ºC.

Separation and purification of the compounds were performed by flash column chromatography (FCC) using Kieselgel 60 (230-400 mesh, Merck) and an appropriate eluent.

4.4.1.3 Analytical techniques and equipment

Melting points were measured using a BUCHI melting point B-540 apparatus and were uncorrected.

IR spectra were obtained on a Fourier transform spectrometer, using the KBr pellets method. KBr pellets were prepared with a mixture of about 2 mg of the solid compound diluted with 198 mg of KBr, ground to a fine powder and pressed at around 12000 psi for 5 min, to obtain a thin and transparent pellet.

^{1}H and ^{13}C NMR spectra were recorded on Brucker Digital NMR–Avance 400 spectrometer, using $CDCl_3$ as internal standard. The chemical shifts (δ) are reported in parts per million (ppm), and coupling constants (*J*) are reported in hertz (Hz).

The mass spectrometry was carried out on Quadrupole/Ion Trap Mass Spectrometer (QIT-MS) (LCQ Advantage MAX, THERMO FINNINGAN). HRMS was performed on a Fourier Transform Ion Cyclotron Resonance (FT-ICR) mass spectrometer (Bruker Apex Ultra with a 7 Tesla actively shielded magnet).

The elemental analysis was performed on an Analyzer Elemental Carlo Erba 1108 apparatus by chromatographic combustion.

4.4.1.4 Synthesis of asiatic acid derivatives

Methyl 2*α*,3β,23-trihydroxyurs-12-en-28-oate (4.1)

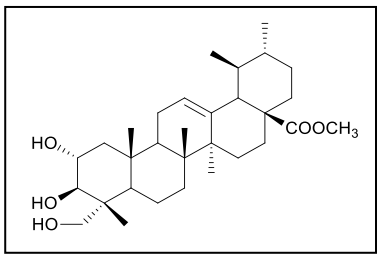

To a stirred solution of asiatic acid **1.27** (1000 mg, 2.05 mmol) and anhydrous potassium carbonate (707.20 mg, 5.12 mmol) in dry DMF (20 mL), methyl iodide (254.7 µl; 4.04 mmol) was added. The reaction mixture was stirred at room temperature in anhydrous conditions. After 2 hours the reaction mixture was evaporated under reduced pressure to remove the organic phase. The crude obtained was dispersed with water (100 mL) and extracted with ethyl acetate (3 × 100 mL). The resulting organic phase was washed with 5% aqueous HCl (2 × 100 mL), 10% aqueous $NaHCO_3$ (2 × 100 mL), 10% aqueous Na_2SO_3 (100 mL), water (100 mL) and brine (100 mL), dried over Na_2SO_4, filtered, and concentrated under vacuum to afford **4.1** as a white powder (1040 mg, quantitative). Mp: 211.6–214.1 °C. ν_{max}/cm^{-1} (KBr): 3419.17, 2946.70, 2925.48, 2873.42, 1725.98, 1454.06, 1049.09. ^1H NMR (400MHz, $CDCl_3$): δ = 5.23 (t, *J* = 3.1 Hz, 1H, H12), 3.79–3.71 (m, 1H, H2), 3.59 (m, 4H), 3.40 (d. *J* = 10.0 Hz, 1H, H23), 3.38 (d, *J* = 10.3 Hz, 1H, H23), 1.07 (s, 3H), 1.01 (s, 3H), 0.94 (d, *J* = 5.9 Hz, 3H), 0.85 (d, *J* = 6.5 Hz, 3H), 0.81 (s, 3H), 0.72 (s, 3H) ppm. ^{13}C NMR (100MHz, $CDCl_3$): δ = 178.1 (C28), 138.2 (C13), 125.2 (C12), 79.8, 69.5, 68.7, 52.8, 51.4, 48.6, 48.0, 47.4, 46.3, 42.6, 42.0, 39.5, 39.0, 38.8, 38.1, 36.6, 32.5, 30.6, 27.9, 24.2, 23.7, 23.3, 21.2, 18.2, 17.1, 17.0, 16.9, 12.9 ppm. DI-ESI-MS *m/z* $[M+H]^+$: 502.98. Anal. Calcd. for $C_{31}H_{50}O_5.0.25H_2O$: C, 73.41; H, 10.03. Found: C, 73.29; H, 10.46%.

Ethyl 2*α*,3β,23-trihydroxyurs-12-en-28-oate (4.2)

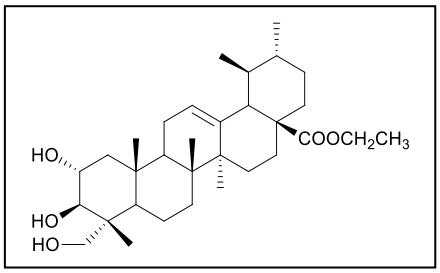

Accordingly to the method described for **4.1,** using asiatic acid **1.27** (500 mg, 1.02 mmol), anhydrous potassium carbonate (353.50 mg, 2.56 mmol), dry DMF (10 mL) and ethyl iodide (246.77 µl; 3.07 mmol) for 3 hours at room temperature, to afford **4.2** as a white powder (507.3 mg, 96%). Mp: 177.5–179.1 °C. ν_{max}/cm^{-1} (KBr): 3417.24, 2973.70, 2925.48, 2871.49, 1724.05, 1454.06, 1037.52. ^1H NMR (400MHz, $CDCl_3$): δ = 5.24 (t, *J* = 3.1 Hz, 1H,

H12), 4.05 (q, *J* = 7.2 Hz, 2H, COO$\underline{CH_2}CH_3$), 3.79–3.72 (m, 1H, H2), 3.66 (d, *J* = 10.4 Hz, 1H, H3), 3.44 (d, *J* = 9.0 Hz, 1H, H23), 3.41 (d, *J* = 9.4 Hz, 1H, H23), 1.21 (t, *J* = 7.0 Hz, 3H, COOCH$_2\underline{CH_3}$), 1.08 (s, 3H), 1.03 (s, 3H), 0.94 (d, *J* = 6.0 Hz, 3H), 0.87 (s, 3H), 0.85 (d, *J* = 6.2 Hz, 3H), 0.76 (s, 3H) ppm.^{13}C NMR (100MHz, $CDCl_3$): δ = 177.5 (C28), 138.2 (C13), 125.2 (C12), 68.7, 60.0, 52.8, 47.8, 47.5, 46.2, 42.1, 39.6, 39.1, 38.8, 38.1, 38.6, 32.7, 30.6, 27.9, 24.1, 23.6, 23.3, 21.2, 18.3, 17.2, 17.1, 17.0, 14.2, 12.8 ppm. DI-ESI-MS *m/z* $[M+H]^+$: 516.97. Anal. Calcd. for $C_{32}H_{52}O_5.0.5H_2O$: C, 73.10; H, 10.16. Found: C, 73.31; H, 10.32%.

2*α*,23-Lactol-3-formyl- urs-12-en-28-oic acid (4.3)

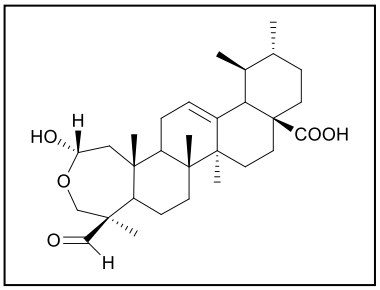

To a stirred solution of asiatic acid **1.27** (200 mg, 0.41 mmol) in methanol/water (5 mL/0.25 mL (20:1)), $NaIO_4$ (131.30 mg; 0.61 mmol) was added. The reaction mixture was stirred at room temperature. After 2 hours the reaction mixture was evaporated under reduced pressure to remove the organic phase. The crude obtained was dispersed with water (40 mL) and extracted with ethyl acetate (3 × 40 mL). The resulting organic phase was washed with water (4 × 40 mL) and brine (40 mL), dried over Na_2SO_4, filtered, and concentrated under vacuum to afford **4.3** as a white powder (quantitative). Mp: 198.5–201.4 °C. ν_{max}/cm^{-1} (KBr): 3421.1, 2948.63, 2927.41, 2871.49, 2732.64, 2630.43, 1716.34, 1695.12, 1456.99, 1378.85, 1037.52. ^{1}H NMR (400MHz, $CDCl_3$): δ = 9.94 (s, 1H, CHO), 5.29 (t, *J* = 3.2 Hz, 1H, H12), 5.14–5.11 (m, 1H, H2), 3.94 (d, *J* = 13.4 Hz, 1H), 3.75 (d, *J* = 13.2 Hz, 1H), 1.08 (s, 3H), 1.06 (s, 3H), 0.99 (s, 3H), 0.95 (d, *J* = 6.0 Hz, 3H), 0.86 (s, 3H), 0.85 (d, *J* =5.4 Hz, 3H) ppm. ^{13}C NMR (100MHz, $CDCl_3$): δ = 206.1 (CHO), 182.9 (C28), 138.0 (C13), 126.0 (C12), 93.7, 65.4, 61.2, 53.4, 62.7, 48.1, 45.1, 43.6, 42.6, 40.0, 39.9, 38.9, 38.8, 38.6, 33.6, 30.6, 27.8, 24.6, 24.1, 23.2, 21.1, 20.6, 20.4, 17.9, 16.9, 14.6 ppm. DI-ESI-MS *m/z* $[M+H]^+$: 487.15. Anal. Calcd. for $C_{30}H_{46}O_5.H_2O$: C, 71.39; H, 9.59. Found: C, 71.49; H, 9.85%.

Methyl 2α,23-lactol-3-formyl-urs-12-en-28-oate (4.4)

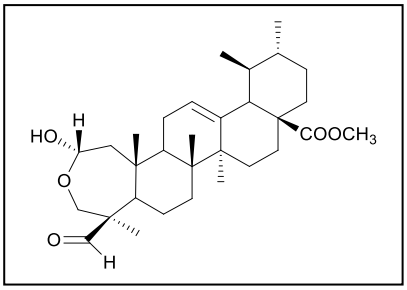

Accordingly to the method described for **4.3,** using compound **4.1** (1000 mg, 1.99 mmol), methanol / water (25 mL/1.25 mL [20:1]) and $NaIO_4$ (645.60 mg 3.02 mmol) for 3 hours to afford **4.4** as a white powder (978.70 mg, 98%). Mp: 144.7–147.1 °C. ν_{max}/cm^{-1} (KBr): 3444.24, 2948.63, 2927.41, 2871.49, 2730.71, 2626.57, 1722.12, 1454.06, 1378.85, 1037.52. ^{1}H NMR (400MHz, $CDCl_3$): δ = 9.94 (s, 1H, CHO), 5.30 (t, *J* = 3.3 Hz, H12), 5.13–5.09 (m, 1H, H2), 3.93 (d, *J* = 13.3 Hz, 1H), 3.74 (d, *J* = 13.3 Hz, 1H), 3.60 (s, 3H, COO$\underline{CH_3}$), 1.08 (s, 3H), 1.06 (s, 3H), 0.99 (s, 3H), 0.94 (d, *J* = 6.0 Hz), 0.85–0.83 (m, 6H) ppm. ^{13}C NMR (100MHz, $CDCl_3$): δ = 205.8 (CHO), 178.0 (C28); 138.3 (C13); 125.7 (C12); 93.7; 65.4, 61.1, 53.4, 53.0, 51.5, 48.2, 45.2, 43.7, 42.6, 40.0, 40.0, 38.9, 38.8, 36.5, 33.6, 30.6, 27.9, 24.6, 24.2, 23.2, 21.1, 20.6, 20.4, 17.9, 17.0, 14.5 ppm. DI-ESI-MS *m/z* $[M+H]^+$: 500.99. Anal. Calcd. for $C_{31}H_{48}O_5.0.25H_2O$: C, 73.70; H, 9.68. Found: C, 73.75; H, 9.97%.

Ethyl 2α,23-lactol-3-formyl-urs-12-en-28-oate (4.5)

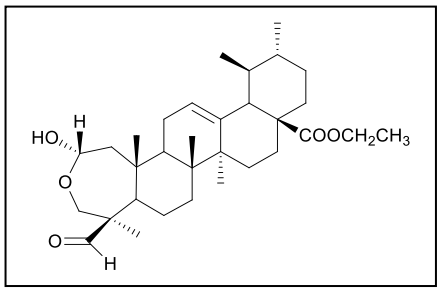

Accordingly to the method described for **4.3,** using compound **4.2** (480 mg, 0.93 mmol), methanol/water (12.90 mL/ 0.65 mL [20:1]) and $NaIO_4$ (299.45 mg, 1.40 mmol) for 1 h 30 min to afford **4.5** as a white powder (477.90 mg, quantitative). Mp: 138.1–142.0 °C. ν_{max}/cm^{-1} (KBr): 3444.24, 2950.55, 2927.41, 2971.49, 2732.64, 1720.19, 1454.06, 1378.85, 1230.36, 1141.65, 1037.52. ^{1}H NMR (400MHz, $CDCl_3$): δ = 9.94 (s, 1H, CHO), 5.29 (t, *J* = 3.1 Hz, 1H, H12), 5.12–5.09 (m, 1H, H2), 4.06 (q, *J* = 7.1 Hz, 2H, COO$\underline{CH_2}CH_3$), 3.93 (d, J = 13.3 Hz, 1H), 3.75 (d, *J* = 13.3 Hz, 1H), 1.21 (t, *J* = 7.1 Hz, 3H, $COOCH_2\underline{CH_3}$), 1.08 (s, 3H), 1.06 (s, 3H), 0.99 (s, 3H), 0.94 (d, *J* = 6.1 Hz, 3H), 0.84 (m, 6H) ppm. ^{13}C NMR (100MHz, $CDCl_3$): δ = 205.8 (CHO), 177.4 (C28), 138.3 (C13), 125.7 (C12), 93.6, 65.4, 61.1, 60.0, 53.4, 53.0, 48.0, 45.2, 43.7, 42.6, 40.1, 39.9, 39.0, 38.8, 36.5, 33.7, 30.7, 27.8, 24.6, 24.1, 23.1, 21.1, 20.6, 20.4, 18.0, 16.9, 14.5, 14.2 ppm. DI-ESI-MS *m/z* $[M+H]^+$: 514.92. Anal. Calcd. for $C_{32}H_{50}O_5.0.25H_2O$: C, 74.02; H, 9.80. Found: C, 73.84; H, 10.05%.

2-Formyl-23-hydroxy-A(1)-norursa-2,12-dien-28-oic acid (4.6)

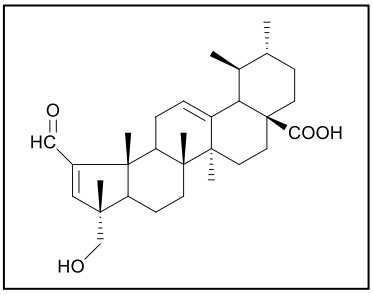

To a stirred solution of compound **4.3** (500 mg, 1.03 mmol) in dry benzene (50 mL), piperidine (3 mL) and acetic acid (3 mL) were added. The resultant solution was heated at 60 °C. After 1 hour, anhydrous magnesium sulfate (500 mg) was added and the reaction mixture was heated at 60 °C under nitrogen atmosphere for 4 h 20 min. The reaction mixture was evaporated under reduced pressure to remove the organic phase. The crude obtained was dispersed with water (50 mL) and extracted with ethyl acetate (3 × 50 mL). The resulting organic phase was washed with water (4 × 50 mL) and brine (50 mL), dried over Na_2SO_4, filtered, and concentrated under vacuum to afford a yellow powder. The crude solid was purified by flash column chromatography (petroleum ether/ethyl acetate 3:1 → 1:1), to afford **4.6** as a white solid (353.77 mg, 73%). Mp: 183.5–186.1 °C. ν_{max}/cm^{-1} (KBr): 3428.81, 2946.7, 2925.48, 2869.56, 2726.85, 2632.36, 1689.34, 1581.34, 1454.06, 1380.78, 1041.37. ^{1}H NMR (400MHz, $CDCl_3$): δ = 9.72 (s, 1H, CHO), 6.66 (s, 1H, H3), 5.28 (t, *J* = 3.0 Hz, 1H, H12), 3.62 (d, *J* = 10.7 Hz, 1H, H23), 3.45 (d, *J* = 10.7 Hz, 1H, H23), 1.25 (s, 3H), 1.10 (s, 3H), 1.01 (s, 3H), 0.93 (d, *J* = 6.2 Hz, 3H), 0.88 (s, 3H), 0.84 (d, *J* = 6.3 Hz, 3H) ppm. ^{13}C NMR (100MHz, $CDCl_3$): δ =190.8 (CHO), 183.3 (C28), 159.3 (C3), 158.9 (C2), 137.5 (C13), 126.6 (C12), 69.4, 56.3, 52.6, 50.9, 49.4, 47.9, 44.1, 42.4, 41.4, 38.8 (2C), 36.6, 33.5, 30.5, 28.2, 27.1, 24.0 (2C), 21.2, 19.0, 18.7, 17.3, 17.0, 15.9 ppm. DI-ESI-MS *m/z* $[M+H]^+$: 469.03. Anal. Calcd. for $C_{30}H_{44}O_4.H_2O$: C, 74.04; H, 9.53. Found: C, 73.68; H, 9.75%.

Methyl 2-formyl-23-hydroxy-A(1)-norursa-2,12-dien-28-oate (4.7)

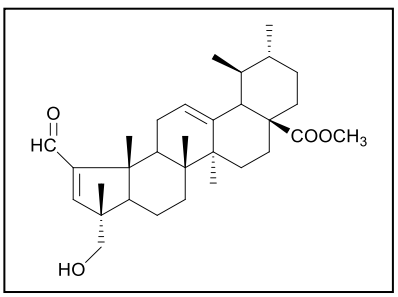

Accordingly to the method described for **4.6**, using compound **4.4** (500 mg, 0.99 mmol), dry benzene (50 mL), piperidine (2.5 mL) acetic acid (2.5 mL) and anhydrous magnesium sulfate (327 mg), to afford compound **4.7** as a yellow powder (488.5 mg, quantitative). Mp: 119.7–122.4 °C. ν_{max}/cm^{-1} (KBr): 3448.10, 2948.63, 2925.48, 2869.56, 2724.92, 2634.29, 1724.05, 1687.41, 1581.34, 1455.99, 1382.71, 1232.29, 1145.51, 1047.16. ^{1}H NMR (400MHz, $CDCl_3$): δ = 9.72 (s,

1H, CHO), 6.66 (s, 1H, H3), 5.28 (t, *J* = 3.2 Hz, 1H, H12), 3.62–3.60 (m, 4H), 3.46 (d, *J* = 10.7 Hz, 1H, H23), 1.25 (s, 3H), 1.09 (s, 3H), 1.02 (s, 3H), 0.93 (d, *J* = 6.1 Hz, 3H), 0.83 (m, 6H) ppm. ^{13}C NMR (100MHz, $CDCl_3$): δ = 190.8 (CHO), 178.1 (C28), 159.2 (C3), 158.9 (C2), 137.7 (C13), 126.3 (C12), 69.4, 56.3, 52.8, 51.4, 50.9, 49.4, 48.0, 44.1, 42.4, 41.3, 38.8, 38.8, 36.6, 33.5, 30.6, 28.2, 27.1, 24.2, 24.0, 21.2, 19.0, 18.7, 17.4, 17.0, 16.0 ppm. DI-ESI-MS *m/z* $[M+H]^+$: 482.98. Anal. Calcd. for $C_{31}H_{46}O_4.0.25H_2O$: C, 76.42; H, 9.62. Found: C, 76.58; H, 9.78%.

Ethyl 2-formyl-23-hydroxy-A(1)-norursa-2,12-dien-28-oate (4.8)

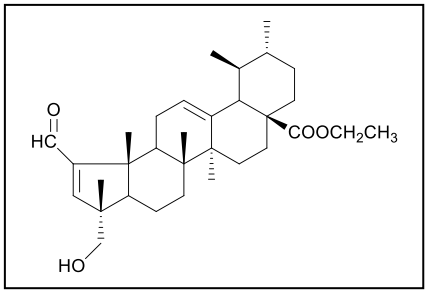

Accordingly to the method described for **4.6**, using compound **4.5** (300 mg, 0.583 mmol), dry benzene (30 mL), piperidine (1.5 mL), acetic acid (1.5 mL) and anhydrous magnesium sulfate (300 mg) to afford a yellow crude. The crude solid was purified by flash column chromatography (petroleum ether/ethyl acetate, 3:1 → 2:1), to afford **4.8** as a white solid (193.2 mg, 67%). Mp: 207.5–209.7 °C. ν_{max}/cm^{-1} (KBr): 3550.31, 2977.55, 2960.20, 2946.70, 2925.48, 2867.63, 2809.78, 2726.85, 1708.62, 1689.34, 1581.34, 1452.11, 1238.08, 1143.58, 1045.23. ^{1}H NMR (400MHz, $CDCl_3$): δ = 9.72 (s, 1H, CHO), 6.66 (s, 1H, H3), 5.28 (t, *J* = 3.0 Hz, 1H, H12), 4.09–4.02 (m, 2H, COO$\underline{CH_2}CH_3$), 3.62 (d, *J* = 8.5 Hz, 1H, H23), 3.46 (d, *J* = 8.8 Hz, 1H, H23), 1.25 (s, 3H), 1.22 (t, *J* = 7.2 Hz, 3H, $COOCH_2\underline{CH_3}$), 1.09 (s, 3H), 1.02 (s, 3H), 0.93 (d, *J* = 6.1 Hz, 3H), 0.86 (s, 3H), 0.83 (d, *J* = 6.5 Hz, 3H) ppm. ^{13}C NMR (100MHz, $CDCl_3$): δ = 190.8 (CHO), 177.6 (C28), 159.3 (C3), 158.9 (C2), 137.8 (C13), 126.3 (C12), 69.4 (C23), 60.0, 56.2, 52.8, 50.9, 49.4, 47.8, 44.1, 42.5, 41.4, 38.8 (2C), 36.6, 33.6, 30.6, 28.2, 27.1, 24.1, 23.9, 21.2, 19.0, 18.8, 17.4, 17.0, 15.9, 14.2 ppm. DI-ESI-MS *m/z* $[M+H]^+$: 497.07. Anal. Calcd. for $C_{32}H_{48}O_4$: C, 77.38; H, 9.74. Found: C, 76.94; H, 10.12%.

Methyl 2α,3β,23-triacetoxyurs-12-en-28-oate (4.9)

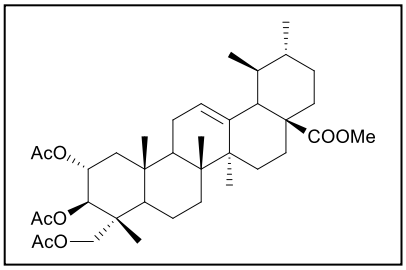

To a stirred solution of compound **4.1** (953 mg, 1.89 mmol) in dry THF (28 mL), acetic anhydride (1163.30 μl; 12.33 mmol) and a catalytic amount of DMAP (95.30 mg) were added. The reaction mixture was stirred at room temperature in anhydrous conditions. After 5 hours the reaction mixture was evaporated under reduced pressure to remove the organic phase. The crude obtained was dispersed with water (80 mL) and extracted with ethyl acetate (3 × 80 mL). The resulting organic phase was washed with 5% aqueous HCl (2 × 80 mL), 10% aqueous $NaHCO_3$ (2 × 80 mL), 10% aqueous Na_2SO_3 (80 mL), water (80 mL) and brine (80mL), dried over Na_2SO_4, filtered, and concentrated under vacuum to afford **4.9** as a white powder (1182 mg, 99% quantitative). Mp: 118.8–121.1 °C. ν_{max}/cm^{-1} (KBr): 2948.63, 2927.41, 2871.49, 1745.26, 1455.99, 1369.21, 1234.22, 1043.30. ^1H NMR (400MHz, $CDCl_3$): δ = 5.24 (t, *J* = 3.0 Hz, 1H, H12), 5.19–5.13 (m, 1H, H2), 5.08 (d, *J* = 10.3 Hz, 1H, H3), 3.85 (d, J = 11.8 Hz, 1H, H23), 3.60 (s, 3H, COO$\underline{CH_3}$), 3.57 (d, *J* = 11.8 Hz, 1H, H23), 2.08 (s, 3H, CH_3CO), 2.01 (s, 3H, CH_3CO), 1.97 (s, 3H, CH_3CO), 1.09 (s, 3H), 1.06 (s, 3H), 0.94 (d, *J* = 6.1 Hz, 3H), 0.88 (s, 3H), 0.84 (d, *J* = 6.2 Hz, 3H), 0.74 (s, 3H) ppm. ^{13}C NMR (100MHz, $CDCl_3$): δ = 177.9 (C28), 170.8 (OCO), 170.4 (OCO), 170.4 (OCO), 138.3 (C13), 125.0 (C12), 74.8, 69.9, 65.3, 52.8, 51.5, 48.0, 47.6, 47.5, 43.7, 42.0, 41.9, 39.5, 39.0, 38.8, 37.8, 36.5, 32.4, 30.6, 27.9, 24.1, 23.4, 23.3, 21.1, 21.1, 20.9, 20.8, 17.9, 17.0, 16.9, 16.8, 13.9 ppm. DI-ESI-MS *m/z* $[M+H]^+$: 629.36. Anal. Calcd. for $C_{37}H_{56}O_8$: C, 70.67; H, 8.98. Found: C, 70.55; H, 8.98%.

Methyl 2α,3β,23-triacetoxy-11-oxours-12-en-28-oate (4.10)

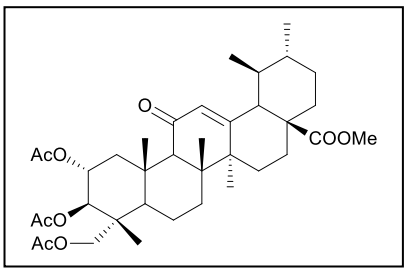

To a stirred solution of compound **4.9** (100 mg, 0.16 mmol) in dry dichloromethane (2 mL), a mixture of $KMnO_4$ (440 mg) and $Fe_2(SO_4)_3.nH_2O$ (220 mg), previous reduced to a fine powder, water (22 μl) and *t*-butanol (0.1 mL) were added. The reaction mixture was stirred at room temperature. After 4h 45 min the reaction mixture was diluted with diethyl ether (20 mL) and filtered through a celite pad, with further washing with

diethyl ether (100 mL). The resulting organic phase was washed with 10% aqueous $NaHCO_3$ (2 × 50 mL) and water (2× 50 mL), dried over Na_2SO_4, filtered, and concentrated under vacuum to afford **4.10** as a white powder (97.5mg, 95%). Mp: 139.2–141.5 °C. ν_{max}/cm^{-1} (KBr): 2977.55, 2950.55, 2875.34, 1747.19, 1662.34, 1457.92, 1369.21, 1234.22, 1043.30. ^{1}H NMR (400MHz, $CDCl_3$): δ = 5.62 (s, 1H, H12), 5.31–5.25 (m. 1H, H2), 5.04 (d, *J* = 10.3 Hz, 1H, H3), 3.83 (d, J = 11.8 Hz, 1H, H23), 3.59 (s, 3H, COO$\underline{CH_3}$), 3.57 (d, *J* = 11.8 Hz, 1H, H23), 2.07 (s, 3H, CH_3CO), 2.00 (s, 3H, CH_3CO), 1.94 (s, 3H, CH_3CO), 1.28 (s, 6H), 0.96 (d, *J* = 6.3 Hz, 3H), 0.90 (s, 6H), 0.85 (d, *J* = 6.5 Hz, 3H) ppm. ^{13}C NMR (100MHz, $CDCl_3$): δ = 198.8 (C11), 177.1 (C28), 170.8 (OCO), 170.5 (OCO), 170.1 (OCO), 163.3 (C13), 130.4 (C12), 74.9, 69.0, 65.2, 61.1, 52.7, 51.9 (2C), 47.6, 47.3, 44.5, 44.2, 43.7, 41.9, 38.6, 37.6, 35.9, 32.4, 30.3, 28.3, 23.8, 21.0, 20.9 (2C), 20.9, 20.7, 18.8, 17.7, 17.0, 17.0, 13.8 ppm. DI-ESI-MS *m/z* $[M+H]^+$: 643.12. Anal. Calcd. for $C_{37}H_{54}O_9.0.25H_2O$: C, 68.65; H, 8.49. Found: C, 68.46; H, 8.38%.

Methyl 2*α*,3β,23-trihydroxy-11-oxours-12-en-28-oate (4.11)

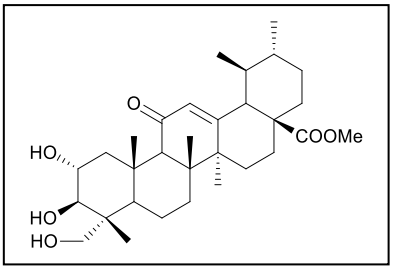

To a stirred solution of compound **4.10** (353 mg, 0.55 mmol) in methanol (23.5 mL), KOH (2350 mg) was added and the reaction mixture was heated under reflux. After 30 min the reaction mixture was evaporated under reduced pressure to remove the methanol, and acidified (pH 5-6) with 6 M aqueous HCl solution. Water (20 mL) was added and the aqueous layer was extracted with ethyl acetate (3 × 80 mL). The resulting organic phase was washed with 10% aqueous $NaHCO_3$ (3 × 50 mL), water (50 mL) and brine (50 mL), dried over Na_2SO_4, filtered, and concentrated under vacuum to afford **4.11** as a white powder (280.2 mg, quantitative). Mp: 174.9–177.3 °C. ν_{max}/cm^{-1} (KBr): 3424.96, 2948.63, 2929.34, 2873.42, 1727.91, 1660.41, 1455.99, 1388.50, 1201.43, 1047.16. ^{1}H NMR (400MHz, $CDCl_3$): δ = 5.60 (s, 1H, H12), 3.87–3.81 (m, 1H, H2), 3.64 (d, *J* = 11.1 Hz, 1H, H23), 3.60 (s, 3H, COO$\underline{CH_3}$), 3.42 (d, *J* = 9.5 Hz, 1H, H3) 3.36 (d, *J* = 11.1 Hz, 2H, H23), 1.30 (s, 3H), 1.21 (s, 3H), 0.96 (d, *J* = 6.1 Hz, 3H), 0.89 (s, 3H), 0.86 (d, *J* = 6.3 Hz, 3H), 0.82 (s, 3H) ppm. ^{13}C NMR (100MHz, $CDCl_3$): δ = 199.7 (C11), 177.2 (C28), 163.5 (C13), 130.4 (C12), 68.5, 61.0, 52.7, 51.8 (2C), 47.6, 46.9, 44.7, 43.9, 42.8, 38.6,

38.6, 38.0, 35.9, 32.5, 30.3, 28.3, 23.9, 21.2, 21.0 (2C), 18.9, 17.9, 17.2, 17.1, 13.0 ppm. DI-ESI-MS *m/z* $[M+H]^+$: 516.93. Anal. Calcd. for $C_{31}H_{48}O_6.H_2O$: C, 69.63; H, 9.42. Found: C, 69.19; H, 8.92%.

Methyl 2*α*,23-lactol-3-formyl- 11-oxours-12-en-28-oate (4.12)

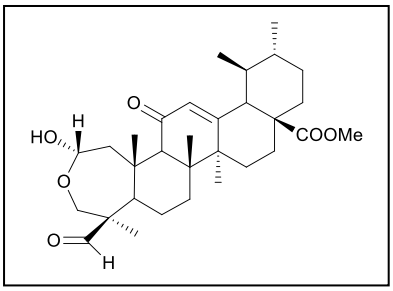

Accordingly to the method described for **4.3**, using compound **4.11** (1950 mg, 3.78 mmol), methanol/water (48.70 mL/ 2.40 mL [20:1]) and $NaIO_4$ (1227.40 mg; 5.74 mmol) for 1 hour at room temperature. The crude solid was purified by flash column chromatography (petroleum ether/ethyl acetate, 4:1 → 1:1), to afford **4.12** as a white solid (1280.30 mg, 66%). Mp: 154.0–157.0 °C. ν_{max}/cm^{-1} (KBr): 3436.53, 2948.63, 2938.98, 2873.42, 2734.57, 1725.98, 1658.48, 1455.99, 1205.29, 1141.65, 1037.52. ^1H NMR (400MHz, $CDCl_3$): δ = 9.97 (s, 1H, CHO), 5.64 (s, 1H, H12), 5.36–5.33 (m, 1H, H2), 3.98 (d, *J* = 13.2 Hz, 1H), 3.71 (d, *J* = 13.6 Hz, 1H), 3.60 (s, 3H, COO$\underline{CH_3}$), 1.34 (s, 3H), 1.32 (s, 3H), 0.97 (m, 6H), 0.93 (s, 3H), 0.86 (d, *J* = 6.4 Hz, 3H) ppm. ^{13}C NMR (100MHz, $CDCl_3$): δ = 205.6 (CHO), 198.9 (C11), 177.1 (C28), 162.7 (C13), 130.9 (C12), 93.5, 65.2, 61.4, 57.4, 53.2, 52.7, 51.9, 47.7, 45.7, 44.6, 44.1, 39.2, 38.6, 38.6, 35.9, 33.2, 30.3, 28.3, 23.9, 20.9, 20.7, 20.5, 19.6, 19.3, 17.0, 14.4 ppm. DI-ESI-MS *m/z* $[M+H]^+$: 515.42. Anal. Calcd. for $C_{31}H_{46}O_6.0.75H_2O$: C, 70.49; H, 9.06. Found: C, 70.31; H, 9.41%.

Methyl 2-formyl-11-oxo-23-hydroxy-A(1)-norursa-2,12-dien-28-oate (4.13)

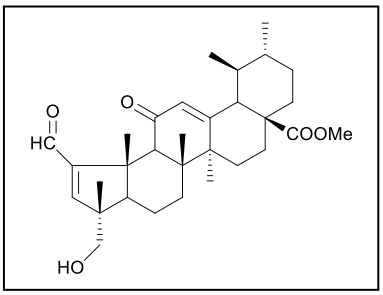

Accordingly to the method described for **4.6**, using compound **4.12** (300 mg, 0.58 mmol), dry benzene (30 mL), piperidine (1.45 mL), acetic acid (1.45 mL) and anhydrous magnesium sulfate (300 mg). The crude solid was purified by flash column chromatography (petroleum ether/ethyl acetate, 2:1 → 1:1), to afford **4.13** as a white solid (142.90 mg, 49%)**.** Mp: 144.8–146.6 °C. ν_{max}/cm^{-1} (KBr): 3442.31, 2977.55, 2948.63, 2929.34, 2871.49, 1727.91, 1662.34, 1614.13, 1581.34, 1455.99, 1226.50. ^1H NMR (400MHz, $CDCl_3$): δ = 10.15 (s, 1H, CHO), 6.35 (s, 1H, H3), 5.67 (s, 1H, H12), 3.62 (s, 3H, COO$\underline{CH_3}$, H28), 3.56 (d, J = 11.1 Hz, 1H), 3.39 (d, *J* = 11.1 Hz, 1H), 1.45

(s, 3H), 1.33 (s, 3H), 1.00 (s, 3H), 0.97 (m, 6H), 0.85 (d, *J* = 6.3 Hz, 3H) ppm. ^{13}C NMR (100MHz, $CDCl_3$): δ = 199.4 (C11), 195.5 (CHO), 177.2 (C28), 164.7 (C13), 157.5 (C2); 144.7 (C3), 129.5 (C12), 69.2, 58.3, 54.8, 53.0, 51.9, 48.7, 48.2, 47.6, 45.8, 44.4, 38.6, 38.4, 35.9, 33.4, 30.2, 28.8, 23.9, 21.4, 21.1, 21.0, 20.5, 17.1, 16.9, 16.1 ppm. DI-ESI-MS *m/z* $[M+H]^+$: 497.47. Anal. Calcd. for $C_{31}H_{44}O_5.0.5H_2O$: C, 73.63; H, 8.97. Found: C, 73.27; H, 8.50%.

2-Cyano-23-hydroxy-A(1)-norursa-2,12-dien-28-oic acid (4.14)

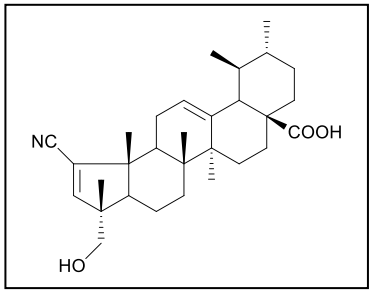

To a stirred solution of compound **4.6** (240 mg, 0.51 mmol) in THF (2.40 mL), aqueous ammonia solution 25% (9.60 mL) and iodine (142.96 mg, 0.56 mmol) were added. The mixture was stirred at room temperature for 2 hours (the dark solution became colorless). The reaction mixture was charged with 5% aqueous $Na_2S_2O_3$ (50 mL) and extracted with ethyl acetate (3 × 60 mL). The resulting organic phase was washed with water (50 mL) and brine (50 mL), dried over Na_2SO_4, filtered, and concentrated under vacuum to afford a yellow powder. The crude solid was purified by flash column chromatography (petroleum ether/ethyl acetate, 4:1 → 2:1), to afford **4.14** as a white solid (134.4 mg, 56%). Mp: 147.1–150.1 °C. ν_{max}/cm^{-1} (KBr): 3423.03, 2948.63, 2925.48, 2871.49, 2217.74, 1697.05, 1455.99, 1382.71, 1043.30. ^{1}H NMR (400MHz, $CDCl_3$): δ = 6.48 (s, 1H, H3), 5.25 (t, *J* = 3.0 Hz, 1H, H12), 3.54 (d, *J* = 10.6 Hz, 1H, H23), 3.38 (d, *J* = 10.6 Hz, 1H, H23), 1.27 (s, 3H), 1.13 (s, 3H), 1.01 (s, 3H), 0.95 (d, *J* = 6.0 Hz, 3H), 0.87 (m, 6H) ppm. $_{13}$C NMR (100MHz, $CDCl_3$): δ = 183.4 (C28), 153.7 (C3), 138.5 (C13), 127.0 (C2), 125.1 (C12), 117.6 (CN), 69.2, 55.3, 52.8, 52.6, 50.8, 47.9, 43.5, 42.4, 40.9, 38.8 (2C), 36.6, 33.4, 30.5, 28.1, 24.5, 24.0, 23.9, 21.1, 19.3, 18.5, 17.6, 17.0, 16.0 ppm. DI-ESI-MS *m/z* $[M+H]^+$: 466.03. Anal. Calcd. for $C_{30}H_{43}NO_3.0.75H_2O$: C, 75.20; H, 9.36; N, 2.92. Found: C, 75.10; H, 9.83; N, 2.79%.

Methyl 2-cyano-23-hydroxy-A(1)-norursa-2,12-dien-28-oate (4.15)

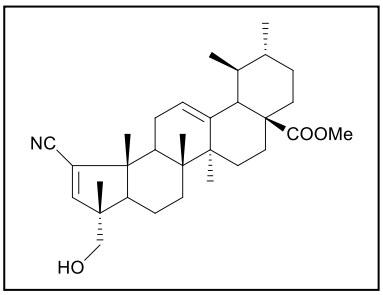

Accordingly to the method described for **4.14**, using compound **4.7** (295 mg, 0.61 mmol), THF (4.40 mL), aqueous ammonia solution 25% (13.70 mL) and iodine (340.75 mg, 1.34 mmol) at room temperature for 8 hours. The crude solid was purified by flash column chromatography (petroleum ether/ethyl acetate, 3:1 → 2:1), to afford **4.15** as a white solid (146.20 mg, 50%). Mp: 115.1–118.1 °C. ν_{max}/cm^{-1}. (KBr): 3504.02, 2948.63, 2925.48, 2871.49, 2215.81, 1724.05, 1652.70, 1587.13, 1455.99, 1362.71, 1234.22, 1197.58, 1145.51, 1049.09. ^{1}H NMR (400MHz, $CDCl_3$): δ = 6.48 (s, 1H, H3), 5.26 (t, *J* = 3.0 Hz, 1H, H12), 3.61 (s, 3H, COO$\underline{CH_3}$), 3.55 (d, *J* = 10.1 Hz, 1H, H23), 3.39 (d, *J* = 9.9 Hz, 1H, H23), 1.27 (s, 3H), 1.13 (s, 3H), 1.02 (s, 3H), 0.94 (d, *J* = 5.4 Hz, 3H), 0.87 (d, *J* = 6.1 Hz, 3H), 0.83 (s, 3H) ppm. ^{13}C NMR (100MHz, $CDCl_3$): δ = 178.0 (C28), 153.6 (C3), 138.7 (C13), 127.2 (C2), 125.0 (C12), 117.6 (CN), 69.3, 55.4, 52.9 (2C), 51.5, 50.8, 48.0, 43.5, 42.4, 40.9, 38.8 (2C), 36.5, 33.4, 30.6, 28.2, 24.5, 24.1, 24.0, 21.2, 19.3, 18.4, 17.6, 17.1, 16.0 ppm. DI-ESI-MS *m/z* $[M+H]^+$: 480.08. Anal. Calcd. for $C_{31}H_{45}NO_3.0.5H_2O$: C, 76.19; H, 9.49; N, 2.87. Found: C, 76.41; H, 9.62; N, 2.97%.

Methyl 2-cyano-11-oxo-23-hydroxy-A(1)-norursa-2,12-dien-28-oate (4.16)

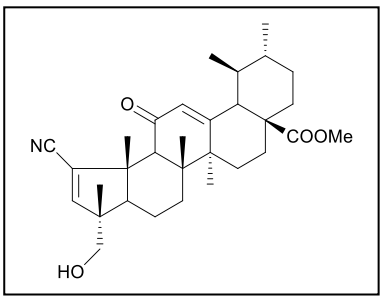

Accordingly to the method described for **4.14**, using compound **4.13** (300 mg, 0.60 mmol), THF (3 mL), aqueous ammonia solution 25% (12 mL) and iodine (168.60 mg, 0.66 mmol) at room temperature for 3 hours. The crude solid was purified by flash column chromatography (petroleum ether/ethyl acetate, 3:1 → 1:1), to afford **4.16** as a white solid (144.6 mg, 48%). Mp: 139.1–142.0 °C. ν_{max}/cm^{-1} (KBr): 3444.24, 2948.63, 2929.34, 2871.49, 2217.74, 1725.98, 1670.05, 1612.2, 1581.34, 1457.92, 1226.50. ^{1}H NMR (400MHz, $CDCl_3$): δ = 6.57 (s, 1H, H3), 5.71 (s, 1H, H12), 3.60 (s, 3H, COO$\underline{CH_3}$), 3.55 (d, J = 10.9 Hz, 1H, H23), 3.38 (d, *J* = 10.9 Hz, 1H, H23), 1.40 (s, 3H), 1.33 (s, 3H), 1.01 (s, 3H), 0.97 (d, *J* = 6.3 Hz, 3H), 0.91 (s, 3H), 0.87 (d, *J* = 6.4 Hz, 3H) ppm. ^{13}C NMR (100MHz, $CDCl_3$): δ = 197.2 (C11), 177.2 (C28), 163.9 (C13), 155.2 (C3), 129.3 (C12), 128.7 (C2), 117.2 (CN), 68.8, 57.2,

54.7, 52.9, 51.9, 50.9, 50.0, 47.6, 45.4, 44.2, 38.6, 38.4, 35.9, 33.1, 30.2, 28.7, 23.8, 21.5, 21.0, 20.8, 20.4, 17.2, 16.9, 15.9 ppm. DI-ESI-MS *m/z* $[M+H]^+$: 494.37. Anal. Calcd. for $C_{31}H_{43}NO_4.0.5H_2O$: C, 74.07; H, 8.82; N, 2.79. Found: C, 74.10; H, 8.83; N, 2.94%.

Methyl 2-formyl-11-oxo-23-acetoxy-A(1)-norursa-2,12-dien-28-oate (4.17)

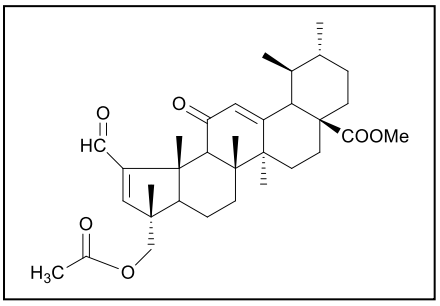

To a stirred solution of compound **4.13** (95 mg, 0.19 mmol) in dry THF (2.85 mL), acetic anhydride (27 µl; 0.29 mmol) and a catalytic amount of DMAP (9.5 mg) were added. The mixture was stirred at room temperature in anhydrous conditions. After 1h 30 min, the reaction mixture was evaporated under reduced pressure to remove the organic phase. The crude obtained was dispersed with water (30 mL) and extracted with ethyl acetate (3 × 30 mL). The resulting organic phase was washed with 5% aqueous HCl (2 × 30 mL), 10% aqueous $NaHCO_3$ (2 × 30 mL), 10% aqueous Na_2SO_3 (30 mL), water (30 mL) and brine (30 mL), dried over Na_2SO_4, filtered, and concentrated under vacuum to afford **4.17** as a white powder (73.2 mg, 71%). Mp: 104.2–107.3 °C. ν_{max}/cm^{-1} (KBr): 2948.63, 2933.20, 2873.42, 1735.62, 1662.34, 1614.13, 1585.2, 1455.99, 1384.84, 1232.29, 1039.44. ^1H NMR (400MHz, $CDCl_3$): δ = 10.15 (s, 1H, CHO), 6.39 (s, 1H, H3), 5.67 (s, 1H, H12), 3.97 (d, J = 10.8 Hz, 1H, H23), 3.89 (d, *J* = 10.8 Hz, 1H, H23), 3.61 (s, 3H, COO$\underline{CH_3}$), 2.05 (s, 3H, C$\underline{H_3}$CO), 1.45 (s, 3H), 1.31 (s, 3H), 1.05 (s, 3H), 0.96 (m, 6H), 0.86 (d, *J* = 6.5 Hz, 3H) ppm. ^{13}C NMR (100MHz, $CDCl_3$): δ = 199.1 (C11), 195.2 (CHO), 177.1 (C28), 171.0 (OCO), 164.6 (C13), 156.4 (C2), 144.0 (C3), 129.5 (C12), 70.7, 58.4, 56.7, 53.0, 51.9, 48.0, 47.6, 46.6, 45.8, 44.4, 38.6, 38.4, 35.8, 33.5, 30.2, 28.7, 23.8, 21.2, 21.0, 20.9, 20.8, 20.2, 17.1, 17.0, 16.3 ppm. DI-ESI-MS *m/z* $[M+H]^+$: 539.88. Anal. Calcd. for $C_{33}H_{46}O_6.0.75H_2O$: C, 71.77; H, 8.67. Found: C, 71.80; H, 8.65%.

Methyl 2-formyl-11-oxo-23-butyroxy-A(1)-norursa-2,12-dien-28-oate (4.18)

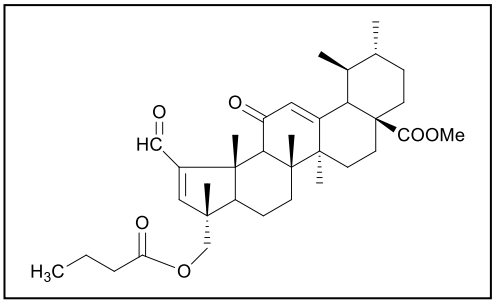

Accordingly to the method described for **4.17**, using compound **4.13** (300 mg, 0.60 mmol), dry THF (9 mL), butyric anhydride (98.80 µl; 0.60 mmol) and a catalytic amount of DMAP (30 mg) at room temperature for 1 hour. The crude solid was purified by flash column chromatography (petroleum ether/ethyl acetate, 7:1 → 5:1), to afford **4.18** as a white solid (59.1 mg, 17%). Mp: 77.8–80.3 °C. ν_{max}/cm^{-1} (KBr): 2950.55, 2933.20, 2873.42, 1731.76, 1662.34, 1614.13, 1585.20, 1457.92, 1224.58, 1197.58, 1174.44. ^{1}H NMR (400MHz, $CDCl_3$): δ = 10.15 (s, 1H, CHO), 6.39 (s, 1H, H3), 5.68 (s, 1H, H12), 3.98 (d, J = 10.8 Hz, 1H, H23), 3.90 (d, *J* = 10.6 Hz, 1H, H23), 3.62 (s, 3H, COOC$\underline{H_3}$), 1.46 (s, 3H), 1.31 (s, 3H), 1.05 (s, 3H), 0.96–0.92 (m, 6H), 0.86 (d, *J* = 6.2 Hz, 3H) ppm. ^{13}C NMR (100MHz, $CDCl_3$): δ = 199.1 (C11), 195.2 (CHO), 177.1 (C28), 173.6 (OCO), 164.6 (C13), 156.4 (C2), 144.1 (C3), 129.5 (C12), 70.3, 58.4, 56.6, 53.0, 51.9, 48.0, 47.6, 46.7, 45.8, 44.4, 38.6, 38.4, 36.2, 35.9, 33.5, 30.2, 28.7, 23.9, 21.2, 21.0, 21.0, 20.3, 18.5, 17.1, 17.0, 16.3, 13.7 ppm. DI-ESI-MS *m/z* $[M+H]^+$: 567.40. Anal. Calcd. for $C_{35}H_{50}O_6$: C, 74.17; H, 8.89. Found: C, 73.79; H, 9.21%.

Methyl 2-formyl-11-oxo-23-cinnamoxy-A(1)-norursa-2,12-dien-28-oate (4.19)

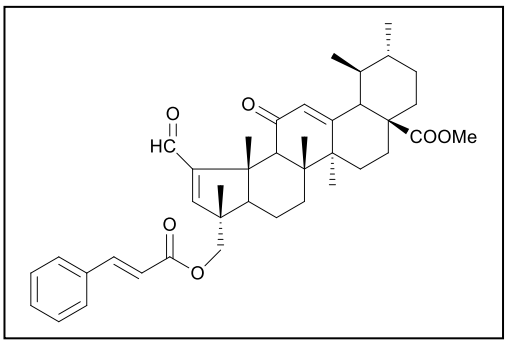

To a stirred solution of compound **4.13** (300 mg, 0.60 mmol) in dry benzene (18 mL), cinnamoyl chloride (402.50 mg, 2.41 mmol) and DMAP (295.20 mg, 2.41 mmol) were added. The mixture was stirred at 60 °C under nitrogen atmosphere. After 3 hours, the reaction mixture was evaporated under reduced pressure to remove the organic phase. The crude obtained was dispersed with water (50 mL) and extracted with ethyl acetate (3 × 50 mL). The resulting organic phase was washed with water (4 × 50 mL) and brine (50 mL), dried over Na_2SO_4, filtered, and concentrated under vacuum to afford a light yellow crude. The crude solid was purified by flash column chromatography (petroleum ether/ethyl acetate, 6:1 → 4:1), to afford **4.19** as a white solid (268.7 mg, 71%). Mp: 97.0–100.2 °C. ν_{max}/cm^{-1} (KBr): 3083.62, 3060.48,

3025.76, 2948.63, 2931.27, 2873.42, 1718.26, 1664.27, 1637.27, 1452.14, 1382.71, 1309.43, 1272.79, 1228.43, 1201.43, 1164.79. ^{1}H NMR (400MHz, $CDCl_3$): δ= 10.17 (s, 1H, CHO), 7.69 (d, *J* = 16.0 Hz, 1H), 7.54–7.52 (m, 2H), 7.40–7.38 (m, 3H), 6.47 (s, 1H, H3), 6.43 (d, *J* = 16.0 Hz, 1H), 5.68 (s, 1H, H12), 4.11 (d, J = 11.0 Hz, 1H, H23), 4.07 (d, *J* = 11.0 Hz, 1H, H23), 3.62 (s, 3H, $COO\underline{CH_3}$), 1.48 (s, 3H), 1.29 (s, 3H), 1.11 (s, 3H), 0.96–0.95 (m, 6H), 0.84 (d, *J* = 6.4 Hz, 3H) ppm. ^{13}C NMR (100MHz, $CDCl_3$): δ = 199.2 (C11), 195.3 (CHO), 177.1 (C28), 166.9 (OCO), 164.7 (C13), 156.4 (C2), 145.3, 144.1 (C3), 134.2, 130.4, 129.4 (C12), 128.9 (2C), 128.2 (2C), 117.6, 70.7, 58.4, 56.7, 53.0, 51.9, 48.0, 47.5, 46.9, 45.8, 44.4, 38.6, 38.3, 35.8, 33.5, 30.2, 28.7, 23.8, 21.2, 21.0, 20.9, 20.3, 17.1, 17.0, 16.4 ppm. DI-ESI-MS^2 *m/z*: 627.36 ($[M+H]^+$,42%), 609.48 (62), 566.37 (72), 479.38 (100), 419.39 (29). Anal. Calcd. for $C_{40}H_{50}O_6.H_2O$: C, 74.50; H, 8.13. Found: C, 74.10; H, 7.76%.

Methyl 2-formyl-11-oxo-23-(1H-imidazole-1-carbonyloxy)-A(1)-norursa-2,12-dien-28-oate (4.20)

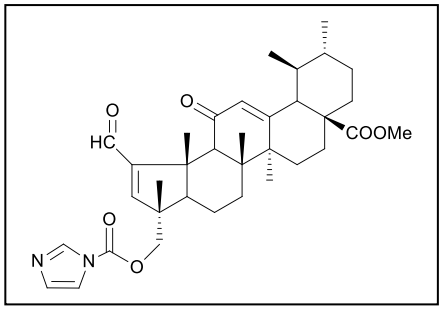

To a stirred solution of compound **4.13** (280 mg, 0.56 mmol) in dry THF (11 mL), CDI (184.10 mg, 1.14 mmol) was added. The reaction mixture was stirred at reflux temperature under nitrogen atmosphere. After 2 hours, the reaction mixture was evaporated under reduced pressure to remove the organic phase. The crude obtained was dispersed with water (50 mL) and extracted with ethyl acetate (3 × 50 mL). The combined organic phase was washed with water (4 × 50 mL) and brine (50 mL), dried over Na_2SO_4, filtered, and concentrated under vacuum to afford a yellowish powder. The crude solid was purified by flash column chromatography (petroleum ether/ethyl acetate, 1:1), to afford **4.20** as a white solid (41.4 mg, 12%). Mp: 111.6–114.1 °C. ν_{max}/cm^{-1} (KBr): 3129.90, 2948.63, 2873.42, 1764.55, 1725.98, 1662.34, 1614.13, 1587.13, 1457.92, 1400.07, 1288.22, 1240.00, 1004.73. ^{1}H NMR (400MHz, $CDCl_3$): δ = 10.14 (s, 1H, CHO), 8.09 (s, 1H, H-Im), 7.36 (s, 1H, H-Im), 7.06 (s, 1H, H-Im), 6.37 (s, 1H, H3), 5.67 (s, 1H, H12), 4.29 (d, J = 10.5 Hz, 1H, H23), 4.24 (d, *J* = 10.3 Hz, 1H, H23), 3.60 (s, 3H, $COO\underline{CH_3}$), 1.24 (s, 3H), 1.13 (s, 3H), 0.95 (s, 6H), 0.84 (d, *J* = 5.4 Hz, 3H) ppm. ^{13}C NMR (100MHz, $CDCl_3$): δ = 198.8 (C11), 194.8 (CHO), 177.1 (C28), 164.8 (C13), 157.1 (C2), 148.6,

142.2 (C3), 136.9, 130.9, 129.3 (C12), 116.9, 73.9 , 58.4, 56.7, 52.9, 51.8, 48.1, 47.5, 46.9, 45.7, 44.3, 38.6, 38.3, 35.8, 33.5, 30.1, 28.7, 23.8, 21.0, 21.0, 20.9, 20.2, 17.1, 17.0, 16.2 ppm. DI-ESI-MS *m/z* $[M+H]^+$: 591.52. Anal. Calcd. for $C_{35}H_{46}N_2O_6$ $0.25H_2O$: C, 70.62; H, 7.87; N, 4.71. Found: C, 70.30; H, 7.71; N, 4.35%.

Methyl 2-formyl-11-oxo-23-(2′-methyl-1H-imidazole-carbonyloxy)-A(1)-norursa-2,12-dien-28-oate (4.21)

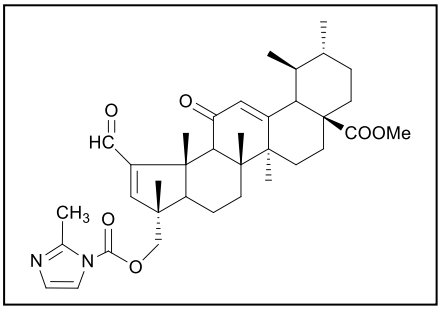

Accordingly to the method described for **4.20**, using compound **4.13** (300 mg, 0.60 mmol), dry THF (12.5 mL), and CBMI (287.20 mg, 1.51 mmol) at reflux temperature under nitrogen atmosphere for 6 hours. The crude solid was purified by flash column chromatography (petroleum ether/ethyl acetate, 2:1 → 1:2), to afford **4.21** as a white solid (121.4 mg, 33%). Mp: 128.7–131.0 °C. ν_{max}/cm^{-1} (KBr): 3122.19, 2948.63, 2931.27, 2873.42, 1758.76, 1725.98, 1660.41, 1614.13, 1587.13, 1552.42, 1511.92, 1457.92, 1398.14, 1295.93, 1143.58. ^1H NMR (400MHz, $CDCl_3$): δ = 10.15 (s, 1H, CHO), 7.28 (d, *J* = 1.5 Hz, 1H, H-Im), 6.84 (d, *J* = 1.5 Hz, 1H, H-Im), 6.39 (s, 1H, H3), 5.67 (s, 1H, H12), 4.27 (d, *J* = 10.8 Hz, 1H, H23), 4.20 (d, *J* = 10.8 Hz, 1H, H23), 3.61 (s, 3H, COO$\underline{CH_3}$), 2.62 (s, 3H, CH_3-Im), 1.47 (s, 3H), 1.23 (s, 3H), 1.13 (s, 3H), 0.97–0.95 (m, 6H), 0.85 (d, *J* = 6.3 Hz, 3H) ppm. ^{13}C NMR (100MHz, $CDCl_3$): δ = 198.8 (C11), 194.8 (CHO), 177.1 (C28), 164.7 (C13), 157.0 (C2), 149.5, 147.9, 142.6 (C3), 129.4 (C12), 128.2, 117.8, 73.3, 58.4, 56.4, 53.0, 51.9, 48.1, 47.5, 46.9, 45.7, 44.3, 38.6, 38.3, 35.8, 33.5, 30.1, 28.7, 23.8, 21.1, 21.0, 20.9, 20.3, 17.1, 16.9, 16.8, 16.3 ppm. DI-ESI-MS *m/z* $[M+H]^+$: 605.40. Anal. Calcd. for $C_{36}H_{48}N_2O_6$: C, 71.50; H, 8.00; N, 4.63. Found: C, 71.16; H, 8.46; N, 4.36%.

Methyl 2-cyano-23-(2′-methyl-1H-imidazole-carbonyloxy)-A(1)-norursa-2,12-dien-28-oate (4.22)

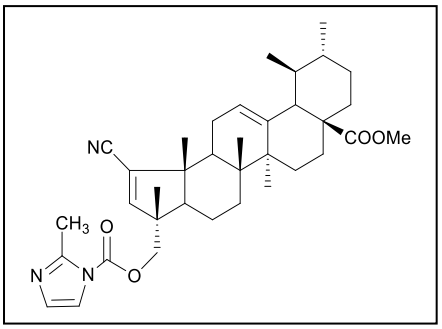

Accordingly to the method described for **4.20**, using compound **4.15** (280 mg, 0.58 mmol), dry THF (11 mL) and CBMI (277.55 mg, 1.46 mmol) at reflux temperature under nitrogen atmosphere for 8 hours. The crude solid was purified by flash column chromatography (petroleum ether/ethyl acetate, 2:1 → 1:1), to afford **4.22** as a white solid (204.1 mg, 59%). Mp: 104.1–107.2 °C. ν_{max}/cm^{-1} (KBr): 3166.54, 2948.63, 2925.48, 2215.81, 1747.19, 1724.05, 1455.99, 1384.64, 1249.65. ^{1}H NMR (400MHz, $CDCl_3$): δ = 7.27 (s, 1H, H-Im), 6.87 (s, 1H, H-Im), 6.47 (s, 1H, H3), 5.27 (t, *J* = 3.0 Hz, 1H, H12), 4.29 (d, *J* = 11.0 Hz, 1H, H23), 4.18 (d, *J* = 11.0 Hz, 1H, H23), 3.60 (s, 3H, COO$\underline{CH_3}$), 2.63 (s, 3H, CH_3-Im), 1.30 (s, 3H), 1.13 (s, 3H), 1.04 (s, 3H), 0.94 (d, *J* = 5.7 Hz, 3H), 0.86 (d, *J* = 6.9 Hz, 3H), 0.84 (s, 3H) ppm. ^{13}C NMR (100MHz, $CDCl_3$): δ = 177.9 (C28), 151.4 (C3), 149.4, 148.0, 138.7 (C13), 128.3, 128.0 (C2), 124.8 (C12), 117.7, 117.0 (CN), 72.3, 56.0, 52.8, 52.7, 51.5, 49.2, 48.0, 43.9, 42.3, 40.9, 38.8, 38.8, 36.5, 33.4, 30.5, 28.1, 24.5, 24.0, 23.7, 21.1, 18.9, 18.4, 17.4, 17.1, 16.8, 16.2 ppm. DI-ESI-MS *m/z* $[M+H]^+$: 588.63. Anal. Calcd. for $C_{36}H_{49}N_3O_4$: C, 73.56; H, 8.40; N, 7.15. Found: C, 73.46; H, 8.79; N, 6.86%.

Methyl 2-cyano-23-acetoxy-A(1)-norursa-2,12-dien-28-oate (4.23)

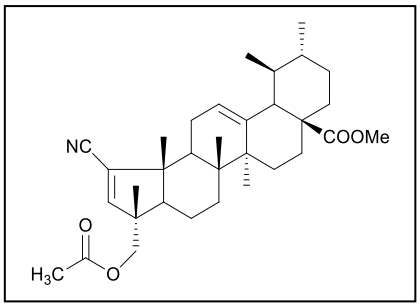

Accordingly to the method described for **4.17**, using compound **4.15** (200 mg, 0.42 mmol), dry THF (6 mL), acetic anhydride (43.30 µl; 0.46 mmol) and a catalytic amount of DMAP (20 mg) at room temperature for 1 hour. The crude solid was purified by flash column chromatography (petroleum ether/ethyl acetate, 6:1 → 4:1), to afford **4.23** as a white solid (126.4 mg, 58%). Mp: 86.7–88.6 °C. ν_{max}/cm^{-1} (KBr): 2948.63, 2925.48, 2871.49, 2215.81, 1745.26, 1724.05, 1650.77, 1589.06, 1455.99, 1382.71, 1236.15, 1039.44. ^{1}H NMR (400MHz, $CDCl_3$): δ = 6.44 (s, 1H, H-3), 5.26 (t, *J* = 2.9 Hz, 1H, H-12), 3.97 (d, *J* = 11.0 Hz, 1H, H-23), 3.90 (d, *J* = 10.9 Hz, 1H, H-23), 3.60 (s, 3H, COO$\underline{CH_3}$), 2.06 (s, 3H, C$\underline{H_3}$CO), 1.26 (s, 3H), 1.11 (s, 3H), 1.05 (s, 3H), 0.94 (d, *J* = 5.9 Hz, 3H), 0.87 (d, *J* = 6.3 Hz, 3H), 0.83 (s, 3H)

ppm. ^{13}C NMR (100MHz, $CDCl_3$): δ = 177.9 (C28), 170.9 (OCO), 152.6 (C3), 138.7 (C13), 127.0 (C2), 124.9 (C12), 117.5 (CN), 69.7, 56.2, 52.9, 52.6, 51.5, 49.0, 48.0, 43.8, 42.3, 40.9, 38.8, 38.8, 36.5, 33.4, 30.5, 28.1, 24.5, 24.1, 23.8, 21.1, 20.8, 19.0, 18.4, 17.5, 17.1, 16.2 ppm. DI-ESI-MS *m/z* $[M+H]^+$: 522.31. Anal. Calcd. for $C_{33}H_{47}NO_4$: C, 75.97; H, 9.08; N, 2.68. Found: C, 76.22; H, 9.25; N, 2.85%.

Methyl 2-cyano-23-butyroxy-A(1)-norursa-2,12-dien-28-oate (4.24)

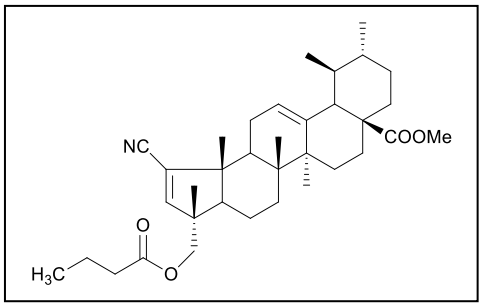

Accordingly to the method described for **4.17**, using compound **4.15** (290 mg, 0.61 mmol), dry THF (11.6 mL), butyric anhydride (108.8 µl, 0.67 mmol) and a catalytic amount of DMAP (30 mg,) at room temperature for 1 h 15 min. The crude solid was purified by flash column chromatography (petroleum ether/ethyl acetate, 7:1 → 6:1), to afford **4.24** as a white solid (101.1 mg, 30%); Mp: 65.5–68.0 °C. ν_{max}/cm^{-1} (KBr): 2948.63, 2927.41, 2873.42, 2215.81, 1735.55, 1652.70, 1589.06, 1455.99, 1172.51. ^{1}H NMR (400MHz, $CDCl_3$): δ = 6.44 (s, 1H, H3), 5.27 (t, *J* = 3.0 Hz, 1H, H12), 3.98 (d, *J* = 10.9 Hz, 1H, H23), 3.90 (d, *J* = 10.9 Hz, 2H, H23), 3.61 (s, 3H, COO$\underline{CH_3}$), 1.27 (s, 3H), 1.10 (s, 3H), 1.04 (s, 3H), 0.97–0.93 (m, 6H), 0.87 (d, *J* = 6.1 Hz, 3H), 0.83 (s, 3H) ppm. ^{13}C NMR (100MHz, $CDCl_3$): δ = 178.0 (C28), 173.4 (OCO), 152.8 (C3), 138.7 (C13), 127.0 (C2), 124.9 (C12), 117.5 (CN), 69.3, 56.0, 52.9, 52.6, 51.5, 49.1, 48.0, 43.8, 42.3, 40.9, 38.8 (2C), 36.5, 36.2, 33.4, 30.5, 28.1, 24.5, 24.1, 23.8, 21.1, 19.1, 18.5, 18.4, 17.4, 17.1, 16.2, 13.7 ppm. DI-ESI-MS *m/z* $[M+H]^+$: 550.33. Anal. Calcd. for $C_{35}H_{51}NO_4$: C, 76.46; H, 9.35; N, 2.55. Found: C, 76.75; H, 9.62; N, 2.58%.

Methyl 2-cyano-23-benzoxy-A(1)-norursa-2,12-dien-28-oate (4.25)

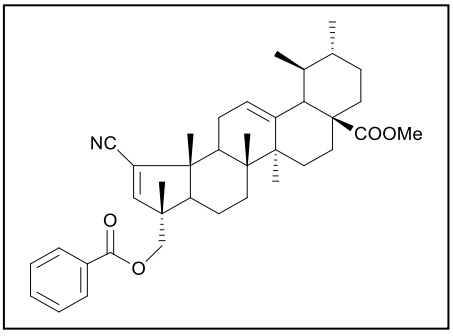

Accordingly to the method described for **4.17**, using compound **4.15** 250 mg, 0.52 mmol), dry THF(10 mL), benzoic anhydride (141.50 mg, 0.63 mmol) and a catalytic amount of DMAP (25 mg) at room temperature for 1 h 30 min. The crude solid was purified by flash column chromatography (petroleum ether/ethyl acetate, 10:1 → 7:1), to afford **4.25** a white solid (158.2 mg,

52%). Mp: 100.2–103.1 °C. ν_{max}/cm^{-1} (KBr): 3089.40, 3060.48, 2948.63, 2925.48, 2871.49, 2215.81, 1722.12, 1602.56, 1585.20, 1452.14, 1270.86, 1112.73. ^{1}H NMR (400MHz, $CDCl_3$): δ = 8.00 (d, *J* = 7.2 Hz, 2H), 7.58 (t, *J* = 7.3 Hz, 1H), 7.45 (t, *J* = 7.7 Hz, 2H), 6.54 (s, 1H, H3), 5.26 (t, *J* = 2.8 Hz, 1H, H12), 4.24 (d, J = 11.0 Hz, 1H, H23), 4.14 (d, *J* = 11.0 Hz, 1H, H23), 3.61 (s, 3H, COOC$\underline{H}_3$), 1.30 (s, 3H), 1.15 (s, 3H), 1.03 (s, 3H), 0.94 (d, *J* = 5.8 Hz, 3H), 0.86 (d, *J* = 6.6 Hz, 3H). 0.84 (s, 3H) ppm. ^{13}C NMR (100MHz, $CDCl_3$): δ = 177.9 (C28), 166.3 (OCO), 152.8 (C3), 138.7 (C13), 133.3, 129.7, 129.5, 128.5, 127.2 (C2), 124.9 (C12), 117.4 (CN), 69.8, 56.1, 52.9, 52.7, 51.5, 49.4, 48.0, 43.9, 42.3, 40.9, 38.8, 38.8, 36.5, 33.5, 30.5, 28.1, 24.6, 24.0, 23.6, 21.1, 19.0, 18.4, 17.5, 17.1, 16.4 ppm. DI-ESI-MS *m/z* $[M+H]^+$: 584.29. Anal. Calcd. for $C_{38}H_{49}NO_4$: C, 78.18; H, 8.46; N, 2.40. Found: C, 77.80; H, 8.58; 2.52%.

Methyl 2-cyano-23-succinoxy-A(1)-norursa-2,12-dien-28-oate (4.26)

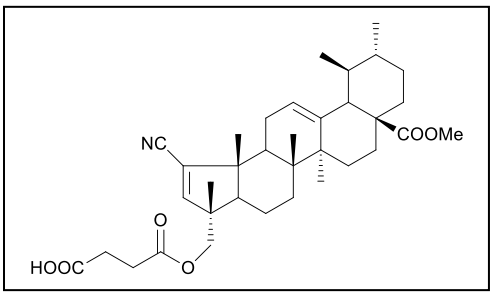

To a stirred solution of compound **4.15** (250 mg, 0.52 mmol) in dry CH_2Cl_2 (15 mL), succinic anhydride (130.38 mg; 1.30 mmol) and DMAP (95.50 mg, 0.78 mmol) were added. The reaction mixture was stirred at room temperature in anhydrous conditions. After 3 hours, the reaction mixture was evaporated under reduced pressure to remove the organic phase. The crude obtained was dispersed with water (60 mL) and extracted with ethyl acetate (3 × 60 mL). The resulting organic phase was washed with 5% aqueous HCl (2 × 60 mL), 10% aqueous Na_2SO_3 (60 mL), water (60 mL) and brine (60 mL), dried over Na_2SO_4, filtered, and concentrated under vacuum to afford a yellow powder. The crude solid was purified by flash column chromatography (petroleum ether/ethyl acetate, 3:1 → 1:1), to afford **4.26** as a white solid (213.9 mg, 71%). Mp: 105.8–107.7 °C. ν_{max}/cm^{-1} (KBr): 2948.63, 2927.41, 2871.49, 2657.43, 2559.08, 2215.81, 1743.33, 1727.91, 1712.48, 1589.06, 1455.99, 1201.43, 1162.87. ^{1}H NMR (400MHz, $CDCl_3$): δ = 6.43 (s, 1H, H3), 5.26 (t, *J* = 2.8 Hz, 1H, H12), 4.01 (d, *J* = 11.0 Hz, 1H, H23), 3.92 (d, *J* = 11.0 Hz, 1H, H23), 3.60 (s, 3H, COOC$\underline{H}_3$), 2.68–2.64 (m, 4H), 1.26 (s, 3H), 1.11 (s, 3H), 1.05 (s, 3H), 0.94 (d, *J* = 6.0 Hz, 3H), 0.87 (d, *J* = 6.3 Hz, 3H), 0.83 (s, 3H). ^{13}C NMR (100MHz, $CDCl_3$): δ = 178.0 (C28), 177.2, 171.9, 152.5 (C3), 138.7 (C13), 128.5, 127.1 (C2), 124.9 (C12), 117.4 (CN), 70.1, 56.2, 52.9, 52.6, 51.5, 49.0, 48.0, 43.7, 42.3, 40.9, 38.8 (2C), 36.5,

33.4, 30.5, 28.8, 28.7, 28.1, 24.5, 24.1, 23.8, 21.1, 19.0, 18.4, 17.5, 17.1, 16.2 ppm. DI-ESI-MS *m/z* $[M+H]^+$: 580.35. Anal. Calcd. for $C_{35}H_{49}NO_6.H_2O$: C, 70.32; H, 8.60; N, 2.34. Found: C, 70.22; H, 8.50; N, 2.38%.

Methyl 2-cyano-23-cinnamoxy-A(1)-norursa-2,12-dien-28-oate (4.27)

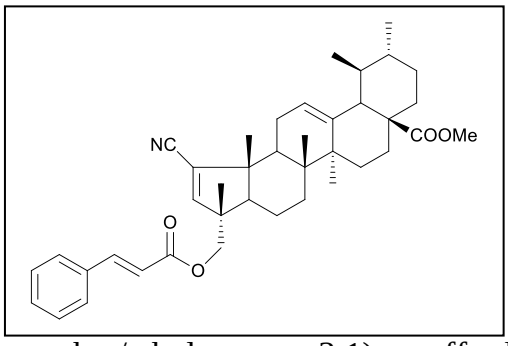

Accordingly to the method described for **4.19**, using compound **4.15 (**300 mg, 0.63 mmol), dry benzene (18 mL), cinnamoyl chloride (416.75 mg, 2.50 mmol) and DMAP (305.60 mg, 2.50 mmol) at 60 °C under nitrogen atmosphere for 1 h 40 min. The crude solid was purified by flash column chromatography (petroleum ether/ethyl acetate, 3:1), to afford **4.27** as a white solid (189 mg, 50%) Mp: 102.3–105.0 °C. ν_{max}/cm^{-1} (KBr): 3083.62, 3060.48, 2946.70, 2925.48, 2871.49, 2215.81, 1718.26, 1637.27, 1579.41, 1496.49, 1452.14, 1162.87. ^1H NMR (400MHz, $CDCl_3$): δ= 7.69 (d, *J* = 16.1 Hz, 1H), 7.54–7.52 (m, 2H), 7.41–7.39 (m, 3H), 6.51 (s, 1H, H3), 6.43 (d, *J* = 16.2 Hz, 1H), 5.27 (t, J = 2.6 Hz, 1H, H12), 4.10 (d, J = 10.9 Hz, 1H, H23), 4.05 (d, *J* = 11.0 Hz, 1H, H23), 3.61 (s, 3H, $COOC\underline{H}_3$), 1.29 (s, 3H), 1.11 (s, 3H), 1.08 (s, 3H), 0.93 (d, *J* = 6.0 Hz, 3H), 0.85–0.84 (m, 6H) ppm. ^{13}C NMR (100MHz, $CDCl_3$): δ = 177.9 (C28), 166.7, 152.8 (C3), 145.5, 138.7 (C13), 134.2, 130.5, 128.9 (2C), 128.2 (2C), 127.1 (C2), 124.9 (C12), 117.5 (CN), 117.4, 69.7, 56.2, 52.9, 52.7, 51.5, 49.2, 48.0, 43.8, 42.3, 40.9, 38.8, 38.8, 36.5, 33.4, 30.5, 28.1, 24.5, 24.0, 23.8, 21.1, 19.1, 18.4, 17.5, 17.1, 16.3 ppm. DI-ESI-MS *m/z* $[M+H]^+$: 610.33. Anal. Calcd. for $C_{40}H_{51}NO_4$: C, 78.78; H, 8.43; N, 2.30. Found: C, 78.82; H, 8.20; N, 2.46%.

Methyl 2-formyl-23-methanesulfonyloxy-A(1)-norursa-2,12-dien-28-oate (4.28)

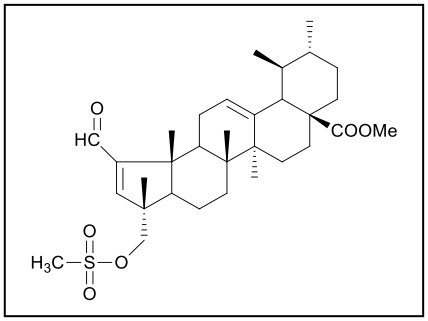

To a stirred solution of compound **4.7** (250 mg, 0.52 mmol) in dry dicloromethane (10 mL), triethylamine (144.60 µl; 1.04 mmol) and methanesulfonyl chloride (80.20 µl, 1.04 mmol) were added. The reaction mixture was stirred at room temperature. After 4 hours, the reaction mixture was evaporated under reduced pressure to remove the organic phase. The crude obtained

was dispersed with water (50 mL) and extracted with ethyl acetate (3 × 50 mL). The resulting organic phase was washed with water (4 × 50 mL) and brine (50 mL), dried over Na_2SO_4, filtered, and concentrated under vacuum to afford a yellow crude. The crude solid was purified by flash column chromatography (petroleum ether/ethyl acetate, 4:1 → 2:1), to afford **4.28** as a white solid (206.9 mg, 71 %). Mp: 105.6–107.2 °C. ν_{max}/cm^{-1} (KBr): 2948.63, 2925.48, 2871.49, 2728.78, 1722.12, 1689.34, 1585.2, 1455.99, 1357.64, 1176.36, 958.45. ^{1}H NMR (400MHz, $CDCl_3$): δ = 9.73 (s, 1H, CHO), 6.60 (s, 1H, H3), 5.26 (t, *J* = 3.0 Hz, 1H, H12), 4.13 (d, *J* = 9.6 Hz, 1H, H23), 4.06 (d, *J* = 9.6 Hz, 1H, H23), 3.61 (s, 3H, COOC$\underline{H_3}$), 3.03 (s, 3H, (S-C$\underline{H_3}$), 1.25 (s, 3H), 1.10 (s, 3H), 1.08 (s, 3H), 0.93 (d, *J* = 5.9 Hz, 3H), 0.84–0.83 (m, 6H) ppm. ^{13}C NMR (100MHz, $CDCl_3$): δ = 190.6 (CHO), 178.0 (C28), 158.9 (C2), 155.8 (C3), 137.8 (C13), 126.1 (C12), 74.7, 56.9, 52.8, 51.4, 50.8, 48.0, 47.7, 44.3, 42.4, 41.3, 38.8, 38.8, 37.5, 36.5, 33.4, 30.6, 28.2, 27.0, 24.1, 23.9, 21.2, 18.8, 18.7, 17.3, 17.0, 15.9 ppm. DI-ESI-MS *m/z* [M+H]$^+$: 560.91. Anal. Calcd. for $C_{32}H_{48}O_6S.0.5H_2O$: C, 67.45; H, 8.67; S, 5.63. Found: C, 67.56; H, 8.73; S, 5.27%.

Methyl 2-formyl-11-oxo-23-methanesulfonyloxy-A(1)-norursa-2,12-dien-28-oate (4.29)

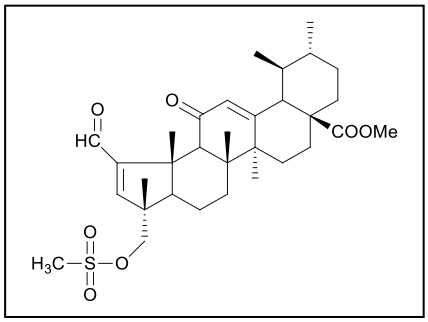

Accordingly to the method described for **4.28**, using compound **4.13** (300 mg, 0.60 mmol), dry CH_2Cl_2 (12.50 mL), triethylamine (168.50 µl; 1.21 mmol) and methanesulfonyl chloride (93.50 µl, 1.21 mmol) at room temperature in anhydrous conditions for 1 h 10 min. The crude solid was purified by flash column chromatography (petroleum ether/ethyl acetate, 5:1 → 1.5:1), to afford **4.29** as a white solid (183.1 mg, 53%). Mp: 114.0–116.5 °C. ν_{max}/cm^{-1} (KBr): 2948.63, 2933.20, 2873.42, 1725.98, 1662.34, 1614.13, 1587.13, 1457.92, 1355.71, 1174.44, 958.45 cm^{-1}. ^{1}H NMR (400MHz, $CDCl_3$): δ = 10.15 (s, 1H, CHO), 6.30 (s, 1H, H3), 5.68 (s, 1H, H12), 4.07 (d, *J* = 10.0 Hz, 1H, H23), 4.04 (d, *J* = 10.0 Hz, 1H, H23), 3.62 (s, 3H, COOC$\underline{H_3}$), 3.01 (s, 3H, S-C$\underline{H_3}$), 1.46 (s, 3H), 1.33 (s, 3H), 1.09 (s, 3H), 0.97–0.96 (m, 6H), 0.86 (d, *J* = 6.2 Hz, 3H) ppm. ^{13}C NMR (100MHz, $CDCl_3$): δ = 199.0 (C11), 194.9 (CHO), 177.1 (C28), 164.9 (C13), 157.2 (C2), 142.0 (C3), 129.3 (C12), 75.1, 58.3, 56.1, 53.0, 51.9, 48.1, 47.6, 46.9, 45.7, 44.4, 38.6, 38.3, 37.5, 35.8, 33.3, 30.2, 29.7, 23.8, 21.2, 21.0, 20.9, 20.3, 17.1, 16.9, 16.1 ppm. DI-ESI-MS *m/z*: 575.42

([M+H]$^+$), 597.30 ([M+Na]$^+$). Anal. Calcd. for $C_{32}H_{46}O_7S$: C, 66.87; H, 8.07; S, 5.58. Found: C, 66.48; H, 8.45; S, 5.20%.

Methyl 2-cyano-23-methanesulfonyloxy-A(1)-norursa-2,12-dien-28-oate (4.30)

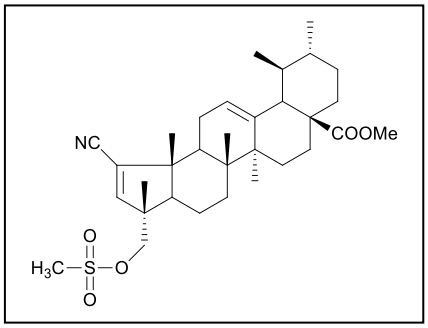

Accordingly to the method described for **4.28**, using compound **4.15** (250 mg, 0.52 mmol), dry CH_2Cl_2 (10.7 mL), triethylamine (145.40 µl; 1.04 mmol) and methanesulfonyl chloride (80.65 µl, 1.04 mmol) at room temperature, in anhydrous conditions for 4 hours. The crude solid was purified by flash column chromatography (petroleum ether/ethyl acetate, 4:1 → 3:1), to afford **4.30** as a white solid (179.2 mg, 62%). Mp: 109.50–112.10 °C. ν_{max}/cm^{-1} (KBr): 2948.63, 2925.48, 2871.49, 2217.74, 1722.12, 1455.99, 1359.57, 1176.36, 960.38. ^{1}H NMR (400MHz, $CDCl_3$): δ = 6.43 (s, 1H, H3), 5.27 (t, *J* = 2.5 Hz, 1H, H12), 4.05 (d, *J* = 9.8, 1H, H23), 4.00 (d, *J* = 10.0 Hz, 1H, H23), 3.60 (s, 3H, COOC$\underline{H_3}$), 3.02 (s, 3H, S-C$\underline{H_3}$), 1.28 (s, 3H), 1.12 (s, 3H), 1.10 (s, 3H), 0.94 (d, *J* = 5.9 Hz, 3H), 0.87 (d, *J* = 6.4 Hz, 3H), 0.83 (s, 3H) ppm. ^{13}C NMR (100MHz, $CDCl_3$): δ = 177.9 (C28), 150.9 (C3), 138.8 (C13), 128.0 (C2), 124.8 (C12), 117.1 (CN), 74.1, 55.9, 52.9, 52.8, 51.5, 49.1, 48.0, 43.7, 42.4, 40.9, 38.8, 38.8, 37.6, 36.5, 33.3, 30.5, 28.1, 24.5, 24.0, 23.9, 21.1, 19.0, 18.4, 17.5, 17.2, 16.0. DI-ESI-MS *m/z* [M+H]$^+$: 558.28. Anal. Calcd. for $C_{32}H_{47}NO_5S.0.25H_2O$: C, 68.35; H, 8.51; N, 2.49; S, 5.70. Found: C, 68.55; H, 8.51; N, 2.67; S, 5.30%.

4.4.2 Biology

4.4.2.1 Cells and reagents

MCF-7, HT-29, Jurkat, PC-3, A375, MIA PaCa-2, HeLa and BJ cell lines were obtained from the American Type Culture Collection (USA).

Dulbecco's Modified Eagle Medium (DMEM), RPMI 1640 Medium, Dulbecco's Phosphate Buffered Saline (DPBS), and L-glutamine were obtained from Biowest. Minimum Essential Medium (MEM), a penicilin/streptomicin solution, and

Fetal Bovine Serum (FBS) were obtained from Gibco. A MTT powder and the XTT cell proliferation kit were purchased from Applichem Panreac. A sodium pyruvate solution 100 mM and Trypsin/EDTA were obtained from Biological Industries. A sodium bicarbonate solution (7.5%) and glucose solution (45%) were purchased from Sigma-Aldrich Co.

Primary antibodies against $p21^{cip1/waf1}$ (sc-397), Bcl-2 (sc-509), Bax (sc-493), and cyclin D_3 (sc-182) were obtained from Santa Cruz Biotechnology, Inc. Primary antibodies against $p27^{kip1}$ (#610242), Bid (#550365) and poly-(ADP-ribose)-polymerase (PARP) (#556493) were obtained from BD Biosciences. Primary antibodies against caspase 3 (#9662), caspase 8 (#9746S) and caspase 9 (#9502) were purchased from Cell Signaling. The primary antibody against α-actin (#69100) was obtained from MP Biomedicals. Secondary antibodies [anti-mouse (P0260) and anti-rabbit (NA934)] were obtained from Dako and from Amersham Biosciences, respectively.

Cisplatin was obtained from Sigma-Aldrich Co.

4.4.2.2 Preparation and storage of the stock solutions

Asiatic acid and its derivatives were suspended in DMSO at 20 mM as stock solutions, which were stored at –80 °C. To obtain final assay concentrations, the stock solutions were diluted with culture medium on the day of testing. The final concentration of DMSO in working solutions was always equal or lower than 0.5%.

4.4.2.3 Cell culture

HT-29, PC-3, A375, MIA PaCa-2 and HeLa cells were routinely maintained in DMEM supplemented with 10% heat-inactivated fetal bovine serum (FBS) and 1% penicillin/streptomycin. MCF-7 cells were maintained in MEM supplemented with 10% heat-inactivated FBS, 0.1% penicillin/streptomycin, 2 mM L-glutamine, 1 mM sodium pyruvate, 0.01 mg/mL of insulin, 10 mM glucose, and 1× MEM-EAGLE non essential aminoacids. BJ cells were routinely maintained in DMEM supplemented with 10% heat-inactivated FBS, 110 mg/L sodium pyruvate, 1% penicillin/streptomycin,

and 1.5 g/L of bicarbonate. Jurkat cells were cultured in RPMI 1640 supplemented with 10% FBS, 1% penicillin/streptomycin and 2 mM L-glutamine. All cell lines were incubated in a 5% CO_2 humidified atmosphere at 37 °C.

4.4.2.4 Cell viability assay

The antiproliferative activities of compounds against the MCF-7, HT-29, PC-3, A375, MIA PaCa-2, HeLa, and BJ cell lines were evaluated via MTT assay. Briefly, 8 $\times 10^2$ to 1 $\times 10^4$ cells per well were plated in 96-well plates in 200 µl of medium and were left to grow. After 24 h of culture, the culture medium was removed and replaced by new medium (200 µl) containing the tested compounds at different concentrations, in triplicate. After 72 h of incubation, 100 µl of MTT solution (0.5 mg/ml) were used to replace the supernatant in each well. After 1 h of incubation, the supernatant was removed and 100 µl of DMSO were added to each well. Relative cell viability was measured by absorbance at 550 nm on an ELISA plate reader (Tecan Sunrise MR20-301, TECAN, Salzburg, Austria).

The antiproliferative activities of compounds against Jurkat cells were determined using the XTT assay. Briefly, Jurkat cells were seeded at a density of 4 $\times$ 10^3 cells per well in 96-well plates in 100 µl of medium. After 24 h of incubation, 100 µL of medium containing the tested compounds at different concentration, in triplicate, were added. After 72 h of incubation, 100 µl of XTT solution were added to each well and the plates were incubated for an additional 4 h at 37 °C. Relative cell viability was measured by absorbance at 450 nm on an ELISA plate reader (Tecan Sunrise MR20-301, TECAN, Salzburg, Austria). Nontreated cells were used as the control.

IC_{50} values represent the concentration of each compound that inhibited the cell growth by 50%, compared with nontreated cells. The IC_{50} values were estimated from the dose-response curves using 9 different concentrations in triplicate. Each IC_{50} value was expressed as the mean IC_{50} ± standard deviation (SD) of three independent experiments.

4.4.2.5 Cell-cycle assay

HeLa cells were seeded at a density of 1×10^5 cells per well in 6-well plates with 2 mL of medium and incubated at 37 °C for 24 h. Cells were then treated with compound **4.29** at the specified concentrations for 24 h. Cells were harvested by mild trypsinization, centrifuged, washed twice with PBS and then stained with Tris-buffered saline (TBS) containing 50 mg/mL of PI, 10 mg/mL Rnase-free Dnase, and 0.1% Igepal CA-630 for 1 hour at 4 °C in the dark. Cell cycle was assessed by flow cytometry using a fluorescence activated cell sorting (FACS) apparatus. FACS analysis was carried out at 488 nm on an Epics XL flow cytometer (coulter Corporation, Hialeah, FL). Data from 1×10^4 cells were collected and analyzed using the multicycle software (phoenix Flow Systems, San Diego, CA). Experiments were performed in triplicate, with two replicates per experiment.

4.4.2.6 Annexin V-FITC/PI flow cytometry assay

HeLa cells were plated in 6-well plates at a density of 1×10^5 cells/well and incubated at 37 °C for 24 h. Cells were then treated with compound **4.29**, at the specified concentrations, for 24 h. Subsequently, cells were harvested by mild trypsinization, collected by centrifugation, and suspended in 95 µl of binding buffer (10 mM HEPES/NaOH, pH 7.4, 10 mM NaCl, 2.5 mM $CaCl_2$). Cells were then stained with annexin V-FITC conjugate for 30 min at room temperature and protected from the light. Then, 500 µl of binding buffer were added to each vial of cells. Approximately 2 min before FACS analysis, 20 µl of a 1mg/mL PI solution were added to each vial and the samples were analyzed by flow cytometry. Data from 1×10^4 cells were collected and analyzed. Experiments were performed in triplicate, with two replicates per experiment.

4.4.2.7 Morphological analysis using phase–contrast microscopy

In this experiment, 1×10^5 HeLa cells per well were seeded in 6-well plates containing 2 mL of medium and incubated at 37 °C for 24 h. Cells were then treated

with compound **4.29** at the specified concentrations. After 24 h, morphological changes were observed using an inverted phase–contrast microscope (Olympus IMT-2) with a 40× objective and a digital camera [*Fujifilm* A2O5S (*Fuji Foto Film*, CO. LTD)].

4.4.2.8 Hoechst 33258 staining

HeLa cells were seeded at a density of 1×10^5 cells per well in 6-well plates containing 2 mL of medium and incubated at 37 °C for 24 h. Cells were then treated with compound **4.29** at the indicated concentrations. After 24 h, the culture medium was removed and cells were harvested by mild trypsinization, collected by centrifugation, and washed twice with PBS. The cells were then stained with 500 µl of Hoechst 33258 solution (2 µg/mL in PBS) for 15 min at room temperature and protected from the light. Subsequently, the Hoechst 33258 solution was removed and cells were washed twice with PBS, resuspended in 10 µl of PBS and then mounted on a slide. The morphological modifications were analyzed by fluorescence microscopy using a fluorescence microscope (DMRB Leica Microssystems, Weltzar, germany) using a DAPI filter.

4.4.2.9 Preparation of total protein extract

To prepare the total protein extracts, HeLa cells (5.6×10^4) were seeded in 100 mm plates containing 10 mL of culture medium and incubated at 37 °C for 24 h. Cells were then treated with the indicated concentrations of compound **4.29.** After 24 h of incubation, HeLa cells were washed twice with ice cold PBS and resuspended in ice cold lysis buffer [20 mM Tris/acetate (pH 7.5), 270 mM sucrose, 1 mM EDTA (pH 8.8), 1 mM EGTA (pH 8.8), 1% Triton X-100, and 1% protease inhibitor cocktail (Sigma-Aldrich)]. The samples were homogenized by sonication, incubated on ice for 15 min, and centrifuged at 12000 rpm for 5 min at 4 °C. The protein content in supernatants was determined using the bicinchoninic acid (BCA) assay kit (Pierce Biotechnology, Rockford). After quantification, the supernatants were stored at –80 °C.

4.4.2.10 Western blotting

The protein extracts were separated on 10% or 15% SDS–polyacrilamide gels[276] and then transferred to polyvinyl nitrocellulose membranes (BioRad Laboratories, Richmond). Transferred membranes were blocked with TBS buffer (20 mM Tris (pH 7.5) and 132 mM NaCl) containing 0.1% Tween and 5% BSA or nonfat dry milk for 1 h at room temperature. The membranes were then incubated with a primary specific antibody overnight at 4 °C. Subsequently, membranes were washed five times (5 min each time) with TBS–0.1% Tween and incubated with the appropriate secondary antibody for 1 h at room temperature. After incubation, membranes were washed five times (5 min each time) with TBS–0.1% Tween, treated with Immobilon ECL Western Blotting Detection Kit Reagent (Millipore) and developed after exposure to an autoradiography film in a film cassette.

Chapter 5

Synthesis and anticancer evaluation of amide and hydroxamic acid derivatives of asiatic acid

Design, synthesis, and biological evaluation of novel asiatic acid derivatives as potential anticancer agents

Bruno M. F. Gonçalves, Jorge A. R. Salvador, Diana S. M. Santos, Sílvia Marín and Marta Cascante

RSC Advances, 2016, 6, 39296–39309.

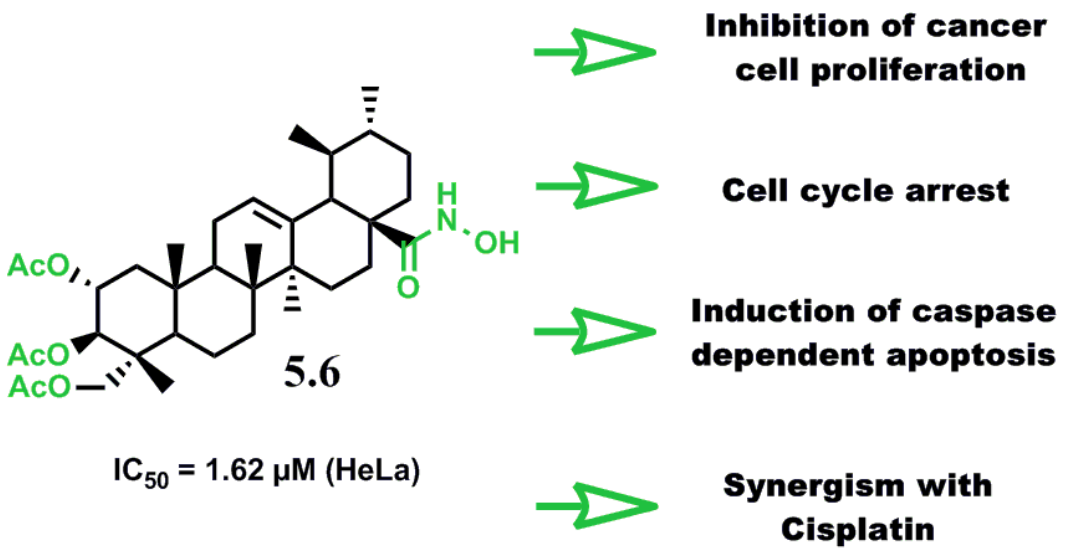

5.1 Introduction

Despite the anticancer potential of asiatic acid **1.27,** its clinical utility in the treatment of cancer is limited by its moderate activity. The chemical modification of the asiatic acid **1.27** backbone had a high impact on its biological activity and may represent the solution to improving its antitumor activity.[211,214]

One of the most common modifications performed in the backbone of several pentacyclic triterpenoids is the replacement of the C28 carboxylic acid with amide side chains, and some of the semisynthetic derivatives obtained exhibited significantly enhanced anticancer activities acompared with the parental compounds.[302] In the case of asiatic acid **1.27**, similar results were reported recently; the introduction of amino moieties at C28 significantly improved its anticancer activity against several cancer cell lines.[211,214,215] Modifications of the A-ring of asiatic acid **1.27** were also reported to have a positive impact on the anticancer activity of the parental compound.[139]

Moreover, in recent decades, medicinal chemists have gained a renewed interest in hydroxamic acids and their derivatives, because these compounds display a wide spectrum of pharmacological activities, including anti-HIV, anti-Alzheimer, anti-inflammatory, and anti-melanogenic properties.[303–306] The hydroxamic acid derivatives also proved to be valuable compounds in the field of anticancer drug discovery.[307–313] The hydroxamic acid derivatives are well-known inhibitors of metal-containing enzymes, such as matrix metalloproteinases (MMPs) and histone deacetylases (HDACs), which are two enzyme families that are important for tumor development.[310,314,315] In the particular case of triterpenoid compounds, previous studies reported the synthesis of hydroxamate derivatives of glycyrrhetinic acid that were selective inhibitors of 11β-hydroxysteroid dehydrogenase 2.[316,317] Recently, ursolic and oleanolic acid-derived hydroxamates were reported to exhibit increased cytotoxic activities against several human tumor cell lines compared with the parental compounds (ursolic acid and oleanolic acid).[318] However, the preparation of hydroxamic acid derivatives of asiatic acid **1.27** was not explored.

Several methods have been described in literature for the preparation of hydroxamic acids from carboxylic acids.[319–322] In this chapter, hydroxamic acid derivatives of asiatic acid **1.27** were prepared via the reaction of CDI-activated carboxylic acids with hydroxylamine or *N*-methylhydroxylamine hydrochloride.[321]

Considering all these facts, a panel of new asiatic acid **1.27** derivatives bearing amide or hydroxamic acid groups at C28, combined with modifications at the A-ring was designed and prepared to search for novel antitumor drug candidates.

5.2 Results

5.2.1 Chemistry

5.2.1.1 Synthesis and structural elucidation

As shown in scheme 5.1 the synthesis started with the preparation of the intermediates **5.1**, **5.2**, **5.3**, **5.4** and **5.5**. The lactol derivative **5.1** was obtained by treatment of asiatic acid **1.27** with sodium periodate in methanol/water, by adapting a previously reported procedure.[252] The treatment of derivative **5.1** with acetic acid and piperidine in dry benzene gave the α,β-unsaturated aldehyde **5.2**. This compound was then reduced with sodium borohydride in anhydrous methanol, affording the diol derivative **5.3** in good yield (92 %).[139,323] The two hydroxyl groups of compound **5.3** were diacetylated with acetic anhydride and DMAP in THF, affording the intermediate **5.4.** The triacetate derivative **5.5** was obtained in good yield by treating the commercially available asiatic acid **1.27** with acetic anhydride. The intermediates **5.4** and **5.5** were then used as starting point for the preparation of new derivatives of asiatic acid **1.27** (Schemes 5.2, 5.3 and 5.4).

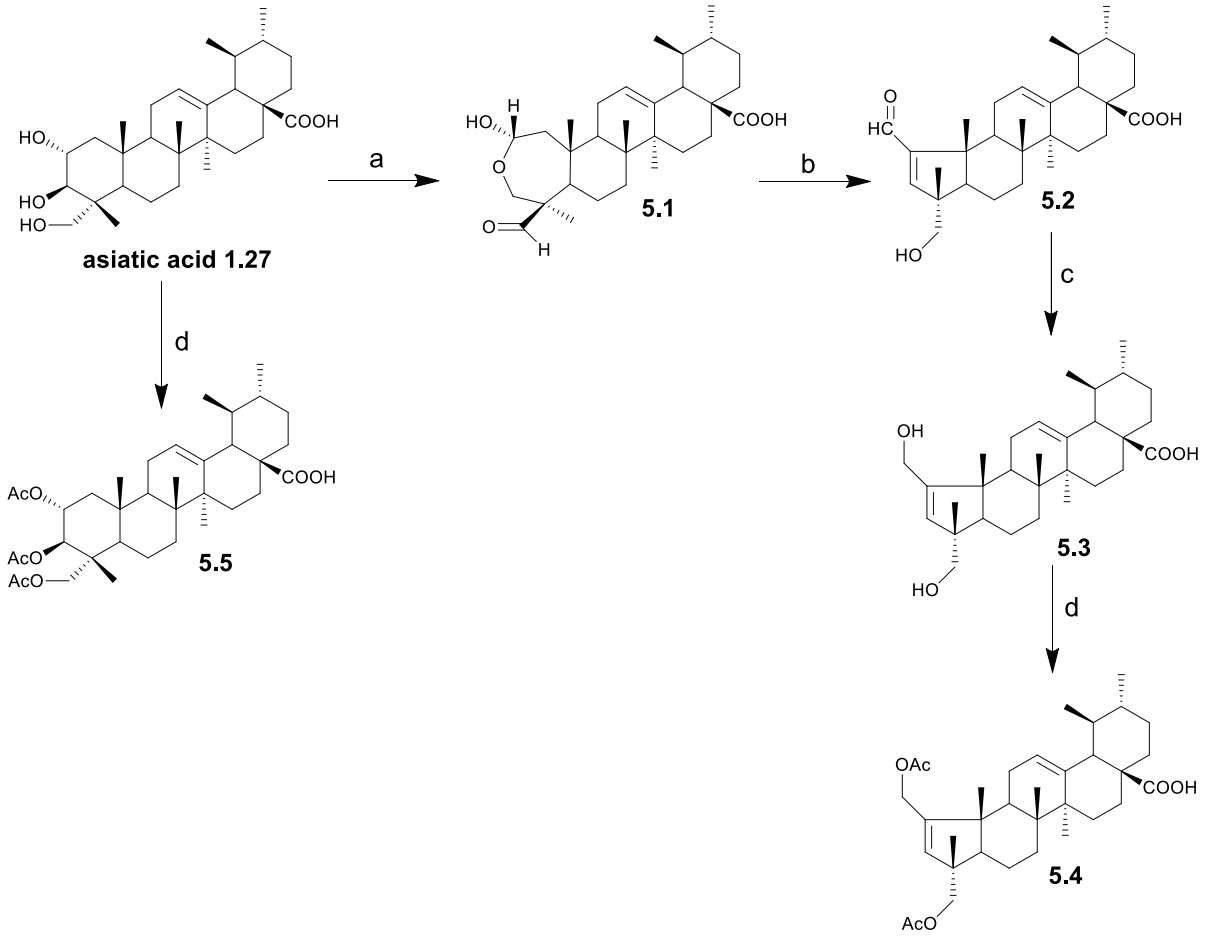

Scheme 5.1 Synthesis of derivatives **5.1–5.5.** *Reagents and conditions:* a) $NaIO_4$, $MeOH/H_2O$, rt.; b) i- Acetic acid, piperidine, dry benzene, 60 °C, N_2; ii -Anhydrous $MgSO_4$, 60 °C, N_2; c) $NaBH_4$, MeOH, rt; d) Acetic anhydride, DMAP, THF, rt.

In this study, the hydroxamic acid derivatives of asiatic acid **1.27** were prepared through the activation of carboxylic acids with CDI, followed by the reaction with hydroxylamine or *N*-methylhydroxylamine hydrochloride. As CDI promoted the deprotonation of hydroxylamine hydrochloride, no additional base was necessary. The by-products are water soluble and therefore easily removed during the work-up.[321] The carboxylic acid derivative **5.5** was treated with CDI in THF to afford the respective *N*-acylimidazole intermediate, which was reacted with hydroxylamine hydrochloride or *N*-methylhydroxilamine hydrochloride to give the corresponding hydroxamic acid derivatives **5.6** and **5.7**, in good yields (Scheme 5.2). The hydroxamic acid derivative **5.8** was prepared from **5.4**, according to the procedure described for compound **5.6** and using hydroxylamine hydrochloride.

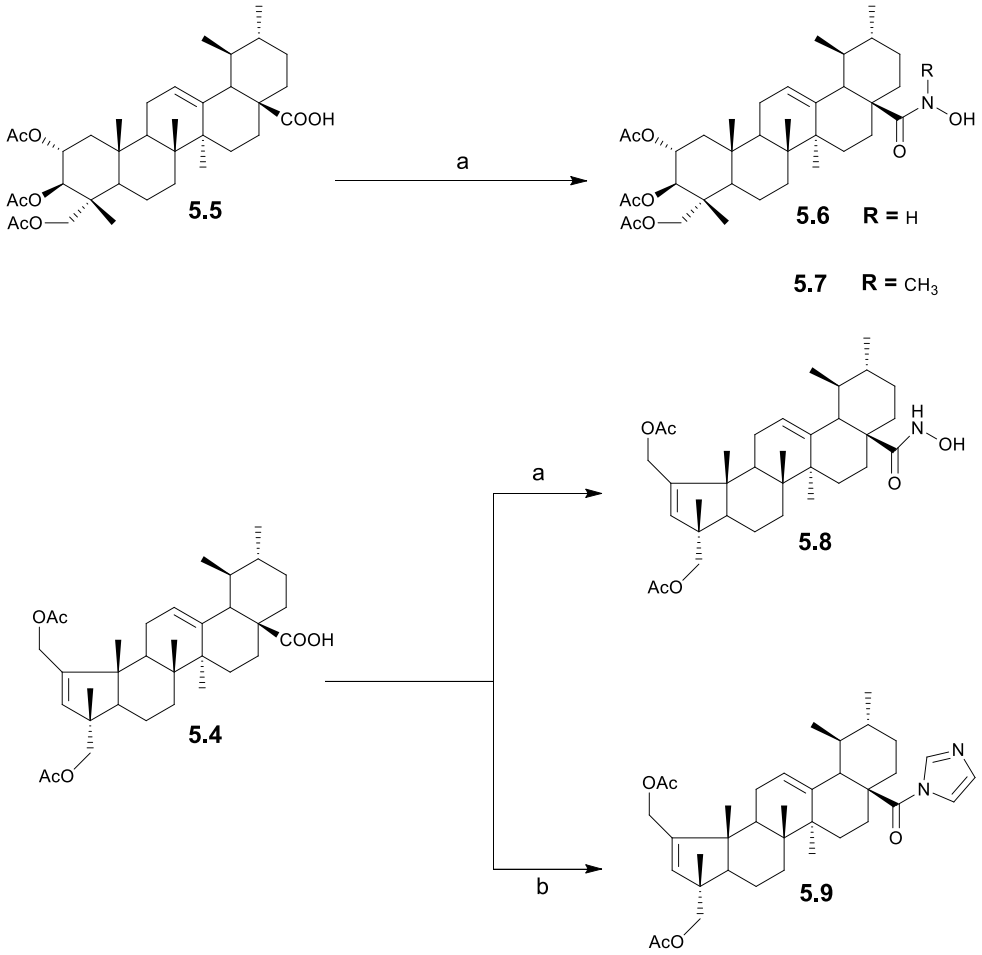

Scheme 5.2 Synthesis of derivatives **5.6–5.9.** *Reagents and conditions:* a) i-THF, CDI, reflux, N_2; ii-Hydroxylamine hydrochloride or *N*-methylhydroxylamine hydrochloride, rt.; b) THF, CDI, reflux, N_2.

The structures of the derivatives synthesized were elucidated by IR, 1D NMR and MS. To characterize the intermediates (**5.1–5.5**), spectral data from the literature were also used for comparison.[139] The formation of the hydroxamic acid derivatives **5.6** and **5.8** was confirmed by the presence of a signal in the ^{1}H NMR spectra at around 6.25–6.27 ppm, corresponding to the proton attached to the nitrogen atom of the hydroxamic acid (Fig. 5.1). In addition, in the ^{13}C NMR spectrum, the signal of the carbonyl carbon of hydroxamic acid was observed at 178.4 ppm, which was a lower value than that observed for the corresponding carbonyl carbon of carboxylic acid (at 183.1–183.6 ppm, in compounds **5.4** and **5.5**) (Fig. 5.2).

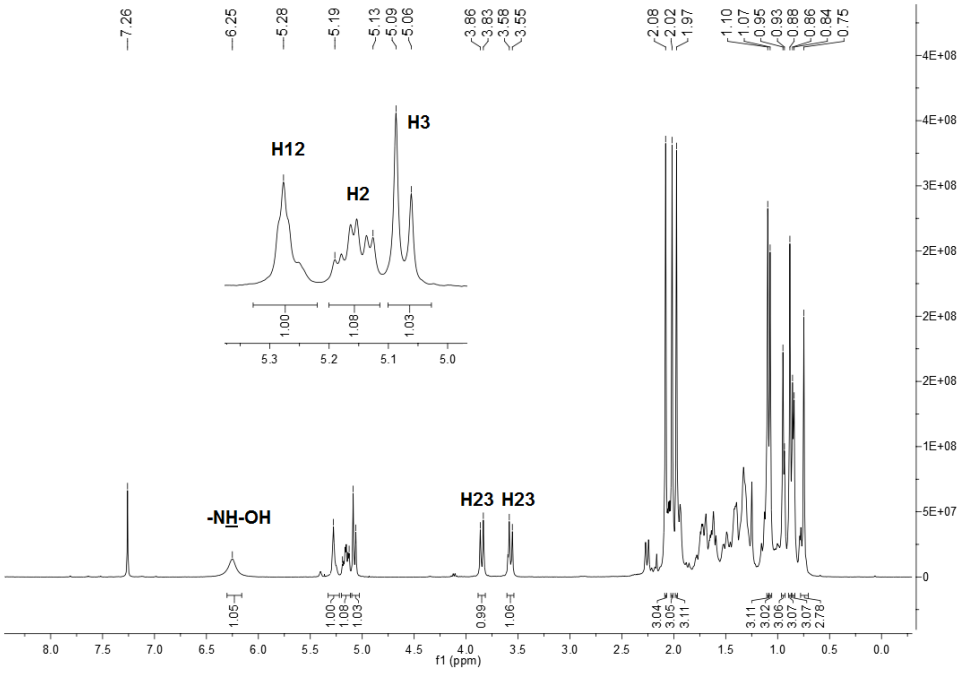

Figure 5.1 ^{1}H NMR Spectrum of compound **5.6**.

The ester carbonyl carbons of compound **5.6** appeared in the ^{13}C NMR spectrum (Fig. 5.2) as three signals at 170.8, 170.4 and 170.4 ppm. The signals for quaternary C13 appeared at 137.9 ppm. The signal at 125.5 ppm corresponded to the tertiary C12, as this signal was present on DEPT 135 (Fig. 5.3).

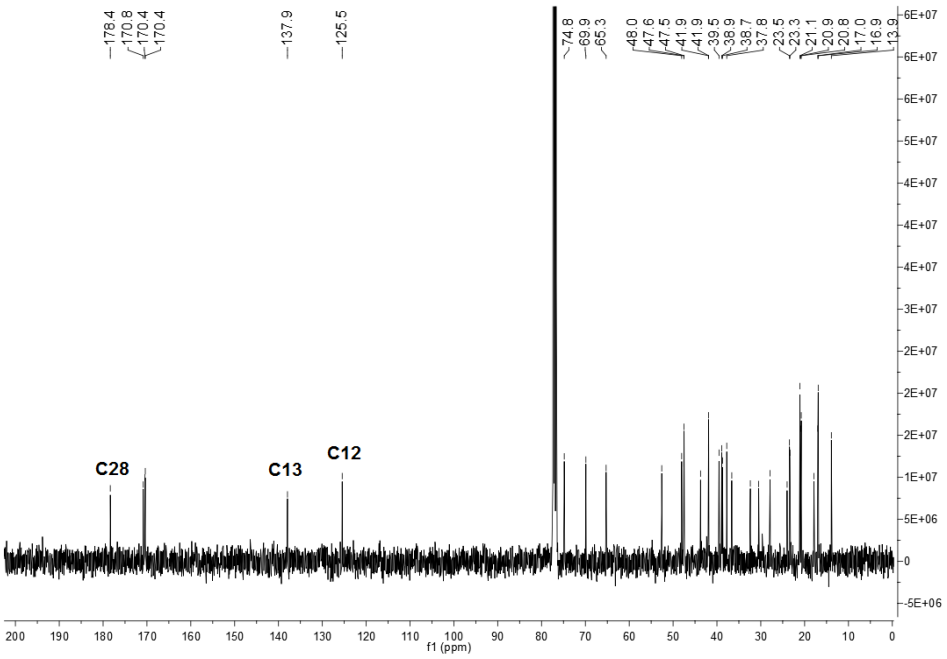

Figure 5.2 ^{13}C NMR spectrum of compound **5.6**.

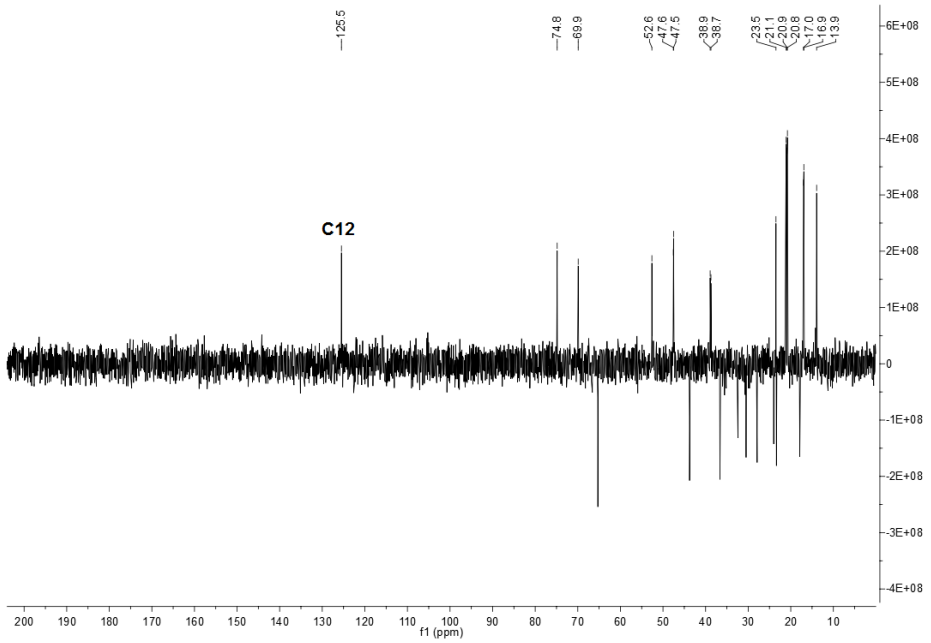

Figure 5.3 DEPT 135 spectrum of compound **5.6**.

The preparation of the derivative **5.7** was confirmed by a signal at 2.76 ppm in the ^{1}H NMR spectrum, corresponding to the methyl protons of the *N*-methyl hydroxamic acid group (Fig. 5.4). The signals corresponding to protons H12, H2, and H3 appeared as a triplet, a multiplet, and a doublet at 5.29, 5.19–5.12 and 5.08 ppm, respectively.

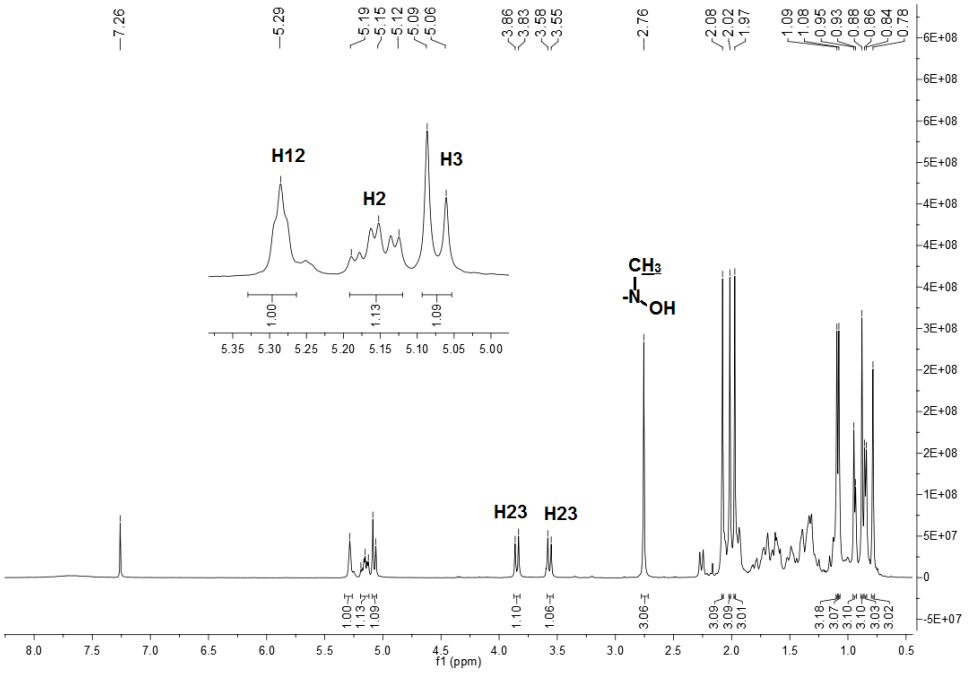

Figure 5.4 ^{1}H NMR spectrum of compound **5.7**.

In the ^{13}C NMR spectrum of compound **5.7**, the signal of carbon C28 appeared at 177.6 ppm, and the signals for the ester carbonyl carbons were observed at 170.9, 170.4, and 170.4 ppm. The signals detected at 137.9 ppm corresponded to the quaternary C13, whereas the signal observed at 125.4 ppm corresponded to the tertiary carbon C12 (Fig. 5.5).

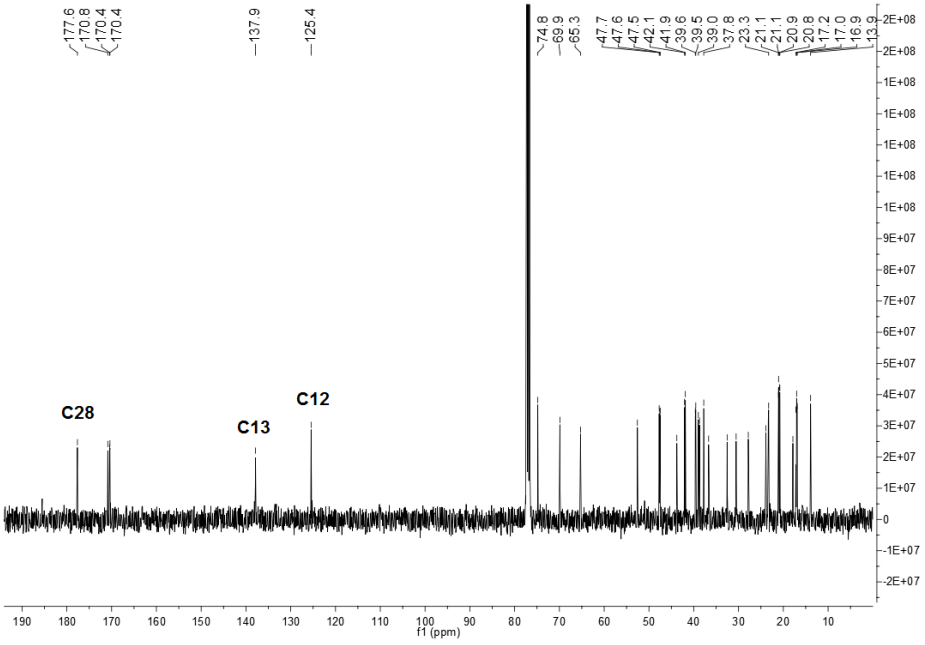

Figure 5.5 ^{13}C NMR spectrum of compound **5.7**.

Previous studies revealed that the introduction of an imidazole ring at the C28 position of triterpenoid compounds improved their cytotoxic activities.[254–256] Thus the *N*-acylimidazole derivative **5.9** was prepared in 62.55% yield via the reaction of compound **5.4** with CDI in THF at reflux and under an inert atmosphere (Scheme 5.2). The presence of the imidazole ring in compound **5.9** was confirmed by the three signals observed at 8.23, 7.52, and 7.03 ppm in the ^{1}H NMR spectrum (Fig. 5.6), which were typical of the three imidazole protons and are consistent with data reported in the literature. [256]

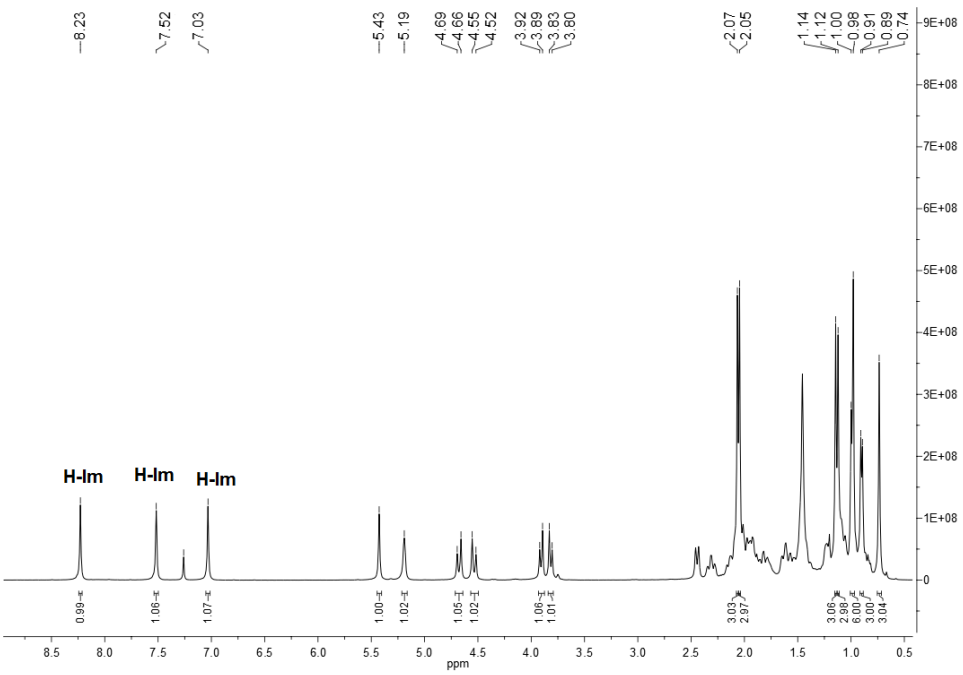

Figure 5.6 ^{1}H NMR spectrum of compound **5.9**.

In the ^{13}C NMR spectrum of compound **5.9** were presented ten δ signals greater than 70 ppm. The signal at 174.7 ppm corresponded to the C28 carbon (Fig. 5.7), which was different from the signal observed for the C28 carbon of carboxylic acid at 183.6 ppm (in the ^{13}C NMR spectrum of compound **5.4**). The signals at 151.1 and 137.7 ppm were attributed to the quaternary carbons C2 and C13, respectively, based on the comparison with the ^{13}C NMR spectrum of compound **5.4**. The signals at 132.0 and 126.1 ppm were attributed to the tertiary carbons C3 and C12, respectively, as these signals appeared in the DEPT 135 (Fig. 5.8). The signals of the three tertiary carbons of the imidazole ring were observed at 137.1, 129.7 and 117.4 ppm, which were in accordance with the data from literature.[256]

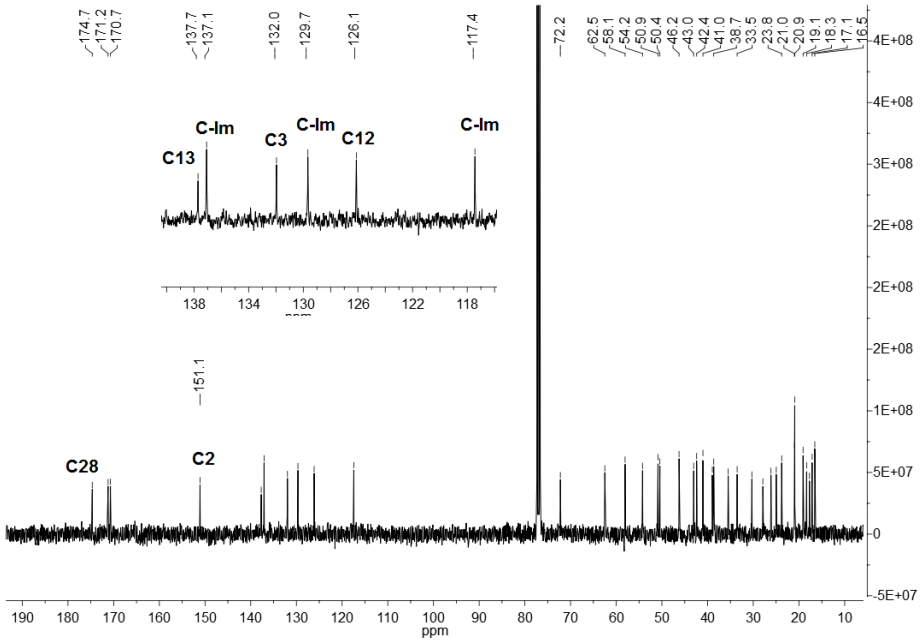

Figure 5.7 ^{13}C NMR spectrum of compound **5.9**.

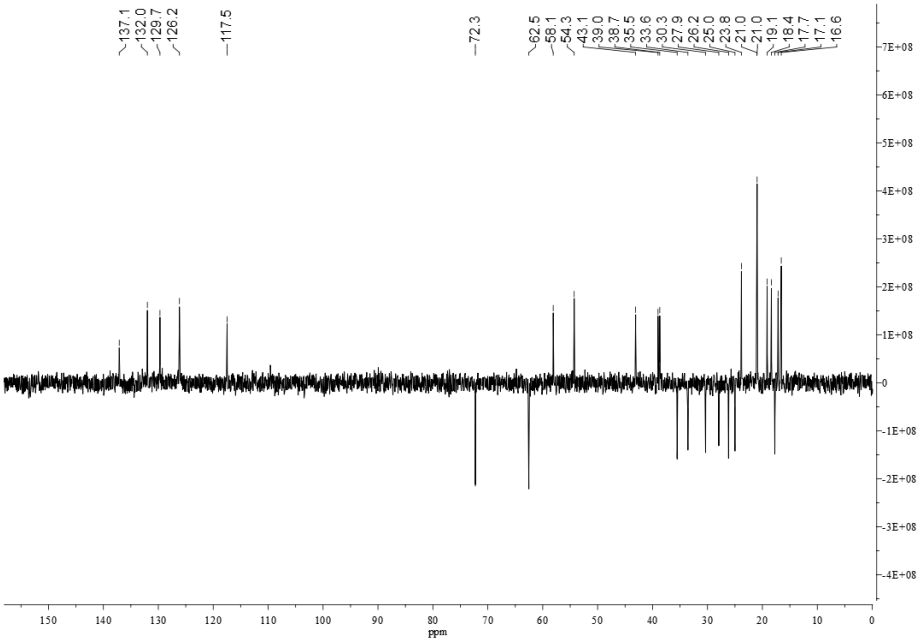

Figure 5.8 DEPT 135 spectrum of compound **5.9**.

As depicted in Scheme 5.3, the treatment of compound **5.4** with thionyl chloride in dry benzene, gave the acyl chloride derivative, followed by treatment with the respective amines in dry dichloromethane afforded the amide derivatives **5.10**–**5.14** in good yields.

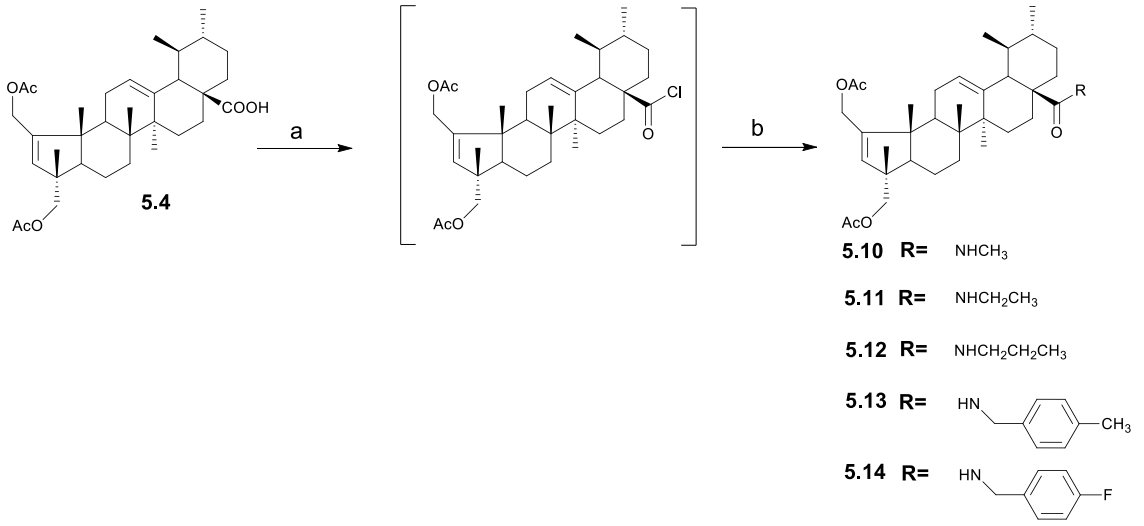

Scheme 5.3 Synthesis of derivatives **5.10**–**5.14.** *Reagents and conditions:* a) $SOCl_2$, benzene, reflux temperature; b) methylamine or ethylamine or propylamine or 4-methylbenzylamine or 4-fluorobenzylamine, Et_3N, dichloromethane, rt.

The formation of an amide bond at C28 in derivatives **5.10**–**5.14** was confirmed by the presence of a strong N-H bending band at 1509–1527 cm^{-1} in the IR spectra. In addition, the absorption band corresponding to the carbonyl stretching vibration of the amide was observed at 1635.0–1635.5 cm^{-1}, which was a lower frequency than that observed for the carbonyl stretching of the carboxylic acid (1694.5 cm^{-1}) (see as example the IR spectra of compound **5.11**, Fig. 5.9).

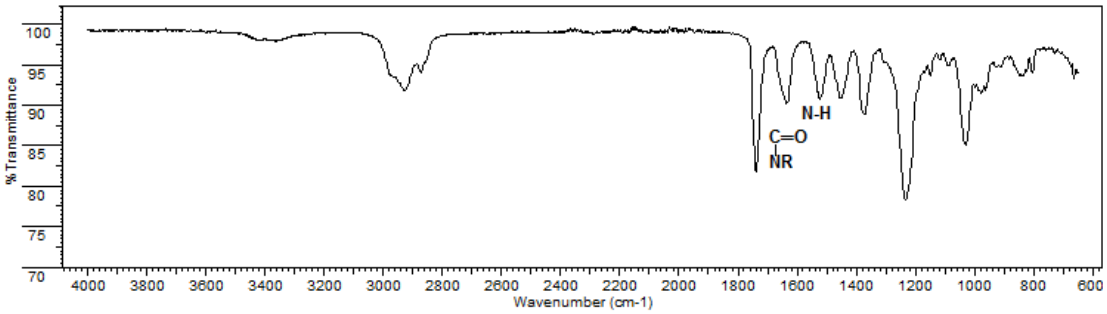

Figure 5.9 IR spectrum of compound **5.11**.

On the ^{1}H NMR spectrum of compound **5.11** (Fig. 5.10), the signal of the amide proton (NH) was observed as a triplet at 5.81 ppm, with a coupling constant of 4.4 *Hz*. On the ^{13}C NMR spectrum (Fig. 5.11), the signal for the amide carbonyl carbon was

observed at 177.8 ppm, which was a lower value than that observed for the carbonyl carbon of carboxylic acid (at 183.6 ppm). Similar structural data were obtained for the other amide derivatives (**5.10**, **5.12**, **5.13**, and **5.14**), as described in the experimental section.

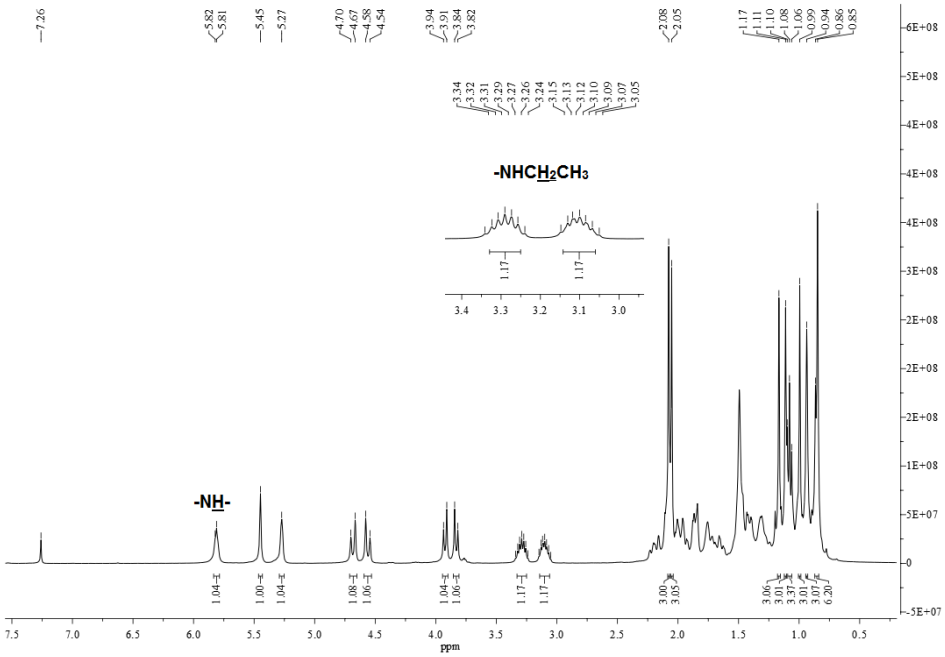

Figure 5.10 ^{1}H NMR spectrum of compound **5.11**.

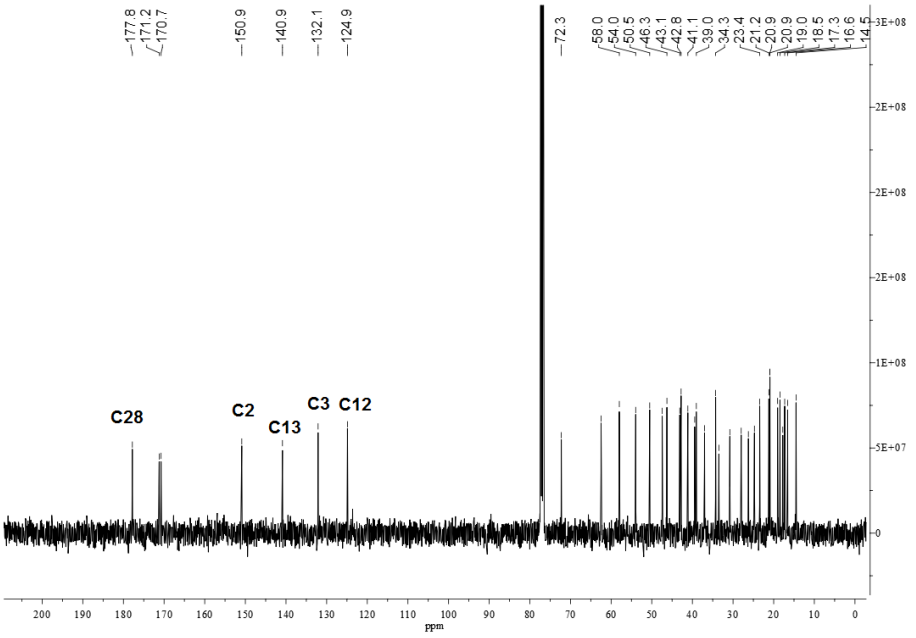

Figure 5.11 ^{13}C NMR spectrum of compound **5.11**.

The methyl ester amino acid derivatives **5.15** and **5.16** were obtained by treating **5.4** with thionyl chloride, to give the acyl chloride intermediate, which was further reacted with the corresponding amino acid methyl ester hydrochloride (Scheme 5.4).

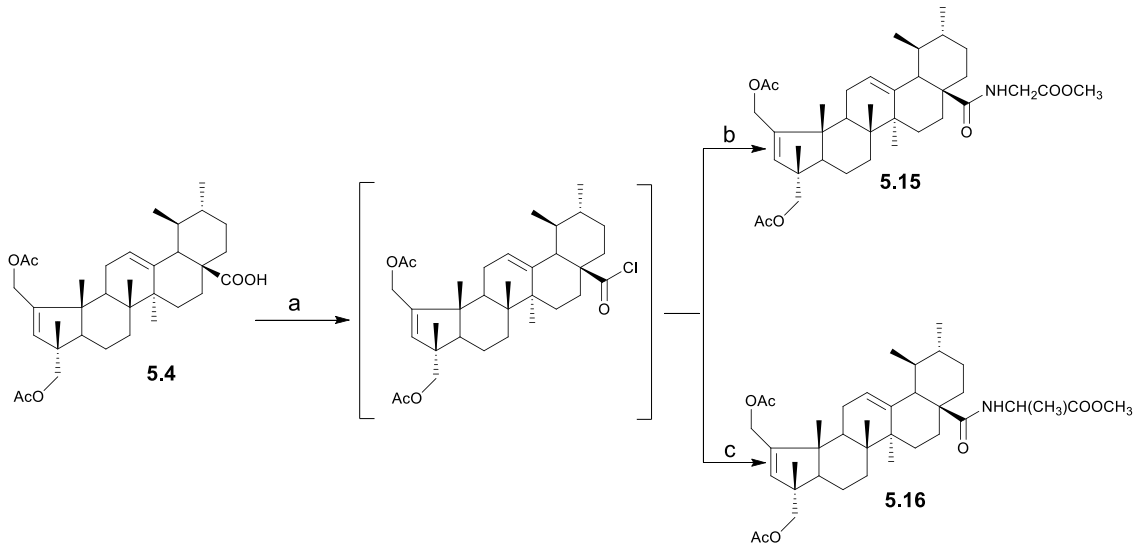

Scheme 5.4 Synthesis of derivatives **5.15** and **5.16.** *Reagents and conditions:* a) $SOCl_2$, benzene, reflux temperature; b) glycine methyl ester, Et_3N, THF, rt; c) L-alanine methyl ester, Et_3N, THF, rt.

The amino acid derivatives **5.15** and **5.16** presented an N-H bending band in the IR spectrum at 1507.5–1520.5 cm^{-1}, as well as a band at 1650.0–1655.5 cm^{-1} corresponding to the carbonyl stretching vibration of the amide. In the ^{1}H NMR spectrum of compound **5.16** (Fig 5.12), the signal for the amide proton (NH) appeared as a doublet at 6.59 ppm, with a coupling constant of 5.8 Hz. The signal detected at 177.3 ppm in the ^{13}C NMR spectrum was identified as the quaternary carbon C28 (Fig. 5.13).

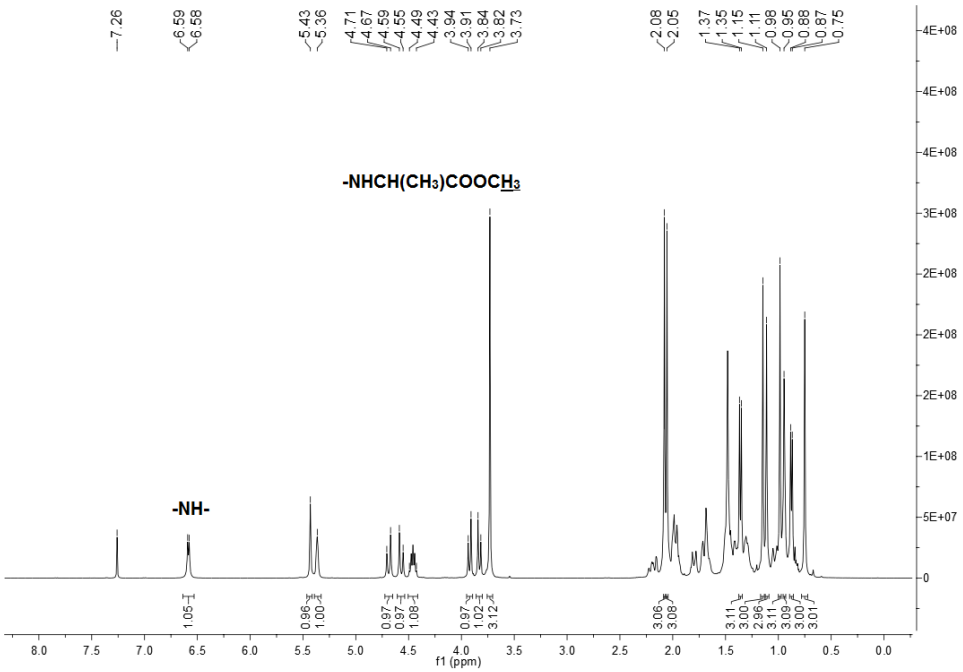

Figure 5.12 ^{1}H NMR spectrum of compound **5.16**.

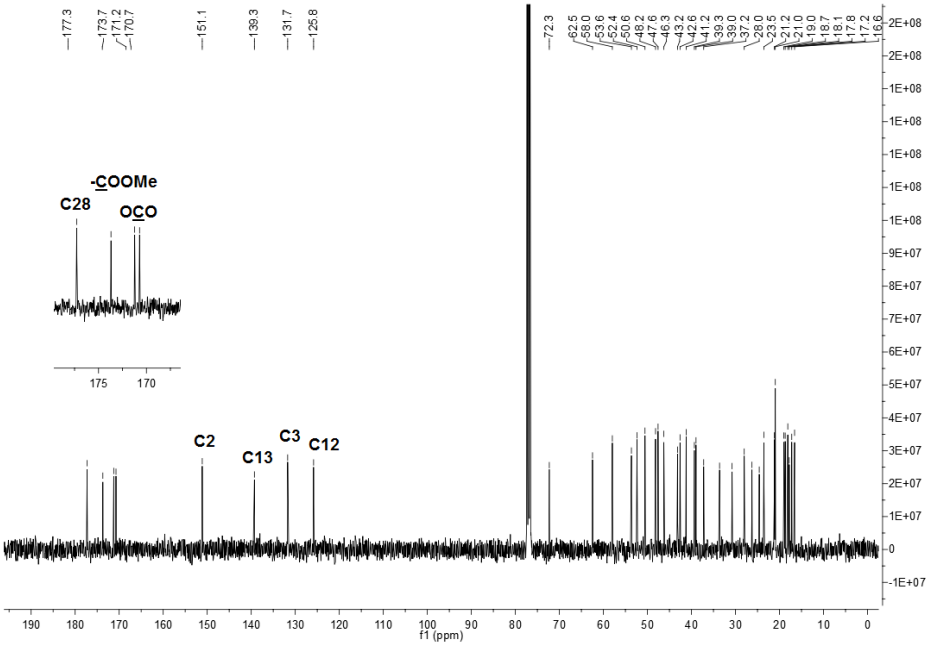

Figure 5.13 ^{13}C NMR spectrum of compound **5.16**.

5.2.2 Biological evaluation

5.2.2.1 Evaluation of the antiproliferative activity

The *in vitro* antiproliferative activity of the newly synthesized derivatives was evaluated against colon cancer (HT-29) and cervix cancer (HeLa) cell lines using the MTT assay. The clinically used antineoplastic drug **cisplatin** was evaluated in parallel as the reference drug. The results, which are expressed as the concentration of compound required for 50% of cell growth inhibition (IC_{50}), are summarized in Table 5.1 and Figure 5.14. The IC_{50} values determined in HeLa cells were used to establish a SAR (Fig. 5.15). As depicted in Table 5.1, all new derivatives exhibited improved antiproliferative activity against HeLa cells compared with asiatic acid **1.27**, as they showed IC_{50} values ranging from 1.62 to 45 μM.

As shown in Table 5.1 and Fig. 5.14, the hydroxamic **5.6** and the *N*-methyl hydroxamic **5.7** derivatives exhibited remarkable antiproliferative activities against HT-29 and HeLa cells compared with asiatic acid **1.27**. Compound **5.6** showed IC_{50} values of 4.12 and 1.62 μM against HT-29 and HeLa cell lines, respectively. This compound was 32.4-fold more potent than asiatic acid **1.27** and 3.7-fold more potent than **5.5** against HeLa cells (Fig. 5.15). Compound **5.6** also exhibited a stronger antiproliferative activity against HeLa cells than did the cisplatin (IC_{50} = 2.28 μM). Derivative **5.7** was 13.9- and 1.6-fold more active against HeLa cells than asiatic acid **1.27** and compound **5.5**, respectively. The conversion of the carboxylic acid group of compound **5.4** into a hydroxamic acid group afforded derivative **5.8**, with an improvement of 4.7- and 10.9-fold in antiproliferative activity against HeLa cells compared with **5.4** and asiatic acid **1.27**, respectively. These combined results suggest that the introduction of a hydroxamic acid moiety at C28 has a positive impact on the anticancer activity.

Table 5.1 Cytotoxic activities, expressed as IC_{50}, of asiatic acid **1.27**, its derivatives and cisplatin against human colon adenorcarcinoma (HT-29) and human cervical cancer (HeLa) cell lines.[a]

Compound	Cell line/IC_{50}[b](μM ± SD)	
	HT-29	HeLa
asiatic acid **1.27**	64.33 ± 3.21	52.47 ± 0.06
5.1	N.D.	21.67 ± 1.04
5.2	N.D.	5.30 ± 0.20
5.3	N.D.	45.00 ± 1.55
5.4	N.D.	22.50 ± 0.75
5.5	N.D.	6.10 ± 0.28
5.6	4.12 ± 0.30	1.62 ± 0.10
5.7	7.03 ± 0.06	3.77 ± 0.23
5.8	19.00 ± 0.71	4.80 ± 0.28
5.9	13.15 ± 0.78	6.25 ± 0.07
5.10	16.15 ± 0.92	7.60 ± 0.42
5.11	14.53 ± 1.45	4.54 ± 0.84
5.12	14.10 ± 1.27	6.50 ± 0.50
5.13	>60	6.25 ± 0.35
5.14	>60	5.38 ± 0.53
5.15	22.00 ± 1.41	10.65 ± 0.35
5.16	13.75 ± 0.35	7.23 ± 0.39
Cisplatin	6.11[262 c]	2.28 ± 0.26

[a] HT-29 and HeLa cells were treated with increasing concentrations of each compound for 72 h. Viable cells were determined by MTT assay and IC_{50} values are expressed as the mean ± SD of three independent experiments. N.D.- not determined.

[b] IC_{50} is the concentration of compound that inhibits 50% of cell growth.

[c] IC_{50} value obtained from literature, determined using the same experimental methodology and included here for comparison.

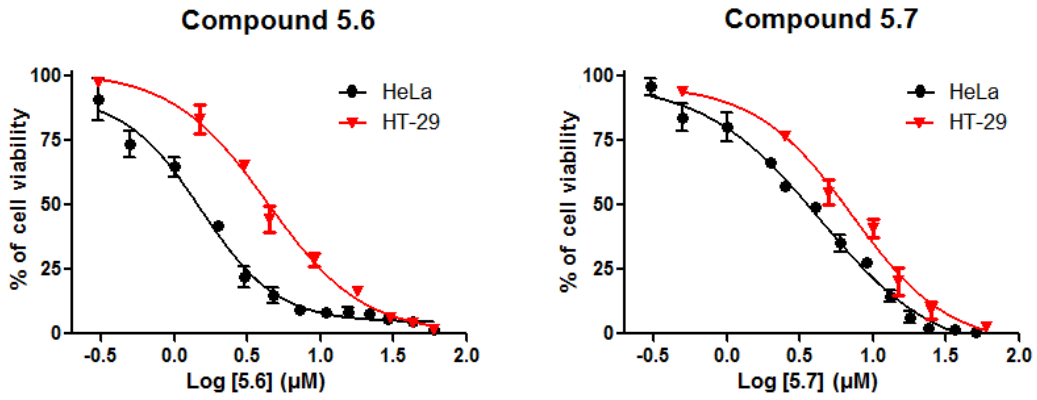

Figure 5.14 Dose-response curves of the antiproliferative effect of derivatives **5.6** and **5.7** against HeLa and HT-29 cancer cell lines. Results are presented as the mean ± SD of three independent experiments.

The introduction of an imidazole ring at C28 of compound **5.4**, to afford compound **5.9**, led to an increase in cell-growth-inhibition activity. The *N*-acylimidazole derivative **5.9** was 3.6- and 8.4-fold more active than **5.4** and asiatic acid **1.27**, respectively, in HeLa cells (Table 5.1). These results are in good agreement with previous reports.[254]

Finally, the comparison of the IC_{50} values of compounds **5.10–5.16** revealed that the introduction of the amide functionality at C28 of compound **5.4** resulted in a significant improvement of antiproliferative activity against HeLa cells**.** Compound **5.11** was 11.6-fold more potent than asiatic acid **1.27** and 4.9-fold more potent than compound **5.4**. Derivatives **5.15** and **5.16**, bearing a methyl ester amino acid residue at C28, exhibited better antiproliferative activity in HeLa cells than did compound **5.4**.

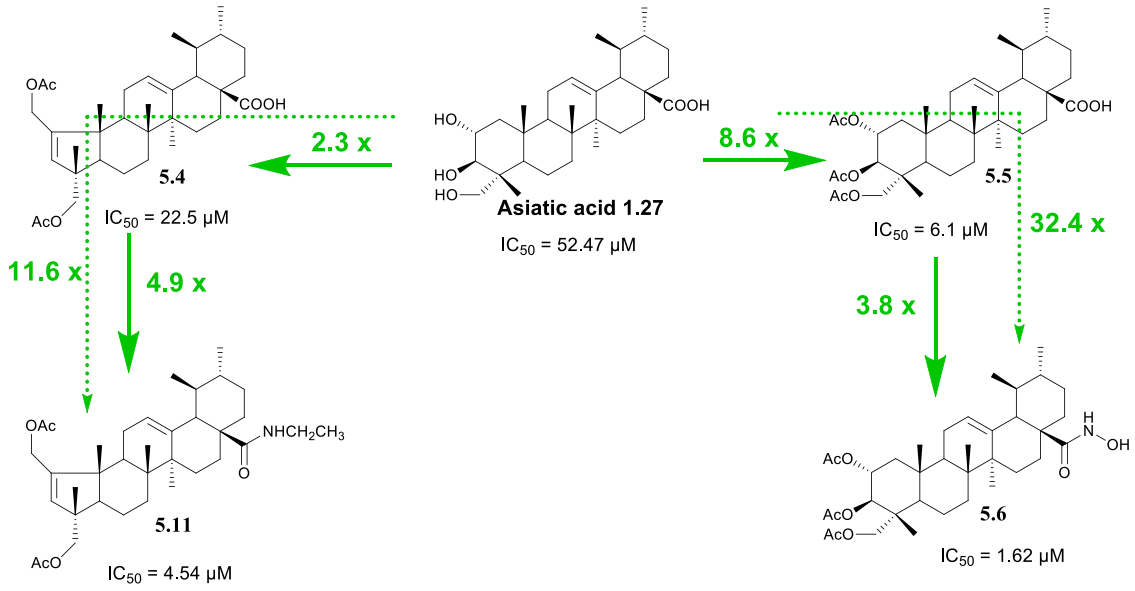

Figure 5.15 Schematic representation of the SAR for the antiproliferative activity of the various semisynthetic derivatives of asiatic acid **1.27** against the HeLa cell line. The SAR was established based on IC_{50} values. The esterification of C2, C3, and C23 hydroxyl groups improved antiproliferative activity: compound **5.5** was 8.6-fold more potent than asiatic acid **1.27**. The introduction of the hydroxamic moiety at C28 led to an increase in activity: compound **5.6** was 32.4- and 3.8-fold more active than asiatic acid **1.27** and compound **5.5**, respectively. The conversion of the hexameric A-ring of asiatic acid **1.27** into the pentameric A-ring of compound **5.4** led to an increase in antiproliferative activity: compound **5.4** was 2.3-fold more active than asiatic acid **1.27** The introduction of amide moieties at C28 of compound **5.4** resulted in an increase in activity: compound **5.11** was 4.9-fold more active than the precursor compound **5.4** and 11.6-fold more active than asiatic acid **1.27**.

As compounds **5.6** and **5.7** were the most active compounds, they were selected, and their antiproliferative activity was further tested in breast (MCF-7), leukemia (Jurkat), and

prostate (PC-3) cancer cell lines. As depicted in Table 5.2, both compounds exhibited a much higher antiproliferative activity against the tested cancer cell lines than did asiatic acid **1.27**.

Table 5.2 Cytotoxic activities, expressed as IC_{50}, of asiatic acid **1.27** and compounds **5.6** and **5.7** against several cancer cell lines (MCF-7, Jurkat, PC-3) and the nontumor human fibrobast cell line BJ.[a]

Compound	Cell line / IC_{50}[b](μM ± SD)			
	MCF-7	**Jurkat**	**PC-3**	**BJ**
Asiatic acid **1.27**	68.5 ± 2.5	37.17 ± 3.75	67.25 ± 0.35	88.7 ± 0.58
5.6	9.93 ± 1.01	2.47 ± 0.12	3.73 ± 0.46	59 ± 0.27
5.7	9.17 ± 0.58	2.43 ± 0.21	3.8 ± 0.8	N.D.
Cisplatin	19 ± 4.5	1.94 [265 c]	4.6 [266 c]	10.10 ± 2.00

[a] The cell lines were treated with increasing concentrations of each compound for 72 h. Viable cells were determined by MTT assay in MCF-7, PC-3 and BJ cell lines and by XTT assay in Jurkat cell line. IC_{50} values are expressed as the mean ± SD of three independent experiments. N.D.- not determined.

[b] IC_{50} is the concentration of compound that inhibits 50% of cell growth.

[c] IC_{50} values obtained from literature determined using the same experimental methodology and included here for comparison.

Moreover, the selectivity of compound **5.6** was assessed on the nontumor fibroblast cell line BJ. The analysis of the selectivity index (IC_{50} in the BJ cell line/ IC_{50} in the cancer cell line) (Table 5.3) values revealed that compound **5.6** was 6 to 36 times more active in cancer cell lines than on nontumor BJ cells. This index ranged from 1.3 to 2.4 for asiatic acid **1.27**. These results clearly suggest that **5.6** is more selective for cancer cells than asiatic acid **1.27**. As compound **5.6** displayed the strongest antiproliferative effect, it was chosen for further studies in HeLa cells aimed at exploring the possible mechanism underlying its anticancer activity.

Table 5.3 Selectivity index of asiatic acid **1.27** and compound **5.6** towards cancer cell lines.

Compound	Selectivity Index (IC_{50} BJ cell line/ IC_{50} cancer cell line)				
	HT-29	**HeLa**	**MCF-7**	**Jurkat**	**PC-3**
asiatic acid **1.27**	1.36	1.69	1.29	2.39	1.32
5.6	14.32	36.42	5.95	23.90	15.81

5.2.2.2 Effects of compound 5.6 on the cell cycle distribution

To gain a deeper insight into the mechanism underlying the growth inhibition afforded by compound **5.6**, its effects on cell-cycle distribution were evaluated. HeLa cells were treated with different concentrations of **5.6** (2, 4 and 6 µM) for 24 h, and the cell-cycle distribution was analyzed by flow cytometry after staining the cellular DNA with PI. The results revealed that treatment of HeLa cells with 4 and 6 µM **5.6** led to a dose-dependent accumulation of cells in the G0/G1 phase (Fig. 5.16). The percentage of cells in the G0/G1 phase rose from 49.45% in control cells to 65.97% in cells treated with 6 µM of compound **5.6**. Concomitantly, the percentage of cells in the S and G2/M phases was gradually reduced. An analysis of cell-cycle progression indicated that compound **5.6** induced cell-cycle arrest at the G0/G1 phase.

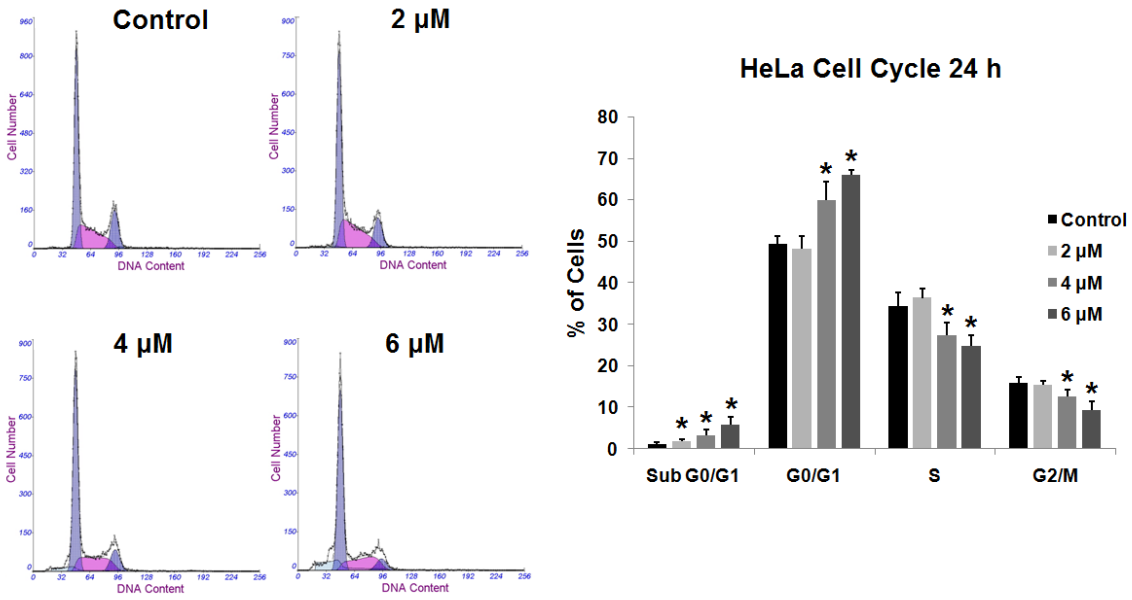

Figure 5.16 Cell-cycle distribution of HeLa cells untreated (control) or treated with the indicated concentrations of compound **5.6** during 24 h. Representative histograms obtained in the cell-cell cycle analysis and graph bar summarizing the variation in the percentage of cells in each phase of cell cycle. Results are presented as the mean ± SD of three independent experiments. Differences between treated and control groups were considered statistically significant at $p < 0.05$ (*).

5.2.2.3 Apoptosis-inducing effect of compound 5.6 evaluated by annexin V-FITC/PI flow cytometry assay

It was also investigated if the anticancer activity of compound **5.6** was related to the induction of apoptosis. In the early stages of apoptosis, the cell membrane loses it asymmetry and PS translocates from the inner to the outer side of the membrane. The externalized PS can be detected using Annexin V-FITC, a fluorescent active dye that selectively binds to PS.[299] Therefore, to explore whether compound **5.6** has the ability to induce apoptosis, HeLa cells were treated with different concentrations of compound **5.6** (2, 4, and 6 µM) for 24 h and analyzed by FACS after double staining with Annexin V-FITC/PI. The combined results of three independent experiments are depicted in Fig. 5.17. HeLa cells treated with **5.6** at 2 µM for 24 h showed an increase in the percentage of Annexin-V-positive cells, from 4.94% in control cells to 10.53% in treated cells (5.70% of early apoptotic cells and 4.83% of late apoptotic cells). Increasing the concentration of the drug to 4 and 6 µM, the percentage of

Annexin-V-positive cells rose to 19.55% and 29.18%, respectively. These results suggest that compound **5.6** induces apoptosis in HeLa cells in a concentration-dependent manner.

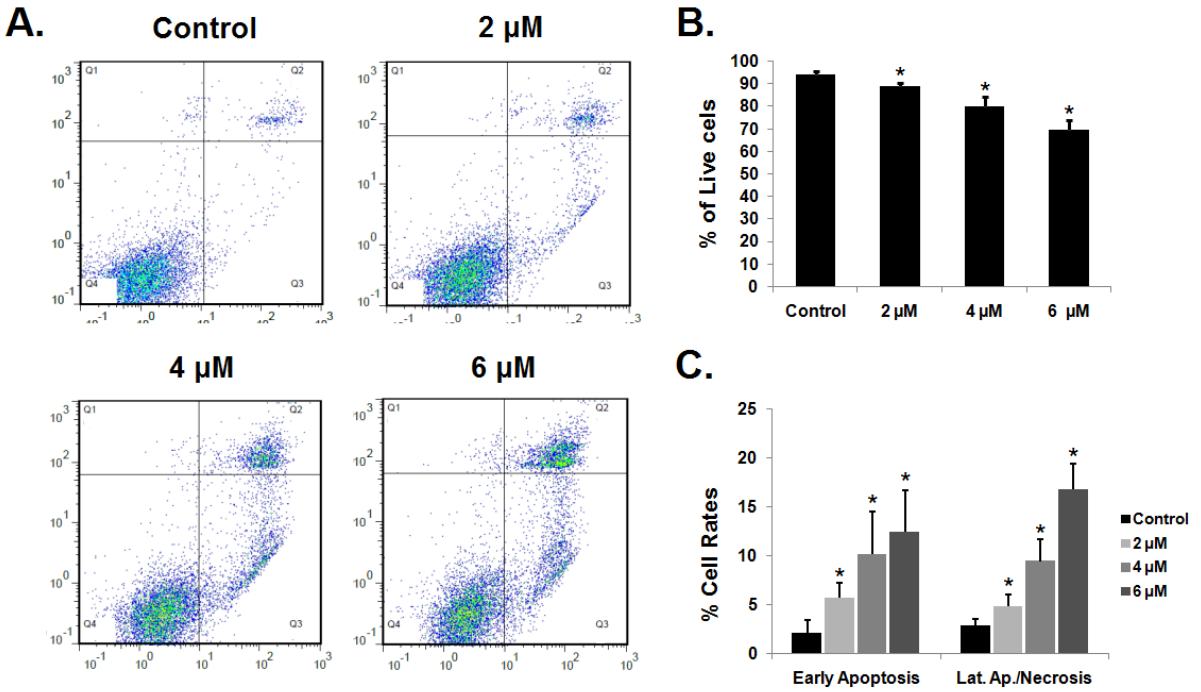

Figure 5.17 Annexin V-FITC/PI assay of HeLa cells untreated (control) or treated with the indicated concentrations of compound **5.6** for 24 h. **A.** Representative flow cytometry histograms that depict the variation in the percentage of cells that are alive (lower-left quadrant), in early apoptosis (lower-right quadrant) and in late apoptosis/necrosis (upper-left and upper-right quadrants). **B.** Graph bar that summarizes the variation in the percentage of live cells. **C.** Graph bar that summarizes the variation in the percentage of cells that are in early apoptosis and in late apoptosis/necrosis. Results are presented as the mean ± SD of three independent experiments. Differences between treated and control groups were considered statistically significant at $p < 0.05$ (*).

5.2.2.4 Apoptosis-inducing effect of compound 5.6 evaluated by morphological analysis after Hoechst 33258 staining

Taking into consideration that cells in apoptosis acquire a series of typical morphological features, the morphological changes in HeLa cells after treatment with **5.6** were accessed using the Hoechst 33258 staining technique to observe in greater detail the chromatin configuration. Hoechst 33258 is a membrane-permeable blue fluorescent dye that intercalates within cellular DNA. HeLa cells treated with compound **5.6** for 24 h were stained with Hoechst 33258 and analyzed by fluorescence microscopy. Non treated cells were used as control.

As depicted in Figure 5.18, control cells were uniformly stained and presented a normal round morphology; without obvious morphological changes. Conversely, typical apoptotic features, such as chromatin condensation and formation of apoptotic bodies, were observed in cells treated with 4 and 6 µM compound **5.6**. Moreover, an evident reduction in the number of cells with increasing concentrations of the drug was also observed. These results are in agreement with the proapoptotic effect of compound **5.6** in HeLa cells.

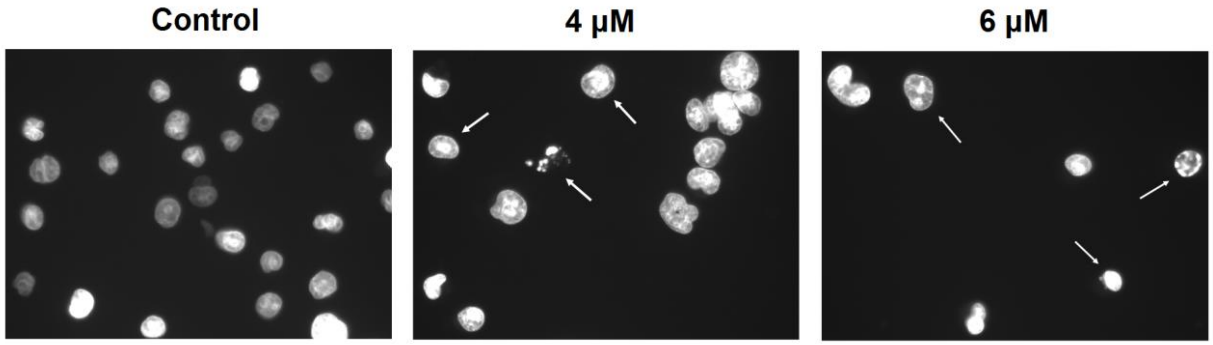

Figure 5.18 Representative fluorescence microscopic images of HeLa cells untreated or treated with the indicated concentrations of compound **5.6** during 24 h. Hela cells were stained with Hoechst 33258 before the fluorescence microscopic observation. White arrows represent apoptotic cells.

5.2.2.5 Effect of compound 5.6 on caspases

One of the most important mechanisms involved in apoptotic cell death is the activation of caspases. To explore if caspase activation was involved in the apoptotic cell death induced by compound **5.6**, was used the general caspase inhibitor z-VAD-fmk. HeLa cells pretreated or not for 45 min with 50 μM z-VAD-fmk were treated for 24 h with compound **5.6** at 6 μM. The effects of z-VAD-fmk on compound **5.6**-induced apoptosis were evaluated by flow cytometry after staining with Annexin V-FITC/PI. Pretreatment with z-VAD-fmk did not affect the number of annexin-V-positive cells in control cells (Fig. 5.19). However, the percentage of apoptotic cells among HeLa cells treated with compound **5.6** was significantly reduced when cells were pretreated with the caspase inhibitor (29.18% of total apoptotic cells in non pretreated cells vs 6.31% of apoptotic cells in cells pretreated with the caspase inhibitor), as shown in Figure 5.19. These results suggest that compound **5.6** induces apoptosis via a caspase-dependent mechanism.

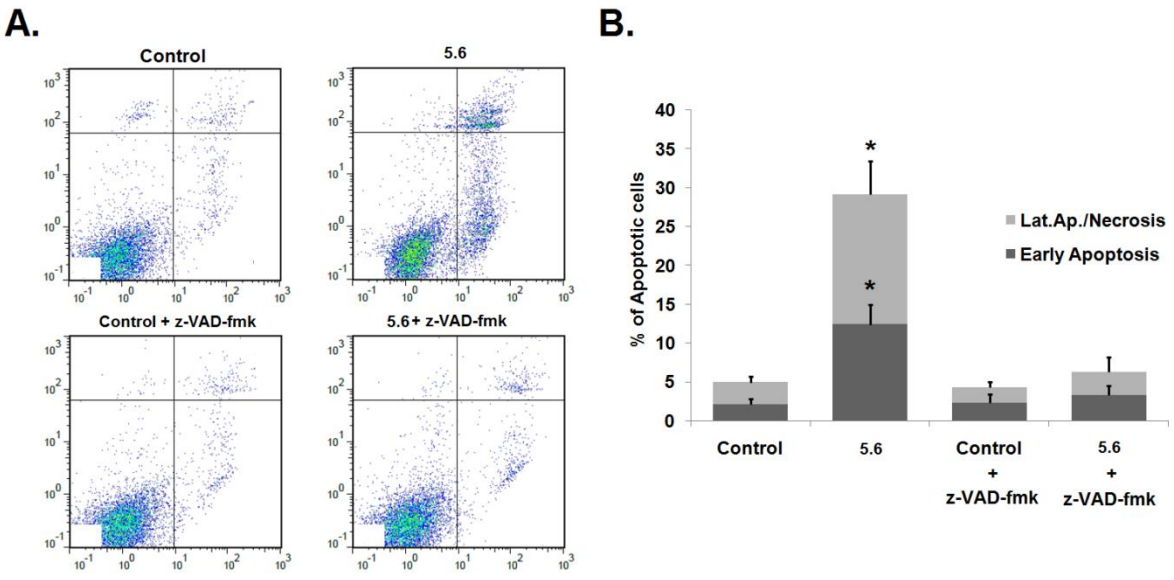

Figure 5.19 Annexin V-FITC/PI assay of HeLa cells untreated (control) or treated with compound **5.6** at 6 μM during 24 h, pretreated or not for 45 min with z-VAD-fmk at 50 μM. **A.** Representative flow cytometry histograms that depict the variation in the percentage of cells that are alive (lower-left quadrant), in early apoptosis (lower-right quadrant) and in late apoptosis/necrosis (upper-left and upper-right quadrants). **B.** Graph bar that summarizes the variation in the percentage of cells that are in early apoptosis (dark gray bars) and in late apoptosis/necrosis (light gray bars). Results are presented as the mean ± SD of three independent experiments. Differences between treated and control groups were considered statistically significant at $p < 0.05$ (*).

5.2.2.6 Evaluation of synergism between cisplatin and compound 5.6

Drug side effects and the development of resistance are limitations to the use of cisplatin [324,325], which is one of the most powerful chemotherapeutic agents that are in current clinical use for the treatment of several types of cancer.[324] Drug-combination therapies have been widely employed to achieve a synergistic therapeutic effect that allows the minimization of toxicity and resistance effects.[326] Keeping that in mind, we hypothesized that the combined use of the derivative **5.6** and cisplatin exerts a synergistic inhibitory effect on the proliferation of HeLa cells. The proliferation assays revealed that compound **5.6** alone exhibited an IC_{50} of 1.62 μM in HeLa cells, which is about 1.5 times lower than the IC_{50} of cisplatin in the same cell line (2.28 μM). To confirm our hypothesis, HeLa cells were treated simultaneously with cisplatin and compound **5.6** at different concentration combinations (maintaining the ratio of 2:1 between the concentrations of cisplatin and compound **5.6**, respectively) for 72 h, and the combination index (CI) values were calculated based on the Chou–Talalay method using the CompuSyn software.[327] As shown in Table 5.4, the CI values obtained were lower than 1 for all the combinations tested. These data suggest the existence of a synergistic effect between cisplatin and compound **5.6** in the inhibition of HeLa cells viability.

Table 5.4 Combination Index (CI) for combinations of cisplatin and compound **5.6** at a constant ratio of 2:1, in HeLa cell line. CI values were calculated using the Chou-Talalay method and the CompuSyn software. CI values <1 indicate the existence of synergism.

Cispatin (μM)	5.6 (μM)	1 - Viability	CI
0.42	0.21	0.30	0.57
1.02	0.51	0.46	0.84
1.80	0.90	0.71	0.69
3.00	1.50	0.77	0.91
4.20	2.10	0.88	0.73
6.00	3.00	0.89	0.92
10.20	5.10	0.97	0.64
18.00	9.00	0.99	0.46

HeLa cells were treated with compound **5.6** and cisplatin simultaneously, for 72 h.

5.3 Conclusions

A panel of new amide and hydroxamic acid derivatives of asiatic acid **1.27** modified in the A ring were successfully developed and synthesized.

The new derivatives showed improved antiproliferative activities against several cancer cell lines compared with asiatic acid **1.27**.

Compound **5.6**, bearing a hydroxamic acid at C28, displayed the best antiproliferative activity among all derivatives tested and was more selective toward cancer cell lines than asiatic acid **1.27**.

Further studies revealed that compound **5.6** led to cell-cycle arrest at the G0/G1 phase and induced apoptosis apparently mediated by caspases in the HeLa cell line. Moreover, a synergistic inhibitory effect on the proliferation of HeLa cells between compound **5.6** and cisplatin was observed.

5.4 Experimental section

5.4.1 Chemistry

5.4.1.1 Reagents and solvents

Asiatic acid, sodium periodate ($NaIO_4$), sodium sulfate (Na_2SO_4), piperidine, acetic acid, magnesium sulfate ($MgSO_4$), sodium borohydride ($NaBH_4$), acetic anhydride, 4-(dimethyamino)pyridine (DMAP), hydrochloric acid 37%, sodium bicarbonate ($NaHCO_3$), sodium sulfite (Na_2SO_3), 1,1′-carbonyldiimidazole (CDI), hydroxylamine hydrochloride, N-methylhydroxylamine hydrochloride, potassium bisulfate ($KHSO_4$), thionyl chloride ($SOCl_2$), triethylamine, methylamine solution 33% (w/v) in ethanol, ethylamine, propylamine, 4-methylbenzylamine, 4-fluorobenzylamine, glycine methyl ester hydrochloride and L-alanine methyl ester hydrochloride were purchased from Sigma–Aldridch Co. The solvents (analytical grade) [methanol, ethyl acetate, benzene, acetone, tetrahydrofuran (THF), petroleum ether and dichloromethane] were bought from Merck Co. The solvents used in reactions were purified and dried, if it was necessary, according to usual procedures

described in the literature.[274] The solvents used in the workup procedures were purchased from VWR Portugal.

5.4.1.2 Chromatographic techniques

Thin layer chromatography (TLC) was performed using Kieselgel 60HF254/Kieselgel 60G.

The purification of the synthesized compounds was performed by FCC, using Kieselgel 60 (230-400 mesh, Merck) and an appropriate eluent.

5.4.1.3 Analytical techniques and equipment

Melting points were determined on a BUCHI Melting point B-540 apparatus and were uncorrected.

IR spectra were obtained in a Fourier transform spectrometer. The IR measurements were performed using the ATR and KBr pellets methods. To prepare the KBr pellets, about 2 mg of the solid compound was diluted with 198 mg of KBr. The mixture was ground to a fine powder and pressed at around 12000 psi for 5 min, to obtain a thin and transparent pellet.

NMR spectra were recorded using a Brucker Digital NMR–Avance 400 spectrometer, with $CDCl_3$ or DMSO-d6 as internal standards. The chemical shifts (δ) are reported in parts per million (ppm), and coupling constants (J) are reported in hertz (Hz).

Mass spectra were recorded on a Quadrupole/Ion Trap Mass Spectrometer (QIT-MS) (LCQ Advantage MAX, THERMO FINNINGAN).

HRMS was performed on a Fourier Transform Ion Cyclotron Resonance (FT-ICR) mass spectrometer (Bruker Apex Ultra with a 7 Tesla actively shielded magnet).

The elemental analysis was performed on an Analyzer Elemental Carlo Erba 1108 apparatus by chromatographic combustion.

5.4.1.4 Synthesis of asiatic acid derivatives

2*α*,23-Lactol-3-formyl-urs-12-en-28-oic acid (5.1)

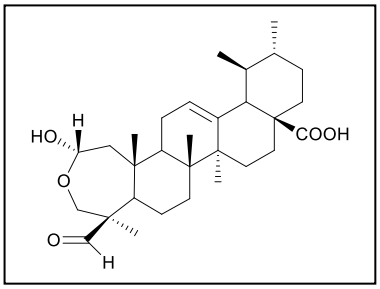

To a stirred solution of asiatic acid **1.27** (200 mg, 0.41 mmol) in methanol/water [5 mL/0.25 mL (20:1)], $NaIO_4$ (131.30 mg, 0.61 mmol) was added. The reaction mixture was stirred at room temperature. After 2 h the reaction mixture was evaporated under reduced pressure to remove the organic phase. The crude obtained was dispersed with water (40 mL) and extracted with ethyl acetate (3 × 40 mL). The resulting organic phase was washed with water (4 × 40 mL) and brine (40 mL), dried over Na_2SO_4, filtered, and concentrated under vacuum to afford **5.1** as a white powder (quantitative). Mp: 198.5–201.4 °C. ν_{max}/cm^{-1} (KBr): 3421.1, 2948.6, 2927.4, 2871.5, 2732.6, 2630.4, 1716.3, 1695.1, 1457.0, 1378.9, 1037.5. ^{1}H NMR (400 MHz, $CDCl_3$): δ = 9.94 (s, 1H, CHO), 5.29 (t, *J* = 3.3 Hz, 1H, H12), 5.14–5.11 (m, 1H, H2), 3.94 (d, *J* = 13.4 Hz, 1H), 3.75 (d, *J* = 13.2 Hz, 1H), 1.08 (s, 3H), 1.06 (s, 3H), 0.99 (s, 3H), 0.95 (d, *J* = 6.0 Hz, 3H), 0.86 (s, 3H), 0.85 (d, *J* = 5.4 Hz, 3H) ppm. ^{13}C NMR (100MHz, $CDCl_3$): δ = 206.1 (CHO), 182.9 (C28), 138.1 (C13), 126.0 (C12), 93.7, 65.4, 61.2, 53.4, 62.7, 48.1, 45.2, 43.7, 42.6, 40.1, 40.0, 38.9, 38.8, 38.6, 33.6, 30.6, 27.8, 24.6, 24.1, 23.2, 21.1, 20.6, 20.4, 17.9, 16.9, 14.6 ppm. DI-ESI-MS *m/z* $[M+H]^+$: 487.15. Anal. Calcd. for $C_{30}H_{46}O_5.H_2O$: C, 71.39; H, 9.59. Found: C, 71.49, H, 9.85%.

2-Formyl-23-hydroxy-A(1)-norursa-2,12-dien-28-oic acid (5.2)

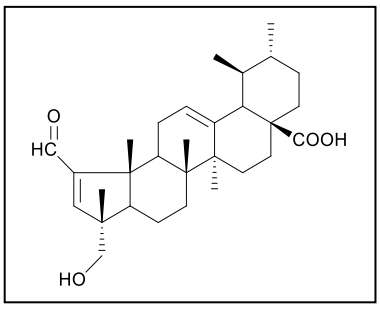

To a stirred solution of compound **5.1** (500 mg, 1.03 mmol) in dry benzene (50 mL), piperidine (3 mL) and acetic acid (3 mL) were added. The resultant solution was heated at 60 °C. After 1 hour, anhydrous magnesium sulfate (500 mg) was added and the reaction mixture was heated at 60 °C under nitrogen atmosphere for 4 h 20 min. The reaction mixture was evaporated under reduced pressure to remove the organic phase. The crude obtained was dispersed with water (50 mL) and extracted with ethyl acetate (3 × 50 mL). The resulting organic phase was washed with water (4 × 50 mL)

and brine (50 mL), dried over Na_2SO_4, filtered, and concentrated under vacuum to afford a yellow powder. The crude solid was purified by flash column chromatography (petroleum ether/ethyl acetate 3:1 → 1:1), to afford **5.2** as a white solid (353.77 mg, 73%). Mp: 183.5–186.1 °C. ν_{max}/cm^{-1} (KBr): 3428.8, 2946.7, 2925.5, 2869.6, 2726.9, 2632.4, 1689.3, 1581.3, 1454.1, 1380.8, 1041.4. ^{1}H NMR (400 MHz, $CDCl_3$): δ = 9.72 (s, 1H, CHO), 6.66 (s, 1H, H3), 5.28 (t, *J* = 3.1 Hz, 1H, H12), 3.62 (d, *J* = 10.7 Hz, 1H, H23), 3.45 (d, *J* = 10.7 Hz, 1H, H23), 1.25 (s, 3H), 1.10 (s, 3H), 1.01 (s, 3H), 0.93 (d, *J* = 6.2 Hz, 3H), 0.88 (s, 3H), 0.84 (d, *J* = 6.3 Hz, 3H) ppm. ^{13}C NMR (100MHz, $CDCl_3$): δ =190.9 (CHO), 183.3 (C28), 159.3 (C3), 158.9 (C2), 137.5 (C13), 126.6 (C12), 69.4, 56.3, 52.6, 50.9, 49.4, 47.9, 44.1, 42.4, 41.4, 38.8 (2C), 36.6, 33.5, 30.6, 28.2, 27.1, 24.0 (2C), 21.2, 19.0, 18.7, 17.4, 17.0, 15.9 ppm. DI-ESI-MS *m/z* $[M+H]^+$: 469.03. Anal. Calcd. for $C_{30}H_{44}O_4.H_2O$: C, 74.04; H, 9.53. Found: C, 73.68; H, 9.75%.

2-Hydroxymethyl-23-hydroxy-A(1)-norursa-2,12-dien-28-oic acid (5.3)

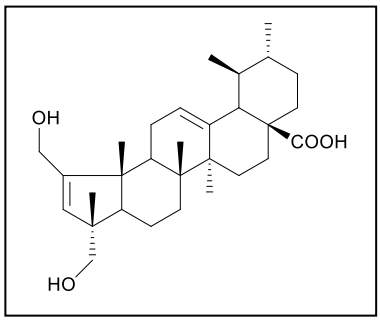

To a stirred solution of **5.2** (500 mg, 1.07 mmol) in anhydrous methanol (15 mL), sodium borohydride (101.20 mg, 2.67 mmol) was added. The resultant solution was stirred at room temperature. After 2 h, some drops of acetone were added to consume the excess of sodium borohydride and the reaction mixture was evaporated under reduced pressure to remove the organic phase.[139] The crude obtained was dispersed with water (50 mL) and extracted with ethyl acetate (3 × 50 mL). The resulting organic phase was washed with water (50 mL) and brine (50 mL), dried over Na_2SO_4, filtered, and concentrated under vacuum to afford **5.3** as a white solid (465 mg, 92%). ν_{max}/cm^{-1} (ATR): 3369.0, 2925.5, 2871.5, 1695.0, 1455.5, 1380.0. ^{1}H NMR (400 MHz, DMSO-d6): δ = 5.34 (s, 1H), 5.12 (s, 1H), 4.58 (t, *J* = 4.8 Hz, 1H), 4.46 (t, *J* = 5.3 Hz, 1H), 4.04–3.99 (m, 1H), 3.95–3.90 (m, 1H), 3.24–3.20 (m, 1H), 3.13–3.09 (m, 1H) 1.09 (s, 3H), 1.07 (s, 3H), 0.92 (s, 3H), 0.87 (s, 3H), 0.82 (d, *J* = 6.3 Hz, 3H), 0.80 (s, 3H) ppm. ^{13}C NMR (101 MHz, DMSO-d6): δ = 178.3 (C28), 156.2 (C2), 138.6 (C13), 129.8 (C3), 124.6 (C12), 70.1, 59.3, 57.0, 52.5, 49.8, 47.2, 46.8, 42.7, 42.0, 40.6, 38.5, 38.1, 36.2, 33.4, 30.1, 27.8, 25.8, 23.7, 23.5, 21.0, 19.1, 18.5, 17.6, 17.0, 16.7 ppm. DI-ESI-MS *m/z* $[M+H]^+$: 471.02.

2-Acetoxymethyl-23-acetoxy-A(1)-norursa-2,12-dien-28-oic acid (5.4)

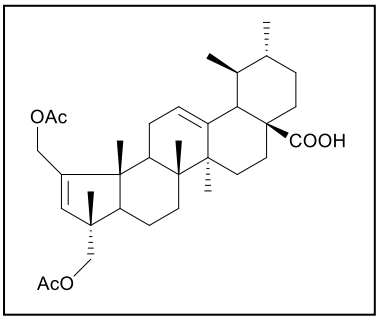

To a stirred solution of **5.3** (500 mg, 1.06 mmol) in dry THF (15 mL), acetic anhydride (250.50 µl; 2.66 mmol) and a catalytic amount of DMAP (50 mg) were added. The mixture was stirred at room temperature, in anhydrous conditions. After 2 hours, the reaction mixture was evaporated under reduced pressure to remove the organic phase. The crude obtained was dispersed with water (50 mL) and extracted with ethyl acetate (3 × 50 mL). The resulting organic phase was washed with 5% aqueous HCl (2 × 50 mL), 10% aqueous $NaHCO_3$ (2 × 50 mL), 10% aqueous Na_2SO_3 (50 mL), water (50 mL) and brine (50 mL), dried over Na_2SO_4, filtered, and concentrated under vacuum to afford **5.4** as a white powder (574 mg, 97 %). Mp: 93.5–95.6 °C. ν_{max}/cm^{-1} (ATR): 2926.0, 2870.0, 1739.0, 1694.5, 1455.5, 1381.0, 1234.5, 1031.5. ^1H NMR (400 MHz, $CDCl_3$): δ = 5.44 (s, 1H, H3), 5.22 (t, *J* = 2.9 Hz, 1H, H12), 4.70 (d, *J* = 14.3 Hz, 1H), 4.57 (d, *J* = 14.1 Hz, 1H), 3.93 (d, *J* = 10.7 Hz, 1H, H23), 3.84 (d, *J* = 10.7 Hz, 1H, H23), 2.08 (s, 3H, OCOC$\underline{H_3}$), 2.06 (s, 3H, OCOC$\underline{H_3}$), 1.17 (s, 3H), 1.10 (s, 3H), 0.99 (s, 3H), 0.94 (d, *J* = 5.6 Hz), 0.85 (d, *J* = 6.6 Hz), 0.83 (s, 3H) ppm. ^{13}C NMR (100MHz, $CDCl_3$): δ = 183.6 (C28), 171.3 (OCO), 170.8 (OCO), 151.3 (C2), 138.7 (C13), 131.8 (C3), 125.3 (C12), 72.3, 62.6, 58.0, 52.6, 50.7, 47.9, 46.3, 43.1, 42.3, 41.1, 38.8, 38.8, 36.6, 33.7, 30.5, 28.2, 26.2, 24.0, 23.8, 21.2, 21.0 (2C), 19.1, 18.6, 17.8, 17.0, 16.6 ppm. DI-ESI-MS *m/z* $[M+H]^+$: 555.04.

2α,3β,23-Triacetoxyurs-12-en-28-oic acid (5.5)

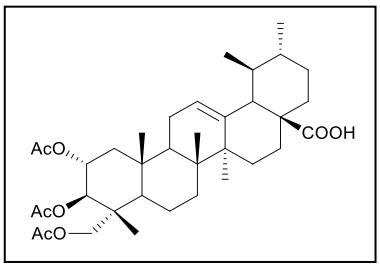

To a stirred solution of asiatic acid **1.27** (1000 mg, 2.05 mmol) in dry THF (30 mL), acetic anhydride (1.15 mL, 12.28 mmol) and a catalytic amount of DMAP (100 mg) were added. The mixture was stirred at room temperature in anhydrous conditions. After 4 h, the reaction mixture was evaporated under reduced pressure to remove the organic phase. The crude obtained was dispersed with water (150 mL) and aqueous phase was extracted with ethyl acetate (3 × 150 mL). The resulting organic phase was washed with 5% aqueous HCl (2 × 100 mL), 10% aqueous $NaHCO_3$ (2 × 100 mL), 10% aqueous Na_2SO_3 (100 mL), water (100 mL) and brine (100 mL), dried over Na_2SO_4,

filtered, and concentrated under vacuum to afford compound **5.5** as a white powder (quantitative). Mp: 150–152 °C. ν_{max}/cm^{-1} (KBr): 3463.5, 2948.6, 2871.5, 1816.6, 1747.2, 1456.0, 1369.2, 1236.2, 1045.2. ^{1}H NMR (400 MHz, $CDCl_3$): δ = 5.23 (t, *J* = 3.2 Hz, 1H, H12), 5.19–5.13 (m, 1H, H2), 5.08 (d, *J* = 10.3 Hz, 1H, H3), 3.85 (d, *J* = 11.9 Hz, 1H, H23), 3.58 (d, *J* = 12.0 Hz, 1H, H23), 2.08 (s, 3H, CH_3CO), 2.02 (s, 3H, CH_3CO), 1.97 (s, 3H, CH_3CO), 1.10 (s, 3H), 1.07 (s, 3H), 0.94 (d, *J* = 5.3 Hz, 3H), 0.87 (s, 3H), 0.85 (d, *J* = 5.4 Hz, 3H), 0.76 (s, 3H) ppm. ^{13}C NMR (100MHz, $CDCl_3$): δ = 183.1 (C28), 170.9 (OCO), 170.5 (OCO), 170.4 (OCO), 138.0, 125.3, 74.8, 69.9, 65.3, 52.5, 47.9, 47.6, 47.8, 43.7, 41.9, 41.9, 39.5, 39.0, 38.8, 37.8, 36.6, 32.4, 30.5, 27.9, 24.0, 23.4, 23.3, 21.1, 21.1, 20.9, 20.8, 17.9, 17.0, 16.9, 16.9, 13.9 ppm. DI-ESI-MS *m/z* $[M+H]^+$: 615.3. ESI-HRMS *m/z* calcd for $C_{36}H_{54}O_8$ $[M + Na]^+$: 637.3716, found: 637.3711.

N-Hydroxy-(2α,3β,23-triacetoxyurs-12-en-28-oyl)amine (5.6)

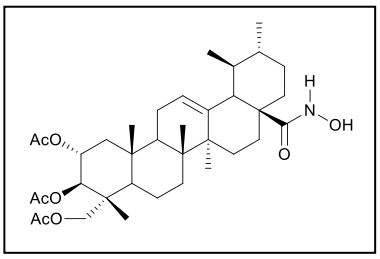

To a stirred solution of **5.5** (153 mg, 0.25 mmol) in anhydrous THF (6.5 mL), CDI (201.35 mg, 1.24 mmol) was added. The mixture was stirred at reflux temperature and under nitrogen atmosphere. After 28 h, the heating was stopped and powdered hydroxylamine hydrochloride (103.50 mg, 1.49 mmol) was added. The resulting mixture was stirred at room temperature. After 23 h 35 min the reaction mixture was evaporated under reduced pressure to remove the organic phase. The crude obtained was diluted with 5% aqueous $KHSO_4$ (50 mL) and extracted with ethyl acetate (3 × 50 mL). The combined organic phase was washed with brine (50 mL), dried over Na_2SO_4, filtered and concentrated under vacuum to give **5.6** as a white powder (140.4 mg, 90%); Mp: 152.1–154.8 °C. ν_{max}/cm^{-1} (ATR): 3302.2, 2947.0, 2921.6, 2870.0, 1739.0, 1455.5, 1368.5, 1228.5, 1042.5, 1028.5. ^{1}H NMR (400 MHz, $CDCl_3$): δ = 6.25 (s, 1H, N<u>H</u>-OH), 5.28 (t, *J* = 3.0 Hz, 1H, H12), 5.19–5.13 (m, 1H, H2), 5.08 (d, *J* = 10.3 Hz, 1H, H3), 3.84 (d, *J* = 11.9 Hz, 1H, H23), 3.57 (d, *J* = 11.8 Hz, 1H, H23), 2.08 (s, 3H, $OCOCH_3$), 2.02 (s, 3H, $OCOCH_3$), 1.97 (s, 3H, $OCOCH_3$), 1.10 (s, 3H), 1.07 (s, 3H), 0.94 (d, *J* = 5.8 Hz, 3H), 0.88 (s, 3H), 0.85 (d, *J* = 6.2 Hz, 3H), 0.75 (s, 3H) ppm. ^{13}C NMR (100MHz, $CDCl_3$): δ = 178.4 (C28), 170.8 (OCO), 170.5 (OCO), 170.4 (OCO), 137.9 (C13), 125.5 (C12), 74.8, 69.9, 65.3, 52.6, 48.0, 47.6, 47.5, 43.7, 41.9, 41.9,

39.5, 38.9, 38.7, 37.8, 36.6, 32.4, 30.5, 27.9, 24.0, 23.5, 23.3, 21.1 (2C), 20.9, 20.8, 17.9, 17.0, 16.9 (2C), 13.9 ppm. DI-ESI-MS *m/z*: 630.12 ($[M+H]^+$), 652.46 ($[M+Na]^+$). Anal. Calcd. for $C_{36}H_{55}NO_8$: C, 68.65; H, 8.80; N, 2.22. Found: C, 69.01; H, 9.20; N, 1.84.

N-Hydroxy-N-methyl-(2*α*,3β,23-triacetoxyurs-12-en-28-oyl)amine (5.7)

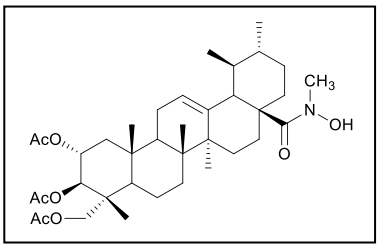

To stirred a solution of **5.5** (300 mg, 0.49 mmol) in anhydrous THF (12.9 mL), CDI (276.90 mg, 1.71 mmol) was added. The mixture was stirred under reflux and nitrogen atmosphere. After 31 h the heating was stopped and powdered *N*-methylhydroxylamine hydrochloride (203.80 mg, 2.44 mmol) was added. The resulting mixture was stirred at room temperature. After 21 h the reaction mixture was evaporated under reduced pressure to remove the organic phase. The crude obtained was diluted with 5% aq. $KHSO_4$ (50 mL) and extracted with ethyl acetate (3 × 50 mL). The combined organic phase was washed with brine (50 mL), dried over Na_2SO_4 filtered and concentrated under vacuum to afford **5.7** as a white powder (308.6 mg, 98%). Mp.: 119.5–121.9 °C. ν_{max}/cm^{-1} (ATR): 3244.0, 2947.0, 2926.5, 2871.5, 1740.0, 1455.5, 1368.5, 1228.0, 1043.0, 1028.5. ^{1}H NMR (400 MHz, $CDCl_3$): δ = 5.29 (t, *J* = 3.0 Hz, 1H, H12), 5.19–5.12 (m, 1H, H2), 5.08 (d, *J* = 10.3 Hz, 1H, H3), 3.85 (d, *J* = 11.9 Hz, 1H, H23), 3.57 (d, *J* = 11.9 Hz, 1H, H23), 2.76 (s, 3H, N-C$\underline{H}_3$), 2.08 (s, 3H, $OCOCH_3$), 2.02 (s, 3H, $OCOCH_3$), 1.97 (s, 3H, $OCOCH_3$), 1.09 (s, 3H), 1.08 (s, 3H), 0.94 (d, *J* = 6.1 Hz, 3H), 0.88 (s, 3H), 0.85 (d, *J* = 6.3 Hz, 3H), 0.78 (s, 3H) ppm. ^{13}C NMR (100MHz, $CDCl_3$): δ = 177.6 (C28), 170.8 (OCO), 170.4 (OCO), 170.4 (OCO), 137.9 (C13), 125.4 (C12), 74.8, 69.9, 65.3, 52.6, 47.7, 47.6, 47.5, 43.8, 42.1, 41.9, 39.7, 39.6, 39.0, 38.7, 37.8, 36.7, 32.5, 30.5, 27.8, 23.9, 23.4, 23.3, 21.1, 21.1, 20.9, 20.8, 17.9, 17.2, 17.0, 16.9, 13.9 ppm. DI-ESI-MS *m/z*: 644.21 ($[M+H]^+$), 666.45 ($[M+Na]^+$). Anal. Calcd. for $C_{37}H_{57}NO_8$: C, 69.02; H, 8.92; N, 2.18. Found: C, 68.62; H, 9.30; N, 2.21.

N-Hydroxy-[2-acetoxymethyl-23-acetoxy-A(1)-norursa-2,12-dien-28-oyl]amine (5.8)

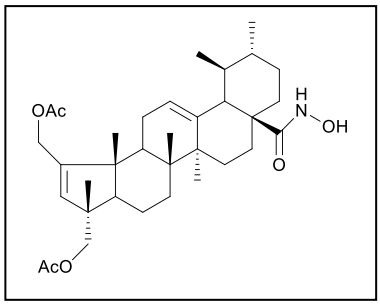

To a stirred solution of compound **5.4** (150 mg, 0.27 mmol) in anhydrous THF (6 mL), CDI (219.22 mg, 1.35 mmol) was added. The reaction mixture was stirred at reflux temperature and under nitrogen atmosphere. After 24 hours the heating was stopped and powdered hydroxylamine hydrochloride (112.75 mg, 1.62 mmol) was added. The resulting mixture was stirred at room temperature. After 48 h the reaction mixture was evaporated under reduced pressure to remove the organic phase. The crude obtained was diluted with 5% aqueous $KHSO_4$ (50 mL) and extracted with ethyl acetate (3 × 50 mL). The combined organic phase was washed with brine (50 mL), dried over Na_2SO_4, filtered and concentrated under vacuum to give a light yellow oil, which was purified by flash column chromatography (petroleum ether/ethyl acetate 4:1 → 2:1), to afford **5.8** as a white solid (46.6 mg, 30%). Mp: 86.1–88.8 °C. ν_{max}/cm^{-1} (ATR): 3250.5, 2926.0, 2.871.5, 1741.0, 1380.5, 1233.0, 1029.5. ^{1}H NMR (400 MHz, $CDCl_3$): δ = 6.27 (s, 1H, N<u>H</u>OH), 5.44 (s, 1H, H3), 5.26 (s, 1H), 4.70 (d, *J* = 14.2 Hz, 1H), 4.57 (d, *J* = 14.2 Hz, 1H), 3.93 (d, *J* = 10.5 Hz, 1H, H23), 3.84 (d, *J* = 10.5 Hz, 1H, H23), 2.08 (s, 3H, $OCOCH_3$), 2.06 (s, 3H, $OCOCH_3$), 1.17 (s, 3H), 1.11 (s, 3H), 1.00 (s, 3H), 0.95 (s, 3H), 0.86–0.81 (3, 6H) ppm. ^{13}C NMR (100 MHz, $CDCl_3$): δ = 178.4 (C28), 171.3 (OCO), 170.8 (OCO), 151.2 (C2), 138.6 (C13), 131.8 (C3), 125.5 (C12), 72.3, 62.6, 58.1, 52.7, 50.6,. 48.1, 46.3, 43.1, 42.3, 41.1, 38.7, 38.7, 36.6, 33.7, 30.5, 28.2, 26.1, 24.0, 23.8, 21.1, 21.0 (2C), 19.1, 18.5, 17.8, 17.0, 16.6 ppm. DI-ESI-MS *m/z* $[M+H]^+$: 570.09.

2-Acetoxymethyl-23-acetoxy-A(1)-norursa-2,12-dien-28-yl-1H-imidazole-1-carboxylate (5.9)

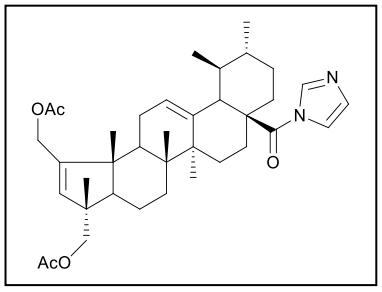

To a stirred solution of compound **5.4** (200 mg, 0.36 mmol) in anhydrous THF (8 mL) at 60 °C, CDI (263.0 mg, 1.63 mmol) was added. The reaction mixture was stirred overnight at reflux temperature and N_2 atmosphere. The reaction mixture was evaporated under reduced pressure to remove the organic phase. The crude obtained was dispersed with water (50 mL) and extracted with ethyl acetate (3 × 50

mL). The combined organic phase was washed with water (4 × 50 mL) and brine (50 mL), dried over Na_2SO_4, filtered, and concentrated under vacuum to afford a yellowish powder. The crude solid was purified by flash column chromatography (petroleum ether/ethyl acetate, 3:1 → 2:1), to afford **5.9** as a white solid (136.3 mg, 63%). Mp: 85.4–88.0 °C. ν_{max}/cm^{-1} (ATR): 3135.0, 2927.0, 2872.5, 1737.5, 1458.5, 1367.5, 1226.5, 1034.0. ^1H NMR (400 MHz, $CDCl_3$): δ = 8.23 (s, 1H, H-Im), 7.52 (s, 1H, H-Im), 7.03 (s, 1H, H-Im), 5.43 (s, 1H, H3), 5.19 (t, *J* = 3.0 Hz, 1H, H12), 4.67 (d, *J* = 14.2 Hz, 1H), 4.54 (d, *J* =14.2 Hz, 1H), 3.91 (d, *J* = 10.6 Hz, 1H, H23), 3.82 (d, *J* = 10.6 Hz, 1H, H23), 2.07 (s, 3H, $OCOCH_3$), 2.05 (s, 3H, $OCOCH_3$), 1.14 (s, 3H), 1.12 (s, 3H), 1.00–0.98 (m, 6H), 0.90 (d, *J* = 6.1 Hz, 3H), 0.74 (s, 3H) ppm. ^{13}C (100 MHz, $CDCl_3$): δ = 174.7 (C28), 171.2 (OCO), 170.7 (OCO), 151.1 (C2), 137.7, 137.1, 132.0 (C3), 129.7, 126.1 (C12), 117.4, 72.2, 62.5, 58.1, 54.2, 50.9, 50.4, 46.3, 43.1, 42.4, 41.0, 39.0, 38.7, 35.5, 33.5, 30.3, 27.9, 26.1, 25.0, 23.8, 21.0, 20.9 (2C), 19.1, 18.3, 17.7, 17.1, 16.5 ppm. DI-ESI-MS *m/z* $[M+H]^+$: 604.89. Anal. Calcd. for $C_{37}H_{52}N_2O_5.0.5H_2O$: C, 72.40; H, 8.70; N, 4.56. Found: C, 72.66; H, 8.77; N, 4.48.

N-[2-Acetoxymethyl-23-acetoxy-A(1)-norursa-2,12-dien-28-oyl]methylamine (5.10)

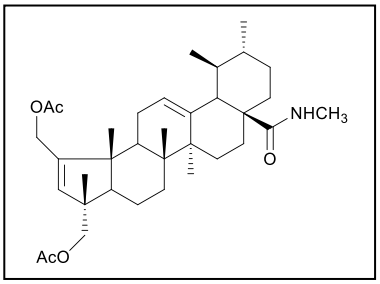

To a stirred solution of **5.4** (200 mg, 0.36 mmol), in dry benzene (8 mL), thionyl chloride (54.90 µl, 0.76 mmol) was slowly added. The resultant solution was heat-refluxed at 80 °C. After 3 h, the solvent was removed by evaporation under reduced pressure, and petroleum ether (aprox. 2 mL) was added to the residue and concentrated to dryness to give the acyl chloride intermediate. Without purification, the acyl chloride obtained was dissolved in dry dichloromethane (8 mL), basified to pH 8–9 with triethylamine, and a solution of methylamine (sol. 33% w/v in ethanol) (135.70 µl, 1.44 mmol) was added. The resultant mixture was stirred at room temperature. After 45 min, the solvent was removed by evaporation under reduced pressure. The crude obtained was dispersed with water (50 mL) acidified with 5% aqueous HCl (pH 3-4) and extracted with ethyl acetate (3 × 50 mL). The combined organic phase was washed with 10% aqueous $NaHCO_3$ (2 × 50 mL), water (50 mL) and brine (50 mL), dried over Na_2SO_4, filtered, and concentrated under vacuum to afford a light yellow solid. The crude solid was purified by flash column chromatography (petroleum

ether/ethyl acetate 4:1 → 2:1), to afford **5.10** as a white solid (187.2 mg, 91 %). Mp: 94.8–97.0 °C. ν_{max}/cm^{-1} (ATR): 3418.5, 2927.0, 2870.5, 1739.5, 1635.0, 1527.0, 1454.5, 1376.5, 1235.5, 1033.5. ^{1}H NMR (400 MHz, $CDCl_3$): δ = 5.91 (d, *J* = 4.4 Hz, 1H, N<u>H</u>CH_3), 5.45 (s, 1H, H3), 5.28 (t, *J* = 3.0 Hz, 1H, H12), 4.69 (d, *J* = 14.2 Hz, 1H), 4.57 (d, *J* = 14.2 Hz, 1H), 3.93 (d, *J* = 10.6 Hz, 1H, H23), 3.84 (d, *J* = 10.6 Hz, 1H, H23), 2.72 (d, *J* = 4.6 Hz, 3H, NHC<u>H</u>$_3$), 2.08 (s, 3H, $OCOCH_3$), 2.06 (s, 3H, $OCOCH_3$), 1.17 (s, 3H), 1.11 (s, 3H), 1.00 (s, 3H), 0.94 (s, 3H), 0.86 (d, *J* = 6.4 Hz, 3H), 0.82 (s, 3H) ppm. ^{13}C (100 MHz, $CDCl_3$): δ = 178.7 (C28), 171.2 (OCO), 170.8 (OCO), 150.8 (C2), 141.1 (C13), 132.1 (C3), 124.9 (C12), 72.3, 62.5, 58.0, 53.9, 50.5, 47.6, 46.3, 43.1, 42.7, 41.0, 39.4, 39.1, 36.8, 33.3, 30.8, 28.0, 26.2, 26.2, 24.9, 23.6, 21.2, 21.0, 20.9, 19.0, 18.2, 17.2, 17.3, 16.6 ppm. DI-ESI-MS *m/z*: 568.52 ([M+H]$^+$), 590.49 ([M+Na]$^+$).

N-[2-Acetoxymethyl-23-acetoxy-A(1)-norursa-2,12-dien-28-oyl]ethylamine (5.11)

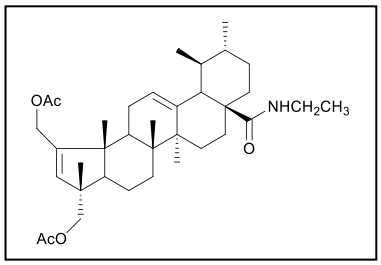

Accordingly to the method described for **5.10**, using compound **5.4 (**150 mg, 0.27 mmol), dry benzene (6 mL), thionyl chloride (41.20 µl, 0.57 mmol) and ethylamine (70.75 µl, 1.08 mmol). The crude solid was purified by flash column chromatography (petroleum ether/ethyl acetate 4:1 → 2:1), to afford **5.11** as a white solid (113 mg, 72 %). Mp: 83.5–86.0 °C. ν_{max}/cm^{-1} (ATR): 3404.5, 2929.5, 2871.5, 1739.0, 1635.5, 1522.5, 1450.5, 1360.0, 1234.0, 1028.0. ^{1}H NMR (400 MHz, $CDCl_3$): δ = 5.81 (t, *J* = 4.4 Hz, 1H, N<u>H</u>CH_2CH_3), 5.45 (s, 1H, H3), 5.27 (t, *J* = 3.0 Hz, 1H, H12), 4.69 (d, *J* = 14.3 Hz, 1H), 4.56 (d, *J* = 14.3 Hz, 1H), 3.93 (d, *J* = 10.6 Hz, 1H, H23), 3.83 (d, *J* = 10.6 Hz, 1H, H23), 3.34–3.24 (m, 1H, NHC<u>H</u>$_2$$CH_3$), 3.15–3.05 (m, 1H, NHC<u>H</u>$_2$$CH_3$), 2.08 (s, 3H, $OCOCH_3$), 2.05 (s, 3H, $OCOCH_3$), 1.17 (s, 3H), 1.11 (s, 3H), 1.08 (t, *J* = 7.4 Hz, 3H, $NHCH_2C$<u>H</u>$_3$), 0.99 (s, 3H), 0.94 (s, 3H), 0.86–0.85 (m, 6H) ppm. ^{13}C (100 MHz, $CDCl_3$): δ = 177.8 (C28), 171.2 (OCO), 170.7 (OCO), 150.9 (C2), 140.9 (C13), 132.1 (C3), 124.9 (C12), 72.3, 62.5, 58.0, 54.0, 50.5, 47.4, 46.3, 43.1, 42.2, 41.1, 39.4, 39.0, 37.0, 34.3, 33.5, 30.8, 28.0, 26.2, 24.7, 23.4, 21.2, 21.0, 20.9, 19.0, 18.5, 17.8, 17.3, 16.6, 14.5 ppm. DI-ESI-MS *m/z*: 582.50 ([M+H]$^+$), 604.51 ([M+Na]$^+$). Anal. Calcd. for $C_{36}H_{55}NO_5.0.25H_2O$: C, 73.74; H, 9.54; N, 2.39. Found: C, 73.65; H, 9.93; N, 2.43.

N-[2-acetoxymethyl-23-acetoxy-A(1)-norursa-2,12-dien-28-oyl]propylamine (5.12)

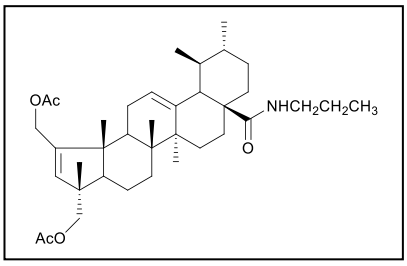

Accordingly to the method described for **5.10**, using compound **5.4** (200 mg, 0.36 mmol), dry benzene (8 mL), thionyl chloride (54.90 µl, 0.76 mmol), dichloromethane (8 mL) and propylamine (118.50 µl, 1.44 mmol). The crude solid was purified by flash column chromatography (petroleum ether/ethyl acetate 4:1 → 3:1), to afford **5.12** as a white solid (122 mg, 57%). Mp: 77.0–79.5 °C. ν_{max}/cm^{-1} (ATR): 3368.5, 2959.0, 2921.5, 2872.5, 1739.5, 1635.0, 1525.0, 1455.5, 1369.0, 1234.5, 1033.5. ^{1}H NMR (400 MHz, $CDCl_3$): δ = 5.87 (t, *J* = 4.3 Hz, 1H, N<u>H</u>$CH_2CH_2CH_3$), 5.44 (s, 1H, H3), 5.27 (t, *J* = 3.0 Hz, 1H, H12), 4.68 (d, *J* = 14.2 Hz, 1H), 4.56 (d, *J* = 14.2 Hz, 1H), 3.92 (d, *J* = 10.6 Hz, 1H, H23), 3.83 (d, *J* = 10.6 Hz, 1H, H23), 3.32–3.24 (m, 1H, NHC<u>H</u>$_2CH_2CH_3$), 2.99–2.92 (m, 1H, NHC<u>H</u>$_2CH_2CH_3$), 2.07 (s, 3H, $OCOCH_3$), 2.05 (s, 3H, $OCOCH_3$), 1.16 (s, 3H), 1.11 (s, 3H), 0.99 (s, 3H), 0.94 (s, 3H), 0.89 (t, *J* = 7.5 Hz, 7.49 Hz, 3H, $NHCH_2CH_2C$<u>H</u>$_3$), 0.86 (d, *J* = 6.6 Hz, 3H), 0.84 (s, 3H) ppm. ^{13}C (100 MHz, $CDCl_3$): δ = 177.8 (C28), 171.2 (OCO), 170.7 (OCO), 150.9 (C2), 140.9 (C13), 132.1 (C3), 124.9 (C12), 72.3, 62.5, 58.0, 54.0, 50.5, 47.6, 46.3, 43.1, 42.8, 41.1, 41.1, 39.4, 39.0, 37.1, 33.5, 30.8, 28.0, 26.2, 24.7, 23.5, 22.5, 21.2, 20.9, 20.9, 19.0, 18.5, 17.8, 17.3, 16.6, 11.5 ppm. DI-ESI-MS *m/z*: 596.54 ([M+H]$^+$), 618.53 ([M+Na]$^+$).

N-[2-acetoxymethyl-23-acetoxy-A(1)-norursa-2,12-dien-28-oyl]4-methylbenzylamine (5.13)

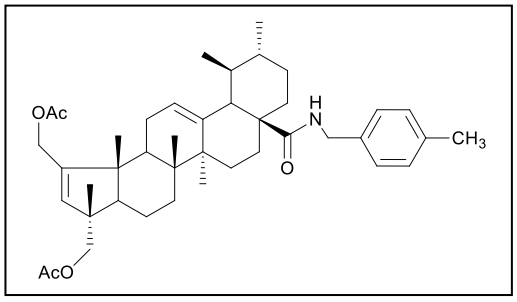

Accordingly to the method described for **5.10**, using compound **5.4** (150 mg, 0.27 mmol), dry benzene (6 mL), thionyl chloride (41.20 µl, 0.57 mmol), dichloromethane (6 mL) and 4-methylbenzilamine (137.70 µl, 1.08 mmol). The crude solid was purified by flash column chromatography (petroleum ether/ethyl acetate 4:1), to afford **5.13** as a white solid (140.3 mg, 79%). Mp: 82.1–84.9 °C. ν_{max}/cm^{-1} (ATR): 3367.0, 2923.0, 2870.5, 1739.5, 1635.5, 1516.5, 1455.5, 1376.0, 1235.0, 1031.0. ^{1}H NMR (400 MHz, $CDCl_3$): δ = 7.13 (s, 4H, H-Ar), 6,07 (t, *J* = 4.2 Hz, 1H, N<u>H</u>CH_2ArCH_3), 5.45 (s, 1H, H3), 5.18 (t, *J* =

2.6 Hz, 1H, H12), 4.67 (d, *J* = 14.2 Hz, 1H), 4.56 (d, *J* = 14.3 Hz, 1H), 4.49 (dd, J_1 = 14.4 Hz, J_2 = 5.9 Hz, 1H, NHC$\underline{H}_2$ArCH$_3$), 4.13 (dd, J_1 = 14.5 Hz, J_2 = 4.3 Hz, 1H, NHC$\underline{H}_2$ArCH$_3$) 3.93 (d, *J* = 10.6 Hz, 1H, H23), 3.84 (d, *J* = 10.6 Hz, 1H, H23), 2.34 (s, 3H, NHCH$_2$ArC$\underline{H}_3$), 2.08 (s, 3H, OCOCH$_3$), 2.06 (s, 3H, OCOCH$_3$), 1.14 (s, 3H), 1.11 (s, 3H), 1.00 (s, 3H), 0.94 (s, 3H), 0.84 (d, *J* = 6.6 Hz, 3H) 0.75 (s, 3H) ppm. ^{13}C NMR (100 MHz, CDCl$_3$): δ = 177.6 (C28), 171.2 (OCO), 170.8 (OCO), 150.9 (C2), 140.7, 137.1, 135.3 (Ar-C), 132.0 (C3), 129.3 (2C, Ar-C), 128.1 (2C, Ar-C), 125.1 (C12), 72.3, 62.5, 58.0, 54.0, 50.3, 47.7, 46.3, 43.4, 43.1, 42.8, 41.1, 39.4, 39.0, 37.1, 33.5, 30.8, 28.0, 26.1, 24.7, 23.5, 21.2, 21.1, 20.9 (2C), 19.0, 18.6, 17.8, 17.2, 16.6 ppm. DI-ESI-MS *m/z*: 658.29 ([M+H]$^+$), 680.40 ([M+Na]$^+$). Anal. Calcd. for $C_{42}H_{59}NO_5$: C, 76.67; H, 9.04; N, 2.13. Found: C, 76.32; H, 9.14; N, 2.23.

N-[2-acetoxymethyl-23-acetoxy-A(1)-norursa-2,12-dien-28-oyl]4-fluorobenzylamine (5.14)

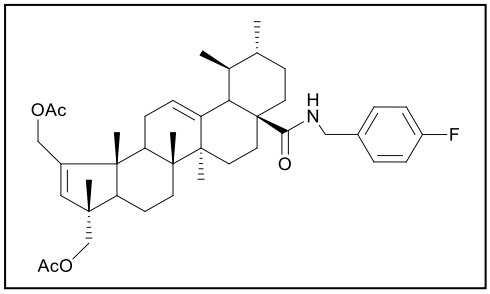

According to the method described for **5.10**, using compound **5.4** (150 mg, 0.27 mmol), dry benzene (6 mL), thionyl chloride (41.20 µl, 0.57 mmol), dichloromethane (6 mL) and 4-fluorobenzylamine (126.60 µl, 1.08 mmol). The crude solid was purified by flash column chromatography (petroleum ether/ethyl acetate 4:1 → 2:1), to afford **5.14** as a white solid (108.8 mg, 61%). Mp: 82.9–85.3 °C. ν_{max}/cm^{-1} (ATR): 3413.0, 2928.0, 2870.5, 1739.0, 1635.5, 1509.5, 1455.0, 1381.0, 1220.5, 1033.5. ^{1}H NMR (400 MHz, CDCl$_3$): δ =7.22–7.19 (m, 2H), 7.00 (t, *J* = 8.61 Hz, 2H), 6.13 (t, *J* = 5.1 Hz, 1H, N$\underline{H}$CH$_2$ArF), 5.44 (s, 1H, H3), 5.19 (t, *J* = 2.5 Hz, 1H, H12), 4.67 (d, *J* = 14.3 Hz, 1H), 4.55 (d, *J* = 14.3 Hz, 1H), 4.49 (dd, J$_1$ = 14.5 Hz, J_2 = 5.9 Hz, 1H, NHC$\underline{H}_2$ArF), 4.14 (dd, J_1 = 14.9 Hz, J_2 = 4.7 Hz, 14.6 Hz, 1H, NHC$\underline{H}_2$ArF), 3.92 (d, *J* = 10.6 Hz, 1H, H23), 3.83 (d, *J* = 10.7 Hz, 1H, H23), 2.07 (s, 3H, OCOCH$_3$), 2.05 (s, 3H, OCOCH$_3$), 1.13 (s, 3H), 1.10 (s, 3H), 0.99 (s, 3H), 0.94 (s, 3H), 0.84 (d, *J* = 6.2 Hz, 3H), 0.72 (s, 3H) ppm. ^{13}C NMR (100 MHz, CDCl$_3$): δ = 177.8 (C28), 171.2 (OCO), 170.7 (OCO), 162.1 (d, J = 245.2 Hz), 150.9 (C2), 140.7 (C13), 134.2, 132.1 (C3), 129.6, 129.5, 125.1 (C12), 115.5, 115.3, 72.2, 62.5, 58.0, 54.0, 50.5, 47.7, 46.3, 43.1, 42.9, 42.7, 41.1, 39.4, 39.0, 37.2, 33.5, 30.8, 28.0, 26.1, 24.7, 23.4, 21.1, 20.9 (2C), 19.0, 18.5, 17.8, 17.2, 16.6 ppm. DI-

ESI-MS *m/z* $[M+H]^+$: 662.40. Anal. Calcd. for $C_{41}H_{56}FNO_5.0.25H_2O$: C, 73.90; H, 8.55; N, 2.10. Found: C, 73.95; H, 8.60; N, 2.23.

Methyl N-[2-acetoxymethyl-23-acetoxy-A(1)-norursa-2,12-dien-28-oyl]gycinate (5.15)

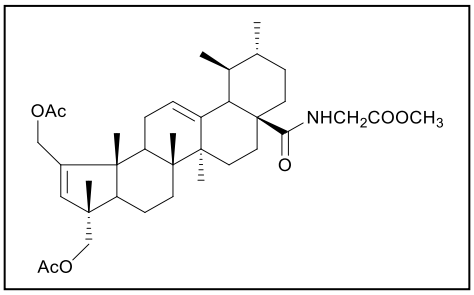

To a stirred solution of compound **5.4** (200 mg, 0.36 mmol), in dry benzene (8 mL), thionyl chloride (54.90 µl, 0.76 mmol) was slowly added. The resultant solution was heat-refluxed at 80 °C. After 3 h, the solvent was removed by evaporation under reduced pressure, and petroleum ether (aprox. 2 mL) was added to the residue, concentrated to dryness to give the acyl chloride intermediate. Without purification the acyl chloride was dissolved in dichloromethane (8 mL), basified to pH 8–9 with triethylamine, and glycine methyl ester hydrochloride (72.40 mg, 0.58 mmol) was added. The resultant mixture was stirred at room temperature. After 45 min, the solvent was removed by evaporation under reduced pressure. The crude obtained was dispersed with water (50 mL) acidified with 5% aqueous HCl (pH 3-4) and extracted with ethyl acetate (3 × 60 mL). The combined organic phase was washed with 10% aqueous $NaHCO_3$ (2 × 50 mL), water (50 mL) and brine (50 mL), dried over Na_2SO_4, filtered, and concentrated under vacuum to afford a light yellow solid. The crude solid was purified by flash column chromatography (petroleum ether/ethyl acetate 2:1), to afford **5.15** as a white solid (179 mg, 79%). Mp: 74.5–76.6 °C. ν_{max}/cm^{-1} (ATR): 3395.0, 2923.5, 2871.5, 1739.0, 1650.0, 1520.5, 1451.0, 1368.0, 1234.0, 1031.0. ^1H NMR (400 MHz, $CDCl_3$): δ = 6.50 (t, *J* = 4.1 Hz, 1H, -N<u>H</u>CH_2COOCH_3) 5.44 (s, 1H, H3), 5.38 (t, *J* = 3.1 Hz, 1H, H12), 4.69 (d, *J* = 14.3 Hz, 1H), 4.57 (d, *J* = 14.2 Hz, 1H), 4.09 (dd, J_1 = 18.5 Hz, J_2 = 5.3 Hz and, 1H, -NHC<u>H</u>$_2COOCH_3$), 3.93 (d, *J* = 10.5 Hz, 1H, H23), 3.84 (dd, J_1 = 18.5 Hz, J_2 = 3.9 Hz, 1H, -NHC<u>H</u>$_2COOCH_3$), 3.83 (d, *J* = 10.7 Hz, 1H, H23), 3.75 (s, 3H, -$NHCH_2COOC$<u>H</u>$_3$), 2.08 (s, 3H, $OCOCH_3$), 2.06 (s, 3H, $OCOCH_3$), 1.15 (s, 3H), 1.12 (s, 3H), 0.99 (s, 3H), 0.95 (s, 3H), 0.88 (d, *J* = 6.3 Hz, 3H), 0.77 (s, 3H) ppm. ^{13}C NMR (100MHz, $CDCl_3$): δ = 178.1, 171.2, 170.7 (OCO), 170.6 (OCO), 151.0 (C2), 140.0 (C13), 131.9 (C3), 125.7 (C12), 72.3, 62.5, 58.0, 53.7, 52.3, 50.5, 47.7, 46.3, 43.2, 42.6, 41.5, 41.1, 39.4, 39.0, 36.9, 33.5, 30.8, 28.0, 26.3, 24.8, 23.6, 21.2, 21.0,

21.0, 19.0, 18.0, 17.8, 17.2, 16.6 ppm. DI-ESI-MS *m/z*: 626.27 ($[M+H]^+$), 648.42 ($[M+Na]^+$).

Methyl N-[2-acetoxymethyl-23-acetoxy-A(1)-norursa-2,12-dien-28-oyl]alaninate (5.16)

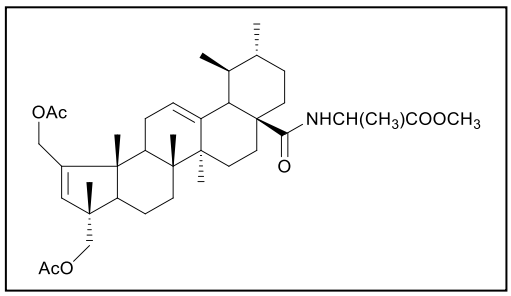

Accordingly to the method described for **5.15**, using compound **5.4** (200 mg, 0.36 mmol), dry benzene (8 mL), thionyl chloride (54.90 µl, 0.76 mmol), dichloromethane (8 mL) and *L*-alanine methyl ester hydrochloride (80.51 mg, 0.58 mmol). The crude solid was purified by flash column chromatography (petroleum ether/ethyl acetate 4:1 → 3:1), to afford **5.16** as a white solid (140 mg, 61 %). Mp: 68.9–71.6 °C. ν_{max}/cm^{-1} (ATR): 3405.0, 2925.0, 2872.0, 1738.0, 1655.5, 1507.5, 1448.5, 1371.5, 1234.5, 1028.0. ^1H NMR (400 MHz, $CDCl_3$): δ = 6.59 (d, *J* = 5.8 Hz, 1H, N<u>H</u>CH(CH_3)COOH), 5.43 (s, 1H, H3), 5.36 (t, *J* = 3.0 Hz, 1H, H12), 4.69 (d, *J* = 14.4 Hz, 1H), 4.57 (d, J = 14.4 Hz, 1H), 4.50–4.42 (m, 1H, NHC<u>H</u>(CH_3)$COOCH_3$), 3.93 (d, *J* = 10.7 Hz, 1H, H23), 3.83 (d, *J* = 10.6 Hz, 1H, H23), 3.73 (s, 3H, NHCH(CH_3)$COOC\underline{H}_3$), 2.08 (s, 3H, $OCOCH_3$), 2.05 (s, 3H, $OCOCH_3$), 1.36 (d, *J* = 7.0 Hz, 3H, NHCH($C\underline{H}_3$)$COOCH_3$), 1.15 (s, 3H), 1.11 (s, 3H), 0.98 (s, 3H), 0.95 (s, 3H), 0.88 (d, *J* = 6.4 Hz, 3H), 0.75 (s, 3H) ppm. ^{13}C (100 MHz, $CDCl_3$): δ = 177.3, 173.7, 171.3 (OCO), 170.2 (OCO), 151.1 (C2), 139.3 (C13), 131.7 (C3), 125.9 (C12), 72.3, 62.5, 58.0, 53.6, 52.4, 50.6, 48.2, 47.6, 46.3, 43.2, 42.6, 41.2, 39.3, 39.0, 37.2, 33.6, 30.8, 28.0, 26.3, 24.6, 23.5, 21.2, 21.0 (2C), 19.0, 18.7, 18.1, 17.8, 17.2, 16.6 ppm. DI-ESI-MS *m/z* $[M+H]^+$: 640.20.

5.4.2 Biology

5.4.2.1 Cells and reagents

MCF-7, HT-29, Jurkat, PC-3, HeLa and BJ cell lines were obtained from the American Type Culture Collection (USA).

Dulbecco's Modified Eagle Medium (DMEM), Dulbecco's Phosphate Buffered Saline (DPBS), and L-glutamine were obtained from Biowest. Minimum Essential

Medium (MEM), a penicilin/streptomicin solution, and Fetal Bovine Serum (FBS) were obtained from Gibco. The MTT powder and the XTT cell proliferation kit were purchased from Applichem Panreac. A sodium pyruvate solution (100 mM) and Trypsin/EDTA were obtained from Biological Industries. A sodium bicarbonate solution (7.5%) and glucose solution (45%) were purchased from Sigma-Aldrich Co. Cisplatin was obtained from Sigma-Aldrich Co.

5.4.2.2 Preparation and storage of the stock solutions

Asiatic acid and its derivatives were suspended in dimethyl sulfoxide (DMSO) to prepare 20 mM stock solutions, which were stored at –80 °C. To obtain final assay concentrations, the stock solutions were diluted in culture medium in the day of testing. The final concentration of DMSO in working solutions was always equal or lower than 0.5%.

5.4.2.3 Cell culture

HT-29, PC-3, and HeLa cells were grown in DMEM high glucose supplemented with 10% heat-inactivated FBS, 100 units/ml penicillin, and 100 µg/ml streptomycin. MCF-7 cells were maintained in MEM supplemented with 10 % heat-inactivated FBS, 10 units/ml penicillin, 10 µg/ml streptomycin, 2 mM L-glutamine, 1 mM sodium pyruvate, 0.01 mg/ml insulin, 10 mM glucose, and 1× MEM-EAGLE Non Essential Amino acids. BJ cells were cultured in DMEM high glucose supplemented with 10% heat-inactivated FBS, 110 mg/L of sodium pyruvate, 100 units/ml penicillin, 100 µg/ml streptomycin, and 1.5 g/L of sodium bicarbonate. Jurkat cells were grown in RPMI 1640 supplemented with 10% heat-inactivated FBS, 100 units/ml penicillin, 100 µg/ml streptomycin, and 2 mM L-glutamine. All cell lines were incubated in a humidified atmosphere of 5.0% CO_2 at 37 °C.

5.4.2.4 Cell viability assay

For MCF-7, HT-29, PC-3, HeLa, and BJ cell lines, the cell viability was determined by MTT assay. In brief, cells were seeded at a concentration of 8×10^2 to 1×10^4 cells/well in 96-well plates and were left to grow. After 24 h of culture, the culture medium was removed and replaced by new medium containing the tested compounds at different concentrations. After 72 h of incubation, cells were incubated with 100 µL of MTT solution (0.5 mg/ml) for 1 h. After incubation, the MTT solution was removed and 100 µL of DMSO were added to each well to dissolve the formazan crystals. The relative cell viability, compared with the viability of nontreated cells, was analyzed by measuring the absorbance at 550 nm on an ELISA plate reader (Tecan Sunrise MR20-301, TECAN, Salzburg, Austria).

For Jurkat cells, the cell viability was determined using the XTT assay. Briefly, 4×10^3 cells/well were seeded in 96-well plates with 100 µL of medium. After 24 h of incubation, 100 µL of new medium containing the tested compounds at different concentrations were added. After an incubation period of 72 hours, 100 µL of XTT solution were added to each well and the plates were incubated for an additional 4 h at 37 °C. Relative cell viability, compared with the viability of nontreated cells, was analyzed by measuring the absorbance at 450 nm on an ELISA plate reader (Tecan Sunrise MR20-301, TECAN, Salzburg, Austria).

IC_{50} values represent the concentration of each compound that inhibited the cell growth by 50%, compared with nontreated cells. The IC_{50} values were estimated from the dose-response curves using 9 different concentrations in triplicate. Each IC_{50} value was expressed as the mean IC_{50} ± standard deviation (SD) of three independent experiments.

5.4.2.5 Cell-cycle assay

Briefly, 2.2×10^4 HeLa cells were seeded per well in 6-well plates with 2 mL of medium. After an incubation period of 24 h, cells were treated with the indicated concentrations of compound **5.6**. After 24 h of incubation, cells were harvested by mild trypsinization, centrifuged, washed twice with PBS, and stained in Tris-buffered saline (TBS) containing 50 mg/mL of PI, 10 mg/mL Rnase-free Dnase, and 0.1% Igepal CA-630 (Sigma-Aldrich), for 1 hour, at 4 °C in the dark. The cell cycle was assessed by

flow cytometry, using a fluorescence-activated cell sorting (FACS) apparatus, and was carried out at 488 nm on an Epics XL flow cytometer (Coulter Corporation, Hialeah, FL). Data from 1×10^4 cells was collected and analyzed using the multicycle software (Phoenix Flow Systems, San Diego, CA). Experiments were performed in triplicate, with two replicates per experiment.

5.4.2.6 Annexin V-FITC/PI flow cytometry assay

HeLa cells were plated in 6-well plates at a density of 2.2×10^4 cells per well. After 24 h, the cells with or without pretreatment for 45 min of 50 μM z-VAD-fmk, were treated with compound **5.6** at the indicated concentrations. After 24 h of incubation, cells were harvested by mild trypsinization, collected by centrifugation, and suspended in 95 μL of binding buffer (10 mM HEPES/NaOH, pH 7.4, 10 mM NaCl, 2.5 mM $CaCl_2$). Cells were stained with the annexin V-FITC conjugate for 30 min at room temperature and protected from light. After the incubation period, 500 μl of binding buffer were added to each vial of cells and approximately 2 min before FACS analysis, 20 μl of a 1 mg/mL PI solution were also added. The samples were analyzed by flow cytometry. Approximately 1×10^4 cells were analyzed for each histogram. Experiments were performed in triplicate, with two replicates per experiment.

5.4.2.7 Hoechst 33258 staining

In this experiment, 2.2×10^4 cells per well were seeded in 6-well plates with 2 mL of medium and incubated for 24 h at 37 °C. After incubation, the cells were treated with the indicated concentrations of compound **5.6**. After 24 h of treatment, the culture medium was removed and cells were harvested by mild trypsinization, and collected by centrifugation. After being washed twice with PBS, the cells were stained with 500 μL of Hoechst 33258 solution (2 μg/mL in PBS) for 15 min in the dark. After incubation, the Hoechst 33258 solution was removed and cells were washed twice with PBS, resuspended in 10 μL of PBS, and mounted on a slide. Morphological changes were

analyzed by fluorescence microscopy using a fluorescence microscope DMRB (Leica Microsystems, Weltzar, germany) and a DAPI filter.

5.4.2.8 Synergy study

Briefly, 7.5×10^2 cells per well were seeded in 96-well plates. After 24 h of culture, cells were treated with compound **5.6** and cisplatin at different concentrations (the ratio between the concentrations of cisplatin and compound **5.6** was constant: the concentration of cisplatin was always 2-fold that of compound **5.6**). After 72 h of incubation, the medium in each well was replaced by 100 µL of filtered MTT solution (0.5 mg/mL). One hour later, the MTT solution was replaced by 100 µM DMSO. The relative cell viability compared with the viability of untreated cells was analyzed by measuring the absorbance at 550 nm on an ELISA plate reader (Tecan Sunrise MR20-301, TECAN, Salzburg, Austria). The effect of compounds **5.6** and cisplatin, alone or in combination, on HeLa cell viability was evaluated, and the results were analyzed via the CompuSyn software, which was used to calculate the Combination Index (CI). A CI value < 1 indicates the existence of synergism.

Chapter 6

Concluding remarks

Chemotherapy is one of the most used strategies for cancer treatment, either alone or in combination with other therapies such as surgery or radiation. However, one of the major limitations of chemotherapy is its lack of selectivity for cancer cells. This low specificity of chemotherapeutic drugs results in toxicity against rapidly proliferating normal cells, severe side effects, and inefficiency of the treatments.[328] Because of these limitations, it is urgent to develop new drugs with increased potency and selectivity, which will lead to better anticancer efficiency.

Asiatic acid **1.27** is a pentacyclic triterpenoid with recognized anticancer properties. The chemical modification of the asiatic acid **1.27** skeleton can originate compounds with increased anticancer activity and improved value for the development of new chemotherapeutic drugs.

In this work, three panels of new asiatic acid **1.27** semisynthetic derivatives were designed and successfully prepared by adopting different strategies of synthesis. As described in Chapter 3, the preparation of new fluorinated derivatives of asiatic acid **1.27** containing fluorolactone or fluorolactam moieties was accomplished using the electrophilic fluorination reagent Selectfluor®. In Chapter **4**, the synthesis of asiatic acid **1.27** derivatives containing a pentameric A-ring was explored. The strategies of synthesis adopted allowed the preparation of new pentameric A-ring derivatives containing α,β-unsaturated aldehyde or α,β-unsaturated nitrile groups. The preparation of nitrile-containing derivatives was performed in moderate yields using a simple, economic, and environmentally friendly method. The strategies of synthesis depicted in Chapter **5** allowed the successful preparation of a series of new amide and hydroxamic acid derivatives of asiatic acid **1.27**. The hydroxamic acid derivatives were obtained in good yields using a simple, cost-effective, and easy-to-handle method. The structures of all new derivatives were elucidated via the analysis of the information obtained using different techniques, including IR, ^{1}H NMR, ^{13}C NMR and MS.

The new derivatives of asiatic acid **1.27** synthesized here were evaluated regarding their ability to inhibit the proliferation of several cancer cell lines. In general, the synthesized compounds exhibited better antiproliferative activities than did asiatic acid **1.27**. As the compounds were particularly active against the HeLa cell line, an SAR was established for each panel of derivatives based on the IC_{50} values determined in this cell line. The general conclusions of the SAR analysis were:

- The conversion of the hexameric A-ring of asiatic acid **1.27** into a pentameric A-ring with an α,β-unsaturated aldehyde led to a significant increase in activity, thus generating the most active compounds among all the derivatives prepared in this project (compounds **3.9**–**3.16**, **4.6**–**4.8**, **4.13**, **4.17**–**4.21**, **4.28** and **4.29**).
- The presence of a methanesulfonyloxy moiety at C23 of pentameric A-ring asiatic acid **1.27** derivatives slightly increase the antiproliferative activity (compounds **4.28** and **4.29**).
- The introduction of amide or hydroxamic acid moieties at C28 had a positive impact in antiproliferative activity (compounds **5.6**, **5.7**, and **5.8** and **5.9**–**5.16**).

The most active compounds of each panel (**3.12**, **3.14**, **4.13**, **4.28**, **4.29**, and **5.6**) were further tested in a nontumor fibroblast cell line (BJ), to access selectivity. The compounds tested exhibited lower toxicity toward nontumor BJ cells than they did toward cancer cells. Additional studies were performed to shed some light on the possible anticancer mechanism of the most active compound of each panel (**3.14**, **4.29**, and **5.6**). Compounds **3.14**, **4.29** and **5.6** induced arrest of the cell cycle at the G0/G1 phase in the HeLa cell line. In the case of compounds **3.14** and **4.29**, this effect was related with the upregulation of $p27^{kip1}$ and $p21^{cip1/waf1}$ and the downregulation of cyclin D3. These three compounds also induced apoptosis in HeLa cells. The results suggested that proapoptotic effects of compounds **3.14** and **4.29** were mediated by the activation of caspases 8 and 3, the downregulation of Bcl-2, and the upregulation of Bax. Finally, compound **5.6** exhibited a synergistic effect with cisplatin to inhibit the growth of HeLa cells.

This study provided some insights into the possible mechanism of action of the most active compounds **3.14**, **4.29**, and **5.6**. However, additional studies are needed to further precise the molecular pathways that drive their anticancer action. These compounds should also be subjected to an *in vivo* evaluation, to confirm their anticancer potential. Additionally, the existence of synergism between cisplatin and other semisynthetic derivatives of asiatic acid **1.27** should be further explored.

In summary, we accomplished the preparation of several new semisynthetic derivatives of asiatic acid **1.27** that proved to be significantly more active in inhibiting cancer cell growth than was the parental asiatic acid **1.27**. Thus, the SAR analysis established in this thesis is a useful tool for the design of new modifications in the asiatic acid **1.27** backbone in

order to increase its anticancer properties. Taking into account all of the results obtained in the present work, some of the new asiatic acid **1.27** derivatives synthesized here may be promising candidates for the development of effective chemotherapeutic agents.

Chapter 7

References

(1) Torre, L. A.; Bray, F.; Siegel, R. L.; Ferlay, J.; Lortet-Tieulent, J.; Jemal, A. Global Cancer Statistics, 2012. *CA Cancer J Clin* **2015**, *65* (2), 87–108.

(2) Siegel, R.; Miller, K.; Jemal, A. Cancer Statistics , 2015 . *CA Cancer J Clin* **2015**, *65* (1), 29.

(3) Ferlay, J.; Steliarova-Foucher, E.; Lortet-Tieulent, J.; Rosso, S.; Coebergh, J. W. W.; Comber, H.; Forman, D.; Bray, F. Cancer Incidence and Mortality Patterns in Europe: Estimates for 40 Countries in 2012. *Eur. J. Cancer* **2013**, *49* (6), 1374–1403.

(4) American Cancer Society. Global Cancer Facts & Figures 3rd Edition. *Am. Cancer Soc.* **2015**, No. 800, 1–64.

(5) Ministério da Saúde - Direção-Geral de Saúde. Portugal, Doenças Oncológicas Em Números – 2014. *Programa Nac. para as Doenças Oncológicas* **2014**, 1–85.

(6) World Health Organization. Cancer: Fact sheet N° 297 Updated February 2015 http://www.who.int/mediacentre/factsheets/fs297/en/ (accessed Jul 15, 2016).

(7) Anand, P.; Kunnumakara, A. B.; Sundaram, C.; Harikumar, K. B.; Tharakan, S. T.; Lai, O. S.; Sung, B.; Aggarwal, B. B. Cancer Is a Preventable Disease That Requires Major Lifestyle Changes. *Pharm. Res.* **2008**, *25* (9), 2097–2116.

(8) Barrett, J. C. Mechanisms of Multistep Carcinogenesis and Carcinogen Risk Assessment. *Environ. Health Perspect.* **1993**, *100* (12), 9–20.

(9) Vogelstein, B.; Kinzler, K. W. The Multistep Nature of Cancer. *Trends Genet.* **1993**, *9* (4), 138–141.

(10) Hanahan, D.; Weinberg, R. A. The Hallmarks of Cancer. *Cell* **2000**, *100* (1), 57–70.

(11) Migliore, L.; Coppedè, F. Genetic and Environmental Factors in Cancer and Neurodegenerative Diseases. *Mutat. Res. Mutat. Res.* **2002**, *512* (2-3), 135–153.

(12) Lodish, H.; Berk, A.; Zipursky, S. L. et. al. Proto-Oncogenes and Tumor-Suppressor Genes. http://www.ncbi.nlm.nih.gov/books/NBK21662/ (accessed Jun 10, 2016).

(13) Marshall, C. J. Tumor Suppressor Genes. *Cell* **1991**, *64* (2), 313–326.

(14) Fearon, E. R. Cancer Progression. *Curr. Biol.* **1999**, *9* (23), R873–R875.

(15) Strahm, B.; Capra, M. Insights into the Molecular Basis of Cancer Development. *Curr. Paediatr.* **2005**, *15* (4), 333–338.

(16) Roth, J. A. Molecular Events in Lung Cancer. *Lung Cancer* **1995**, *12* (SUPPL. 2), S3–S15.

(17) Hanahan, D.; Weinberg, R. A. Hallmarks of Cancer: The next Generation. *Cell* **2011**, *144* (5), 646–674.

(18) Fernald, K.; Kurokawa, M. Evading Apoptosis in Cancer. *Trends Cell Biol.* **2013**, *23* (12), 620–633.

(19) Raynaud, C. M.; Sabatier, L.; Philipot, O.; Olaussen, K. A.; Soria, J. C. Telomere Length, Telomeric Proteins and Genomic Instability during the Multistep Carcinogenic Process. *Crit. Rev. Oncol. Hematol.* **2008**, *66* (2), 99–117.

(20) Nishida, N.; Yano, H.; Nishida, T.; Kamura, T.; Kojiro, M. Angiogenesis in Cancer. *Vasc. Health Risk Manag.* **2006**, *2* (3), 213–219.

(21) Geiger, T. R.; Peeper, D. S. Metastasis Mechanisms. *Biochim. Biophys. Acta - Rev. Cancer* **2009**, *1796* (2), 293–308.

(22) Laszczyk, M. N. Pentacyclic Triterpenes of the Lupane, Oleanane and Ursane Group as Tools in Cancer Therapy. *Planta Med.* **2009**, *75* (15), 1549–1560.

(23) Vermeulen, K.; Van Bockstaele, D. R.; Berneman, Z. N. The Cell Cycle: A Review of Regulation, Deregulation and Therapeutic Targets in Cancer. *Cell Prolif.* **2003**, *36* (3), 131–149.

(24) Collins, K.; Jacks, T.; Pavletich, N. P. The Cell Cycle and Cancer. *Proc. Natl. Acad. Sci. U. S. A.* **1997**, *94* (7), 2776–2778.

(25) Diaz-Moralli, S.; Tarrado-Castellarnau, M.; Miranda, A.; Cascante, M. Targeting Cell Cycle Regulation in Cancer Therapy. *Pharmacol. Ther.* **2013**, *138* (2), 255–271.

(26) Lim, S.; Kaldis, P. Cdks, Cyclins and CKIs: Roles beyond Cell Cycle Regulation. *Development* **2013**, *140* (15), 3079–3093.

(27) Alberts, B.; Johnson, A.; Lewis, J.; Raff, M.; Roberts, K.; Walter, P. Components of the Cell-Cycle Control System http://www.ncbi.nlm.nih.gov/books/NBK26824/ (accessed Jul 10, 2015).

(28) Giacinti, C.; Giordano, A. RB and Cell Cycle Progression. *Oncogene* **2006**, *25* (38), 5220–5227.

(29) Neganova, I.; Lako, M. G1 to S Phase Cell Cycle Transition in Somatic and Embryonic Stem Cells. *J. Anat.* **2008**, *213* (1), 30–44.

(30) Malumbres, M.; Barbacid, M. Cell Cycle, CDKs and Cancer: A Changing Paradigm. *Nat. Rev. Cancer* **2009**, *9* (3), 153–166.

(31) Clurman, B. E.; Roberts, J. M. Cell Cycle and Cancer. *J. Natl. Cancer Inst.* **1995**, *87* (20), 1499–1501.

(32) Park, M. T.; Lee, S. J. Cell Cycle and Cancer. *J. Biochem. Mol. Biol.* **2003**, *36* (1), 60–65.

(33) Williams, G. H.; Stoeber, K. The Cell Cycle and Cancer. *J. Pathol.* **2012**, *226* (2), 352–364.

(34) Ouyang, L.; Shi, Z.; Zhao, S.; Wang, F. T.; Zhou, T. T.; Liu, B.; Bao, J. K. Programmed Cell Death Pathways in Cancer: A Review of Apoptosis, Autophagy and Programmed Necrosis. *Cell Prolif.* **2012**, *45* (6), 487–498.

(35) Martin, S. J. Caspases: Executioners of Apoptosis. In *Pathobiology of Human Disease: A Dynamic Encyclopedia of Disease Mechanisms*; Mcmanus, L. M., Mitchel, R. N., Eds.; Elsevier Inc.: Amsterdam, **2014**; pp. 145–152.

(36) Abud, H. E. Shaping Developing Tissues by Apoptosis. *Cell Death Differ.* **2004**, *11* (8), 797–799.

(37) Kalimuthu, S.; Se-Kwon, K. Cell Survival and Apoptosis Signaling as Therapeutic Target for Cancer: Marine Bioactive Compounds. *Int. J. Mol. Sci.* **2013**, *14* (2), 2334–2354.

(38) Roos, W. P.; Kaina, B. DNA Damage-Induced Cell Death: From Specific DNA Lesions to the DNA Damage Response and Apoptosis. *Cancer Lett.* **2013**, *332* (2), 237–248.

(39) Taylor, R. C.; Cullen, S. P.; Martin, S. J. Apoptosis: Controlled Demolition at the Cellular Level. *Nat. Rev. Mol. Cell Biol.* **2008**, *9* (3), 231–241.

(40) Tait, S. W.; Green, D. R. Mitochondria and Cell Death: Outer Membrane Permeabilization and beyond. *Nat Rev Mol Cell Biol* **2010**, *11* (9), 621–632.

(41) Wlodkowic, D.; Telford, W.; Skommer, J.; Darzynkiewicz, Z. Apoptosis and Beyond: Cytometry in Studies of Programmed Cell Death. In *Methods in Cell Biology*; Darzynkiewicz, Z., Holden, E., Orfao, A., Telford, W., Wlodkowic, D., Eds.; Elsevier Inc., **2011**; Vol. 103, pp. 55–98.

(42) Saraste, A.; Pulkki, K. Morphologic and Biochemical Hallmarks of Apoptosis. *Cardiovasc. Res.* **2000**, *45* (3), 528–537.

(43) Kumar, S. Caspase Function in Programmed Cell Death. *Cell Death Differ.* **2007**, *14* (1), 32–43.

(44) Li, J.; Yuan, J. Caspases in Apoptosis and Beyond. *Oncogene* **2008**, *27* (48), 6194–6206.

(45) Puccini, J.; Kumar, S. Caspases. In *Encyclopedia of Cell Biology*; Bradshaw, R. A., Stahl, P. D., Eds.; Elsevier Ltd., **2016**; Vol. 3, pp. 364–373.

(46) Shi, Y. Review Mechanisms of Caspase Activation and Inhibition during Apoptosis. *Mol. Cell* **2002**, *9*, 459–470.

(47) Fulda, S.; Debatin, K. M. Extrinsic versus Intrinsic Apoptosis Pathways in Anticancer Chemotherapy. *Oncogene* **2006**, *25*, 4798–4811.

(48) Guicciardi, M. E.; Gores, G. J. Life and Death by Death Receptors. *FASEB J.* **2009**, *23* (6), 1625–1637.

(49) Safa, A. R.; Pollok, K. E. Targeting the Anti-Apoptotic Protein c-FLIP for Cancer Therapy. *Cancers (Basel).* **2011**, *3* (2), 1639–1671.

(50) Li, H.; Zhu, H.; Xu, C. J.; Yuan, J. Cleavage of BID by Caspase 8 Mediates the Mitochondrial Damage in the Fas Pathway of Apoptosis. *Cell* **1998**, *94* (4), 491–501.

(51) Czabotar, P. E.; Lessene, G.; Strasser, A.; Adams, J. M. Control of Apoptosis by the BCL-2 Protein Family: Implications for Physiology and Therapy. *Nat. Rev. Mol. Cell Biol.* **2014**, *15* (1), 49–63.

(52) Wong, R. S. Apoptosis in Cancer: From Pathogenesis to Treatment. *J. Exp. Clin. Cancer Res.* **2011**, *30* (87).

(53) Kasibhatla, S.; Tseng, B. Why Target Apoptosis in Cancer Treatment ? *Mol. Cancer Ther.* **2003**, *2* (June), 573–580.

(54) Schug, Z. T.; Gonzalvez, F.; Houtkooper, R. H.; Vaz, F. M.; Gottlieb, E. BID Is Cleaved by Caspase-8 within a Native Complex on the Mitochondrial Membrane. *Cell Death Differ.* **2011**, *18* (3), 538–548.

(55) Candé, C.; Cohen, I.; Daugas, E.; Ravagnan, L.; Larochette, N.; Zamzami, N.; Kroemer, G. Apoptosis-Inducing Factor (AIF): A Novel Caspase-Independent Death Effector Released from Mitochondria. *Biochimie* **2002**, *84* (2-3), 215–222.

(56) Kliche, K. O.; Höffken, K. The Role of Apoptosis in Hematologic Malignancies and Modulation of Apoptosis as a New Therapeutic Approach. *J. Cancer Res. Clin. Oncol.* **1999**, *125* (3), 226–231.

(57) Cragg, G. M.; Grothaus, P. G.; Newman, D. J. Impact of Natural Products on Developing New Anti-Cancer Agents . *Chem. Rev.* **2009**, *109*, 3012–3043.

(58) Cragg, G. M.; Newman, D. J. Natural Products: A Continuing Source of Novel Drug Leads. *Biochim. Biophys. Acta - Gen. Subj.* **2013**, *1830* (6), 3670–3695.

(59) Blunt, J. W.; Copp, B. R.; Munro, M. H. G.; Northcote, P. T.; Prinsep, M. R. Marine Natural Products. *Nat. Prod. Rep.* **2011**, *28* (2), 196–268.

(60) Romano, G.; Costantini, M.; Sansone, C.; Lauritano, C.; Ruocco, N.; Ianora, A. Marine Microorganisms as a Promising and Sustainable Source of Bioactive Molecules. *Mar. Environ. Res.* **2016**.

(61) Newman, D. J. Natural Products as Drug Leads: An Old Process or the New Hope for Drug Discovery? *J. Med. Chem.* **2008**, *51* (9), 2589–2599.

(62) Harvey, A. L.; Edrada-Ebel, R.; Quinn, R. J. The Re-Emergence of Natural Products for Drug Discovery in the Genomics Era. *Nat. Rev. Drug Discov.* **2015**, *14* (2), 111–129.

(63) Molinari, G. Chapter 2 Natural Products in Drug Discovery: Present Status and Perspectives. In *Pharmaceutical Biotechnology: Advances in Experimental Medicine and Biology*; **2009**; Vol. 655, pp 13–27.

(64) Atanasov, A. G.; Waltenberger, B.; Pferschy-Wenzig, E. M.; Linder, T.; Wawrosch, C.; Uhrin, P.; Temml, V.; Wang, L.; Schwaiger, S.; Heiss, E. H.; et al. Discovery and Resupply of Pharmacologically Active Plant-Derived Natural Products: A Review. *Biotechnol. Adv.* **2015**, *33* (8), 1582–1614.

(65) da Rocha, A. Natural Products in Anticancer Therapy. *Curr. Opin. Pharmacol.* **2001**, *1* (4), 364–369.

(66) Newman, D. J.; Cragg, G. M. Natural Products as Sources of New Drugs over the 30 Years from 1981 to 2010. *J. Nat. Prod.* **2012**, *75* (3), 311–335.

(67) Cragg, G. M.; Newman, D. J. Plants as a Source of Anti-Cancer Agents. *J. Ethnopharmacol.* **2005**, *100* (1-2), 72–79.

(68) Prakash, O.; Kumar, A.; Kumar, P.; Ajeet, A. Anticancer Potential of Plants and Natural Products: A Review. *Am. J. Pharmacol. Sci.* **2013**, *1* (6), 104–115.

(69) Mondal, S.; Bandyopadhyay, S.; Ghosh, M. K.; Mukhopadhyay, S.; Roy, S.; Mandal, C. Natural Products: Promising Resources for Cancer Drug Discovery. *Anticancer. Agents Med. Chem.* **2012**, *12* (1), 49–75.

(70) Graham, J. G.; Quinn, M. L.; Fabricant, D. S.; Farnsworth, N. R. Plants Used against Cancer - An Extension of the Work of Jonathan Hartwell. *J. Ethnopharmacol.* **2000**, *73* (3), 347–377.

(71) Hartwell, J. L. *Plants Used Against Cancer: A SurVey*; Quarterman Publishers Inc.: Lawrence MA, **1982**.

(72) Demain, A. L.; Vaishnav, P. Natural Products for Cancer Chemotherapy. *Microb. Biotechnol.* **2011**, *4* (6), 687–699.

(73) Khazir, J.; Mir, B. A.; Pilcher, L.; Riley, D. L. Role of Plants in Anticancer Drug Discovery. *Phytochem. Lett.* **2014**, *7* (1), 173–181.

(74) Moudi, M.; Go, R.; Yien, C. Y. S.; Nazre, M. Vinca Alkaloids. *Int. J. Prev. Med.* **2013**,

4 (11), 1131–1135.

(75) Rowinsky, E. The Vinca Alkaloids http://www.ncbi.nlm.nih.gov/books/NBK12718/ (accessed Jun 9, 2016).

(76) Kittakoop, P. Anticancer Drugs and Potential Anticancer Leads Inspired by Natural Products. In *Studies in Natural Products Chemistry*; Atta-Ur-Rahman, F., Ed.; Elsevier: Amsterdam, **2015**, Vol. 44, pp. 251–307.

(77) Sears, J. E.; Boger, D. L. Total Synthesis of Vinblastine, Related Natural Products, and Key Analogues and Development of Inspired Methodology Suitable for the Systematic Study of Their Structure-Function Properties. *Acc. Chem. Res.* **2015**, *48* (3), 653–662.

(78) Keglevich, P.; Hazai, L.; Kalaus, G.; Szántay, C. Modifications on the Basic Skeletons of Vinblastine and Vincristine. *Molecules* **2012**, *17* (5), 5893–5914.

(79) Fauzee, N. J. S.; Dong, Z.; Wang, Y. L. Taxanes: Promising Anti-Cancer Drugs. *Asian Pacific J. Cancer Prev.* **2011**, *12* (4), 837–851.

(80) Rowinsky, E. K. The Development and Clinical Utility of the Taxane Class of Antimicrotubule Chemotherapy Agents. *Annu. Rev. Med.* **1997**, *48* (1), 353–374.

(81) Press Announcements - FDA approves Abraxane for late-stage pancreatic cancer http://www.fda.gov/NewsEvents/Newsroom/PressAnnouncements/ucm367442.htm (accessed Jul 5, 2016).

(82) Mita, A. C.; Figlin, R.; Mita, M. M. Cabazitaxel: More than a New Taxane for Metastatic Castrate-Resistant Prostate Cancer? *Clin. Cancer Res.* **2012**, *18* (24), 6574–6579.

(83) Abal, M.; Andreu, J. M.; Barasoain, I. Taxanes: Microtubule and Centrosome Targets, and Cell Cycle Dependent Mechanisms of Action. *Curr. Cancer Drug Targets* **2003**, *3*, 193–203.

(84) Gordaliza, M.; Castro, M. A.; del Corral, J. M.; Feliciano, A. S. Antitumor Properties of Podophyllotoxin and Related Compounds. *Curr. Pharm. Des.* **2000**, *6* (18), 1811–1839.

(85) You, Y. Podophyllotoxin Derivatives: Current Synthetic Approaches for New Anticancer Agents. *Curr. Pharm. Des.* **2005**, *11* (13), 1695–1717.

(86) Hande, K. R. Topoisomerase II Inhibitors. *Update Cancer Ther.* **2008**, *3* (1), 13–26.

(87) Nitiss, J. L. Targeting DNA Topoisomerase II in Cancer Chemotherapy. *Nat. Rev. Cancer* **2009**, *9* (5), 338–350.

(88) Pommier, Y. Topoisomerase I Inhibitors: Camptothecins and Beyond. *Nat. Rev. Cancer* **2006**, *6* (10), 789–802.

(89) Wahid, M.; Bano, Q. Structure Activity Relationship and Clinical Development Perspective of Analogs. *J. Appl. Pharm.* **2014**, *6* (3), 286–295.

(90) Pommier, Y. DNA Topoisomerase I Inhibitors: Chemistry, Biology, and Interfacial Inhibition. *Chem. Rev.* **2009**, *109* (7), 2894–2902.

(91) Xu, Y.; Her, C. Inhibition of Topoisomerase (DNA) I (TOP1): DNA Damage Repair and Anticancer Therapy. *Biomolecules* **2015**, *5* (3), 1652–1670.

(92) Oberlies, N. H.; Kroll, D. J. Camptothecin and Taxol: Achievements in Natural

Products Research. *J. Nat. Prod.* **2004**, *67*, 129–135.

(93) FDA. Press Announcements- FDA aproves new treatment for advanced pancreatic cancer http://www.fda.gov/NewsEvents/Newsroom/PressAnnouncements/ucm468654.htm (accessed Jun 25, 2016).

(94) Staker, B. L.; Hjerrild, K.; Feese, M. D.; Behnke, C. A.; Burgin, A. B.; Stewart, L. The Mechanism of Topoisomerase I Poisoning by a Camptothecin Analog. *Proc. Natl. Acad. Sci. U. S. A.* **2002**, *99* (24), 15387–15392.

(95) Nagaiah, G.; Remick, S. C. Combretastatin A4 Phosphate: A Novel Vascular Disrupting Agent. *Futur. Oncol.* **2010**, *6* (8), 1219–1228.

(96) Nathan, P.; Zweifel, M.; Padhani, A. R.; Koh, D. M.; Ng, M.; Collins, D. J.; Harris, A.; Carden, C.; Smythe, J.; Fisher, N.; et al. Phase I Trial of Combretastatin A4 Phosphate (CA4P) in Combination with Bevacizumab in Patients with Advanced Cancer. *Clin. Cancer Res.* **2012**, *18* (12), 3428–3439.

(97) A Safety and Efficacy Study of Carboplatin, Paclitaxel, Bevacizumab and CA4P in Non-Small Cell Lung Cancer https://clinicaltrials.gov/ct2/show/NCT00653939 (accessed Jul 5, 2016).

(98) Tholl, D. Biosynthesis and Biological Functions of Terpenoids in Plants. *Adv. Biochem. Eng. Biotechnol.* **2015**, *148*, 63–106.

(99) Breitmaier, E. Terpenes: Importance, General Structure, and Biosynthesis. In *Terpenes: Flavors, Fragrances, Pharmaca, Pheromones*; Wiley-VCH Verlag GmbH & Co. KGaA: Weinheim, Germany, **2006**; pp. 1–9.

(100) Dzubak, P.; Hajduch, M.; Vydra, D.; Hustova, A.; Kvasnica, M.; Biedermann, D.; Markova, L.; Urban, M.; Sarek, J. Pharmacological Activities of Natural Triterpenoids and Their Therapeutic Implications. *Nat. Prod. Rep.* **2006**, *23* (3), 394–411.

(101) Salvador, J. A. R.; Moreira, V. M.; Gonçalves, B. M. F.; Leal, A. S.; Jing, Y. Ursane-Type Pentacyclic Triterpenoids as Useful Platforms to Discover Anticancer Drugs. *Nat. Prod. Rep.* **2012**, *29* (12), 1463–1479.

(102) Nagegowda, D. A. Plant Volatile Terpenoid Metabolism: Biosynthetic Genes, Transcriptional Regulation and Subcellular Compartmentation. *FEBS Lett.* **2010**, *584* (14), 2965–2973.

(103) Sheng, H.; Sun, H. Synthesis, Biology and Clinical Significance of Pentacyclic Triterpenes: A Multi-Target Approach to Prevention and Treatment of Metabolic and Vascular Diseases. *Nat. Prod. Rep.* **2011**, *28* (3), 543–593.

(104) Xu, R.; Fazio, G. C.; Matsuda, S. P. T. On the Origins of Triterpenoid Skeletal Diversity. *Phytochemistry* **2004**, *65* (3), 261–291.

(105) Thimmappa, R.; Geisler, K.; Louveau, T.; O'Maille, P.; Osbourn, A. Triterpene Biosynthesis in Plants. *Annu. Rev. Plant Biol.* **2014**, *65* (January), 16.1–16.33.

(106) Hill, R. A.; Connolly, J. D. Triterpenoids. *Nat. Prod. Rep.* **2015**, *29* (2), 273–327.

(107) Sawai, S.; Uchiyama, H.; Mizuno, S.; Aoki, T.; Akashi, T.; Ayabe, S. I.; Takahashi, T. Molecular Characterization of an Oxidosqualene Cyclase That Yields Shionone, a Unique Tetracyclic Triterpene Ketone of Aster Tataricus. *FEBS Lett.* **2011**, *585* (7), 1031–1036.

(108) Andre, C. M.; Legay, S.; Nieuwenhuizen, N.; Punter, M.; Cooney, J. M.; Lateur, M.; Larondelle, Y.; Laing, W. A. Multifunctional Oxidosqualene Cyclases and Cytochrome P450 Involved in the Biosynthesis of Apple Fruit Triterpenic Acids. *New Phytol.* **2016**, 1–16.

(109) Salvador, J. A. R.; Leal, A. S.; Alho, D. P. S.; Gonçalves, B. M. F.; Valdeira, A. S.; Mendes, V. I. S.; Jing, Y. Highlights of Pentacyclic Triterpenoids in the Cancer Settings. *Stud. Nat. Prod. Chem.* **2014**, *41*, 33–73.

(110) Loizzo, M. R.; Menichini, F.; Tundis, R. Recent Insights into the Emerging Role of Triterpenoids in Cancer Therapy: Part I in *Studies in Natural Products Chemistry*, Atta-ur-Rahman, Eds. Elsevier B.V. All rights reserved, Amsterdam, **2013**, Vol. 40, pp. 1-31.

(111) Shanmugam, M. K.; Dai, X.; Kumar, A. P.; Tan, B. K. H.; Sethi, G.; Bishayee, A. Oleanolic Acid and Its Synthetic Derivatives for the Prevention and Therapy of Cancer: Preclinical and Clinical Evidence. *Cancer Lett.* **2014**, *346* (2), 206–216.

(112) Shanmugam, M. K.; Nguyen, A. H.; Kumar, A. P.; Tan, B. K. H.; Sethi, G. Targeted Inhibition of Tumor Proliferation, Survival, and Metastasis by Pentacyclic Triterpenoids: Potential Role in Prevention and Therapy of Cancer. *Cancer Lett.* **2012**, *320* (2), 158–170.

(113) Kamble, S. M.; Goyal, S. N.; Patil, C. R. Multifunctional Pentacyclic Triterpenoids as Adjuvants in Cancer Chemotherapy: A Review. *RSC Adv.* **2014**, *4*, 33370.

(114) Shanmugam, M. K.; Dai, X.; Kumar, A. P.; Tan, B. K. H.; Sethi, G.; Bishayee, A. Ursolic Acid in Cancer Prevention and Treatment: Molecular Targets, Pharmacokinetics and Clinical Studies. *Biochem. Pharmacol.* **2013**, *85* (11), 1579–1587.

(115) Król, S. K.; Kielbus, M.; Rivero-Müller, A.; Stepulak, A. Comprehensive Review on Betulin as a Potent Anticancer Agent. *Biomed Res. Int.* **2015**.

(116) Liby, K. T.; Sporn, M. B. Synthetic Oleanane Triterpenoids: Multifunctional Drugs with a Broad Range of Applications for Prevention and Treatment of Chronic Disease. *Pharmacol. Rev.* **2012**, *64* (4), 972–1003.

(117) Nakagawa-Goto, K.; Yamada, K.; Taniguchi, M.; Tokuda, H.; Lee, K. H. Cancer Preventive Agents 9. Betulinic Acid Derivatives as Potent Cancer Chemopreventive Agents. *Bioorganic Med. Chem. Lett.* **2009**, *19* (13), 3378–3381.

(118) Yan, X. J.; Gong, L. H.; Zheng, F. Y.; Cheng, K. J.; Chen, Z. S.; Shi, Z. Triterpenoids as Reversal Agents for Anticancer Drug Resistance Treatment. *Drug Discov. Today* **2014**, *19* (4), 482–488.

(119) Yadav, V. R.; Prasad, S.; Sung, B.; Kannappan, R.; Aggarwal, B. B. Targeting Inflammatory Pathways by Triterpenoids for Prevention and Treatment of Cancer. *Toxins (Basel).* **2010**, *2* (10), 2428–2466.

(120) Liby, K. T.; Yore, M. M.; Sporn, M. B. Triterpenoids and Rexinoids as Multifunctional Agents for the Prevention and Treatment of Cancer. *Nat. Rev. Cancer* **2007**, *7* (5), 357–369.

(121) Coussens, L. M.; Werb, Z. Inflammation and Cancer. *Nature* **2002**, *420* (6917), 860–867.

(122) Lu, H.; Ouyang, W.; Huang, C. Inflammation, a Key Event in Cancer Development. *Mol Cancer Res* **2006**, *4* (4), 221–233.

(123) Vannini, N.; Lorusso, G.; Cammarota, R.; Barberis, M.; Noonan, D. M.; Sporn, M. B.; Albini, A. The Synthetic Oleanane Triterpenoid, CDDO-Methyl Ester, Is a Potent Antiangiogenic Agent. *Mol. Cancer Ther.* **2007**, *6* (12), 3139–3146.

(124) Kanjoormana, M.; Kuttan, G. Antiangiogenic Activity of Ursolic Acid. *Integr. Cancer Ther.* **2010**, *9* (2), 224–235.

(125) M. R. Patlolla, J.; V. Rao, C. Triterpenoids for Cancer Prevention and Treatment: Current Status and Future Prospects. *Curr. Pharm. Biotechnol.* **2012**, *13* (1), 147–155.

(126) Hong, D. S.; Kurzrock, R.; Supko, J. G.; He, X.; Naing, A.; Wheler, J.; Lawrence, D.; Eder, J. P.; Meyer, C. J.; Ferguson, D. A.; et al. A Phase I First-in-Human Trial of Bardoxolone Methyl in Patients with Advanced Solid Tumors and Lymphomas. *Clin. Cancer Res.* **2012**, *18* (12), 3396–3406.

(127) Günther, B.; Wagner, H. Quantitative Determination of Triterpenes in Extracts and Phytopreparations of Centella Asiatica (L.) Urban. *Phytomedicine* **1996**, *3* (1), 59–65.

(128) Brinkhaus, B.; Lindner, M.; Schuppan, D.; Hahn, E. G. Chemical, Pharmacological and Clinical Profile of the East Asian Medical Plant Centella Aslatica. *Phytomedicine* **2000**, *7* (5), 427–448.

(129) Gohil, K. J.; Patel, J. A.; Gaijar, A. K. Pharmacological Review on Centella Asiatica: A Potential Herbal Cure-All. *Indian J. Pharm. Sci.* **2010**, *72* (5), 546–556.

(130) Sawatdee, S.; Choochuay, K.; Chanthorn, W.; Srichana, T. The Efficacy of Topical Spray Containing Centella Asiatica Extract on Excision Wound Healing in Rats. *Acta Parm.* **2016**, *66* (2), 233–244.

(131) Inamdar, P. K.; Yeole, R. D.; Ghogare, A. B.; de Souza, N. J. Determination of Biologically Active Constituents in Centella Asiatica. *J. Chromatogr. A* **1996**, *742* (1-2), 127–130.

(132) Rush, W. R.; Murray, G. R.; Graham, D. J. M. The Comparative Steady-State Bioavailability of the Active Ingredients of Madecassol. *Eur. J. Drug Metab. Pharmacokinet.* **1993**, *18* (4), 323–326.

(133) Somboonwong, J.; Kankaisre, M.; Tantisira, B.; Tantisira, M. H. Wound Healing Activities of Different Extracts of Centella Asiatica in Incision and Burn Wound Models: An Experimental Animal Study. *BMC Complement. Altern. Med.* **2012**, *12* (1), 103–109.

(134) de Fátima, A.; Modolo, L. V; Sanches, A. C. C.; Porto, R. R. Wound Healing Agents: The Role of Natural and Non-Natural Products in Drug Development. *Mini Rev. Med. Chem.* **2008**, *8* (9), 879–888.

(135) Bonte, F.; Dumas, M.; Chaudagne, C.; Meybeck, A. . Influence of Asiatic Acid, Madecassic Acid, and Asiaticoside on Human Collagen I Synthesis. *Planta Med.* **1994**, *60* (2), 133–135.

(136) Grimaldi, R.; Ponti, F. De; D'Angelo, L.; Caravaggi, M.; Guidi, G.; Lecchini, S.; Frigo, G.M., Crema, A. Phamacokinetics of the Total Triterpenic Fraction of Centella Asiatica After Single and Multiple Administrations to Healthy Volunteers. A New Assay for Asiatic Acid. *J. Ethnopharmacol.* **1990**, *28*, 235–241.

(137) Zheng, X. C.; Wang, S. H. Determination of Asiatic Acid in Beagle Dog Plasma after Oral Administration of Centella Asiatica Extract by Precolumn Derivatization RP-HPLC. *J. Chromatogr. B. Analyt. Technol. Biomed. Life Sci.* **2009**, *877* (5-6), 477–481.

(138) Bontems, J. E. A New Heteroside, Asiaticoside, Isolated from Hydrocotyle Asiatica L (Umbelliferae). *Bull. Sci. Pharmacol* **1941**, *49*, 186–191.

(139) Jew, S. S.; Park, H.; Kim, H.; Jung, Y. Asiatic Acid Derivatives Having Modified A-Ring, US Patent 6071898, **2000**.

(140) Polonsky, J. Sur La Constitution Chimique de L'asiaticoside et Notamment de L'acide Asiatique (III). Sur La Lactonisation et La Décarboxylation de L'acide Asiatique. *Comptes. Rend.* **1950**, *230*, 1784–1786.

(141) Polonsky, J. Sur La Constitution Chimique de L'asiaticoside et Notamment de L'acide Asiatique (IV). Sur La Nature Des OH de La Fonction Glycol-1.2. *Comptes. Rend.* **1951**, *232*, 1878–1880.

(142) Shim, P. J.; Park, J. H.; Chang, M. S.; Lim, M. J.; Kim, D. H.; Jung, Y. H.; Jew, S. S.; Park, E. H.; Kim, H. D. Asiaticoside Mimetics as Wound Healing Agent. *Bioorg. Med. Chem. Lett.* **1996**, *6* (24), 2937–2940.

(143) Jeong, B. S. Structure-Activity Relationship Study of Asiatic Acid Derivatives for New Wound Healing Agent. *Arch. Pharm. Res.* **2006**, *29* (7), 556–562.

(144) Maquart, F. X.; Bellon, G.; Gillery, P.; Yanusz, W.; Borel, J. P. Stimulation of Collagen Synthesis in Fibroblast Cultures by a Triterpene Extracted from Centella Asiatica. *Connect. Tissue Res.* **1990**, *24* (2), 107–120.

(145) Rehm, J.; Samokhvalov, A. V.; Shield, K. D. Global Burden of Alcoholic Liver Diseases. *J. Hepatol.* **2013**, *59* (1), 160–168.

(146) Jeong, B. S.; Lee, M. K.; Kim, Y. C.; Lee, E. S. Modification of C2 Functional Group on Asiatic Acid and the Evaluation of Hepatoprotective Effects. *Arch Pharm Res* **2007**, *30* (3), 282–289.

(147) Zhao, L.; Park, H.; Jew, S.; Lee, M. K.; Kim, Y. C.; Thapa, P.; Karki, R.; Jahng, Y.; Jeong, B. S.; Lee, E. S. Modification of C11, C28, C2,3,23 or C2,23,28 Functional Groups on Asiatic Acid and Evaluation of Hepatoprotective Effects. *Bull. Korean Chem. Soc.* **2007**, *28* (6), 970–976.

(148) Wei, J.; Huang, Q.; Huang, R.; Chen, Y.; Lv, S.; Wei, L.; Liang, C.; Liang, S.; Zhuo, L.; Lin, X. Asiatic Acid from Potentilla Chinensis Attenuate Ethanol-Induced Hepatic Injury via Suppression of Oxidative Stress and Kupffer Cell Activation. *Biol. Pharm. Bull.* **2013**, *36* (12), 1980–1989.

(149) Yan, S. L.; Yang, H. T.; Lee, Y. J.; Lin, C. C.; Chang, M. H.; Yin, M. C. Asiatic Acid Ameliorates Hepatic Lipid Accumulation and Insulin Resistance in Mice Consuming High Fat Diet. *J. Agric. Food Chem.* **2014**, *62*, 4625–4631.

(150) Gao, J.; Chen, J.; Tang, X.; Pan, L.; Fang, F.; Xu, L.; Zhao, X.; Xu, Q. Mechanism Underlying Mitochondrial Protection of Asiatic Acid against Hepatotoxicity in Mice. *J. Pharm. Pharmacol.* **2006**, *58* (2), 227–233.

(151) Ma, K.; Zhang, Y.; Zhu, D.; Lou, Y. Protective Effects of Asiatic Acid against D-Galactosamine/lipopolysaccharide-Induced Hepatotoxicity in Hepatocytes and Kupffer Cells Co-Cultured System via Redox-Regulated Leukotriene C4 Synthase Expression

Pathway. *Eur. J. Pharmacol.* **2009**, *603* (1-3), 98–107.

(152) Tang, L.; He, R.; Yang, G.; Tan, J.; Zhou, L.; Meng, X.; Huang, X. R.; Lan, H. Y. Asiatic Acid Inhibits Liver Fibrosis by Blocking TGF-beta/Smad Signaling in Vivo and in Vitro. *PLoS One* **2012**, *7* (2), e31350.

(153) Guo, W.; Liu, W.; Hong, S.; Liu, H.; Qian, C.; Shen, Y.; Wu, X.; Sun, Y.; Xu, Q. Mitochondria-Dependent Apoptosis of Con A-Activated T Lymphocytes Induced by Asiatic Acid for Preventing Murine Fulminant Hepatitis. *PLoS One* **2012**, *7* (9), e46018.

(154) Nasir, M. N.; Habsah, M.; Zamzuri, I.; Rammes, G.; Hasnan, J.; Abdullah, J. Effects of Asiatic Acid on Passive and Active Avoidance Task in Male Spraque-Dawley Rats. *J. Ethnopharmacol.* **2011**, *134* (2), 203–209.

(155) Kumar, M. V.; Gupta, Y. K. Effect of Centella Asiatica on Cognition and Oxidative Stress in an Cerebroventricular Streptozotocin Model of Alzheimer's Disease in Rats. *Clin. Exp. Parmacology Physiol.* **2003**, *30*, 336–342.

(156) Orhan, I. E. Centella Asiatica (L.) Urban: From Traditional Medicine to Modern Medicine with Neuroprotective Potential. *Evid. Based. Complement. Alternat. Med.* **2012**, 946259.

(157) Soumyanath, A.; Zhong, Y. P.; Henson, E.; Wadsworth, T.; Bishop, J.; Gold, B. G.; Quinn, J. F. Centella Asiatica Extract Improves Behavioral Deficits in a Mouse Model of Alzheimer's Disease: Investigation of a Possible Mechanism of Action. *Int. J. Alzheimers. Dis.* **2012**, 1–9.

(158) Sousa, J. N.; Shah, V.; Desai, P. D.; Inamdar, P. K.; D'Sa, A.; Ammanamanchi, R.; Dohadwalia, A. N.; Lakdwaia, A. D.; Mandrekar, S. S.; Blumbach, J. 2,3,23-Trihydroxy-Urs-12-Ene and Its Derivatives, Processes for Their Preparation and Their Use. EP 0383171 A2, **1990**.

(159) Jew, S. S.; Park, H. G.; Kim, H.; Jung, Y. H.; Kim, Y. C.; Kim, S. R.; Seo, S. K.; Nam, T. G.; Han, D.; Yoo, C. H.; et al. Medicines for Treating Dementia or Cognitive Disorder, Which Comprises Asiatic Acid Derivatives. WO Patent 9823278, **1998**.

(160) Mook-Jung, I.; Shin, J. E.; Yun, S. H.; Huh, K.; Koh, J. Y.; Park, H. K.; Jew, S. S.; Jung, M. W. Protective Effects of Asiaticoside Derivatives against Beta-Amyloid Neurotoxicity. *J. Neurosci. Res.* **1999**, *58* (3), 417–425.

(161) Jew, S. S.; Yoo, C. H.; Lim, D. Y.; Kim, H.; Mook-Jung, I.; Jung, M. W.; Choi, H.; Jung, Y. H.; Park, H. G. Structure-Activity Relationship Study of Asiatic Acid Derivatives against Beta Amyloid (A Beta)-Induced Neurotoxicity. *Bioorg. Med. Chem. Lett.* **2000**, *10* (2), 119–121.

(162) Xu, M.; Xiong, Y.; Liu, J.; Qian, J.; Zhu, L.; Gao, J. Asiatic Acid, a Pentacyclic Triterpene in Centella Asiatica, Attenuates Glutamate-Induced Cognitive Deficits in Mice and Apoptosis in SH-SY5Y Cells. *Acta Pharmacol. Sin.* **2012**, *33* (5), 578–587.

(163) Xiong, Y.; Ding, H.; Xu, M.; Gao, J. Protective Effects of Asiatic Acid on Rotenone- or H2O2-Induced Injury in SH-SY5Y Cells. *Neurochem. Res.* **2009**, *34* (4), 746–754.

(164) Zhang, X.; Wu, J.; Dou, Y.; Xia, B.; Rong, W.; Rimbach, G.; Lou, Y. Asiatic Acid Protects Primary Neurons against C2-Ceramide-Induced Apoptosis. *Eur. J. Pharmacol.* **2012**, *679* (1-3), 51–59.

(165) Krishnamurthy, R. G.; Senut, M. C.; Zemke, D.; Min, J.; Frenkel, M. B.; Greenberg, E. J.; Yu, S. W.; Ahn, N.; Goudreau, J.; Kassab, M.; et al. Asiatic Acid, a Pentacyclic Triterpene from Centella Asiatica, Is Neuroprotective in a Mouse Model of Focal Cerebral Ischemia. *J. Neurosci. Res.* **2009**, *87* (11), 2541–2550.

(166) Lee, K. Y.; Bae, O.; Weinstock, S.; Kassab, M.; Majid, A. Neuroprotective Effect of Asiatic Acid in Rat Model of Focal Embolic Stroke. *Biol. Pharm. Bull.* **2014**, *37* (8), 1397–1401.

(167) Sirichoat, A.; Chaijaroonkhanarak, W.; Prachaney, P.; Pannangrong, W.; Leksomboon, R.; Chaichun, A.; Wigmore, P.; Welbat, J. Effects of Asiatic Acid on Spatial Working Memory and Cell Proliferation in the Adult Rat Hippocampus. *Nutrients* **2015**, *7* (10), 8413–8423.

(168) Umka Welbat, J.; Sirichoat, A.; Chaijaroonkhanarak, W.; Prachaney, P.; Pannangrong, W.; Pakdeechote, P.; Sripanidkulchai, B.; Wigmore, P. Asiatic Acid Prevents the Deleterious Effects of Valproic Acid on Cognition and Hippocampal Cell Proliferation and Survival. *Nutrients* **2016**, *8* (5), 303.

(169) Chao, P.; Lee, H.; Yin, M. Asiatic Acid Attenuated Apoptotic and Inflammatory Stress in the Striatum of MPTP-Treated Mice. *Food Funct.* **2016**, *7* (4), 1999–2005.

(170) Jiang, W.; Li, M.; He, F.; Bian, Z.; He, Q.; Wang, X.; Yao, W.; Zhu, L. Neuroprotective Effect of Asiatic Acid against Spinal Cord Injury in Rats. *Life Sci.* **2016**, *157*, 45–51.

(171) Liu, J.; He, T.; Lu, Q.; Shang, J.; Sun, H.; Zhang, L. Asiatic Acid Preserves Beta Cell Mass and Mitigates Hyperglycemia in Streptozocin-Induced Diabetic Rats. *Diabetes. Metab. Res. Rev.* **2010**, *26* (6), 448–454.

(172) Ramachandran, V.; Saravanan, R.; Senthilraja, P. Antidiabetic and Antihyperlipidemic Activity of Asiatic Acid in Diabetic Rats, Role of HMG CoA: In Vivo and in Silico Approaches. *Phytomedicine* **2014**, *21* (3), 225–232.

(173) Inzucchi, S. E.; Sherwin, R. S. Type 2 Diabetes Mellitus. In *Goldman's Cecil Medicine*; Goldman, L., Schafer, A. I., Eds.; Elsevier Inc., **2014**, pp. 1489–1499.

(174) Treadway, J. Glycogen Phosphorylase Inhibitors for Treatment of Type 2 Diabetes Mellitus. *Expert Opin. Investig. Drugs* **2001**, *10* (3), 439–454.

(175) Baker, D. J.; Timmons, J. A.; Greenhaff, P. I. Glycogen Phosphorylase Inhibition in Type 2 Diabetes Therapy. *Diabetes* **2005**, *54*, 2453–2459.

(176) Wen, X.; Sun, H.; Liu, J.; Cheng, K.; Zhang, P.; Zhang, L.; Hao, J.; Zhang, L.; Ni, P.; Zographos, S. E.; et al. Naturally Occurring Pentacyclic Triterpenes as Inhibitors of Glycogen Phosphorylase: Synthesis, Structure-Activity Relationships, and X-Ray Crystallographic Studies. *J. Med. Chem.* **2008**, *51* (12), 3540–3554.

(177) Zhang, L.; Chen, J.; Gong, Y.; Liu, J.; Zhang, L.; Hua, W.; Sun, H. Synthesis and Biological Evaluation of Asiatic Acid Derivatives as Inhibitors of Glycogen Phosphorylases. *Chem. Biodivers.* **2009**, *6* (6), 864–874.

(178) Ramachandran, V.; Saravanan, R. Efficacy of Asiatic Acid, a Pentacyclic Triterpene on Attenuating the Key Enzymes Activities of Carbohydrate Metabolism in Streptozotocin-Induced Diabetic Rats. *Phytomedicine* **2012**, *20* (3-4), 230–236.

(179) Ramachandran, V.; Saravanan, R. Glucose Uptake through Translocation and

Activation of GLUT4 in PI3K/Akt Signaling Pathway by Asiatic Acid in Diabetic Rats. *Hum. Exp. Toxicol.* **2015**, *34* (9), 884–893.

(180) Fan, Y. M.; Xu, L. Z.; Gao, J.; Wang, Y.; Tang, X. H.; Zhao, X. N.; Zhang, Z. X. Phytochemical and Antiinflammatory Studies on Terminalia Catappa. *Fitoterapia* **2004**, *75* (3-4), 253–260.

(181) Yun, K. J.; Kim, J.Y.; Kim, J. B.; Lee, K.W.; Jeong, S.Y.; Park, H. J.; Jung, H. J.; Cho, Y. W.; Yun, K.; Lee, K. T. Inhibition of LPS-Induced NO and PGE2 Production by Asiatic Acid via NF-Kappa B Inactivation in RAW 264.7 Macrophages: Possible Involvement of the IKK and MAPK Pathways. *Int. Immunopharmacol.* **2008**, *8* (3), 431–441.

(182) Nhiem, N. X.; Tai, B. H.; Quang, T. H.; Kiem, P. Van; Minh, C. Van; Nam, N. H.; Kim, J. H.; Im, L. R.; Lee, Y. M.; Kim, Y. H. A New Ursane-Type Triterpenoid Glycoside from Centella Asiatica Leaves Modulates the Production of Nitric Oxide and Secretion of TNF-α in Activated RAW 264.7 Cells. *Bioorg. Med. Chem. Lett.* **2011**, *21* (6), 1777–1781.

(183) Tsao, S. M.; Yin, M. C. Antioxidative and Antiinflammatory Activities of Asiatic Acid, Glycyrrhizic Acid, and Oleanolic Acid in Human Bronchial Epithelial Cells. *J. Agric. Food Chem.* **2015**, *63* (12), 3196–3204.

(184) Huang, S. S.; Chiu, C. S.; Chen, H. J.; Hou, W. C.; Sheu, M. J.; Lin, Y. C.; Shie, P. H.; Huang, G. J. Antinociceptive Activities and the Mechanisms of Anti-Inflammation of Asiatic Acid in Mice. *Evid. Based. Complement. Alternat. Med.* **2011**, 895857.

(185) Yang, G. X.; Zhang, R. Z.; Lou, B.; Cheng, K. J.; Xiong, J.; Hu, J. F. Chemical Constituents from Melastoma Dodecandrum and Their Inhibitory Activity on Interleukin-8 Production in HT-29 Cells. *Natural product research*. Taylor & Francis **2014**, pp. 1383–1387.

(186) Meng, X.; Nikolic-Paterson, D. J.; Lan, H. Y. TGF-β: The Master Regulator of Fibrosis. *Nat. Rev. Nephrol.* **2016**.

(187) Xu, C.; Wang, W.; Xu, M.; Zhang, J. Asiatic Acid Ameliorates Tubulointerstitial Fibrosis in Mice with Ureteral Obstruction. *Exp. Ther. Med.* **2013**, *6* (3), 731–736.

(188) Meng, X.; Zhang, Y.; Huang, X.; Ren, G.; Li, J. Treatment of Renal Fibrosis by Rebalancing TGF-β / Smad Signaling with the Combination of Asiatic Acid and Naringenin. *Oncotarget* **2015**, *6* (35), 36984–36997.

(189) Liu, W.; Liu, T. C.; Mong, M. Antibacterial Effects and Action Modes of Asiatic Acid. *BioMedicine* **2015**, *5* (3), 16.

(190) Norzaharaini, M.; Wan Norshazwani, W.; Hasmah, A.; Nor Izani, N.; Rapeah, S. A Preliminary Study on the Antimicrobial Activities of Asiaticoside and Asiatic Acid against Selected Gram Positive and Gram Negative Bacteria. *Heal. Environ. J.* **2011**, *2* (1), 23–26.

(191) Wong, K. C.; Hag Ali, D. M.; Boey, P. L. Chemical Constituents and Antibacterial Activity of Melastoma Malabathricum L. *Nat. Prod. Res.* **2012**, *26* (7), 609–618.

(192) Wilson, R.; Dowling, R. B. Pseudomonas Aeruginosa and Other Related Species. *Thorax* **1998**, *53* (3), 213–219.

(193) Garo, E.; Eldridge, G. R.; Goering, M. G.; Pulcini, E. D.; Hamilton, M. A.; Costerton,

J. W.; James, G. A. Asiatic Acid and Corosolic Acid Enhance the Susceptibility of Pseudomonas Aeruginosa Biofilms to Tobramycin. *Antimicrob. Agents Chemother.* **2007**, *51* (5), 1813–1817.

(194) Si, L.; Xu, J.; Yi, C.; Xu, X.; Wang, F.; Gu, W.; Zhang, Y.; Wang, X. Asiatic Acid Attenuates Cardiac Hypertrophy by Blocking Transforming Growth Factor-β1-Mediated Hypertrophic Signaling in Vitro and in Vivo. *Int. J. Mol. Med.* **2014**, *34* (2), 499–506.

(195) Xu, X.; Si, L.; Xu, J.; Yi, C.; Wang, F.; Gu, W.; Zhang, Y.; Wang, X. Asiatic Acid Inhibits Cardiac Hypertrophy by Blocking Interleukin- 1 β -Activated Nuclear Factor-κ B Signaling in Vitro and in Vivo. *J. Thorac. Dis.* **2015**, *7* (10), 1787–1797.

(196) Ma, Z. G.; Dai, J.; Wei, W. Y.; Zhang, W. B.; Xu, S. C.; Liao, H. H. Asiatic Acid Protects against Cardiac Hypertrophy through Activating AMPK α Signalling Pathway. *Int. J. Biol. Sci.* **2016**, *12*, 861–871.

(197) Huo, L.; Shi, W.; Chong, L.; Wang, J.; Zhang, K.; Li, Y. Asiatic Acid Inhibits Left Ventricular Remodeling and Improves Cardiac Function in a Rat Model of Myocardial Infarction. *Exp. Ther. Med.* **2015**, *11* (1), 57–64.

(198) Chan, C. Y.; Mong, M. C.; Liu, W. H.; Huang, C. Y.; Yin, M. C. Three Pentacyclic Triterpenes Protect H9c2 Cardiomyoblast Cells against High-Glucose-Induced Injury. *Free Radic. Res.* **2014**, *48* (4), 402–411.

(199) Li, Z. W.; Piao, C. D.; Sun, H. H.; Ren, X. S.; Bai, Y. S. Asiatic Acid Inhibits Adipogenic Differentiation of Bone Marrow Stromal Cells. *Cell Biochem. Biophys.* **2013**, *68* (2), 437–442.

(200) Bunbupha, S.; Pakdeechote, P.; Kukongviriyapan, U.; Prachaney, P. Asiatic Acid Reduces Blood Pressure by Enhancing Nitric Oxide Bioavailability with Modulation of eNOS and p47 Phox Expression in L -NAME-Induced Hypertensive Rats. *Phyther. Res.* **2014**, *28* (10), 1506–15012.

(201) Bunbupha, S.; Pakdeechote, P.; Kukongviriyapan, U.; Prachaney, P. Asiatic Acid Reduces Blood Pressure and Improves Vascular Function in Nitric Oxide Deficient Hypertensive Rats. *Srinagarind Med. J.* **2013**, *28*, 234–238.

(202) Maneesai, P.; Bunbupha, S.; Kukongviriyapan, U.; Prachaney, P.; Tangsucharit, P.; Kukongviriyapan, V.; Pakdeechote, P. Asiatic Acid Attenuates Renin-Angiotensin System Activation and Improves Vascular Function in High-Carbohydrate, High-Fat Diet Fed Rats. *BMC Complement. Altern. Med.* **2016**, *16* (123).

(203) Bharitkar, Y. P.; Banerjee, M.; Kumar, S.; Paira, R.; Meda, R.; Kuotsu, K.; Mondal, N. B. Search for a Potent Microbicidal Spermicide from the Isolates of Shorea Robusta Resin. *Contraception* **2013**, *88* (1), 133–140.

(204) Mavondo, G. A.; Mkhwananzi, B. N.; Mabandla, M. V. Pre-Infection Administration of Asiatic Acid Retards Parasitaemia Induction in Plasmodium Berghei Murine Malaria Infected Sprague-Dawley Rats. *Malar. J.* **2016**, *15* (226).

(205) Soo Lee, Y.; Jin, D. Q.; Beak, S. M.; Lee, E. S.; Kim, J. A. Inhibition of Ultraviolet-A-Modulated Signaling Pathways by Asiatic Acid and Ursolic Acid in HaCaT Human Keratinocytes. *Eur. J. Pharmacol.* **2003**, *476* (3), 173–178.

(206) Lee, Y. S.; Jin, D. Q.; Kwon, E. J.; Park, S. H.; Lee, E. S.; Jeong, T. C.; Nam, D. H.; Huh, K.; Kim, J. A. Asiatic Acid, a Triterpene, Induces Apoptosis through Intracellular

Ca2+ Release and Enhanced Expression of p53 in HepG2 Human Hepatoma Cells. *Cancer Lett.* **2002**, *186* (1), 83–91.

(207) Park, B. C.; Bosire, K. O.; Lee, E. S.; Lee, Y. S.; Kim, J. A. Asiatic Acid Induces Apoptosis in SK-MEL-2 Human Melanoma Cells. *Cancer Lett.* **2005**, *218* (1), 81–90.

(208) Park, B. C.; Paek, S. H.; Lee, Y. S.; Kim, S. J.; Lee, E. S.; Choi, H. G.; Young, C. S.; Kim, J. A. Inhibitory Effects of Asiatic Acid and 12-O-Tetradecanoylphorbol 13-Acetate-Induced Tumor Promotion in Mice. *Biol. Pharm. Bull.* **2007**, *30* (1), 176–179.

(209) Chen, J.; Xu, Q.; Xu, H.; Huang, Z. Asiatic Acid Promotes p21 WAF1 / CIP1 Protein Stability through Attenuation of NDR1 / 2 Dependent Phosphorylation of p21 WAF1 / in HepG2 Human Hepatoma Cells. *Asian Pacific J. Cancer Prev.* **2014**, *15*, 963–967.

(210) Lu, Y.; Liu, S.; Wang, Y.; Wang, D.; Gao, J.; Zhu, L. Asiatic Acid Uncouples Respiration in Isolated Mouse Liver Mitochondria and Induces HepG2 Cells Death. *Eur. J. Pharmacol.* **2016**, *786* (5), 212–223.

(211) Jing, Y.; Wang, G.; Ge, Y.; Xu, M.; Gong, Z. Synthesis, Anti-Tumor and Anti-Angiogenic Activity Evaluations of Asiatic Acid Amino Acid Derivatives. *Molecules* **2015**, *20*, 7309–7324.

(212) Zhao, C. H.; Zhang, C. L.; Shi, J. J.; Hou, X. Y.; Feng, B.; Zhao, L. X. Design, Synthesis, and Biofunctional Evaluation of Novel Pentacyclic Triterpenes Bearing O-[4-(1-Piperazinyl)-4-Oxo-Butyryl Moiety as Antiproliferative Agents. *Bioorganic Med. Chem. Lett.* **2015**, *25* (20), 4500–4504.

(213) Wang, L.; Xu, J.; Zhao, C.; Zhao, L.; Feng, B. Antiproliferative, Cell-Cycle Dysregulation Effects of Novel Asiatic Acid Derivatives on Human Non-Small Cell Lung Cancer Cells. *Chem. Pharm. Bull. (Tokyo).* **2013**, *61* (October), 1015–1023.

(214) Li, J. F.; Huang, R. Z.; Yao, G. Y.; Ye, M.Y.; Wang, H. S.; Pan, Y. M.; Xiao, J. T. Synthesis and Biological Evaluation of Novel Aniline-Derived Asiatic Acid Derivatives as Potential Anticancer Agents. *Eur. J. Med. Chem.* **2014**, *86*, 175–188.

(215) Meng, Y.; Li, Y.; Li, F.; Song, Y.; Wang, H.; Chen, H.; Cao, B. Synthesis and Antitumor Activity Evaluation of New Asiatic Acid Derivatives. *J. Asian Nat. Prod. Res.* **2012**, *14* (9), 844–855.

(216) Jirasripongpun, K.; Jirakanjanakit, N.; Sakulsom, P.; Wongekalak, L. O.; Hongsprabhas, P. Influences of Food Matrices on Cytotoxicity of Asiatic Acid in Mammalian Cell Models. *Int. J. Food Sci. Technol.* **2012**, *47* (9), 1970–1976.

(217) Wongekalak, L.; Sakulsom, P.; Jirasripongpun, K.; Hongsprabhas, P. Potential Use of Antioxidative Mungbean Protein Hydrolysate as an Anticancer Asiatic Acid Carrier. *Food Res. Int.* **2011**, *44* (3), 812–817.

(218) Jing, Y.; Wang, G.; Ge, Y.; Xu, M.; Tang, S.; Gong, Z. AA-PMe , a Novel Asiatic Acid Derivative , Induces Apoptosis and Suppresses Proliferation , Migration , and Invasion of Gastric Cancer Cells. *Onco Targets Ther.* **2016**, *9*, 1605–1621.

(219) Yoshida, M.; Fuchigami, M.; Nagao, T.; Okabe, H.; Matsunaga, K.; Takata, J.; Karube, Y.; Tsuchihashi, R.; Kinjo, J.; Mihashi, K.; et al. Antiproliferative Constituents from Umbelliferae Plants VII. Active Triterpenes and Rosmarinic Acid from Centella Asiatica. *Biol. Pharm. Bull.* **2005**, *28* (1), 173–175.

(220) Bunpo, P.; Kataoka, K.; Arimochi, H.; Nakayama, H.; Kuwahara, T.;

Vinitketkumnuen, U.; Ohnishi, Y. Inhibitory Effects of Asiatic Acid and CPT-11 on Growth of HT-29 Cells. *J. Med. Invest.* **2005**, *52* (1-2), 65–73.

(221) Tang, X. L.; Yang, X. Y.; Jung, H. J.; Kim, S. Y.; Jung, S. Y.; Choi, D. Y.; Park, W. C.; Park, H. Asiatic Acid Induces Colon Cancer Cell Growth Inhibition and Apoptosis through Mitochondrial Death Cascade. *Biol. Pharm. Bull.* **2009**, *32* (8), 1399–1405.

(222) Hsu, Y.; Kuo, P.; Lin, L.; Lin, C. Asiatic Acid , a Triterpene , Induces Apoptosis and Cell Cycle Arrest through Activation of Extracellular Signal-Regulated Kinase and p38 Mitogen-Activated Protein Kinase Pathways in Human Breast Cancer Cells. *J. Pharmacol. Exp. Ther.* **2005**, *313* (1), 333–344.

(223) Longxuan, Z.; Mingzhu, T.; Liji, J.; Xinglong, H.; Ping, S.; Xiaocui, Z.; Junwei, Y. Synthesis and Characterization of Derivatives of Asiatic Acid and Primary Study on Anti-Cancer Activity. *Chinese J. Org. Chem.* **2011**, *31*, 646–652.

(224) Takaya, M.; Nomura, M.; Takahashi, T.; Kondo, Y.; Lee, K. T.; Kobayashi, S. 23-Hydroxyursolic Acid Causes Cell Growth-Inhibition by Inducing Caspase-Dependent Apoptosis in Human Cervical Squamous Carcinoma HeLa Cells. *Anticancer Res.* **2009**, *29* (4), 995–1000.

(225) Ren, L.; Cao, Q. X.; Zhai, F. R.; Yang, S. Q.; Zhang, H.X. Asiatic Acid Exerts Anticancer Potential in Human Ovarian Cancer Cells via Suppression of PI3K/Akt/mTOR Signalling. *Pharm. Biol.* **2016**, *0209* (March), 1–6.

(226) Gurfinkel, D. M.; Chow, S.; Hurren, R.; Gronda, M.; Henderson, C.; Berube, C.; Hedley, D. W.; Schimmer, A. D. Disruption of the Endoplasmic Reticulum and Increases in Cytoplasmic Calcium Are Early Events in Cell Death Induced by the Natural Triterpenoid Asiatic Acid. *Apoptosis* **2006**, *11* (9), 1463–1471.

(227) Zhang, J.; Ai, L.; Lv, T.; Jiang, X.; Liu, F. Asiatic Acid, a Triterpene, Inhibits Cell Proliferation through Regulating the Expression of Focal Adhesion Kinase in Multiple Myeloma Cells. *Oncol. Lett.* **2013**, *6* (6), 1762–1766.

(228) Garanti, T.; Stasik, A.; Burrow, A. J.; Alhnan, M. A.; Wan, K.-W. Anti-Glioma Activity and the Mechanism of Cellular Uptake of Asiatic Acid-Loaded Solid Lipid Nanoparticles. *Int. J. Pharm.* **2016**, *500* (1-2), 305–315.

(229) Mabuchi, S.; Kuroda, H.; Takahashi, R.; Sasano, T. The PI3K/AKT/mTOR Pathway as a Therapeutic Target in Ovarian Cancer. *Gynecol. Oncol.* **2015**, *137* (1), 173–179.

(230) Zhao, X. F.; Guan, J. L. Focal Adhesion Kinase and Its Signaling Pathways in Cell Migration and Angiogenesis. *Adv Drug Deliv Rev.* **2012**, *63* (8), 610–615.

(231) Kavitha, C. V; Agarwal, C.; Agarwal, R.; Deep, G. Asiatic Acid Inhibits pro-Angiogenic Effects of VEGF and Human Gliomas in Endothelial Cell Culture Models. *PLoS One* **2011**, *6* (8), e22745.

(232) Cho, C. W.; Choi, D. S.; Cardone, M. H.; Kim, C. W.; Sinskey, A. J.; Rha, C. Glioblastoma Cell Death Induced by Asiatic Acid. *Cell Biol. Toxicol.* **2006**, *22* (6), 393–408.

(233) Kavitha, C. V.; Jain, A. K.; Agarwal, C.; Pierce, A.; Keating, A.; Huber, K. M.; Serkova, N. J.; Wempe, M. F.; Agarwal, R.; Deep, G. Asiatic Acid Induces Endoplasmic Reticulum Stress and Apoptotic Death in Glioblastoma Multiforme Cells Both in Vitro and in Vivo. *Mol. Carcinog.* **2014**, No. April.

(234) Furuya, T.; Kamlet, A. S.; Ritter, T. Catalysis for Fluorination and Trifluoromethylation. *Nature* **2011**, *473* (7348), 470–477.

(235) Gillis, E. P.; Eastman, K. J.; Hill, M. D.; Donnelly, D. J.; Meanwell, N. A. Applications of Fluorine in Medicinal Chemistry. *J. Med. Chem.* **2015**, *58* (21), 8315–8359.

(236) Böhm, H. J.; Banner, D.; Bendels, S.; Kansy, M.; Kuhn, B.; Müller, K.; Obst-Sander, U.; Stahl, M. Fluorine in Medicinal Chemistry. *Chembiochem* **2004**, *5* (5), 637–643.

(237) Filler, R.; Saha, R. Fluorine in Medicinal Chemistry: A Century of Progress and a 60-Year Retrospective of Selected Highlights. *Future Med. Chem.* **2009**, *1* (5), 777–791.

(238) Ojima, I. Exploration of Fluorine Chemistry at the Multidisciplinary Interface of Chemistry and Biology. *J. Org. Chem.* **2013**, *78* (13), 6358–6383.

(239) Hagmann, W. K. The Many Roles for Fluorine in Medicinal Chemistry. *J. Med. Chem.* **2008**, *51* (15), 4359–4369.

(240) Isanbor, C.; O'Hagan, D. Fluorine in Medicinal Chemistry: A Review of Anti-Cancer Agents. *J. Fluor. Chem.* **2006**, *127* (3), 303–319.

(241) Abad, A.; Agulló, C.; Cuñat, A. C.; González-Coloma, A.; Pardo, D. Preparation of 9 α-Fluorinated Sesquiterpenic Drimanes and Evaluation of Their Antifeedant Activities. *European J. Org. Chem.* **2010**, (11), 2182–2198.

(242) Liang, T.; Neumann, C. N.; Ritter, T. Introduction of Fluorine and Fluorine-Containing Functional Groups. *Angew. Chemie Int. Ed.* **2013**, *32*, 8214–8264.

(243) Beaulieu, F.; Beauregard, L.; Courchesne, G.; Couturier, M.; Heureux, A. L. Aminodifluorosulfinium Tetrafluoroborate Salts as Stable and Crystalline Deoxofluorinating Reagents. *Org. Lett.* **2009**, *11* (21), 5050–5053.

(244) Singh, R. P.; Shreeve, J. M. Recent Advances in Nucleophilic Fluorination Reactions of Organic Compounds Using Deoxofluor and DAST. *Synthesis (Stuttg).* **2002**, No. 17, 2561–2578.

(245) Jerôme Baudoux; Dominique Cahard. Electrophilic Fluorination with N-F Reagents. In *Organic Reactions*; Overman, L. E., et.al., Eds.; John Wiley & Sons, Inc., **2007**; Vol. 69, pp. 347–672.

(246) Rajendra P. Sing and Jean'Ne M. Shreeve. Recent Highlights in Electrophilic Fluorination with 1-Cloromethyl-4-Fluoro-1,4-diazoniabicyclo[2.2.2]octane Bis(tetrafluoroborate). *Acc. Chem. Res.* **2004**, *37* (1), 31–44.

(247) Nyffeler, P. T.; Durón, S. G.; Burkart, M. D.; Vincent, S. P.; Wong, C. Selectfluor : Mechanistic Insight and Applications Angewandte. *Angew. Chem. Int. Ed. Engl.* **2005**, *44*, 192–212.

(248) Aoyagi, Y.; Hitotsuyanagi, Y.; Hasuda, T. Fluorination of Triptolide and Its Analogues and Their Cytotoxicity. *Bioorg. Med. Chem. Lett.* **2008**, *18*, 2459–2463.

(249) Biedermann, D.; Sarek, J.; Klinot, J.; Hajduch, M.; Dzubak, P. Fluorination of Betulinines and Other Triterpenoids with DAST. *Synthesis (Stuttg).* **2005**, No. Scheme 1, 1157–1163.

(250) Leal, A. S.; Wang, R.; Salvador, J. A. R.; Jing, Y. Semisynthetic Ursolic Acid Fluorolactone Derivatives Inhibit Growth with Induction of p21(waf1) and Induce Apoptosis with Upregulation of NOXA and Downregulation of c-FLIP in Cancer Cells.

ChemMedChem **2012**, *7* (9), 1635–1646.

(251) Subba Rao, G. S. R.; Kondaiah, P.; Singh, S. K.; Ravanan, P.; Sporn, M. B. Chemical Modifications of Natural Triterpenes-Glycyrrhetinic and Boswellic Acids: Evaluation of Their Biological Activity. *Tetrahedron* **2008**, *64* (51), 11541–11548.

(252) Singh, B.; Rastogi, R. P. A Reinvestigation of the Triterpenes of Centella Asiatica. *Phytochemistry* **1969**, *8* (1960), 917–921.

(253) Anachatchairatana, T. T.; Remner, B. B.; Hokchaisiri, R. C.; Uksamrarn, A. S. Antimycobacterial Activity of Cinnamate-Based Esters of the Triterpenes Betulinic , Oleanolic and Ursolic Acids. *Chem. Pharm. Bull. (Tokyo).* **2008**, *56* (2), 194–198.

(254) Leal, A. S.; Wang, R.; Salvador, J. A. R.; Jing, Y. Synthesis of Novel Heterocyclic Oleanolic Acid Derivatives with Improved Antiproliferative Activity in Solid Tumor Cells. *Org. Biomol. Chem.* **2013**, *11* (10), 1726–1738.

(255) Leal, A. S.; Wang, R.; Salvador, J. A. R.; Jing, Y. Synthesis of Novel Ursolic Acid Heterocyclic Derivatives with Improved Abilities of Antiproliferation and Induction of p53, p21waf1 and NOXA in Pancreatic Cancer Cells. *Bioorg. Med. Chem.* **2012**, *20* (19), 5774–5786.

(256) Santos, R. C.; Salvador, J. A. R.; Marín, S.; Cascante, M. Novel Semisynthetic Derivatives of Betulin and Betulinic Acid with Cytotoxic Activity. *Bioorg. Med. Chem.* **2009**, *17* (17), 6241–6250.

(257) Santos, R. C.; Salvador, J. A. R.; Marín, S.; Cascante, M.; Moreira, J. N.; Dinis, T. C. P. Synthesis and Structure-Activity Relationship Study of Novel Cytotoxic Carbamate and N-Acylheterocyclic Bearing Derivatives of Betulin and Betulinic Acid. *Bioorg. Med. Chem.* **2010**, *18* (12), 4385–4396.

(258) Santos, R. C.; Salvador, J. A. R.; Cortés, R.; Pachón, G.; Marín, S.; Cascante, M. New Betulinic Acid Derivatives Induce Potent and Selective Antiproliferative Activity through Cell Cycle Arrest at the S Phase and Caspase Dependent Apoptosis in Human Cancer Cells. *Biochimie* **2011**, *93* (6), 1065–1075.

(259) Fleming, F. F.; Yao, L.; Ravikumar, P. C.; Funk, L.; Shook, B. C. Nitrile-Containing Pharmaceuticals: Efficacious Roles of the Nitrile Pharmacophore. *J. Med. Chem.* **2010**, *53* (22), 7902–7917.

(260) Nikolić, A. R.; Petri, E. T.; Klisurić, O. R.; Ćelić, A. S.; Jakimov, D. S.; Djurendić, E. a; Penov Gaši, K. M.; Sakač, M. N.; Gaši, K. M. P.; Sakač, M. N. Synthesis and Anticancer Cell Potential of Steroidal 16,17-Seco-16,17a-Dinitriles: Identification of a Selective Inhibitor of Hormone-Independent Breast Cancer Cells. *Bioorg. Med. Chem.* **2015**, *23*, 703–711.

(261) Talukdar, S.; Hsu, J. L.; Chou, T. C.; Fang, J. M. Direct Transformation of Aldehydes to Nitriles Using Iodine in Ammonia Water. *Tetrahedron Lett.* **2001**, *42* (6), 1103–1105.

(262) Chu, F.; Xu, X.; Li, G.; Gu, S.; Xu, K.; Gong, Y.; Xu, B.; Wang, M.; Zhang, H.; Zhang, Y.; et al. Amino Acid Derivatives of Ligustrazine-Oleanolic Acid as New Cytotoxic Agents. *Molecules* **2014**, *19*, 18215–18231.

(263) Siewert, B.; Pianowski, E.; Csuk, R. Esters and Amides of Maslinic Acid Trigger Apoptosis in Human Tumor Cells and Alter Their Mode of Action with Respect to the Substitution Pattern at C-28. *Eur. J. Med. Chem.* **2013**, *70*, 259–272.

(264) Sporn, M. B.; Liby, K. T.; Yore, M. M.; Fu, L.; Lopchuk, J. M.; Gribble, G. W. New Synthetic Triterpenoids: Potent Agents for Prevention and Treatment of Tissue Injury Caused by Inflammatory and Oxidative Stress. *J. Nat. Prod.* **2011**, *74* (3), 537–545.

(265) Antunovic, M.; Kriznik, B.; Ulukaya, E.; Yilmaz, V. T.; Mihalic, K. C.; Madunic, J.; Marijanovic, I. Cytotoxic Activity of Novel Palladium-Based Compounds on Leukemia Cell Lines. *Anticancer. Drugs* **2015**, *26*, 180–186.

(266) Dhar, S.; Daniel, W. L.; Giljohann, D. A.; Mirkin, C. A.; Lippard, S. J. Polyvalent Oligonucleotide Gold Nanoparticle Conjugates as Delivery Vehicles for platinum(IV) Warheads. *J. Am. Chem. Soc.* **2009**, *131* (41), 14652–14653.

(267) Rajic, Z.; Zorc, B.; Raic-Malic, S.; Ester, K.; Kralj, M.; Pavelic, K.; Balzarini, J.; De Clercq, E.; Mintas, M. Hydantoin Derivatives of L- and D-Amino Acids: Synthesis and Evaluation of Their Antiviral and Antitumoral Activity. *Molecules* **2006**, *11* (11), 837–848.

(268) Porchia, M.; Dolmella, A.; Gandin, V.; Marzano, C.; Pellei, M.; Peruzzo, V.; Refosco, F.; Santini, C.; Tisato, F. Neutral and Charged Phosphine/scorpionate copper(I) Complexes: Effects of Ligand Assembly on Their Antiproliferative Activity. *Eur. J. Med. Chem.* **2013**, *59*, 218–226.

(269) Krysko, D. V; Vanden Berghe, T.; Parthoens, E.; D'Herde, K.; Vandenabeele, P. Methods for Distinguishing Apoptotic from Necrotic Cells and Measuring Their Clearance. *Methods Enzymol.* **2008**, *442* (08), 307–341.

(270) Hengartner, M. O. The Biochemistry of Apoptosis. *Nature* **2000**, *407*, 770–776.

(271) Soldani, C.; Scovassi, a I. Poly(ADP-Ribose) Polymerase-1 Cleavage during Apoptosis: An Update. *Apoptosis.* **2002**, pp. 321–328.

(272) Zhao, Y.; Li, R.; Xia, W.; Neuzil, J.; Lu, Y.; Zhang, H.; Zhao, X.; Zhang, X.; Sun, C.; Wu, K. Bid Integrates Intrinsic and Extrinsic Signaling in Apoptosis Induced by α-Tocopheryl Succinate in Human Gastric Carcinoma Cells. *Cancer Lett.* **2010**, *288* (1), 42–49.

(273) Youle, R. J.; Strasser, A. The BCL-2 Protein Family: Opposing Activities That Mediate Cell Death. *Nat. Rev. Mol. Cell Biol.* **2008**, *9* (january), 47–59.

(274) Armarego, W. L. F.; Chai, C. L. L. *Purification of Laboratory Chemicals*, Fifth Edit.; Butterworth Heinemann, Elsevier Science, **2003**.

(275) Mosmann, T. Rapid Colorimetric Assay for Cellular Growth and Survival: Application to Proliferation and Cytotoxicity Assays. *J. Immunol. Methods* **1983**, *65* (1-2), 55–63.

(276) Laemmli, U. K. Cleavage of Structural Proteins during Assembly of Head of Bacteriophage-T4. *Nature* **1970**, *227*, 680–685.

(277) Fleming, F. F.; Yao, L.; Ravikumar, P. C.; Funk, L.; Shook, B. C. Nitrile-Containing Pharmaceuticals: Efficacious Roles of the Nitrile Pharmacophore. *J. Med. Chem.* **2010**, *53*, 7902–7917.

(278) Kalgutkar, A. S.; Dalvie, D. K. Drug Discovery for a New Generation of Covalent Drugs. *Expert Opin. Drug Discov.* **2012**, *7*, 561–581.

(279) Berteotti, A.; Vacondio, F.; Lodola, A.; Bassi, M.; Silva, C.; Mor, M.; Cavalli, A. Predicting the Reactivity of Nitrile-Carrying Compounds with Cysteine: A Combined Computational and Experimental Study. *ACS Med. Chem. Lett.* **2014**, *5* (5), 501–505.

(280) Murphy, S. T.; Case, H. L.; Ellsworth, E.; Hagen, S.; Huband, M.; Joannides, T.; Limberakis, C.; Marotti, K. R.; Ottolini, A. M.; Rauckhorst, M.; et al. The Synthesis and Biological Evaluation of Novel Series of Nitrile-Containing Fluoroquinolones as Antibacterial Agents. *Bioorg. Med. Chem. Lett.* **2007**, *17*, 2150–2155.

(281) Altmann, E.; Cowan-Jacob, S. W.; Missbach, M. Novel Purine Nitrile Derived Inhibitors of the Cysteine Protease Cathepsin K. *J. Med. Chem.* **2004**, *47*, 5833–5836.

(282) Mannhold, R.; Höltje, H. D.; Koke, V. Importance of Nitrile Substitution for the Ca Antagonistic Action. *Arch. Pharm. (Weinheim).* **1986**, *319*, 990–998.

(283) Frizler, M.; Lohr, F.; Furtmann, N.; Kläs, J.; Gütschow, M. Structural Optimization of Azadipeptide Nitriles Strongly Increases Association Rates and Allows the Development of Selective Cathepsin Inhibitors. *J. Med. Chem.* **2011**, *54*, 396–400.

(284) Bag, S.; Tawari, N. R.; Degani, M. S. A New, Mild and High Yielding Protocol for the Preparation of Nitriles from Aldehydes Using Iodosobenzene Diacetate in Aqueous Ammonia. *Arkivoc* **2009**, (14), 118–123.

(285) Shie, J.; Fang, J. Microwave-Assisted One-Pot Tandem Reactions for Direct Conversion of Primary Alcohols and Aldehydes to Triazines and Tetrazoles in Aqueous Media. *J. Org. Chem.* **2007**, *72* (8), 3141–3144.

(286) Erman, M. B.; Snow, J. W.; Williams, M. J. A New Efficient Method for the Conversion of Aldehydes into Nitriles Using Ammonia and Hydrogen Peroxide. *Tetrahedron Lett.* **2000**, *41*, 6749–6752.

(287) Zhu, J. L.; Lee, F. Y.; Wu, J. D.; Kuo, C. W.; Shia, K. S. An Efficient New Procedure for the One-Pot Conversion of Aldehydes into the Corresponding Nitriles. *Synlett* **2007**, No. 8, 1317–1319.

(288) Sarvari, M. H.; Sharghi, H. Graphite as an Efficient Catalyst for One-Step Conversion of Aldehydes into Nitriles in Dry Media. *Synthesis (Stuttg).* **2003**, No. 2, 243–246.

(289) Rokade, B. V.; Prabhu, K. R. Chemoselective Schmidt Reaction Mediated by Triflic Acid: Selective Synthesis of Nitriles from Aldehydes. *J. Org. Chem.* **2012**, *77* (12), 5364–5370.

(290) Telvekar, V. N.; Rane, R. A.; Namjoshi, T. V. Novel System for the Synthesis of Nitriles from Aldehydes Using Aqueous Ammonia and [Bis(Trifluoroacetoxy) Iodo] Benzene. *Synth. Commun.* **2010**, *40* (4), 494–497.

(291) Zolfigol, M. A.; Hajjami, M.; Ghorbani-Choghamarani, A. A Simple and One-Pot Oxidative Conversion of Alcohols or Aldehydes to the Nitriles Using NaIO4/KI in Aqueous NH3. *Bull. Korean Chem. Soc.* **2011**, *32* (12), 4191–4194.

(292) Dornan, L. M.; Cao, Q.; Flanagan, J. C. a; Crawford, J. J.; Cook, M. J.; Muldoon, M. J. Copper/TEMPO Catalysed Synthesis of Nitriles from Aldehydes or Alcohols Using Aqueous Ammonia and with Air as the Oxidant. *Chem. Commun.* **2013**, *49* (54), 6030–6032.

(293) Shie, J. J.; Fang, J. M. Direct Conversion of Aldehydes to Amides, Tetrazoles, and Triazines in Aqueous Media by One-Pot Tandem Reactions. *J. Org. Chem.* **2003**, *68* (3), 1158–1160.

(294) Upadhyay, S.; Chandra, A.; Singh, R. M. A One Pot Method of Conversion of Aldehydes into Nitriles Using Iodine in Ammonia Water: Synthesis of 2-Chloro-3-

Cyanoquinolines. *Indian J. Chem. - Sect. B* **2009**, *48B* (1), 152–154.

(295) Salvador, J. A. R.; Sá E Melo, M. L.; Campos Neves, A. S. Oxidations with Potassium Permanganate - Metal Sulphates and Nitrates. β-Selective Epoxidation of Δ5-Unsaturated Steroids. *Tetrahedron Lett.* **1996**, *37* (5), 687–690.

(296) Tu, H. Y.; Huang, A. M.; Wei, B. L.; Gan, K. H.; Hour, T. C.; Yang, S. C.; Pu, Y. S.; Lin, C. N. Ursolic Acid Derivatives Induce Cell Cycle Arrest and Apoptosis in NTUB1 Cells Associated with Reactive Oxygen Species. *Bioorg. Med. Chem.* **2009**, *17* (20), 7265–7274.

(297) Csuk, R.; Schwarz, S.; Kluge, R.; Ströhl, D. Does One Keto Group Matter? Structure-Activity Relationships of Glycyrrhetinic Acid Derivatives Modified at Position C-11. *Arch. Pharm. (Weinheim).* **2012**, *345*, 28–32.

(298) Malumbres, M.; Carnero, A. Cell Cycle Deregulation: A Common Motif in Cancer. *Prog. Cell Cycle Res.* **2003**, *5*, 5–18.

(299) Vermes, I.; Haanen, C.; Steffens-Nakken, H.; Reutelingsperger, C. A Novel Assay for Apoptosis. Flow Cytometric Detection of Phosphatidylserine Expression on Early Apoptotic Cells Using Fluorescein Labelled Annexin V. *J. Immunol. Methods* **1995**, *184* (95), 39–51.

(300) Häcker, G. The Morphology of Apoptosis. *Cell Tissue Res.* **2000**, *301*, 5–17.

(301) Budihardjo, I.; Oliver, H.; Lutter, M.; Luo, X.; Wang, X. Biochemical Pathways of Caspase Activation during Apoptosis. *Annu. Rev. Cell Dev. Biol.* **1999**, *15*, 269–290.

(302) Chen, H.; Gao, Y.; Wang, A.; Zhou, X.; Zheng, Y.; Zhou, J. Evolution in Medicinal Chemistry of Ursolic Acid Derivatives as Anticancer Agents. *Eur. J. Med. Chem.* **2015**, *92*, 648–655.

(303) Apfel, C.; Banner, D. W.; Bur, D.; Dietz, M.; Hirata, T.; Hubschwerlen, C.; Locher, H.; Page, M. G.; Pirson, W.; Rossé, G.; et al. Hydroxamic Acid Derivatives as Potent Peptide Deformylase Inhibitors and Antibacterial Agents. *J. Med. Chem.* **2000**, *43* (12), 2324–2331.

(304) Baek, H.; Rho, H.; Yoo, J.; Ahn, S. The Inhibitory Effect of New Hydroxamic Acid Derivatives on Melanogenesis. *Bull. Korean Chem. Soc.* **2008**, *29* (1), 43–46.

(305) Rho, H. S.; Baek, H. S.; Ahn, S. M.; Yoo, J. W.; Kim, D. H.; Kim, H. G. Hydroxamic Acid Derivatives as Anti-Melanogenic Agents: The Importance of a Basic Skeleton and Hydroxamic Acid Moiety. *Bull. Korean Chem. Soc.* **2009**, *30* (2), 475–478.

(306) Stranix, B. R.; Wu, J. J.; Milot, G.; Beaulieu, F.; Bouchard, J. E.; Gouveia, K.; Forte, A.; Garde, S.; Wang, Z.; Mouscadet, J. F.; et al. Pyridoxine Hydroxamic Acids as Novel HIV-Integrase Inhibitors. *Bioorganic Med. Chem. Lett.* **2016**, *26* (4), 1233–1236.

(307) Butler, L. M.; Agus, D. B.; Scher, H. I.; Higgins, B.; Rose, A.; Cordon-Cardo, C.; Thaler, H. T.; Rifkind, R. A.; Marks, P. A.; Richon, V. M. Suberoylanilide Hydroxamic Acid, an Inhibitor of Histone Deacetylase, Suppresses the Growth of Prostate Cancer Cells in Vitro and in Vivo. *Cancer Res* **2000**, *60* (18), 5165–5170.

(308) Pal, D.; Saha, S. Hydroxamic Acid - A Novel Molecule for Anticancer Therapy. *J. Adv. Pharm. Technol. Res.* **2012**, *3* (2), 92–99.

(309) Saban, N.; Bujak, M. Hydroxyurea and Hydroxamic Acid Derivatives as Antitumor

Drugs. *Cancer Chemother. Pharmacol.* **2009**, *64*, 213–221.

(310) Jiang, J.; Thyagarajan-Sahu, A.; Krchňák, V.; Jedinak, A.; Sandusky, G. E.; Sliva, D. NAHA, a Novel Hydroxamic Acid-Derivative, Inhibits Growth and Angiogenesis of Breast Cancer in Vitro and in Vivo. *PLoS One* **2012**, *7* (3), 1–10.

(311) Zhang, Y.; Feng, J.; Jia, Y.; Wang, X.; Zhang, L.; Liu, C.; Fang, H.; Xu, W. Development of Tetrahydroisoquinoline-Based Hydroxamic Acid Derivatives: Potent Histone Deacetylase Inhibitors with Marked in Vitro and in Vivo Antitumor Activities. *J. Med. Chem.* **2011**, *54*, 2823–2838.

(312) Nam, N. H.; Huong, T. L.; Mai Dung, D. T.; Phuong Dung, P. T.; Kim Oanh, D. T.; Quyen, D.; Thao, L. T.; Park, S. H.; Kim, K. R.; Han, B. W.; et al. Novel Isatin-Based Hydroxamic Acids as Histone Deacetylase Inhibitors and Antitumor Agents. *Eur. J. Med. Chem.* **2013**, *70*, 477–486.

(313) Huong, T. T. L.; Dung, D. T. M.; Dung, P. T. P.; Huong, P. T.; Vu, T. K.; Hahn, H.; Han, B. W.; Kim, J.; Pyo, M.; Han, S. B.; et al. Novel 2-Oxoindoline-Based Hydroxamic Acids: Synthesis, Cytotoxicity, and Inhibition of Histone Deacetylation. *Tetrahedron Lett.* **2015**, *56* (46), 6425–6429.

(314) Zask, A.; Gu, Y.; Albright, J. D.; Du, X.; Hogan, M.; Levin, J. I.; Chen, J. M.; Killar, L. M.; Sung, A.; DiJoseph, J. F.; et al. Synthesis and SAR of Bicyclic Heteroaryl Hydroxamic Acid MMP and TACE Inhibitors. *Bioorganic Med. Chem. Lett.* **2003**, *13* (8), 1487–1490.

(315) Marmion, C. J.; Parker, J. P.; Nolan, K. B. Hydroxamic Acids: An Important Class of Metalloenzyme Inhibitors. In *Comprehensive Inorganic Chemistry II: From Elements to Applications*; Reedijk, J., Poeppelmeier, K., Eds.; Elsevier Ltd.: Amsterdam, **2013**, Vol. 3, pp. 683–708.

(316) Stanetty, C.; Czollner, L.; Koller, I.; Shah, P.; Gaware, R.; Cunha, T. Da; Odermatt, A.; Jordis, U.; Kosma, P.; Classen-Houben, D. Synthesis of Novel 3-Amino and 29-Hydroxamic Acid Derivatives of Glycyrrhetinic Acid as Selective 11β-Hydroxysteroid Dehydrogenase 2 Inhibitors. *Bioorg. Med. Chem.* **2010**, *18* (21), 7522–7541.

(317) Gaware, R.; Khunt, R.; Czollner, L.; Stanetty, C.; Cunha, T. Da; Kratschmar, D. V.; Odermatt, A.; Kosma, P.; Jordis, U.; Claßen-Houben, D. Synthesis of New Glycyrrhetinic Acid Derived Ring A Azepanone, 29-Urea and 29-Hydroxamic Acid Derivatives as Selective 11β-Hydroxysteroid Dehydrogenase 2 Inhibitors. *Bioorganic Med. Chem.* **2011**, *19* (6), 1866–1880.

(318) Wiemann, J.; Heller, L.; Csuk, R. Targeting Cancer Cells with Oleanolic and Ursolic Acid Derived Hydroxamates. *Bioorg. Med. Chem. Lett.* **2016**, *26* (3), 907–909.

(319) Reddy, A. S.; Kumar, M. S.; Reddy, G. R. A Convenient Method for the Preparation of Hydroxamic Acids. *Tetrahedron Lett.* **2000**, *41*, 6285–6288.

(320) Giacomelli, G.; Porcheddu, A.; Salaris, M. Simple One-Flask Method for the Preparation of Hydroxamic Acids. *Org. Lett.* **2003**, *5* (15), 2715–2717.

(321) Usachova, N.; Leitis, G.; Jirgensons, A.; Kalvinsh, I. Synthesis of Hydroxamic Acids by Activation of Carboxylic Acids with *N* , *N* ′-Carbonyldiimidazole: Exploring the Efficiency of the Method. *Synth. Commun.* **2010**, *40* (May 2012), 927–935.

(322) Ech-Chahad, A.; Minassi, A.; Berton, L.; Appendino, G. An Expeditious Hydroxyamidation of Carboxylic Acids. *Tetrahedron Lett.* **2005**, *46* (31), 5113–5115.

(323) Jew, S. S.; Park, H. G.; Kim, H. D.; Jung, Y. H.; Kim, Y. C.; Kim, H. P.; Lee, M. K.; Choi, H. S.; Lee, E. S.; Lim, D. Y.; et al. Asiatic Acid Derivatives Having Modified A-Ring, WO9823575, **1998**.

(324) Kohji Takara, Yukihisa Obata, Eri Yoshikawa, Noriaki Kitada, Toshiyuki Sakaeda, Noriaki Ohnishi, T. Y. Molecular Changes to HeLa Cells on Continuous Exposure to Cisplatin or Paclitaxel. *Cancer Chemother. Pharmacol.* **2006**, *58*, 785–793.

(325) Cortés, R.; Tarrado-Castellarnau, M.; Talancón, D.; López, C.; Link, W.; Ruiz, D.; Centelles, J. J.; Quirante, J.; Cascante, M. A Novel Cyclometallated Pt(ii)-Ferrocene Complex Induces Nuclear FOXO3a Localization and Apoptosis and Synergizes with Cisplatin to Inhibit Lung Cancer Cell Proliferation. *Metallomics* **2014**, 622–633.

(326) Chou, T. C. Drug Combination Studies and Their Synergy Quantification Using the Chou-Talalay Method. *Cancer Res.* **2010**, *70*, 440–446.

(327) Chou, T. C.; Talalay, P. Quantitative Analysis of Dose-Effect Relationships: The Combined Effects of Multiple Drugs or Enzyme Inhibitors. *Adv. Enzyme Regul.* **1984**, *22* (C), 27–55.

(328) Liang, X.-J.; Chen, C.; Zhao, Y.; Wang, P. C. Circumventing Tumor Resistance to Chemotherapy by Nanotechnology. *Methods Mol. Biol.* **2010**, *596* (3), 467–488.